Hemanshu Roy Pota

The Essentials of Power System Dynamics and Control

The Essentials of Power System Dynamics and Control

Hemanshu Roy Pota

The Essentials of Power System Dynamics and Control

Springer

Hemanshu Roy Pota
School of Engineering and Information
    Technology
The University of New South Wales
Canberra, ACT
Australia

हस्कराद्विद्युतस्पर्यतो जाता अवन्तु नः। मरुतो मृळयन्तु नः॥ऋग्वेदः १।२३।१२॥

haskārādvidyutasparyato jātā avantu naḥ| maruto mṛḻayantu naḥ||ṛgvedaḥ 1|23|12||

May the winds, born from the shining sky electricity, protect us and give us happiness.

Preface

Every aspect of the power system is undergoing a transformation, and the existing dynamical representation of the power system will change. Engineers from diverse background, often working in one specialised area of the interconnected power system, are contributing to this change. The ability to accurately model the existing complex interconnected power system dynamics with only a few simple differential equations has been a fascinating intellectual achievement. The work of the engineers who are at the forefront of transforming the power system will have a higher impact if the new contributions rest on and are connected with the existing foundations of power system dynamics.

This book is written for students or practising engineers with a background in science or engineering. It is self-contained, starting from phasor analysis and leading the reader to the design of automatic voltage regulators and power system stabilisers for synchronous generators. It includes fundamentals of the linear control systems that enable the design of the controllers. Historically speaking, initially dynamic models for synchronous machines were developed for analysis and immediately after that they were successfully used for voltage and frequency regulation. A solid understanding of power system dynamics is obtained from completing the model, analysis, design, and then model refinement cycle. In this book, the reader is guided through the entire cycle.

The simplification in modelling the power system dynamics is achieved by partitioning the dynamics into fast and slow dynamics. The fast dynamics, also known as the stator or the transmission system dynamics, is assumed to be in steady state during each integration time-step of the slow dynamics, also known as rotor dynamics. Although mathematically straightforward, it is important to understand the steady-state analysis of the slow dynamics. This analysis, also known as the power flow or load flow analysis, is introduced in Chap. 1. A simple technique to solve for the nonlinear steady-state solution is given so that the reader gets a complete appreciation of the problem. Many advanced methods exist for load flow

solution, but an understanding of those methods is not necessary for a deep understanding of power system dynamics.

Magnetic energy is the intermediate energy storage mechanism during the conversion between electrical and mechanical energy. Magnetic circuits can be easily understood in analogy with electrical circuits. Although magnetic circuits have a much smaller linear range, once properly formulated, it is not difficult to include the nonlinear characteristics during the numerical integration process. The first chapter covers a comprehensive analysis of the magnetic circuit of three-phase rotating machines which leads to the principle of operation of synchronous and induction machines.

The dynamics of generators with moving parts has coupled mechanical and electrical dynamic equations. The mechanical dynamics is often equivalent to a mass–spring system driven by the difference between the input mechanical power and the output electrical power. The electrical output power is a function of the generator angular position and terminal voltage, and this couples the mechanical and electrical dynamics of the rotating electrical generators. In most situations, a first-order differential equation accurately represents the voltage dynamics. In Chap. 2, a detailed method is presented that shows how the third-order dynamic equations, for each generator, are coupled to form interconnected system dynamic equations. This chapter is complete in all the details, and every equation is derived fully. The reader is encouraged to derive each expression using symbolic computation software or using the paper-and-pencil method. The fundamental principle is very simple, but the confidence that this simple principle can lead to such complicated models will only sink in if the reader derives each expression and gets convinced that only one simple principle, Faraday's law of induced electromotive force, has such far-reaching consequences. Algebraic transformation using matrix algebra plays an important role in the simplified transient analysis models, and the complete derivation includes all the matrix manipulation required to arrive at the final simple model.

Chapter 2 extends the simple transient model, accurate in the order of hundreds of milliseconds, by adding additional dynamics to make it accurate for tens of milliseconds time frame. Once the understanding of a single coil dynamics is understood well, it is simply a mechanical process to keep adding additional coils to the model to obtain the so called sub-transient model. The chapter further derives the block diagrams used by commercial power system analysis software to model rotating machines. These models are parameterised both in terms of open-circuit and short-circuit time constants. The author has used symbolic manipulation software to derive these results, and the reader is also strongly urged to use similar software, especially since high-quality open-source symbolic manipulation software is available.

Chapter 3 covers essential linear systems analysis for the design of classical controllers, using frequency domain techniques, for voltage regulation and oscillation damping of rotating generators. In this chapter, detailed derivations are given so that the reader is absolutely clear what is frequency response and why is it such a wonderful tool for the design of robust controllers. Almost all classical design tools

are covered in this chapter giving enough information about the utility of the method. With the availability of open-source software tools such as octave and Scilab, this chapter does not detail how to draw various plots for analysis, but it emphasises on what the tools fit in the design process.

Power system analysis is done with the nonlinear models, but control design is more convenient with the linearised models. Chapter 3 gives complete derivation of all the linearised models. Although expressions for the linearised models are given, here again the reader is urged to derive the models themselves so that they have definite expressions which they can own and further use it for control design with a full understanding.

Automatic voltage regulator (AVR) is an essential component of generators, and almost all the commercially available AVRs can be designed using frequency domain techniques covered in Chap. 3. In Chap. 4, AVR design is covered from simple fixed gain controllers to complex multiple-loop proportional–derivative–integral (PID) controllers. The control specifications are given in terms of steady-state error, bandwidth, and phase-margin, and the lag-lead compensator design is used to satisfy these control specifications. These methods have been used to design and implement AVRs for commercial synchronous generators.

There is no inherent mechanical damping in the interconnected system, and the electrical transients couple with the mechanical dynamics to provide damping. Chapter 5 covers a detailed analysis of the magnitude and sign of the damping due to feedback mechanism used for AVRs. Often the damping due to electrical transients is not enough, and in those situations, a power system stabiliser (PSS) is used to increase the damping. The design of PSS is also done using frequency domain methods. Chapter 5 covers the design of the classical PSS, and it completes the model, analysis, and design cycle.

Although this book covers the essentials of power system dynamics with rotating generators, the same ideas are applicable to static generators, such as photo-voltaic solar generators. The material in this book will enable researchers to integrate generator models of the emerging renewable resources-based generators to inter-connected power systems and do control design considering the dynamics of the entire power systems.

The essentials in this book have been very carefully chosen to provide sufficient depth to the reader so that it is easy to integrate the dynamics of emerging devices. The author emphasises that the full benefit from this book can only be realised if the reader derives the expression in this book.

I have taught a ten-week forty-lecture course based on this book thrice to engineers with diverse background, and as a result, some refinement has been done and the author sincerely hopes that it will help engineers from diverse backgrounds to become productive power system engineers. A shorter version of this course has been also taught twice to practising power system consultants. I have incorporated most of the feedback that I received during the course.

I thank my former Ph.D. students who have shaped much of the material in this book by asking questions and giving me an idea of the difficulties faced by a beginning researcher in the area of power system dynamics. I thank Dr. C. S. Kumble

and Mr. Prahlad Tilwalli for engaging me as a consultant and giving me the satisfaction of observing the performance of the controllers designed using the methods in this book on commercial synchronous generators.

Canberra, Australia   Hemanshu Roy Pota

Contents

Chapter 1
Introduction

This chapter covers the basics that will enable a good understanding of the power system dynamics. A power system is a collection of electricity generation, transmission, and consumption. Traditionally the generation and consumption have been geographically separated with a transmission system to connect them. The backbone of the study of power system dynamics is a circuit analysis of the transmission network. In this circuit analysis, generators are modelled as active voltage sources and the consumption devices, also known as loads, are modelled as consuming constant current or power, or as impedances, or a combination of all the three. In developing the basics of power systems we analyse a transmission system exactly the same way as we analyse an electrical circuit. In practice generation devices are not ideal voltage sources and loads are not constant impedances and thus to accommodate practical generation devices and loads the circuit analysis is extended to what is commonly known as the load-flow analysis.

In electrical machines magnetic flux is the medium through which conversion between mechanical and electrical energy takes place. Flux in magnetic circuits is analogous to current in electrical circuits. In this chapter the necessary magnetic circuit analysis to understand synchronous and induction machines is covered.

Next we start with a look at the tools that are needed to analyse circuits with sinusoidal sources, i.e., AC circuits.

1.1 Sinusoidal Steady-State

A transmission network is just like any electrical circuit with steady-state and transient modes of operation. One key assumption about the transmission system in power system analysis is that the transmission network is always in steady-state. This means that we assume that the transients die out much faster than the interval over which the analysis is done. This simplifies the analysis greatly. Let us first look at the sinusoidal steady-state analysis, also known as the phasor analysis, of a simple circuit.

Fig. 1.1 An LC circuit
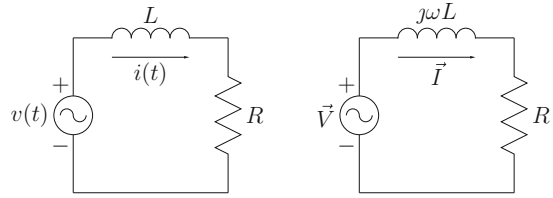
1.1.1 RL Circuit

The circuit in Fig. 1.1 represents a generator supplying an inductive load. The differential equation describing the circuit in Fig. 1.1, with $v(t) = V_m \sin(\omega t)$ is:

$$L\frac{di}{dt} + Ri = V_m \sin(\omega t); i(0) = i_0 \tag{1.1}$$

The complete solution to this first-order differential equation (1.1) is:

$$i(t) = ke^{-t\frac{R}{L}} + I_m \sin(\omega t + \phi) \tag{1.2}$$

where $I_m = \dfrac{V_m}{\sqrt{\omega^2 L^2 + R^2}}$, $\phi = -\tan^{-1}\frac{\omega L}{R}$, and k is chosen to satisfy the initial condition.

The steady-state solution can be written as:

$$i_{ss}(t) = \lim_{t \to \infty} i(t) = I_m \sin(\omega t + \phi). \tag{1.3}$$

The above solution does not depend on the initial conditions and there is an easy method, known as phasor analysis, to obtain I_m and ϕ without actually solving the differential equation.

1.1.2 Phasor Analysis

Phasor analysis converts a linear differential equation problem to an algebra problem with complex variables. A phasor is a complex number $re^{\jmath \phi}$ and it is used as a shorthand notation to represent a sinusoidal waveform $\sqrt{2}r \sin(\omega t + \phi)$. The correspondence between the phasors and time waveforms is shown in Fig. 1.2. A systematic way to do the phasor analysis is to represent all the sinusodal forcing functions as phasors and the circuit elements by their impedances. After the conversion one can use either Kirchhoff's Current Law (KCL) or Kirchhoff's Voltage Law (KVL) to write circuit equations and solve them to obtain node voltages or loop currents. It

Fig. 1.2 Time waveforms and phasors
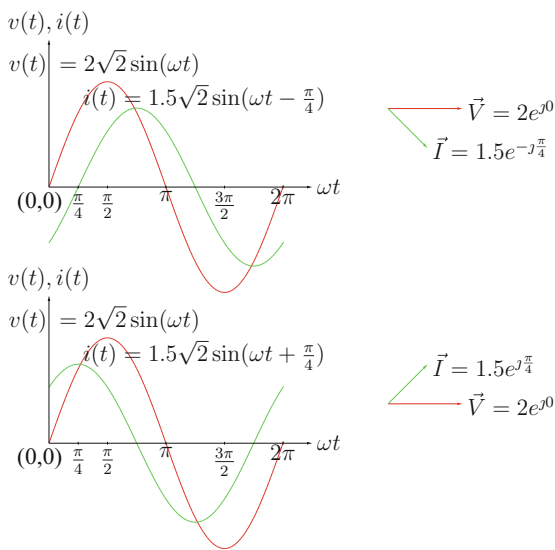
is common to write KCL or nodal equations in power system analysis and solve for nodal voltages.

For phasor analysis, where all voltage and current sources are sinusoids with the same frequency ω, any current or voltage forcing function $f(t) = F_m \sin(\omega t + \phi)$ is written in phasor form as $\vec{F} = \dfrac{F_m}{\sqrt{2}} e^{j\phi}$. The passive circuit elements, inductance, L, capacitance, C, and resistance R, are replaced by their impedances $j\omega L$, $\dfrac{1}{j\omega C}$, and R, respectively. The impedances can be combined using parallel and series circuit rules like resistors in a DC circuit. Equivalent impedance in general will be a complex quantity, $Z = R + jX$, where the real part, R, is called the equivalent resistance, and the imaginary part, X, is called the equivalent reactance which is positive for an inductive and negative for a capacitive circuit.

The equivalent circuit for phasor analysis of the LC circuit is shown on the right in Fig. 1.1. In the phasor analysis we represent $V_m \sin(\omega t)$ as $\vec{V} = \dfrac{V_m}{\sqrt{2}} e^{j0}$, $I_m \sin(\omega t + \phi)$ as $\vec{I} = \dfrac{I_m}{\sqrt{2}} e^{j\phi}$, and $\vec{Z} = R + j\omega L$. Then

$$\vec{I} = \frac{\vec{V}}{\vec{Z}} \Rightarrow \vec{I} = \frac{V_m}{\sqrt{2}} e^{j0} \frac{1}{\sqrt{\omega^2 L^2 + R^2}} e^{j\tan^{-1}\frac{-\omega L}{R}}$$

The magnitude and phase of the phasor $\vec{I}$ directly give the magnitude and the phase of the sinusoidal $i_{ss}(t)$ in (1.3). Phasor representation converts the steady-state solution of linear differential equations with sinusoidal inputs to algebraic equations.

Example In the RL circuit shown in Fig. 1.1, let $v(t) = 5\sin 2\pi 60t\, V$, $R = 3\Omega$, and $L = 0.0106\, H$. Find the steady-state current $i_{ss}(t)$.

$\vec{V} = \dfrac{5}{\sqrt{2}}e^{j0}$ and $\vec{Z} = 3 + j2\pi 60 \times 0.0106\,\Omega = 3 + j4\,\Omega$. This gives $\vec{I} = \dfrac{\vec{V}}{\vec{Z}} = 1.0e^{j(-0.9273)}$ and

$$i_{ss}(t) = \sqrt{2}\sin(2\pi 60t - 0.9273)A$$

1.2 Real and Reactive Power

In an AC system, the power generated and consumed is changing at every instant in time. Although the voltage and current are alternating, the interest is in calculating the average power generated or consumed. The average power is given the name real power. When the voltage and current across a device are in phase the real power is given as the product of the root-mean-squared (rms) values of the voltage and current. When they are not in phase, the real power is given by the product of the rms values and something called the power factor which is always less than one. This means that each device included in the power system analysis is characterised by the real power it consumes or generates and the power factor. The instantaneous power can be obtained from phasor quantities using real power and another term called reactive power, i.e., both real and reactive power are required to completely characterise power using phasor analysis. In the following the concept of reactive power is introduced. In power system analysis it is common to specify real and reactive power for active devices, like generators and motors, and impedances for passive devices.

Figure 1.3 shows an AC generator and a load. The instantaneous power delivered by the voltage source is:

$$
\begin{aligned}
v(t)i(t) &= V_m \sin(\omega t + \alpha)I_m \sin(\omega t + \beta) \\
&= V_m \sin(\omega t + \alpha)I_m \sin(\omega t + \alpha - (\alpha - \beta)) \\
&= V_m I_m \sin(\omega t + \alpha)(\sin(\omega t + \alpha)\cos(\alpha - \beta) - \cos(\omega t + \alpha)\sin(\alpha - \beta)) \\
&= V_m I_m \sin^2(\omega t + \alpha)\cos(\alpha - \beta) - V_m I_m \frac{\sin 2(\omega t + \alpha)}{2}\sin(\alpha - \beta))
\end{aligned}
$$
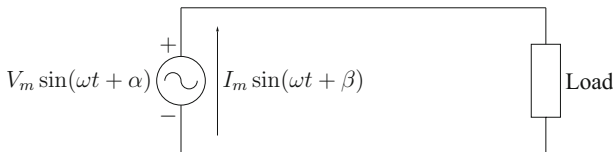
Fig. 1.3 Real and reactive power in steady-state
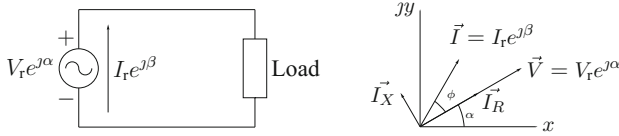
Fig. 1.4 Real and reactive power and phasors

$$= V_m I_m \frac{1 - \cos 2(\omega t + \alpha)}{2} \cos(\alpha - \beta) - V_m I_m \frac{\sin 2(\omega t + \alpha)}{2} \sin(\alpha - \beta))$$
$$= p_R + p_Q$$

The two components of the power delivered by the voltage source can be written as:

$$p_R = V_m I_m \frac{1 - \cos 2(\omega t + \alpha)}{2} \cos(\alpha - \beta) \text{ and } p_Q = -V_m I_m \frac{\sin 2(\omega t + \alpha)}{2} \sin(\alpha - \beta) \tag{1.4}$$

Two quantities P and Q known as real power and reactive power, respectively, are defined as:

$$P = \frac{V_m I_m}{2} \cos(\alpha - \beta) \text{ and } Q = \frac{V_m I_m}{2} \sin(\alpha - \beta) \tag{1.5}$$

It is easy to see that P is the average of p_R over one period and Q is the peak value of p_Q. The unit for the real power is W and for the reactive power it is VAr. The phasor diagram in Fig. 1.4 can be used to better understand the definitions for P and Q.

In Fig. 1.4, $\cos \phi = \cos(\beta - \alpha)$, is known as the power factor, where ϕ is the phase difference between the voltage and current phasors. Let us express the current phasor as the sum of two components. One component, $\vec{I}_R = |I_r \cos \phi| e^{J\alpha}$, in phase and another $\vec{I}_X = |I_r \sin \phi| e^{J(\alpha + 90°)}$, ninety degrees out of phase with the voltage phasor. Let $V_r = \frac{V_m}{\sqrt{2}}, I_r = \frac{I_m}{\sqrt{2}}$, then from the definition in (1.5), we get:

$$P = V_r \left| \vec{I}_R \right| \operatorname{sgn}(\cos \phi) \text{ and } Q = V_r \left| \vec{I}_X \right| \operatorname{sgn}(\sin \phi)$$

This means that the real power is the product of the rms values of the voltage and the current that is in phase with the voltage and the reactive power is the product with the rms current that is ninety degrees out of phase with the voltage. The ninety degree out of phase current produces zero average power, this is the power that gets alternately consumed and delivered by inductors and capacitors.

The convenience of using reactive power instead of power factor to characterise a device is due to the ease with which one can compute the reactive power and the fact that we can treat it as something physical on the same footing as the real power. Next we show that real and reactive powers can be packed into a term called complex power and that there has to be a perfect balance in the network between the sum of

the generated and consumed complex power. It is much easier to understand that the ith load is X_i VAr instead of specifying that it operates at power factor $\cos \phi_i$, since the sum of all X_is has a physical meaning while the sum of the power factors has no meaning. It must be understood that the reactive power, p_Q in (1.4), neither gets consumed nor generated on an average but a balance has to be met between the sum of generated and consumed reactive powers.

Complex power S The complex power S is defined as: $S = P + jQ$, from the vector diagram in Fig. 1.4 it can be seen that:

$$S = \vec{V} \, \vec{I}^* = V_r I_r e^{J(\alpha-\beta)} = V_r I_r \cos(\alpha - \beta) + j V_r I_r \sin(\alpha - \beta) = P + jQ$$

where * means complex conjugate.

Let the load in Fig. 1.4 be made up of a resistor, R, and reactance, X, such that the load impedance, $Z_L = R + jX$. The current $\vec{I}_r = \frac{\vec{V}_r}{R+jX}$, and its magnitude is $I_r = \frac{V_r}{\sqrt{R^2+X^2}}$. Referring to the definitions in Fig. 1.4, we have $\alpha = 0, \beta = -\tan^{-1} \frac{X}{R}$, $\phi = \beta, \cos\beta = \frac{R}{\sqrt{R^2+X^2}}$, and $\sin\beta = \frac{X}{\sqrt{R^2+X^2}}$. This gives the real and reactive power absorbed by the load as: $P = I_r^2 R$ and $Q = I_r^2 X$. This has an interesting interpretation for power absorbed by an impedance. The real power is the power dissipated across the resistor and the reactive power is the power "dissipated" across the reactance.

1.2.1 P and Q Sign Convention

The real and reactive power specifications follow a sign convention in power system analysis. This convention is important as power systems have both loads and generators so it is important to distinguish if one is specifying generated or consumed P and Q.

Figure 1.5 shows two ways one can specify current across a device. In a branch where the current is flowing from the negative polarity of the voltage to the positive polarity, i.e., for a generator convention as in Fig. 1.5a:

1. If P is positive then the real power is generated or supplied by the branch otherwise it absorbs real power.
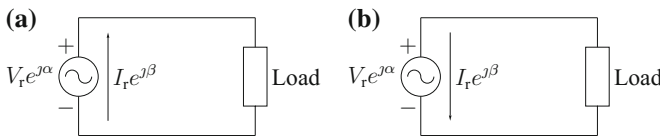
Fig. 1.5 Real and reactive power sign convention

Fig. 1.6 Real and reactive
power (numerical example)
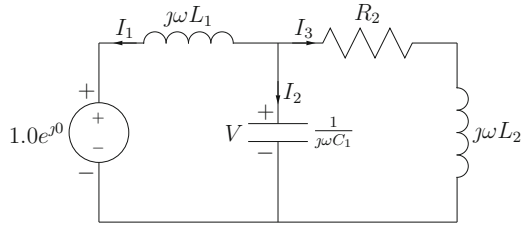
Table 1.1 Complex power

Element	Voltage source	Z_1	Z_2	Z_3
Complex power S	$-1.5385 + j2.3077$	$j0.7692$	$-j7.6923$	$1.5385 + j4.6154$

2. If Q is positive it is supplying positive reactive power otherwise it is absorbing positive reactive power.

In a branch where the current is flowing from the positive polarity of the voltage to the negative polarity, i.e., for a load convention, as in Fig. 1.5b above:

1. If P is positive then the real power is absorbed by the branch otherwise it generates real power.
2. If Q is positive it is absorbing positive reactive power otherwise it is supplying positive reactive power.

For the cases where the phase difference between the voltage and current is limited between $+90°$ and $-90°$, for the generator convention, positive Q means that the current lags the voltage.

Example A schematic of a simple power system with a voltage source and some loads is shown in Fig. 1.6. Let us calculate the real and reactive power generated and consumed in the system.

Let $\omega = 2\pi 60 \,\text{rad s}^{-1}$, $L_1 = \frac{0.1}{\omega} H$, $L_2 = \frac{0.3}{\omega} H$, $C_1 = \frac{5}{\omega} F$, and $R_2 = 0.1 \,\Omega$, note that the source voltage is $\sqrt{2} \sin \omega t \, V$.

Let $Z_1 = j\omega L_1, Z_2 = \frac{1}{j\omega C_1}, Z_3 = R_2 + j\omega L_2$, writing KCL for the node above the capacitor, we have:

$$\frac{V - 1e^{j0}}{Z_1} + \frac{V}{Z_2} + \frac{V}{Z_3} = 0$$

solving the above equation we get, $V = 1.2308 - j0.1538V$, and $I_1 = -1.5385 - j2.3077A$, $I_2 = 0.7692 + j6.1538A$, $I_3 = 0.7692 - j3.8462A$. The complex power *consumed* by each branch is shown in the Table 1.1.

Due to the direction of the current in the circuit diagram in Fig. 1.6 the complex power for the voltage source in Table 1.1 is the consumed power. From Table 1.1 it is clear that all the real powers add up to be zero and so do the reactive powers. We say Z_1 and Z_3 consume positive reactive power and Z_2 consumes negative reactive power.

1.2.2 Real and Reactive Power Balance

Figure 1.7 is a representation of a transmission system. The active power sources are represented as current sources and impedances represent transmission lines and loads.

Let $V_N = \begin{bmatrix} V_1 & V_2 & V_3 & 0 \end{bmatrix}$, $I_B = \begin{bmatrix} I_1 & I_2 & I_3 & I_4 & I_5 \end{bmatrix}^T$ and $I_S = \begin{bmatrix} I_{s1} & 0 & I_{s2} & -I_{s1} & -I_{s2} \end{bmatrix}^T$. Using KCL we can write:

$$
\begin{bmatrix}
-1 & 1 & 0 & 0 & 0 \\
0 & -1 & -1 & 1 & 0 \\
0 & 0 & 0 & -1 & -1 \\
1 & 0 & 1 & 0 & 1
\end{bmatrix}
\begin{bmatrix}
I_1 \\ I_2 \\ I_3 \\ I_4 \\ I_5
\end{bmatrix}
=
\begin{bmatrix}
I_{s1} \\ 0 \\ I_{s2} \\ -I_{s1} - I_{s2}
\end{bmatrix}
$$

Let the matrix above be represented by B (known as the directed incidence matrix) then we have:

$$V_N B I_B^* = V_N I_S^* \tag{1.6}$$

In the above Eq. (1.6) all the real and reactive powers on the left-hand-side are calculated according to the load convention and on the right-hand-side using the generator convention. It can be seen that the left-hand-side of the above equation is the sum of complex power absorbed by each branch and the right-hand-side is the sum of complex power supplied by all the sources. In other words the sum of real and reactive powers across all the loads is equal to the sum of real and reactive power supplied by the sources.

The above analysis has been done for a simple system and it is not too difficult to realise that the proof for real and reactive power balance will hold good for all transmission networks. This analysis shows that one can consider reactive power in a similar way as one thinks of real power. It is common sense that the generated and consumed real powers have to be equal and one can think similarly about reactive power balance. By considering KCL at one node at a time, it can be proved that
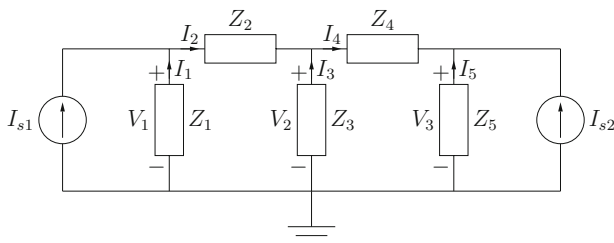
Fig. 1.7 A simple network
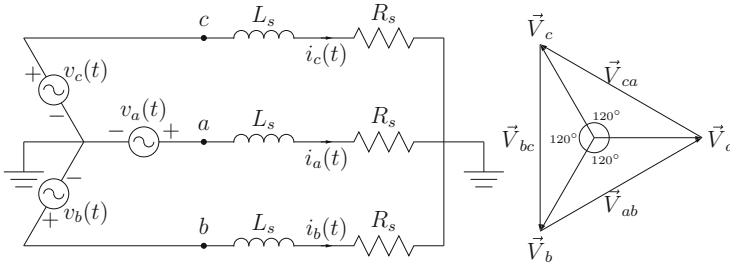
Fig. 1.8 A three-phase star-star connection

the total ingoing and outgoing complex power at every node is equal. This can be easily demonstrated for one the leftmost node in Fig. 1.7; the KCL for the node can be written as:

$$\frac{V_1}{Z_1} + \frac{V_1 - V_2}{Z_2} = I_{s_1} \tag{1.7}$$

Multiplying the complex conjugate of Eq. (1.7) by V_1, we get

$$V_1 \frac{V_1^*}{Z_1^*} + V_1 \frac{V_1^* - V_2^*}{Z_2^*} = V_1 I_{s_1}^* \tag{1.8}$$

In Eq. (1.8), the first term on the left-hand-side is the complex power going down, the second term is the power going to the right, and the term on the right-hand-side is the complex power supplied by the current source.

These ideas form the basis of understanding the operation of power systems. Next we introduce the basic power system analysis called load flow or power flow analysis.

1.3 Load Flow Analysis

In circuit analysis source voltages or current and load impedances are known but in load flow analysis generator power and load power is specified and so the name is changed from circuit analysis to load flow. This does not change the way we formulate the problem but it needs different solution methods. It is common to have a single-line representation of three-phase power systems for load flow analysis. The single-line representation simplifies the analysis greatly for balanced three-phase systems. First let us look at the process for obtaining a single-line representation of a balanced three-phase system.

1.3.1 Three-Phase to Single-Line Diagram

For a balanced three-phase system, shown in Figs. 1.8 and 1.9, $v_a = V_m \sin \omega t$; $v_b = V_m \sin(\omega t - \frac{2\pi}{3})$; $v_c = V_m \sin(\omega t + \frac{2\pi}{3})$. In addition to the line voltages v_a, v_b, and v_c, phase voltages are defined as $v_{ab}(t) = v_a(t) - v_b(t)$, $v_{bc}(t) = v_b(t) - v_c(t)$, and $v_{ca}(t) = v_c(t) - v_a(t)$. The phasor representation of these line ($\vec{V}_a$, $\vec{V}_b$, $\vec{V}_c$) and phase voltages ($\vec{V}_{ab}$, $\vec{V}_{bc}$, $\vec{V}_{ca}$) is shown in Fig. 1.8. From the vector diagram in Fig. 1.8 we can write, line voltage magnitude, $V_L = V_a = V_b = V_c$ and phase voltage magnitude is, $V_P = \sqrt{3}V_L = V_{ab} = V_{bc} = V_{ca}$. Similarly it can be seen that for the delta-connected load in Fig. 1.9, $i_a(t) = i_{ab}(t) - i_{ca}(t)$, $i_b(t) = i_{bc}(t) - i_{ab}(t)$, and $i_c(t) = i_{ca}(t) - i_{bc}(t)$ and $I_L = \sqrt{3}I_P = I_a = I_b = I_c$, where $I_P = I_{ab} = I_{bc} = I_{ca}$.

All the transmission and distribution systems without exception are three-phase networks as shown in Figs. 1.8 and 1.9. For balanced three-phase circuits the three-phase analysis can be replaced by a single-phase analysis and thus the most common representation of power systems is using single-line diagrams. This transformation from a three-phase to a single-line representation is achieved in the following way. Using KVL for each leg of the balanced three-phase circuit of Fig. 1.8, we can write the phasor equations as:

$$\begin{bmatrix} \vec{V}_a \\ \vec{V}_b \\ \vec{V}_c \end{bmatrix} = \begin{bmatrix} R_s + J\omega L_s & J\omega L_M & J\omega L_M \\ J\omega L_M & R_s + J\omega L_s & J\omega L_M \\ J\omega L_M & J\omega L_M & R_s + J\omega L_s \end{bmatrix} \begin{bmatrix} \vec{I}_a \\ \vec{I}_b \\ \vec{I}_c \end{bmatrix} \tag{1.9}$$

where L_M is the mutual inductance among the three inductors. For a balanced three phase system $\vec{I}_b = \vec{I}_a e^{-J\frac{2\pi}{3}}$ and $\vec{I}_c = \vec{I}_a e^{J\frac{2\pi}{3}}$. As $\vec{I}_b + \vec{I}_c = -\vec{I}_a$, we can write the coupled simultaneous equations in (1.9) as three decoupled equations:

$$\vec{V}_a = R_s \vec{I}_a + J\omega(L_s - L_M)\vec{I}_a$$
$$\vec{V}_b = R_s \vec{I}_b + J\omega(L_s - L_M)\vec{I}_b$$
$$\vec{V}_c = R_s \vec{I}_c + J\omega(L_s - L_M)\vec{I}_c$$
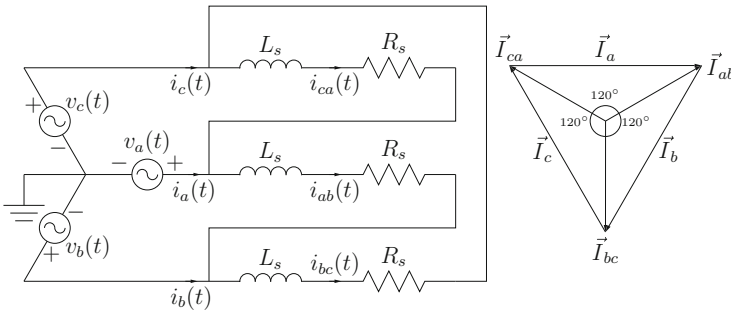
Fig. 1.9 A three-phase star-delta connection

The decoupling of the equations for three-phase balanced networks is the reason why only a single-line diagram is used to represent the system where the equivalent inductance of the transmission lines is given as $L_s - L_M$.

1.3.2 Circuit Analysis Versus Power Systems Analysis

Circuit analysis is simple and most engineers and scientists are familiar with it. One needs to realise that power system analysis is circuit analysis for power transmission networks. In conventional circuit analysis all the elements are either passive components such as resistors, inductors, and capacitors or active components like voltage and current sources. A typical power system, shown in Fig. 1.10, is analysed here as a conventional circuit and then typical power systems constraints are added to highlight the differences between circuit and power system analyses.

Using KCL for the circuit in Fig. 1.10, we can write,

$$\text{Ybus} \begin{bmatrix} \vec{V_1} \\ \vec{V_2} \\ \vec{V_3} \\ \vec{V_4} \end{bmatrix} = \begin{bmatrix} \vec{I_1} \\ 0 \\ 0 \\ \vec{I_4} \end{bmatrix}$$

Matrix Ybus for the circuit is given as below:

$$\begin{bmatrix} \sum_{j=2}^{4} y_{1j} & -y_{12} & -y_{13} & -y_{14} \\ -y_{12} & y_{12} + y_{24} + \frac{1}{Z_2} & 0 & -y_{24} \\ -y_{13} & 0 & y_{13} + y_{34} + \frac{1}{Z_3} & -y_{34} \\ -y_{14} & -y_{24} & -y_{34} & \sum_{j=1}^{3} y_{j4} \end{bmatrix}$$

where z_{ij} is the impedance of the transmission line between nodes i and j and the admittance is given by $y_{ij} = \frac{1}{z_{ij}}$.

Fig. 1.10 Four bus circuit
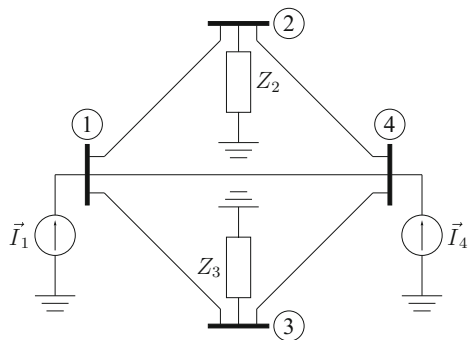
Let the parameters for the four bus example in per units be: $z_t = 0.01 + j0.2$, and $z_t = z_{12} = z_{13} = z_{14} = z_{42} = z_{43}, \vec{I}_1 = \vec{I}_4 = 1, \vec{Z}_2 = 0.9 + j0.275$, and $\vec{Z}_3 = 0.99 + j0.1$.

Solving for bus voltages we get:

$$V bus = \begin{bmatrix} \vec{V}_1 \\ \vec{V}_2 \\ \vec{V}_3 \\ \vec{V}_4 \end{bmatrix} = \begin{bmatrix} 0.9577 + 0.2935j \\ 0.9429 + 0.1922j \\ 0.9626 + 0.1947j \\ 0.9577 + 0.2935j \end{bmatrix}$$

Circuit analysis involves finding the nodal voltages $\vec{V}_1, \ldots, \vec{V}_4$ given $\vec{I}_1$ and $\vec{I}_4$. How is power systems analysis different from circuit analysis? In power systems analysis, the currents $\vec{I}_1$ and $\vec{I}_4$, for the active sources, are not known instead real power generation or voltage magnitude at the node is known. The currents, $\vec{I}_1$ and $\vec{I}_4$, can be written in terms of the known variables and this substitution changes the KCL equations from a set of simultaneous linear equation to a nonlinear set of equations in terms of the new unknown variables. The current sources, like $\vec{I}_1$ and $\vec{I}_4$, are changed to one of the three standard forms depending on the type of the node, i.e., the bus. These three standard forms are discussed next.

1.3.3 Bus Types

Four variables are associated with each node, or a bus, as it is called in power systems analysis. For the ith bus, the variables are P_i, Q_i, V_i, and δ_i. Variables P_i and Q_i are the real and reactive power injected at the bus, respectively; V_i is the bus voltage; I_i is the current injected into the bus; where $\vec{V}_i = V_i e^{J\delta_i}$ and $\vec{I}_i = I_i e^{J(\delta_i + \phi_i)}$. These four variables are related by the following expression for complex power:

$$S_i = P_i + JQ_i = V_i e^{J\delta_i} I_i e^{J(-(\delta_i + \phi_i))} = V_i I_i \cos \phi_i + J V_i I_i \sin \phi_i \qquad (1.10)$$

For any given bus only two of the four variables are known. A bus is characterised by which of the two out of the above four variables are known. The following classification is commonly used in power system analysis:

1. PV bus: P_i and V_i are known
2. PQ bus: P_i and Q_i are known
3. Slack bus: V_i and $\delta_i = 0$ are known

For the nodal analysis, currents through the active sources and impedances of the loads are required. These are obtained using the complex power relationship in (1.10). In particular, $\vec{I}_i$ or Z_i, for each of the three bus types, are obtained as follows ($\phi = \tan^{-1} \frac{Q_i}{P_i}$):

1. PV Bus: known: P_i and V_i, and unknown: ϕ_i (or Q_i) and δ_i

$$\vec{I}_i = \frac{P_i}{V_i \cos \phi_i} e^{J(\delta_i + \phi_i)}$$

2. PQ Bus: known: P_i and Q_i, and unknown: V_i and δ_i

$$Z_i = \frac{V_i^2}{\sqrt{P_i^2 + Q_i^2}} e^{J\phi} \text{ and } \vec{I}_i = \frac{V_i}{Z_i}$$

3. Slack Bus: known: V_i and $\delta_i = 0$, and unknown: ϕ_i (or Q_i) and P_i

$$\vec{I}_i = \frac{P_i}{V_i \cos \phi_i} e^{J\phi_i}$$

The above expressions for $\vec{I}_i$ or Z_i are substituted in the KCL equations which makes the resulting equations nonlinear in the unknown variables. This change to a set of nonlinear equations means that numerical methods have to be used to solve the circuit equations. To see how this works, let us look again at the four-bus system in Fig. 1.10 where Bus 1 is now a PV Bus, $P_1 = 1$ pu and $V_1 = 1$ pu, and Bus 4 is the slack bus with $V_4 = 1$ pu. The KCL system of equations for this four-bus system can now be written as:

$$\text{Ybus} \begin{bmatrix} 1e^{J\delta_1} \\ \vec{V}_2 \\ \vec{V}_3 \\ 1e^{J0} \end{bmatrix} = \begin{bmatrix} \frac{1}{\cos \phi_1} e^{J(\delta_1 + \phi_1)} \\ 0 \\ 0 \\ \vec{I}_4 \end{bmatrix}$$

The above four complex equations give eight equations by equating the real and complex parts of each of the equations. These eight equations can be used to solve for eight variables: $\vec{V}_2$, $\vec{V}_3$, $\vec{I}_4$, δ_1, and ϕ_1. As can be clearly seen that this is a system of nonlinear algebraic equations and we need numerical methods to solve it.

Power Balance Equations In power systems analysis one can start with the KCL nodal equations or have a "power balance" formulation of the KCL as given in Eq. (1.6) which is more convenient for computer solutions.

The power flowing from bus i to bus j, along the transmission line connecting the two buses with impedance $\vec{Z}_{ij}$, is given by:

$$S_{ij} = \vec{V}_i \vec{I}_{ij}^* = \vec{V}_i \frac{\vec{V}_i^* - \vec{V}_j^*}{Z_{ij} e^{-J\theta_{ij}}}$$

At each node the power flows S_{ij} are added up and equated to the power supplied, $S_i = P_i + JQ_i$, and this gives us N power flow equations for an N bus system. Note that at each bus two of the four variables are known and two are unknown and each of the N equations is really two equations, one equating the real part and another the

imaginary part. A single-machine-infinite-bus analysis is given next to familiarise with the basic ideas of the power system analysis.

1.3.4 Single Machine Infinite Bus

A single-machine-infinite-bus (SMIB) system is shown in Fig. 1.11. The system consists of a generator, transmission line, and an infinite bus which represents the grid. In the following analysis we look at real and reactive power flows as a result of varying voltage levels and power injections. An SMIB analysis is used very frequently by experienced power systems engineers to understand what is happening even in complex power systems. A detailed analysis of the SMIB is presented next.

Load-flow Equations The complex power supplied by the generator, G_1, is $\vec{S}_{G_1} = P_{G_1} + JQ_{G_1} = V_1 e^{J\delta_1} \vec{I}_{12}^*$; absorbed by the infinite bus is, $\vec{S}_\infty = P_\infty + JQ_\infty = V_2 e^{J\delta_2}(-\vec{I}_{12}^*)$; and absorbed by the transmission line, is given is, $\vec{S}_Z = \vec{P}_Z + J\vec{Q}_Z = (V_1 e^{J\delta_1} - V_2 e^{J\delta_2})(\vec{I}_{12}^*)$.

The current from the generator to the infinite bus is given as:

$$\vec{I}_{12} = I_{12} e^{J\beta} = \frac{V_1 e^{J\delta_1} - V_2 e^{J\delta_2}}{Z e^{J\theta}} \tag{1.11}$$

where $Z e^{J\theta}$ is the impedance of the transmission line connecting Buses 1 and 2. Substituting for $\vec{I}_{12}$ from (1.11) in the generator complex power expression,

$$P_{G_1} = \frac{1}{Z}\left(V_1^2 \cos\theta - V_1 V_2 \cos(\delta_1 - \delta_2 + \theta)\right) \tag{1.12}$$

$$Q_{G_1} = \frac{1}{Z}\left(V_1^2 \sin\theta - V_1 V_2 \sin(\delta_1 - \delta_2 + \theta)\right) \tag{1.13}$$

$$P_{G_2} = \frac{1}{Z}\left(V_2^2 \cos\theta - V_1 V_2 \cos(\delta_2 - \delta_1 + \theta)\right) \tag{1.14}$$

$$Q_{G_2} = \frac{1}{Z}\left(V_2^2 \sin\theta - V_1 V_2 \sin(\delta_2 - \delta_1 + \theta)\right) \tag{1.15}$$

The above four Eqs. (1.12)–(1.15) are the four power balance equations, two at each bus. Let Bus 1 be a PV bus and Bus 2 be a slack bus, then the SMIB load-flow

Fig. 1.11 Single machine infinite bus–load flow
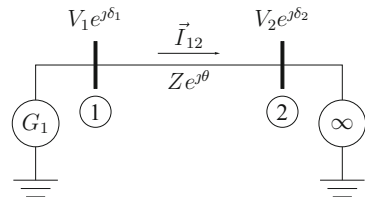
problem has four unknowns, δ_1, Q_{G_1}, P_{G_2}, Q_{G_2}. Let $\delta_{ij} = \delta_i - \delta_j$, then from (1.12), we can write,

$$\delta_{12} = \cos^{-1}\left(\frac{V_1^2 \cos\theta - ZP_{G_1}}{V_1 V_2}\right) - \theta$$

Once δ_1 is known (as δ_2 is reference, we can assume it to be zero.), the other three unknowns are directly calculated from Eqs. (1.13)–(1.15). This completes the load-flow problem for the SMIB system.

Many transmission lines are purely inductive that means the transmission line impedance $\vec{Z} = 0 + _JX \Rightarrow \theta = \frac{\pi}{2}$, putting this in the above we get:

$$P_{G_1} = \frac{V_1 V_2 \sin\delta_{12}}{X} \text{ and } Q_{G_1} = \frac{V_1^2 - V_1 V_2 \cos\delta_{12}}{X}$$

and

$$\delta_{12} = \sin^{-1}\left(\frac{XP_{G_1}}{V_1 V_2}\right).$$

By symmetry or doing the algebra we have:

$$P_{G_2} = \frac{V_1 V_2 \sin\delta_{21}}{X} \text{ and } Q_{G_2} = \frac{V_2^2 - V_1 V_2 \cos\delta_{21}}{X}$$

The power consumed by the purely inductive transmission line ($\theta = \frac{\pi}{2}$) is:

$$P_Z = P_{G_1} + P_{G_2} = \frac{V_1 V_2 \sin\delta_{12}}{X} + \frac{V_1 V_2 \sin\delta_{21}}{X} = 0$$

$$Q_Z = Q_{G_1} + Q_{G_2} = \frac{V_1^2 - V_1 V_2 \cos\delta_{12}}{X} + \frac{V_2^2 - V_1 V_2 \cos\delta_{21}}{X} = \frac{V_1^2 + V_2^2 - 2V_1 V_2 \cos\delta_{12}}{X}$$

Reactive Power Control The SMIB example is a good place to analyse how a variable reactive power supply from generation devices is achieved. The real power output of a generator is equal to the input power (minus the losses) thus the only way to change the output real power of a generator is to change the input mechanical power. As most electrical loads and overhead transmission lines consume reactive power, it is useful to distribute the required reactive power also among the generators indirectly by controlling the generator terminal voltage.

For the SMIB system, Fig. 1.12 shows the variation of the synchronous machine current I_{12} and power factor $\cos\phi$, ($\phi = \beta - \delta_1$), as the field current of the generator, G_1, is changed, i.e., V_1 is changed, when *the output power is constant*. Putting the previous relations together we get:

$$I_{12}^2 = \frac{V_1^2}{X^2} + \frac{V_2^2}{X^2} - \frac{2V_1 V_2 \cos\delta_{12}}{X^2} = \frac{V_1^2}{X^2} + \frac{V_2^2}{X^2} - \frac{2V_1 V_2}{X^2}\sqrt{1 - \left(\frac{P_{G_1}X}{V_1 V_2}\right)^2}$$

(a) Current I_{12} (solid) and Phase difference ϕ (dashed)

(b) Generator Reactive Power (solid) and Power Factor (dashed)
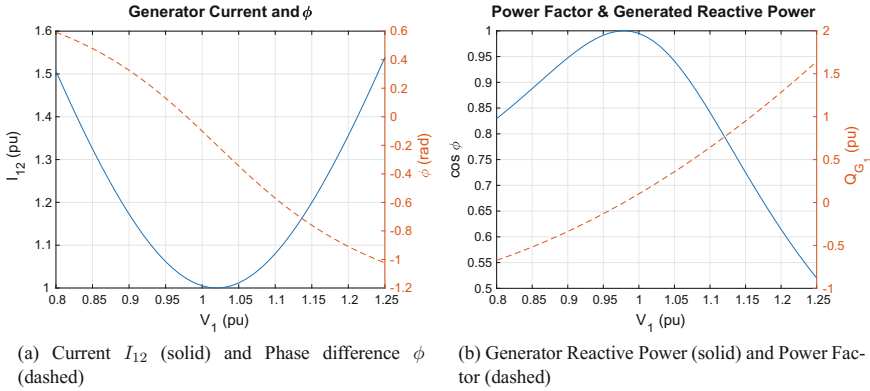
Fig. 1.12 V-curves for an SMIB system

$$\cos \phi = \frac{P_{G_1}}{V_1 I_{12}}$$

Due to the shape of plot of the variation of I_{12} as the generator terminal voltage is changed, seen in Fig. 1.12, the plots are called as V curves. For an SMIB system with $X = 0.2$ pu, $V_2 = 1$ pu, $P_{G_1} = 1$ pu, $\delta_2 = 0$, the V curves are shown in Fig. 1.12. The V curves show the variation of the magnitude of the generator current as the terminal voltage varies as the real power output is held constant. The current magnitude as seen in Fig. 1.12a is a V and the power factor variation seen in Fig. 1.12b is an inverted V. The phase of the current with respect to the terminal voltage is also shown in Fig. 1.12a. It can be seen from Fig. 1.12b that for low terminal voltages the generator absorbs reactive power and for higher terminal voltages it supplies reactive power.

These curves show why synchronous machine is such a popular electricity generation device. The operating characteristics of the synchronous machine enable it to supply or absorb reactive power in a continuous range. It is easy to vary the terminal voltage of the synchronous machine using the field current and by varying the voltage it is possible to supply a load with an arbitrary power factor.

Note that $\left| \vec{I}_{12} \right|^2 = I_{12}^2 = \vec{I}_{12} \vec{I}_{12}^*$ and the reactive power absorbed by the transmission line is:

$$Q_X = \left| \vec{I}_{12} \right|^2 X = I_{12}^2 X = Q_{G_1} + Q_{G_\infty} = \frac{V_1^2 + V_2^2 - 2V_1 V_2 \cos \delta_{12}}{X} \qquad (1.16)$$

From (1.16) it can be seen that for high power transfer, i.e., large $\sin \delta_{12}$, the term $2V_1 V_2 \cos \delta_{12}$ will be small thus the reactive power consumed by the transmission line will increase. For a fixed generator terminal voltage, this increase in the consumption of the reactive power will drop the voltage at the other end. At times this interaction between the need to supply higher real power and associated increase in the reactive power leads to voltage collapse in the grid.

1.3.5   N-Bus System

An N-Bus system is considered in this section. The ideas from the previous sections are put together here to get a general formulation. A simple algorithm to solve the load flow problem is also introduced. Good power system analysis software is available freely and in general there is no need for power system engineers to write their own software routines to solve load flow problems. The educational importance of coding a few load flow algorithm by students cannot be underestimated. We strongly encourage every student to solve a few load flow problems using their own code.

The *i*th bus of an *N*-bus grid is shown in Fig. 1.13. This is a general representation and it is likely that a given bus may not have all the connection or devices attached to it as shown in the figure.

The nodal equations or the KCL equations for the N-bus system with the *i*th Bus shown in Fig. 1.13, can be written as:

$$Ybus\,Vbus = Ibus$$

$$Vbus = \begin{bmatrix} V_1 e^{J\delta_1} \\ \vdots \\ V_i e^{J\delta_i} \\ \vdots \\ V_N e^{J\delta_N} \end{bmatrix} \; ; \quad Ibus = \begin{bmatrix} \vec{I}_1 \\ \vdots \\ \vec{I}_i \\ \vdots \\ \vec{I}_N \end{bmatrix}$$

where $\vec{I}_i = \vec{I}_{G_i} - \vec{I}_{L_i}$

Let the (ij)th element of *Ybus* be $\vec{Y}_{ij} = Y_{ij} e^{J\theta_{ij}}$, then we can write:

$$\vec{I}_{G_i} = \sum_{j=1}^{N} Y_{ij} e^{J\theta_{ij}} V_j e^{J\delta_j} + \vec{I}_{L_i} = \sum_{j=1}^{N} Y_{ij} e^{J\theta_{ij}} V_j e^{J\delta_j} + \frac{P_{L_i} - JQ_{L_i}}{V_i e^{-J\delta_i}} \tag{1.17}$$

Fig. 1.13 The *i*th bus
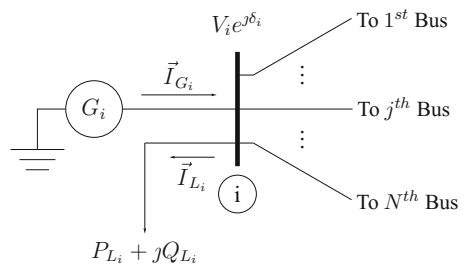
With the expression for the current in (1.17), the complex power supplied by generator G_i can be written as follows:

$$P_{G_i} + JQ_{G_i} = \vec{V}_i\vec{I}_{G_i}^* = V_i e^{J\delta_i} \sum_{j=1}^{N} Y_{ij} e^{-J\theta_{ij}} V_j e^{-J\delta_j} + \frac{V_i e^{J\delta_i}(P_{L_i} + JQ_{L_i})}{V_i e^{J\delta_i}}$$

$$= \sum_{j=1}^{N} V_i V_j Y_{ij} e^{J(\delta_i - \delta_j - \theta_{ij})} + P_{L_i} + JQ_{L_i} \qquad (1.18)$$

$$P_i + JQ_i = \sum_{j=1}^{N} V_i V_j Y_{ij} e^{J(\delta_i - \delta_j - \theta_{ij})}$$

$$= \sum_{j=1}^{N} V_i V_j Y_{ij} \left(\cos(\delta_{ij} - \theta_{ij}) + J \sin(\delta_{ij} - \theta_{ij}) \right) \qquad (1.19)$$

where: $P_i + JQ_i = P_{G_i} + JQ_{G_i} - P_{L_i} - JQ_{L_i}$.

From (1.19), for each node, $i = 1, \ldots, N$, we have

$$P_i = \sum_{j=1}^{N} V_i V_j Y_{ij} \cos(\delta_{ij} - \theta_{ij}); \quad Q_i = \sum_{j=1}^{N} V_i V_j Y_{ij} \sin(\delta_{ij} - \theta_{ij}) \qquad (1.20)$$

The above set of $2N$ Eq. (1.20) are used in most load flow programs. These $2N$ equations are solved for $2N$ unknowns. Please note that for each bus there are four variables P_i, Q_i, V_i, and V_i; in a typical power flow problem two are known and two are unknown.

There is an alternative load flow formulation to the one in (1.20) that is popular for simple but very powerful Gauss-Seidel methods and their variations. Noting that

$$\vec{S}_i = \vec{V}_i\vec{I}_i^* \Rightarrow \vec{I}_i = \frac{\vec{S}_i^*}{\vec{V}_i^*} = \frac{P_i - JQ_i}{V_i e^{-J\delta_i}},$$

the nodal or KCL equations given below is an alternative load-flow formulation:

$$\begin{bmatrix} \vec{Y}_{11} & \ldots & \vec{Y}_{1i} & \ldots & \vec{Y}_{1N} \\ \vdots & \ldots & \vdots & \ldots & \vdots \\ \vec{Y}_{i1} & \ldots & \vec{Y}_{ii} & \ldots & \vec{Y}_{iN} \\ \vdots & \ldots & \vdots & \ldots & \vdots \\ \vec{Y}_{N1} & \ldots & \vec{Y}_{Ni} & \ldots & \vec{Y}_{NN} \end{bmatrix} \begin{bmatrix} \vec{V}_1 \\ \vdots \\ \vec{V}_i \\ \vdots \\ \vec{V}_N \end{bmatrix} = \begin{bmatrix} \frac{P_1 - JQ_1}{\vec{V}_1^*} \\ \vdots \\ \frac{P_i - JQ_i}{\vec{V}_i^*} \\ \vdots \\ \frac{P_N - JQ_N}{\vec{V}_N^*} \end{bmatrix}$$

The Gauss-Seidel algorithms work like this:

1. For all unknown $\vec{V}_i$, $i = 1, \ldots, N$, supply initial guesses; most common guesses are $V_i = 1$ pu and $\delta_i = 0$.
2. Calculate $P_i - jQ_i$, $i = 1, \ldots, N$, using (1.20).
3. Obtain updated values of $\vec{V}_i$, $i = 1, \ldots, N$

$$\vec{V}_i \leftarrow \frac{1}{\vec{Y}_{ii}} \left(-\sum_{\substack{j=1 \\ j \neq i}}^{N} \vec{Y}_{ij} \vec{V}_j + \frac{P_i - jQ_i}{\vec{V}_i^*} \right)$$

4. Iterate over Steps 2 and 3 above till there is a convergence in the values of $\vec{V}_i$, $i = 1, \ldots, N$.

A Three-Bus Example Figure 1.14 is a one-line diagram of a three-bus system. The impedance of the lines connecting nodes i and j is given by $\vec{Z}_{ij} = 0.01 + j0.2$ pu, i.e., all the transmission lines have the same impedance.

1. Bus 1 is a PV bus, i.e., a generator bus: $P_{G_1} = 1$ pu and $V_1 = 1$ pu; Q_1 and δ_1 are unknown.
2. Bus 2 is a slack bus: $V_2 = 1$ pu and $\delta_2 = 0°$; P_2 and Q_2 are unknown.
3. Bus 3 is a PQ bus, i.e., a load bus: $P_{L_3} = 0.5$ pu and $Q_{L_3} = 0.1$ pu; V_3 and δ_3 are unknown.

All the values are expressed in per unit with $P_b = 100$ MW and $V_b = 138$ kV.

The nodal equations or the KCL for the above three-bus system can be written as:

$$\begin{bmatrix} \frac{1}{\vec{Z}_{12}} + \frac{1}{\vec{Z}_{13}} & -\frac{1}{\vec{Z}_{12}} & -\frac{1}{\vec{Z}_{13}} \\ -\frac{1}{\vec{Z}_{12}} & \frac{1}{\vec{Z}_{12}} + \frac{1}{\vec{Z}_{23}} & -\frac{1}{\vec{Z}_{23}} \\ -\frac{1}{\vec{Z}_{13}} & -\frac{1}{\vec{Z}_{23}} & \frac{1}{\vec{Z}_{13}} + \frac{1}{\vec{Z}_{23}} \end{bmatrix} \begin{bmatrix} \vec{V}_1 \\ \vec{V}_2 \\ \vec{V}_3 \end{bmatrix} = \begin{bmatrix} \frac{P_1 - jQ_1}{\vec{V}_1^*} \\ \frac{P_2 - jQ_2}{\vec{V}_2^*} \\ \frac{P_3 - jQ_3}{\vec{V}_3^*} \end{bmatrix}$$

Fig. 1.14 Three bus system
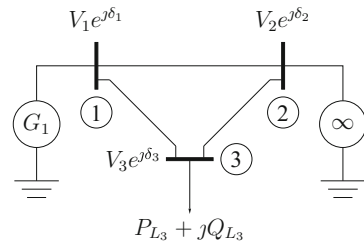
A simple Matlab script to solve the three bus system using Gauss-Seidel algorithm is given below.

```
clear all
j=sqrt(-1);
zt = 0.01 + j*0.2;
yt = 1/zt;
Ybus = [yt+yt -yt -yt; ...
        -yt yt+yt -yt; ...
        -yt -yt yt+yt];
%rectangular to polar form
vec = @(m,ph) m*(cos(ph) + j*sin(ph));
%Known values
pg1 = 1.0; %generator 1 set generation
mV(1) = 1;mV(2) = 1;delta(2) = 0;P(1) = pg1;P(3) = -0.5;Q(3) = -0.1;
%Initial guesses
delta(1) = 0; mV(3) = 1; delta(3) = 0;
%build V
for k = 1:3
    V(k) = vec(mV(k),delta(k));
end;
%Main loop
for m = 1:10
    %calculate bus powers
    V(1) = vec(1,angle(V(1))); %magnitude of V(1) is always 1.
    for k = 1:2 %We calculate powers for buses 1 and 2 only because bus 3 is a load bus
        P(k) = 0; Q(k) = 0;
        for l = 1:3
            P(k) = P(k) + real(V(k)*V(l)'*Ybus(k,l)');
            Q(k) = Q(k) + imag(V(k)*V(l)'*Ybus(k,l)');
        end;
    end;
    P(1) = pg1; %bus 1 is a PV bus
    V(1) = (1/Ybus(1,1))*(-Ybus(1,2)*V(2) - Ybus(1,3)*V(3) + ...
                (P(1) - j*Q(1))/V(1)');
    V(3) = (1/Ybus(3,3))*(-Ybus(1,3)*V(1) - Ybus(2,3)*V(2) + ...
                (P(3) - j*Q(3))/V(3)');
end;
```

The values of the variables as the iteration progresses are shown in Table 1.2. It can be seen that the convergence is a bit slow.

In this three-bus example the current at the load bus (Bus 3), $\vec{I}_3 = I_3 e^{J(\delta_3 + \phi_3)}$ is obtained from the given complex power as follows:

$$P_{L_3} + JQ_{L_3} = V_3 e^{J\delta_3} I_3 e^{-J(\delta_3 + \phi_3)} = V_3 I_3 e^{-J\phi_3} \Rightarrow I_3 e^{J\phi_3} = \frac{P_{L_3} - JQ_{L_3}}{V_3}$$

Frequently the load (such as connected to Bus 3) is represented as a constant impedance load. This can be done as follows by making an assumption that the bus voltage (in this case V_3) doesn't change much:

$$\vec{Z}_3 = \frac{V_3 e^{J\delta_3}}{I_3 e^{J(\delta_3 + \phi_3)}} = \frac{V_3}{I_3 e^{J\phi_3}} = \frac{V_3^2}{P_{L_3} - JQ_{L_3}}$$

Table 1.2 Gauss-Seidel algorithm iterations

Iteration	V_1	V_3	P_{L_2}	Q_{L_2}
1	1.010	0.999	0.000	0.000
2	0.999	0.992	−0.343	0.049
3	1.000	0.992	−0.235	0.073
4	1.000	0.992	−0.206	0.071
5	1.000	0.992	−0.197	0.071
6	1.000	0.992	−0.195	0.070
7	1.000	0.992	−0.195	0.070
8	1.000	0.992	−0.194	0.070
9	1.000	0.992	−0.194	0.070
10	1.000	0.992	−0.194	0.070

1.4   Magnetic Circuits and Inductance

To have a feel for the synchronous machine model, a little understanding of the
magnetic circuit in the synchronous machine is essential. Magnetic circuit analysis
is analogous to electrical circuit analysis where magnetic flux is calculated instead
of currents and voltages. Current through an electrical coil generates a magnetic
field and it is expressed in terms of magnetic field strength, H, with the units of
$A\,m^{-1}$. The inductance of the coil is a property of an electrical coil that is based
on the size of the magnetic flux created by a given magnetic field strength. Here a
basic technique to analyse magnetic circuits is presented. This technique is sufficient
to understand leakage flux, mutual flux, and the related terms leakage and mutual
inductances for transformers and synchronous machines. The basic tool used here is
Ampère's Circuital Law that relates magnetic field strength, H, to the current in the
coil. Magnetic flux density, B, magnetic flux, ϕ, and induced voltages can be easily
derived once the magnetic field strength, H, is known.

1.4.1   An Inductor

Inductance of a coil, such as the one shown in Fig. 1.15, can be obtained using the
following steps.

1. The first step is to calculate the magnetic field strength or intensity, H, which has
   the units of $A\,m^{-1}$. The intensity, $H(l)$, is a vector quantity and it is a function
   of position, l, in the coil.

Fig. 1.15 An inductive coil
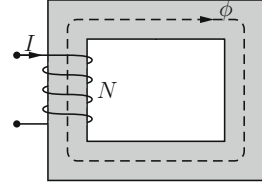
2. Magnetic field intensity, $H(l)$, is a vector quantity with a direction. The direction of $H(l)$ through a coil is obtained using the right-hand rule. To apply this rule, wrap the fingers of the right-hand along the flow of the current and then the direction of the thumb gives the direction of $H(l)$.
3. Ampère's Circuital Law, $\oint H(l) \cdot dl = NI$, is used to obtain H. The path integral is taken along a closed contour. The contour is divided into several segments such that the value of $H(l)$ is constant along each of those segments and then the integral is simply the sum of the length of the segment times the constant value of H along that segment. A contour satisfying this assumption is shown in Fig. 1.15. The right-hand-side, NI, is the total current that is enclosed by the contour. It is NI for the contour chosen in Fig. 1.15 but it can be different depending on the shape of the coil.
4. Next the intensity, H, is related to the flux density, B, which has the units of T (Tesla) which stands for $N s C^{-1} m^{-1}$. Flux density, $B = \mu H$, where μ is the permeability of the magnetic material; B and H are also related by the hysteresis curve for many magnetic materials. The vacuum permeability, known as μ_0, is $4\pi 10^{-7} V s A^{-1} m^{-1}$.
5. The flux, $\phi = BA$, where A is the area of cross-section through which the flux passes, has the units of flux are Wb (Webers). In general there will be multiple paths along which the magnetic flux flows and a calculation of the total flux must consider all the paths. In most problems multiple symmetrical paths can be identified from the geometry of the device.
6. Finally, the coil inductance is given as $L = \dfrac{\text{Total flux linkage}}{\text{Applied current}}$. For the coil in Fig. 1.15 this will be $L = \frac{N\phi}{I}$.
7. Symbol λ is used to denote the total flux linkages in an N turn coil and it is calculated as:

$$\lambda = \sum_{j=1}^{N} \phi_j$$

where flux ϕ_j goes through the jth turn. For the coil in Fig. 1.15 we have the same flux through every turn of the coil $\phi = \phi_i$, $i = 1, \ldots, N$ and $\lambda = N\phi$.
8. In an electrical system with n coils the inductances are defined as:

$$L_{kj} = \frac{\lambda_{kj}}{i_k}$$

Fig. 1.16 Magnetic circuit
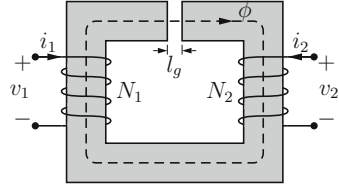
where λ_{kj} are the flux linkages in coil j due to current in coil k; when $k = j$ it is called self-inductance and when $k \neq j$ it is called mutual-inductance.

9. In a system of multiple coils if flux due to current in coil k links only the turns in coil k and no other coil then that flux is called the leakage flux and the inductance due to that flux is called leakage inductance.

The next example illustrates the method detailed above.

Example Two coils with turns $N_1 = 100$ and $N_2 = 1000$ are wound around an iron core with an air-gap of $l_g = 1$ mm. The flux path in the iron core has a length of $l_c = 10$ cm and the cross-section area of the core is $A_c = 1$ cm^{-2}. The relative permeability of the iron core is $\mu_r = 2000$ and $\mu_0 = 4\pi 10^{-7}$ V s A^{-1} m^{-1}. Find the self and the mutual inductance of both the coils.

A closed contour is shown with dashed lines in Fig. 1.16. Two segments can be clearly identified in the closed contour, one in the core and another in the air-gap. The magnetic intensity H is constant along each of those segments. Now, applying Ampère's Circuital Law, we get,

$$N_1 i_1 + N_1 i_1 = \oint H(l) \cdot dl$$
$$= H_c l_c + H_g l_g$$
$$= \frac{B_c}{\mu_r \mu_0} l_c + \frac{B_g}{\mu_0} l_g$$

where H_c (B_c) and H_g (B_g) are the magnetic intensity (flux density) in the core and the air-gap, respectively.

To obtain the self-induction of coil with N_1 turns, we set $I_2 = 0$, and obtain,

$$N_1 i_1 = \frac{\phi}{\mu_r \mu_0 A_c} l_c + \frac{\phi}{\mu_0 A_g} l_g$$

where $\phi = B_c A_c = B_g A_g$ is the flux that goes through the core and the air-gap. Flux is analogous to current in an electrical circuit and as the same current flows through a series circuit so the same flux flows through a series magnetic circuit. In this example it is assumed that there is no leakage flux and the cross-section area of the air-gap is the same as the core.

Analogous to resistance, a term reluctance is defined for magnetic circuits as, $\mathcal{R} = \frac{l}{\mu A}$. For this example, we define, $\mathcal{R}_c = \frac{l_c}{\mu_0 \mu_r A_c}$, and $\mathcal{R}_g = \frac{l_g}{\mu_0 A_g}$, and we get,

$$L_1 = \frac{N_1 \phi}{i_1} = \frac{N_1^2}{\mathcal{R}_c + \mathcal{R}_g}$$

Similarly

$$L_2 = \frac{N_2^2}{\mathcal{R}_c + \mathcal{R}_g} \text{ and } L_{12} = \frac{N_1 N_2}{\mathcal{R}_c + \mathcal{R}_g}$$

The numerical values for this example are: $L_1 = 0.0012\,\text{H}, L_2 = 0.1197\,\text{H}$, and $L_{12} = 0.0120\,\text{H}$.

1.4.2   Rotating Machine

The process discussed above to obtain inductance of coils can be used to obtain inductances of the coils that make up a synchronous machine. The machine in Fig. 1.17 has a salient pole rotor and a stator, with coils on both the rotor and stator. The coil on the rotor is often called the field coil. The stator coil is represented as a single turn coil in Fig. 1.17 but it is distributed sinusoidally in space along the stator. In the following, field coil leakage inductance, field coil self inductance, and the mutual inductance between the field and stator coils will be obtained.

Each coil in synchronous machine has flux linkages due to current in the coil itself and also due to currents in other coils. The flux linkages due to the current in the coil itself and the resulting inductance is called self-inductance and due to the currents in other coils is called mutual inductance. In the following we discuss the essentials of self and mutual inductance of the coils in synchronous machines.

Self-Inductance The first step in calculating coil inductances is to mark the multiple paths taken by the magnetic flux generated due to the current in the coils. In Fig. 1.17 four paths are shown for the flux due to rotor coil current. Flux ϕ_l is the leakage flux that only links the field coil and not the stator coil and flux ϕ_m links both the coils. The leakage and mutual flux follow two symmetrical paths, one above and

Fig. 1.17 Rotor and armature coils
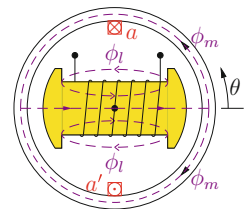
another below the horizontal line of symmetry and the total flux through the rotor is:
$\phi = 2\phi_l + 2\phi_m$.

Leakage Flux—ϕ_l Using Ampère's Law ($\oint H \cdot dl = NI$) we get,

$$H_{l_1}l_1 + H_{l_a}l_a = N_f i_f$$

$$\frac{B_{l_1}}{\mu_1\mu_0}l_1 + \frac{B_{l_a}}{\mu_0}l_a = N_f i_f$$

$$\frac{\phi_l}{\mu_1\mu_0 A_{l_1}}l_1 + \frac{\phi_l}{\mu_0 A_{l_a}}l_a = N_f i_f$$

where subscript '1' refers to rotor and 'a' to the air parameters.

Mutual Flux—ϕ_m Using Ampère's Law ($\oint H \cdot dl = NI$) we get,

$$H_{l_r}l_r + H_{l_g}l_g + H_{l_s}l_s = N_f i_f$$

$$\frac{B_{l_r}}{\mu_r\mu_0}l_r + \frac{B_{l_g}}{\mu_0}l_g + \frac{B_{l_s}}{\mu_s\mu_0}l_s = N_f i_f$$

$$\frac{\phi_m}{\mu_r\mu_0 A_{l_r}}l_r + \frac{\phi_m}{\mu_0 A_{l_g}}l_g + \frac{\phi_m}{\mu_s\mu_0 A_{l_s}}l_s = N_f i_f$$

where subscript 'r' refers to rotor, 'g' to the air-gap and 's' to stator.

Introduction of a term called reluctance that is analogous to resistance in electrical circuits simplifies the above expressions. Reluctance and a few other commonly used terms are defined below.

1. Reluctance $\mathcal{R} = \dfrac{l}{\mu A}$
2. Flux linkages $\lambda = N\phi$
3. Inductance $L = \dfrac{\lambda}{i}$
4. Induced Voltage $e = -\dfrac{d\lambda}{dt} = -\dfrac{d(Li)}{dt}$

With the above definitions we can write:

$$\phi_l = \frac{N_f i_f}{\mathcal{R}_1 + \mathcal{R}_a} \text{ and } \phi_m = \frac{N_f i_f}{\mathcal{R}_r + \mathcal{R}_g + \mathcal{R}_s}$$

$$\lambda_l = \frac{N_f^2 i_f}{\mathcal{R}_1 + \mathcal{R}_a} \text{ and } \lambda_m = \frac{N_f^2 i_f}{\mathcal{R}_r + \mathcal{R}_g + \mathcal{R}_s}$$

$$L_l = \frac{N_f^2}{\mathcal{R}_1 + \mathcal{R}_a} \text{ and } L_m = \frac{N_f^2}{\mathcal{R}_r + \mathcal{R}_g + \mathcal{R}_s}; \ \phi_{ff} = \phi_l + \phi_m \text{ and } L_{ff} = L_l + L_m$$

where L_l is the leakage inductance and L_{ff} is the self-inductance of the field coil.
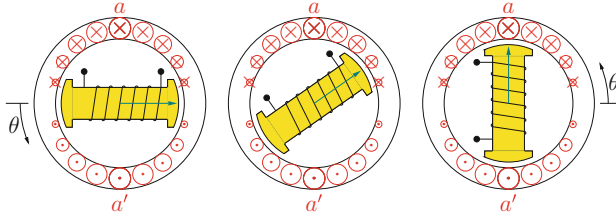
Fig. 1.18 Rotating field coil

Fig. 1.19 Total flux linkage
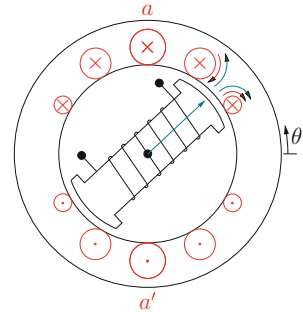
Given the geometry of the machine, the parameters of the magnetic material, and number of turns of the coil, the field coil inductance can be obtained. For practical purposes these inductances are found by performing actual measurements on the field coil. The important thing to note from the above derived expressions for leakage and self induction of the field coil is that since $\mathcal{R}_1 + \mathcal{R}_a >> \mathcal{R}_r + \mathcal{R}_g + \mathcal{R}_s$, the leakage inductance is much smaller than the self inductance and that the self-inductance does not change with the position of the rotor.

Mutual Inductance

Next the mutual inductance between the field and stator coils is derived. As mentioned previously the stator coil is sinusoidally distributed along the stator of the synchronous machine as shown in Fig. 1.18. The stator coils run along the length of the machine and loop back from the front and back of the machine. The standard notation is that $\otimes$ represents current going into the coil and $\odot$ represents current coming out of the coil. Figure 1.18 also shows three different rotor positions. The rotor angle θ increases as the rotor rotates in the anti-clockwise direction.

The aa' windings on the stator are distributed such that at θ the winding density is $\frac{N}{2}\sin\theta$. The total number of windings are:

$$\int_0^\pi \frac{N}{2}\sin\theta\, d\theta = \left[-\frac{N}{2}\cos\theta\right]_0^\pi = N$$

The flux linkage between the rotor and stator coils depends on the angular position of the rotor. Figure 1.19 shows how the rotor flux links the stator coils.

The field flux links all the coils but it links positively with the coils on the left and negatively with the coils on right. In Fig. 1.19, current going into the stator coil generates flux in the clockwise direction (flux line right next to the $\otimes$ coil) and the rotor flux going left after it enters the stator is in the anti-clockwise direction for the $\otimes$ coil. This rotor flux induces current in the stator coil that is in the same direction as the coil current, i.e., into the coil due to the Lenz's law. Similar reasoning shows that the rotor flux that travels after turning right in the stator links negatively with the stator coils.

The stator coil density at θ is $\frac{N}{2} \sin \theta$ and the number of coils linking the rotor flux when it is at θ is obtained as:

$$\int_{\theta}^{\pi} \frac{N}{2} \sin \theta \, d\theta - \int_{0}^{\theta} \frac{N}{2} \sin \theta \, d\theta = N \cos \theta$$

The total number of turns of the coil that link with the field flux when rotor is at θ is given by $N \cos \theta$. Thus the rotor flux linking the stator coils is proportional to $N \cos \theta$. This gives,

$$\phi_{fa} = \phi_m \text{ and } L_{fa}(\theta) = \phi_m N_a \cos \theta$$

where L_{fa} is the mutual impedance between the field coil and the aa' stator coil. Finally, the emf induced in coil aa' is proportional to the rate of change of the flux through the coil and so we write (where ω is the angular velocity of the rotor):

$$v_a(t) = V_m \sin \theta = V_m \sin \omega t$$

1.5 Electromechanical Energy Conversion

In this section energy conversion in electromechanical systems using electromagnetic coupling field, i.e., inductances, is discussed. The starting point to analyse the electromechanical energy conversion problem is the energy balance equation,

Field Energy (W_f) = Supplied Electrical Energy (W_e) + Supplied Mechanical Energy (W_m).

In the analysis of electromechanical systems we start with the system operating in equilibrium and then derive the dynamic equations for the changes from the equilibrium in the energies in the system from the following expression:

$$d W_f(i, x) = d W_e(i, x) + d W_m(i, x). \tag{1.21}$$

For a system with n electrical coils with currents, $i_1, i_2, \ldots, i_n$, and m mechanical parts with displacements, $x_1, x_2, \ldots, x_m$, Eq. (1.21) can be written as:

$$\sum_{j=1}^{n} \frac{\partial W_f(i,x)}{\partial i_j} di_j + \sum_{k=1}^{m} \frac{\partial W_f(i,x)}{\partial x_k} dx_k = \sum_{j=1}^{n} \frac{\partial W_e(i,x)}{\partial i_j} di_j + \sum_{k=1}^{m} \frac{\partial W_e(i,x)}{\partial x_k} dx_k$$

$$+ \sum_{j=1}^{n} \frac{\partial W_m(i,x)}{\partial i_j} di_j + \sum_{k=1}^{m} \frac{\partial W_m(i,x)}{\partial x_k} dx_k$$

$$(1.22)$$

Each of the variation $di_j, j = 1, 2, \ldots, n$ and $dx_k, k = 1, 2, \ldots, m$ are independent and thus $n + m$ Eq. (1.22) can be written as a system of $n + m$ equations by equating the co-efficients of di_j and dx_k in (1.22) as:

$$\frac{\partial W_f(i,x)}{\partial i_j} di_j = \frac{\partial W_e(i,x)}{\partial i_j} di_j + \frac{\partial W_m(i,x)}{\partial i_j} di_j, \quad j = 1, 2, \ldots, n \qquad (1.23)$$

$$\frac{\partial W_f(i,x)}{\partial x_k} dx_k = \frac{\partial W_e(i,x)}{\partial x_k} dx_k + \frac{\partial W_m(i,x)}{\partial x_k} dx_k, \quad k = 1, 2, \ldots, m \qquad (1.24)$$

Equations (1.23) and (1.24) are written in terms of coil currents but they can also be written in terms of coil flux linkages $\lambda_j, j = 1, 2, \ldots, n$ and then the system of equations (1.23) and (1.24) is written in terms of $d\lambda_j, j = 1, 2, \ldots, n$.

General Method The following general steps detail how to use the above Eq. (1.21) to obtain dynamic equations for a given electromechanical system.

1. The input electrical energy supplied to a coil with voltage e_f across its terminals is: $W_e = \int e_f i \, dt = \int \frac{d\lambda}{dt} i \, dt = \int i \, d\lambda$, where i is the current through the coil and λ is the total flux linking the coil. For an n-coil system $\lambda_i(\theta_i) = \sum_{j=1}^{n} L_{ij}(\theta_i, \theta_j) i_j$. Thus the change in the supplied electrical energy in a coil is: $dW_e = i \, d\lambda$.
2. In any system the stored electromagnetic field energy is found by calculating the supplied electrical energy while making the extracted (or supplied) mechanical energy zero, i.e., $dx = 0$ or $d\theta = 0$. For a single coil system $W_f = \frac{1}{2} L(\theta) i^2$.
3. For a rotating part the supplied mechanical energy is: $dW_m = -T_e d\theta$ or $dW_m = -f dx$ for linear displacement.
4. Putting all this together for a rotary machine with m coils and one rotating part, we have: $dW_f(i, \theta) = \sum_{j=1}^{m} i_j d\lambda_j(i, \theta) - T_e d\theta$. This gives:

$$\sum_{j=1}^{m} \frac{\partial W_f}{\partial i_j} di_j + \frac{\partial W_f}{\partial \theta} d\theta = \sum_{j=1}^{m} i_j \frac{\partial \lambda_j}{\partial i_j} di_j + \sum_{j=1}^{m} i_j \frac{\partial \lambda_j}{\partial \theta} d\theta - T_e d\theta \qquad (1.25)$$

5. Equating the co-efficients of $d\theta$ in (1.25), we get:

$$T_e = \sum_{j=1}^{m} i_j \frac{\partial \lambda_j(i, \theta)}{\partial \theta} - \frac{\partial W_f}{\partial \theta} \qquad (1.26)$$

The above general method can be used for multiple moving parts as well. For most electrical machines we have only one moving part called the rotor.

1.5.1 Plunger-Spring System

Figure 1.20 shows the schematic of a plunger system. As the current is applied to the coil, it pulls the mass-damper-spring system into the air-gap. There are three different systems in this plunger system: (a) the electrical system with the voltage and current in the coil, (b) the magnetic system that stores magnetic energy in the magnetic core and the air-gap, and (c) the mass-damper-spring mechanical system. The electrical energy is transferred from the coil to the mechanical system via the magnetic field. The analysis problem related to the plunger system in Fig. 1.20 is to find the change in the position x as a function of time after a step voltage is applied to the field. This is a typical electromechanical energy conversion problem.

The plunger in Fig. 1.20 is h deep (into the paper) and the air-gap between the core and the plunger is g. Assuming that the entire flux travels through the plunger (no leakage), it can be shown that for a core with large air-gap the inductance of the coil is given as,

$$L(x) = \frac{N^2 \mu_0 h x}{2g}.$$

A few observations on this plunger problem give a general idea of the electromechanical system analysis. From Eq. (1.21), it can be seen that if the change in the mechanical energy $d W_m(i, x)$ is zero, i.e., if the plunger is held in one position, all the change in the electrical energy will equal the change in field energy. This observation is useful when we calculate the stored field energy as a function of position and current. As the plunger moves into the gap in the core, it induces an emf in the coil which is in addition to the self-induced emf due to the inductance of the coil. Due to this extra emf, the input electrical energy increases (as compared to when the plunger is held in one position), and that extra energy is converted into mechanical energy. As there is an increase in x, mechanical energy is absorbed by the mass-damper-plunger system thus the supplied mechanical energy is $-f dx$.

Let $\lambda(x, i) = L(x)i$ be the total flux linkage of the coil, where $L(x)$ is the coil inductance, and the stored field energy is $\frac{1}{2}L(x)i^2$. Then Eq. (1.21) for the plunger

Fig. 1.20 An electromechanical plunger system
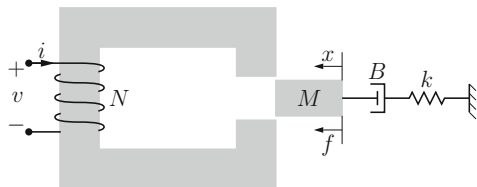
system is:

$$d(\frac{1}{2}L(x)i^2) = id\lambda(x, i) - fdx$$

$$\frac{1}{2}i^2\frac{L(x)}{\partial x}dx + iL(x)di = i^2\frac{L(x)}{\partial x}dx + iL(x)di - fdx$$

Equating the co-efficients of dx, we get

$$\frac{1}{2}i^2\frac{L(x)}{\partial x} = f$$

The electromechanical equation for the system is (R is the coil resistance):

$$Ri + i\frac{\partial L(x)}{\partial x}\frac{dx}{dt} + L(x)\frac{di}{dt} = v \tag{1.27}$$

$$m\frac{d^2x}{dt^2} + B\frac{dx}{dt} + kx = \frac{1}{2}i^2\frac{\partial L(x)}{\partial x} \tag{1.28}$$

Equation (1.27) models the electrical transients and Eq. (1.28) models the mechanical transients. In general the time-constant for electrical transients is much smaller than mechanical transient time-constant.

1.5.2 Rotor-Spring System

The synchronous machine in Fig. 1.21 has a sinusoidally distributed stator winding aa' and a round rotor with field coil ff'. A helical spring connects rotor to a fixed point. The parameters of the system are: $J = 1\,\text{J}\,\text{s}^2, B = 0.2\,\text{J}\,\text{s}, k_s = 0.1\,\text{N}\,\text{m}, L_{aa} = 6\,\text{mH},$ $L_{ff} = 6\,\text{mH}, \hat{L}_{fa} = 5\,\text{mH}, r_f = 1\,\Omega, r_a = 1\,\Omega, v_f = 10\,\text{V},$ and $v_a = 10\,\text{V}$. The mutual inductance between the stator and rotor coils is $L_{fa} = \hat{L}_{fa}\cos\theta$ where θ is the angle between the horizontal line and the magnetic "pole" of the rotor.

DC voltages are applied to the rotor and stator windings at time $t = 0\,\text{s}$. Plot the value of θ with time.

Fig. 1.21 Rotor with a spring
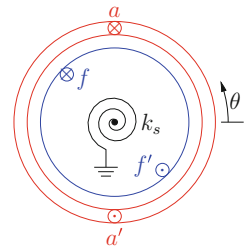
Field energy is the supplied electrical energy with θ constant or $d\theta = 0$. Note that $\lambda_f = i_f L_{ff} + i_a L_{fa}(\theta)$ and $\lambda_a = i_a L_{aa} + i_f L_{fa}(\theta)$.

$$
\begin{aligned}
W_f &= \int i_f\, d\lambda_f + \int i_a\, d\lambda_a \\
&= \int i_f\, d(i_f L_{ff} + i_a L_{fa}(\theta)) + \int i_a\, d(i_a L_{aa} + i_f L_{fa}(\theta)) \\
&= \int i_f\, d(i_f L_{ff}) + \int i_a\, d(i_a L_{aa}) + i_f\, d(i_a L_{fa}(\theta)) \\
&= \frac{1}{2} L_{ff} i_f^2 + i_f i_a L_{fa}(\theta) + \frac{1}{2} L_{aa} i_a^2
\end{aligned}
$$

The integral above is evaluated in two steps. Current i_a is kept constant in the first step and i_f is taken to its final value. In the second step i_f is fixed at its final value and i_a is varied from zero to its final value. The change in electrical energy is:

$$
\begin{aligned}
dW_e &= i_f\, d\lambda_f(i_a, i_f, \theta) + i_a\, d\lambda_a(i_a, i_f, \theta) \\
&= i_f \left(\frac{\partial \lambda_f}{\partial i_f} di_f + \frac{\partial \lambda_f}{\partial i_a} di_a + \frac{\partial \lambda_f}{\partial \theta} d\theta \right) + i_a \left(\frac{\partial \lambda_a}{\partial i_f} di_f + \frac{\partial \lambda_a}{\partial i_a} di_a + \frac{\partial \lambda_a}{\partial \theta} d\theta \right)
\end{aligned}
$$

Using $dW_f(i, \theta) = i\, d\lambda(i, \theta) - T_e d\theta$ and equating co-efficients of $d\theta$, we get

$$
\begin{aligned}
i_f i_a \frac{dL_{fa}(\theta)}{d\theta} &= i_f \frac{\partial \lambda_f}{\partial \theta} + i_a \frac{\partial \lambda_a}{\partial \theta} - T_e \\
&= i_f i_a \frac{dL_{fa}(\theta)}{d\theta} + i_a i_f \frac{dL_{fa}(\theta)}{d\theta} - T_e
\end{aligned}
$$

$$
T_e = i_f i_a \frac{dL_{fa}(\theta)}{d\theta} = -i_f i_a \hat{L}_{fa} \sin\theta
$$

If we want a positive torque as θ increases we can change the direction of the current flow of either i_f or i_a.

The complete system dynamics equations can be written as:

$$
J \frac{d^2\theta}{dt^2} + B \frac{d\theta}{dt} + k_s \theta = T_e
$$

$$
L_{ff} \frac{di_f}{dt} + L_{fa}(\theta) \frac{di_a}{dt} + i_a \frac{dL_{fa}(\theta)}{d\theta} \frac{d\theta}{dt} + R_f i_f = v_f
$$

$$
L_{aa} \frac{di_a}{dt} + L_{fa}(\theta) \frac{di_f}{dt} + i_f \frac{dL_{fa}(\theta)}{d\theta} \frac{d\theta}{dt} + R_a i_a = v_a
$$

Define the states as: $x_1 = \theta$, $x_2 = \frac{d\theta}{dt}$, $x_3 = i_f$, and $x_4 = i_a$ and we have $\frac{dL_{fa}(\theta)}{d\theta}$ $= -\hat{L}_{fa} \sin\theta$.

Fig. 1.22 Rotor position for the spring-machine system
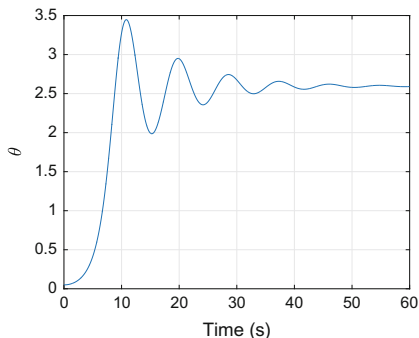
$$\dot{x}_1 = x_2$$

$$\dot{x}_2 = -\frac{1}{J}\left(k_s x_1 + B x_2 + i_f i_a \hat{L}_{fa}\sin\theta\right)$$

$$\text{Let } \mathcal{L} = \begin{bmatrix} L_{ff} & L_{fa}(\theta) \\ L_{fa}(\theta) & L_{aa} \end{bmatrix}$$

$$\text{then } \begin{bmatrix} \dot{x}_3 \\ \dot{x}_4 \end{bmatrix} = [\mathcal{L}]^{-1}\begin{bmatrix} v_f - R_f x_3 + \hat{L}_{fa}x_2 x_4 \sin x_1 \\ v_r - R_r x_4 + \hat{L}_{fa}x_2 x_3 \sin x_1 \end{bmatrix}$$

The step response of the angular position of the rotor due to the rotor and stator voltage steps, $V_f = 10\,\text{V}$, and $V_a = 10\,\text{V}$, is shown in Fig. 1.22. The equilibrium value can be obtained by solving for θ in $k_s x_1 + i_f i_a \hat{L}_{fa}\sin\theta = 0$.

1.6   Rotating Magnetic Field

Nikola Tesla discovered that polyphase stationary coils can generate a rotating magnetic field. His discovery led to the induction machine which does not need energised coils on the rotor. Here we look at how a rotating field is created with three-phase coils.

1. The coil currents are:

$$i_a(t) = I_m \cos(\omega t); \ \ i_b(t) = I_m \cos(\omega t - \frac{2\pi}{3}); \ \ i_c(t) = I_m \cos(\omega t + \frac{2\pi}{3})$$

2. The three stator coils are spatially distributed such that each of them produces a spatially distributed sinusoidal magnetomotive force (mmf) in the air-gap. The spatial location of the maximum value of the mmf due to each coil is shown in Fig. 1.23 as vectors $\hat{F}_a$, $\hat{F}_b$, and $\hat{F}_c$.

Fig. 1.23 Synchronous machine—rotating magnetic field
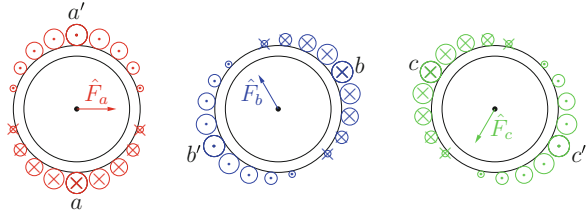
3. For the coil arrangement shown in Fig. 1.23 (θ is wrt the horizontal axis and positive anti-clockwise), the value of the mmf due to each coil as a function of θ is given as:

$$F_a(t, \theta) = \hat{F}_a(t) \cos(\theta); \;\; F_b(t, \theta) = \hat{F}_b(t) \cos(\theta - \frac{2\pi}{3}); \;\; F_c(t, \theta) = \hat{F}_c(t) \cos(\theta + \frac{2\pi}{3})$$

4. The instantaneous peak value of the mmf due to the current in N-turn stator windings is given as:

$$\hat{F}_a(t) = NI_m \cos(\omega t); \;\; \hat{F}_b(t) = NI_m \cos(\omega t - \frac{2\pi}{3}); \;\; \hat{F}_c(t) = NI_m \cos(\omega t + \frac{2\pi}{3})$$

5. The resultant rotating mmf at θ is given as:

$$
\begin{aligned}
F_a(t, \theta) &= NI_m \cos(\omega t)\cos(\theta) + NI_m \cos(\omega t - \frac{2\pi}{3})\cos(\theta - \frac{2\pi}{3}) \\
&\quad + NI_m \cos(\omega t + \frac{2\pi}{3})\cos(\theta + \frac{2\pi}{3}) \\
&= \frac{3}{2}NI_m \cos(\omega t - \theta)
\end{aligned}
$$

6. The resulting mmf, $F_a(t, \theta)$, is sinusoidally distributed as a function of θ and the maximum value of $F(\theta)$, at time t, is at that θ for which $\omega t = \theta$. This means that the mmf is rotating at the rate given by the stator current frequency ω, and thus the number of rotations of the mmf per second are: $\frac{\omega}{2\pi}$.

1.6.1 Synchronous Machine

A three-phase synchronous machine, like most rotating electrical machines, has a rotor and a stator. The rotor has a low resistance and high inductance coil, known as the field coil, energised by a DC current. The rotor itself can have salient poles (Fig. 1.19) or it can be a round rotor (Fig. 1.24). The stator has three sinusoidally distributed coils, each with N turns that are spatially displaced 120° from each other. Each turn of the coil is a pole pitch apart and runs along the length of the coil and loops

Fig. 1.24 Synchronous
machine schematic
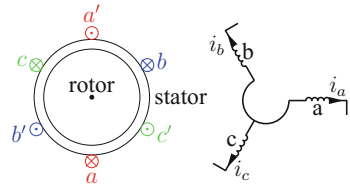
back at both the ends. The pitch of each turn depends on the number of poles on the
rotor. In this book two-pole, i.e., one pole-pair machines are shown in the figures and
analysed. Thermal units normally have two poles and hydro units have ten or higher
number of poles. Figure 1.24 is a schematic of a round rotor two-pole synchronous
machine. The three stator coils, which are shown as 120° displaced lumped coils,
are in reality not lumped but spatially sinusoidally distributed as shown in Fig. 1.23.
When we have multiple pole-pairs the analysis is done for one pole pitch, i.e., 360
electrical degrees. The mechanical rotation, for a P pole machine, is then calculated
using the following formula,

$$360 \text{ mechanical degrees} = \frac{P}{2} \times 360 \text{ electrical degrees.}$$

Principle of Operation Synchronous machine operation is based on an interaction
of two magnetic fields, one due to the rotor field coil and another due to the field
created by the three-phase stator coils. This interaction of the two magnetic fields is
summarised below and it is expanded in Chap. 2.

1. Synchronous machine is made up of a rotating magnetic field (field windings),
   and polyphase (mostly three-phase) stator windings.
2. The three-phase sinusoidal currents in the stator windings create a rotating mag-
   netic field.
3. The rotor spins to prevent emf being induced in the field coils due to the rotating
   field based on Faraday's Law and Lenz's Law.
4. An equilibrium is reached when the rotor speed equals the speed of the rotating
   magnetic field and there is no induced emf in the rotor coil due to the rotating
   magnetic field. This speed is called the synchronous speed.
5. The two fields (the rotating field due to stator and the field due to the rotor rotating
   at the synchronous speed) are not spatially aligned. The rotor field lags or leads
   the stator field depending on if the machine is operating as a generator or a motor.
   The two fields can only be aligned when the machine is running at no load and
   there are no mechanical or electrical losses.

Synchronous Generator: Induced EMF As discussed in Sect. 1.4, the voltage
induced in the sinusoidally stator coils due to the field flux in coil aa' is given
as: $V_m \sin \omega t$, where ω is the angular velocity of the rotor. As the coils bb' and cc'
are spatially displaced by 120° the induced voltage in the two coils will also have a
phase displacement of 120°.
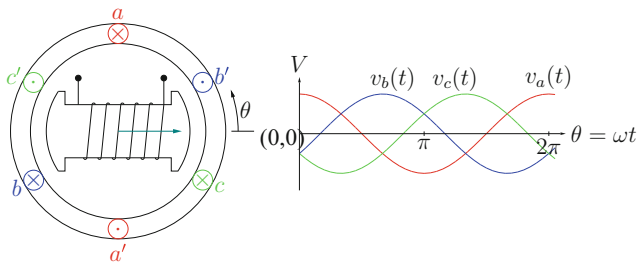
Fig. 1.25 Induced voltages

The induced voltages due to the field coil flux, shown in Fig. 1.25, and for $i_a = i_b = i_c = 0$, are given as:

$$v_a(t) = V_m \cos \omega t$$

$$v_b(t) = V_m \cos(\omega t - \frac{2\pi}{3})$$

$$v_c(t) = V_m \cos(\omega t + \frac{2\pi}{3})$$

Rotor and Stator Field Interaction In a synchronous machine the interaction between the rotor and stator fields, F_r and F_s respectively, shown in Fig. 1.26, is responsible for synchronising the angular velocity of the rotor with the electrical frequency of the current in the stator. For a steady-state operation, the two fields must rotate at the same angular velocity, and thus the following relationship can be obtained between the rotor angular velocity, ω_r, and the supply frequency, ω_s:

$$\omega_r = \frac{\omega_s}{\text{pole pairs on the rotor}} \tag{1.29}$$

For a P pole machine, the machine can be conceptually thought of as $\frac{P}{2}$ "electrical" machines within one mechanical machine. For the purpose of synchronisation the rotor thus moves $\frac{P}{2}$ times slower and yet maintains the synchronisation. Equation (1.29) is often written as:

$$f = \frac{nP}{120} \tag{1.30}$$

where n is the rotor speed in rotations-per-minute and f is the stator supply frequency in Hz.

A few key points about the generator and motor operation, as captured in Fig. 1.26, of the synchronous machine are enumerated below. A full derivation and coverage is provided in the next chapter.

Fig. 1.26 Generator and
motor operations

Generator   Motor
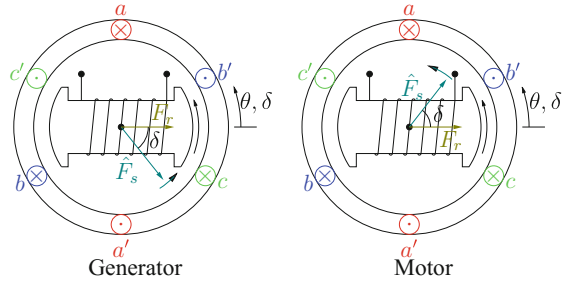
1. The stator coils are connected to the grid. There are two rotating magnetic fluxes, one due to stator currents, $F_s = \hat{F}_s \cos(\omega t - \theta)$, and another due to the field coil, F_r.
2. The interaction between the rotor mmf and the rotating stator mmf due to the stator currents creates synchronous generator and motor actions.
3. If there is no mechanical torque applied to the machine the mmf vectors $\hat{F}_s$ and F_r are aligned.
4. When a mechanical torque is applied to the rotor it will "advance" and F_r will lead $\hat{F}_s$—generator action.
5. When a mechanical torque is applied by the rotor it will "fall back" and F_r will lag $\hat{F}_s$—motor action.
6. The generated real power change results in the change in "δ", also known as the synchronous machine angle.
7. The change in the generated reactive power can be achieved by the change in the magnitude of the generator terminal voltage.

1.6.2 Induction Machine

In a synchronous machine there is a field coil on the rotor but in the induction machine there are coils or no coil on the rotor but in either case the coils are short circuited and not energised. Modern induction machines, called doubly-fed induction machines have energised rotor coils to get extra control capability that is required with wind generators. These advanced machines are discussed in Chap. 2. Here we look at the principle of operation of singly-fed induction machines as shown in Fig. 1.27.

The rotor of the induction machine rotates at an angular velocity, ω_r, which is different from the synchronous speed, ω_s. The three-phase stator coils are connected to a three-phase supply generating a rotating magnetic flux which induces an alternating current of frequency, $\omega_s - \omega_r$, in the rotor coils due to the speed difference between the speed of the rotating magnetic field. This alternating current in the rotor creates a rotating magnetic field at the rotational speed, $\omega_s - \omega_r$, with respect to the rotor. Thus both the magnetic fields, due to the induced rotor currents and the supplied

Fig. 1.27 Induction machine
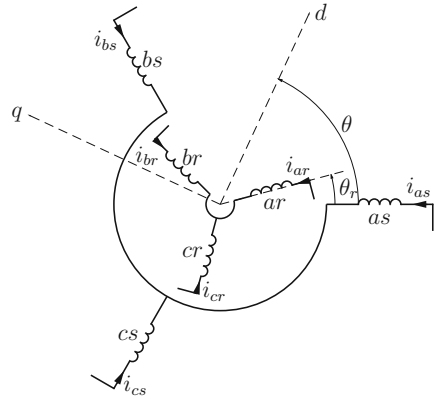
stator currents, rotate at the synchronous speed, ω_s. They are at the same speed but phase displaced, exactly the same way as in a synchronous motor. The magnitude of the induced rotor currents depends on the speed difference, $\omega_s - \omega_r$ and the measure of speed difference is denoted by slip, $s = \frac{\omega_s - \omega_r}{\omega_s}$. A detailed analysis of the dynamics of induction machines is given in Chap. 2.

1.7 Essential Background

1.7.1 Complex Number Algebra

There are multiple ways to write complex numbers (for real x and y):

$$z = x + Jy = re^{J\phi} = r\angle\phi$$

where $|z| = r = \sqrt{x^2 + y^2}$ and $\angle z$ or $\arg z = \phi = \tan^{-1}\frac{y}{x}$, and

$$e^x = 1 + x + \frac{x^2}{2!} + \frac{x^3}{3!} + \frac{x^4}{4!} + \dots$$

$$e^{J\phi} = 1 + J\phi - \frac{\phi^2}{2!} - J\frac{\phi^3}{3!} + \frac{\phi^4}{4!} + \dots$$

$$e^{J\phi} = \cos\phi + J\sin\phi$$

Let $z_1 = x_1 + Jy_1$ and $z_2 = x_2 + Jy_2$ then
$z_1 + z_2 = (x_1 + x_2) + J(y_1 + y_2)$ and $z_1 z_2 = (x_1 x_2 - y_1 y_2) + J(x_1 y_2 + x_2 y_1)$
Let $z_1 = r_1 e^{J\phi_1}$ and $z_2 = r_2 e^{J\phi_2}$ then

$$z_1 + z_2 = (r_1 \cos \phi_1 + r_2 \cos \phi_2) + J (r_1 \sin \phi_1 + r_2 \sin \phi_2)$$
$$= \left(\sqrt{r_1^2 + r_2^2 + r_1 r_2 \cos(\phi_1 - \phi_2)} \right) e^{J \frac{r_1 \cos \phi_1 + r_2 \cos \phi_2}{r_1 \sin \phi_1 + r_2 \sin \phi_2}}$$

$z_1 z_2 = r_1 r_2 e^{J(\phi_1 + \phi_2)}$ Let

$$v_1 = r_1 \sin(\omega t + \phi_1) = r_1 \sin \omega t \cos \phi_1 + r_1 \cos \omega t \sin \phi_1$$
$$v_2 = r_2 \sin(\omega t + \phi_2) = r_2 \sin \omega t \cos \phi_2 + r_2 \cos \omega t \sin \phi_2$$

Then let $v_1 + v_2 = r \sin(\omega t + \phi)$. Is there an easy way to find r and ϕ? Let us write

$$v_1 + v_2 = \left(\sqrt{r_1^2 + r_2^2 + r_1 r_2 \cos(\phi_1 - \phi_2)} \right) \sin \left(\omega t + \tan^{-1} \frac{r_1 \cos \phi_1 + r_2 \cos \phi_2}{r_1 \sin \phi_1 + r_2 \sin \phi_2} \right)$$

It is clear that had we expressed v_1 and v_2 as $V_i = r_i e^{J \phi_i}$ and done a complex addition we would have obtained r and ϕ directly.

Sinusoids are expressed as complex numbers or vectors to make it easy to do algebra. This complex number representation is known as phasors.

1.7.2   Per Unit System

In power systems every quantity is specified in a per unit system. There are so many advantages of using per unit system that after having used it for a while one wonders how could one have lived without it. To establish a per unit system:

1. First base power P_b and base voltage V_b are chosen.
2. The per unit value of power and voltage is obtained by dividing the nominal value with the base value.
3. The base values of all other quantities are derived from the base values of power and voltage, e.g., base current $I_b = \frac{P_b}{V_b}$ and base impedance $Z_b = \frac{V_b}{I_b} = \frac{V_b^2}{V_b}$.
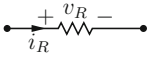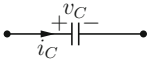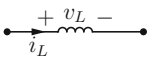
Let $P_b = 100\,\text{MW}$, then $100\,\text{MW}$ is $1\,\text{pu}$, $200\,\text{MW}$ $2\,\text{pu}$, and $50\,\text{MW}$ $0.5\,\text{pu}$. Let $V_b = 138\,\text{kV}$, then $138\,\text{kV}$ is 1 pu, $276\,\text{kV}$ $2\,\text{pu}$, and $69\,\text{kV}$ $0.5\,\text{pu}$.

1.7.3   Circuit Theory in a Nutshell

Kirchhoff's Current Law (KCL) The algebraic sum of all the currents at a node is zero.

Kirchhoff's Voltage Law (KVL) The algebraic sum of all the voltage drops across all elements around a loop is zero.

Table 1.3 Circuit elements

Resistor	$+ \; v_R \; -$ i_R	$v_R = R i_R$
Capacitor	v_C $+ \; -$ i_C	$i_C = C \dfrac{d v_C}{dt}$
Inductor	$+ \; v_L \; -$ i_L	$v_L = L \dfrac{d i_L}{dt}$

The current and voltage relationship for all three circuit elements is given in Table 1.3. These three relationships along with KCL and KVL is circuit theory in a nutshell.

Chapter 2
Modelling Power System Devices

Chapter Organisation

Introduction section gives the basic modelling philosophy of how individual device models fit into an interconnected system. As is common in power system simulations, all voltages and currents are transformed to appropriate dq-frames. A simplification is achieved by writing device models in local dq-frames. This necessitates the transformation between local and global dq-frames. The ideas and equations necessary to perform phasor to dq-frame transformations are given in Sect. 2.1.1. A framework for device models is given in Sect. 2.1.2. In this framework, the inputs to the model are external device inputs and the stator currents, and the outputs are the states and stator voltages. This framework enables the addition of new devices to the interconnected system without having to change the model equations for the existing devices. Section 2.1.3 summarises the framework for writing the network equations.

Section 2.2 covers modelling of synchronous machines. The modelling starts with the transient analysis model and then develops an understanding of the various simplified models used in the analysis and control design. Although a complete subtransient analysis model is later developed for synchronous machines the emphasis is on developing models for transient analysis with a view to using them for control design. The transient analysis of the electrical behaviour of synchronous machines is fully captured by just one differential equation. To emphasise this fact most results used for transient analysis have been so arranged that their relationship to that one single equation is clear. A similar analysis is done for induction machines in Sect. 2.5. A framework for network equations and how all the devices are connected together is covered in detail in Sect. 2.7. Finally the material for the entire chapter is put together by using simulations in Sect. 2.8.

As stated above the synchronous and induction machine models developed in this chapter are comprehensive and cover situations from steady-state to sub-transient analysis. It is ensured that various models used in the literature and presented in many books have been included in this chapter. This is done in a very deliberate way

to enhance student learning. After presenting the essential concepts several relationships and equations are presented in an exercise format where all the conceptual steps are given and the student must carry out the mechanical steps. In this way students at all levels will be able to complete the exercises and be certain of the origins of all the equations used in various models in use in transient analysis and control design.

2.1 Introduction

This section gives an overview of the modelling process for power system devices and their interface to the network. The network interface and simulation of interconnected devices is done by neglecting the stator transients in electrical machines.

2.1.1 The dq0 Transformation

All the models in this book are represented in a dq-frame. The transformation between the phasor quantities and the dq quantities is achieved using the following matrix:

$$K_s = \frac{2}{3} \begin{bmatrix} \cos(\omega t + \phi_r + \phi_s) & \cos(\omega t + \phi_r + \phi_s - \frac{2\pi}{3}) & \cos(\omega t + \phi_r + \phi_s + \frac{2\pi}{3}) \\ -\sin(\omega t + \phi_r + \phi_s) & -\sin(\omega t + \phi_r + \phi_s - \frac{2\pi}{3}) & -\sin(\omega t + \phi_r + \phi_s + \frac{2\pi}{3}) \\ \frac{1}{2} & \frac{1}{2} & \frac{1}{2} \end{bmatrix} \quad (2.1)$$

such that

$$F_{dq0} = K_s F_{abc}, \text{ i.e., } \begin{bmatrix} F_d \\ F_q \\ F_0 \end{bmatrix} = K_s \begin{bmatrix} F_a \\ F_b \\ F_c \end{bmatrix} \quad (2.2)$$

For balanced three-phase phasor quantities

$$F_{abcs} = \begin{bmatrix} F_m \cos(\omega t + \phi_f) \\ F_m \cos(\omega t + \phi_f - \frac{2\pi}{3}) \\ F_m \cos(\omega t + \phi_f + \frac{2\pi}{3}) \end{bmatrix} \quad (2.3)$$

the correspoding $dq0$ variables from (2.2) are:

$$F_d = F_m \cos(\phi_f - (\phi_s + \phi_r)), \; F_q = F_m \sin(\phi_f - (\phi_s + \phi_r)), \text{ and } F_0 = 0. \quad (2.4)$$

The rotating frame in which $\phi_r = 0$ is called the $DQ0$ frame (with upper case letters), shown in Fig. 2.1, and for this case we have:

$$F_D = F_m \cos(\phi_f - \phi_s) \text{ and } F_Q = F_m \sin(\phi_f - \phi_s). \quad (2.5)$$

Fig. 2.1 Rotating frames DQ and dq
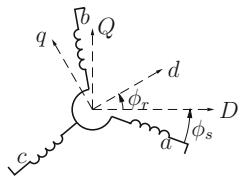
Quantities in frames $dq0$ and $DQ0$ can be related by using Eqs. (2.4) and (2.5)

$$\begin{bmatrix} F_d \\ F_q \end{bmatrix} = \overbrace{\begin{bmatrix} \cos \phi_r & \sin \phi_r \\ -\sin \phi_r & \cos \phi_r \end{bmatrix}}^{R(\phi_r)} \begin{bmatrix} F_D \\ F_Q \end{bmatrix} \tag{2.6}$$

Often the above vector transformation in (2.6) is written as

$$F_d + jF_q = (F_D + jF_Q)\, e^{-j\phi_r} \tag{2.7}$$

Note that in a balanced three-phase system, $F_D + jF_Q$ is the phasor representation of voltage F_a with respect to $DQ0$ and $F_d + jF_q$ is the phasor representation of voltage F_a with respect to the $dq0$. We will consider only balanced three-phase systems. The standard convention of positive increase in angle in the counter clockwise direction is used here.

2.1.1.1 Exercise—Real and Reactive Power

Show that for a three-phase balanced system with

$$V_{abcs} = \begin{bmatrix} V_m \cos(\omega t + \phi_f) \\ V_m \cos(\omega t + \phi_f - \frac{2\pi}{3}) \\ V_m \cos(\omega t + \phi_f + \frac{2\pi}{3}) \end{bmatrix}, \quad I_{abcs} = \begin{bmatrix} I_m \cos(\omega t + \phi_f + \phi) \\ I_m \cos(\omega t + \phi_f - \frac{2\pi}{3} + \phi) \\ I_m \cos(\omega t + \phi_f + \frac{2\pi}{3} + \phi) \end{bmatrix} \tag{2.8}$$

$$S = \frac{3}{2}\left(V_d + jV_q\right)\left(I_d - jI_q\right); \quad P = \frac{3}{2}\left(V_d I_d + V_q I_q\right), \text{ and } Q = \frac{3}{2}\left(V_d I_q - V_q I_d\right) \tag{2.9}$$

We know that for the above three-phase system of voltages and currents $P = \frac{3}{2}V_m I_m \cos\phi$ and $Q = \frac{3}{2}V_m I_m \sin\phi$, where the complex power $S = P + jQ$. Use the $dq0$ expression in (2.7) to obtain V_d, V_q, I_d, and I_q and then simplify to obtain the required relationship.
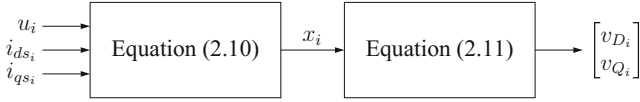
Fig. 2.2 ith device block diagram

2.1.2   Device Models

All the devices are modelled in terms of currents and voltages referred to a dq-frame. In synchronous machines the dq-frame is aligned with the field-axis of the rotor and for other devices it is aligned with the bus voltage to which the device is connected. Let the ith device be connected to bus i with voltage v_{ds_i} and v_{qs_i}, the current being injected by the device into the network is denoted by i_{ds_i} and i_{qs_i}. The voltages and currents with lowercase subscripts d and q refer to the dq-frame attached to the machine which can be different from the DQ-frame (uppercase D and Q) attached to the infinite or the reference bus. Bus voltages and injected currents at the ith bus in DQ-frame are referred as v_{D_i}, v_{Q_i}, i_{D_i}, and i_{Q_i}.

The device model consists of two sets of equations: (a) differential equations representing the device dynamics and (b) algebraic constraints of the network satisfied by the voltages v_{D_i}, v_{Q_i}, currents i_{D_i}, i_{Q_i}, and $R(\phi_{r_i})$ the transformation matrix between the reference DQ-frame and the local dq-frame.

The differential equations for the device connected to bus i, also called the ith device, in terms of state x_i ($n_i \times 1$ column vector), have the device inputs u_i and also the currents i_{ds_i} and i_{qs_i} as inputs:

$$\dot{x}_i = f_i(x_i, i_{ds_i}, i_{qs_i}, u_i) \tag{2.10}$$

The algebraic constraint equations are written as:

$$\begin{bmatrix} v_{D_i} \\ v_{Q_i} \end{bmatrix} = Z_{DQ_i} \begin{bmatrix} i_{D_i} \\ i_{Q_i} \end{bmatrix} + D_{a_i} x_i \quad \text{and} \quad \left(\begin{bmatrix} i_{ds_i} \\ i_{qs_i} \end{bmatrix} = R(\phi_{r_i}) \begin{bmatrix} i_{D_i} \\ i_{Q_i} \end{bmatrix} \right) \tag{2.11}$$

To specify a device model then means to give differential Eqs. (2.10), matrices Z_{DQ_i}, D_{a_i}, and $R(\phi_{r_i})$.

Block diagram for the ith device block is given in Fig. 2.2. In a multi-device system, currents i_{D_i} and i_{Q_i} depend on the state of other devices so we can only perform the integration step after obtaining i_{ds_i} and i_{qs_i} using the network algebraic constraints.

The multimachine simulation proceeds as follows. The initial load flow voltages and currents are used to perform the first integration step for each device using (2.10). From the current state x_i, voltages v_{D_i}, v_{Q_i} are computed using (2.11). These voltages are then used to obtain currents i_{D_i}, i_{Q_i} using the network algebraic constraints. The transformation matrix $R(\phi_{r_i})$ is used to obtain i_{d_i}, i_{q_i} and the next integration step

is performed. If the device is connected to an infinite bus then v_{D_i} and v_{Q_i} are fixed and algebraic solution step is not needed.

2.1.3 Network Modelling

For transmission networks we neglect the transients which also implies neglecting the stator transients of synchronous and induction machines. We can consider the network in sinsusoidal steady-state and express all the currents and voltages as phasors. For the phasor representation of network quantities, we will take the infinite-bus voltage as the reference, i.e., with phase zero. Voltage and current at bus-i can be written as: $\vec{V}_i = v_{Di} + J v_{Qi}$ and $\vec{I}_i = i_{Di} + J i_{Qi}$, upper case D and Q are used for network bus quantities. We use the notation $\vec{V}_a$ and $\vec{I}_a$, to denote vector of phasor voltages and currents at all the active buses (a), etc. A detailed description of network modelling is covered in Sect. 2.7.

2.2 Synchronous Machine

Synchronous machine is a complex device to model. It is the genius of the power system engineers that has led to a simple and accurate model of synchronous machines [2–5]. Not only the models are simple enough to get an insight into power system operation without resorting to computers, the model parameters can be measured with simple experiments too. A right start to the analysis of synchronous machines and a little labour in deriving important relationships can lead to a sound understanding of synchronous machine and power system dynamics. Here we start from *the* field flux linkage equation and then tie everything around it in stages. Students are strongly advised to derive all the relationships developed in this chapter themselves.
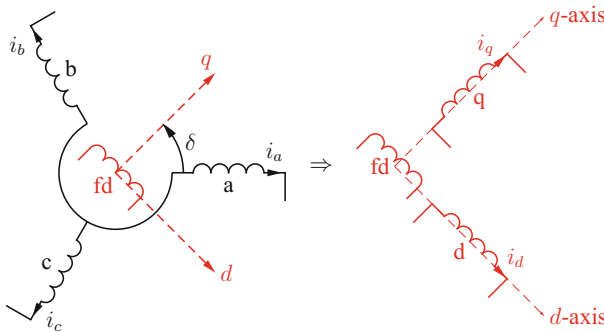
Fig. 2.3 Synchronous machine d and q axis

Let us consider a P_i pole synchronous machine with four windings as shown in Fig. 2.3 with one rotating coil in the centre and three stationary coils. Dynamic equation for the rotor flux in the synchronous generator (for motor operation, change the sign of the stator current terms) connected to bus i,

$$\dot{\lambda}_{\text{fd}_i} = -r_{\text{fd}_i} i_{\text{fd}_i} + v_{\text{fd}_i} \tag{2.12}$$

The torque and rotor speed are related as [6]:

$$J_i \left(\frac{2}{P_i} \right) \dot{\omega}_{r_i} = T_{m_i} - T_{e_i} \tag{2.13}$$

$$\dot{\delta}_{r_i} = \omega_{r_i} \tag{2.14}$$

where T_{m_i} is the applied mechanical torque in case of generators and the load torque for motors,

$$T_{e_i} = \left(\frac{3}{2} \right) \left(\frac{P_i}{2} \right) \left(\lambda_{ds_i} i_{qs_i} - \lambda_{qs_i} i_{ds_i} \right). \tag{2.15}$$

Most symbols have their usual meaning: v, i, and λ, r, L, denote voltage, current, total flux linkages, resistance, and inductance, respectively. Mechanical variables are: δ for angular position, ω for angular velocity, T for torque, J for angular moment of inertia. Subscripts indicate the coil to which the quantity relates: d, q for d-axis and q-axis respectively; s is used for stator and r or fd for rotor; with inductances subscript l is for leakage and m is to indicate mutual inductance. For example, λ_{ds_i} represents flux in the d-axis coil of the stator of the ith generator.

Electrical Torque T_{e_i} The electrical torque, T_{e_i} is normally obtained using the method [6, 7] outlined in Sect. 1.5. For the purposes of modelling the dynamics of synchronous machines for control a simpler method can be used to calculate the electrical torque. It is always true that the input power is equal to the output power minus electrical and mechanical losses. A good approximation for most synchronous generators is to neglect electrical and mechanical losses, thus it can be assumed that the input and the output power are equal.

The electrical power equation in (2.9), when applied to the synchronous machine, can be written as: $\frac{3}{2} \left(v_{ds_i} i_{ds_i} + v_{qs_i} i_{qs_i} \right)$ and the mechanical power is $T_{e_i} \omega_{m_i}$. This gives (ignoring electrical and mechanical losses),

$$\frac{3}{2} \left(v_{ds_i} i_{ds_i} + v_{qs_i} i_{qs_i} \right) = T_{e_i} \omega_{m_i} \tag{2.16}$$

Equation (2.16) is exact when the stored magnetic energy or mutual inductances do not change with the rotor position. In the case of equations that are written in the dq-frame this means that the approximation (2.16) is good whenever the rotor speed is close to the synchronous speed which is normally the case.

The mechanical angular velocity ω_{m_i} and the electrical angular velocity ω_{r_i} are related by $\omega_{r_i} = \frac{P_i}{2}\omega_{m_i}$, giving,

$$T_{e_i} = \frac{P_{e_i}}{\omega_{m_i}} = \frac{P_i}{2}\frac{P_{e_i}}{\omega_{r_i}} = \left(\frac{3}{2}\right)\left(\frac{P_i}{2}\right)\left(\lambda_{ds_i}i_{qs_i} - \lambda_{qs_i}i_{ds_i}\right) \qquad (2.17)$$

The last equality (2.17) is obtained by substituting for v_{ds_i} and v_{qs_i} from Eqs. (2.18) and (2.19) in (2.16). Please note that Eqs. (2.16) and (2.17) cannot be used to obtain T_{e_i} when ω_{m_i} is zero, i.e., during the starting of the machine. In power systems, the starting period of the synchronous machine is seldom of interest thus we can safely use Eq. (2.17) for modelling the dynamics of the synchronous machine.

Interconnection constraints Algebraic equations or constraints, given below, for the synchronous machine connected to bus i are used to obtain expressions for the voltages and currents in the synchronous machine (ω is the angular velocity of the synchronously rotating dq-frame and it is equal to ω_{r_i}),

$$v_{qs_i} = -r_{s_i}i_{qs_i} + \omega\lambda_{ds_i} \qquad (2.18)$$

$$v_{ds_i} = -r_{s_i}i_{ds_i} - \omega\lambda_{qs_i} \qquad (2.19)$$

$$\lambda_{qs_i} = -L_{ls_i}i_{qs_i} + L_{mq_i}\left(-i_{qs_i}\right) \qquad (2.20)$$

$$\lambda_{ds_i} = -L_{ls_i}i_{ds_i} + L_{md_i}\left(-i_{ds_i} + i_{\text{fd}_i}\right) \qquad (2.21)$$

$$\lambda_{\text{fd}_i} = L_{l\text{fd}_i}i_{\text{fd}_i} + L_{md_i}\left(-i_{ds_i} + i_{\text{fd}_i}\right) \qquad (2.22)$$

Equations (2.18)–(2.22) are completely derived later in the chapter.

The model of the synchronous machine is given by the differential Eqs. (2.12)–(2.14) and algebraic Eqs. (2.18) and (2.19) with λ_{ds_i}, λ_{qs_i}, and i_{fd_i} written in terms of i_{ds_i} and i_{qs_i}. Equations (2.20)–(2.22) are solved for λ_{ds_i}, λ_{qs_i}, and i_{fd_i} in terms of i_{ds_i} and i_{qs_i}. The following material till Sect. 2.2.1 gives the details of these manipulations. On first reading these details can be skipped but please be sure to derive all the equations to get familiar with the model.

Direct and quadrature axis inductances A simplification in writing the model equations can be obtained by defining the so called direct and quadrature axis inductances. These inductances also have a physical interpretation and they can be measured experimentally. Inductance parameters used in Eqs. (2.18)–(2.22) are hard to measure and it is harder to obtain their values analytically. The introduction of direct and quadrature axis inductances is one of the main reasons for the accuracy achieved in modelling synchronous machines.

Define

$$L_{d_i} = L_{ls_i} + L_{md_i}, \quad L_{q_i} = L_{ls_i} + L_{mq_i}, \quad L_{\text{fd}_i} = L_{l\text{fd}_i} + L_{md_i}, \qquad (2.23)$$

From (2.22), we get

$$i_{\text{fd}_i} = \frac{1}{L_{\text{fd}_i}}\left(\lambda_{\text{fd}_i} + L_{md_i}i_{ds_i}\right) \qquad (2.24)$$

with this the rotor flux dynamic Eq. (2.12) and the mechanical Eqs. (2.13) and (2.14) can be written as,

$$\dot{\lambda}_{\text{fd}_i} = -\frac{r_{\text{fd}_i}}{L_{\text{fd}_i}} \lambda_{\text{fd}_i} - \frac{r_{\text{fd}_i} L_{md_i}}{L_{\text{fd}_i}} i_{ds_i} + v_{\text{fd}_i} \tag{2.25}$$

$$J_i \left(\frac{2}{P_i} \right) \dot{\omega}_{r_i} = T_{L_i} - \left(\frac{3}{2} \right) \left(\frac{P_i}{2} \right) \left(\left(L_{q_i} - L'_{d_i} \right) i_{qs_i} i_{ds_i} + \frac{L_{md_i}}{L_{\text{fd}_i}} i_{qs_i} \lambda_{\text{fd}_i} \right) \tag{2.26}$$

$$\dot{\delta}_{r_i} = \omega_{r_i} \tag{2.27}$$

and the algebraic constraints (2.18) and (2.19) between the stator voltages and currents can be written as:

$$v_{qs_i} = -r_{s_i} i_{qs_i} - \omega L'_{d_i} i_{ds_i} + \frac{\omega L_{md_i}}{L_{\text{fd}_i}} \lambda_{\text{fd}_i} \tag{2.28}$$

$$v_{ds_i} = -r_{s_i} i_{ds_i} + \omega L'_{q_i} i_{qs_i} \tag{2.29}$$

Define:

$$L'_{d_i} = \frac{L_{l\text{fd}_i} L_{md_i}}{L_{\text{fd}_i}} + L_{ls_i} = L_{d_i} - \frac{L^2_{md_i}}{L_{\text{fd}_i}}, \quad L'_{q_i} = L_{ls_i} + L_{mq_i}, \tag{2.30}$$

$$E'_{q_i} = \frac{\omega L_{md_i}}{L_{\text{fd}_i}} \lambda_{\text{fd}_i}, \quad E_{\text{fd}_i} = \frac{\omega L_{md_i}}{r_{\text{fd}_i}} v_{\text{fd}_i}, \quad T'_{d0_i} = \frac{L_{\text{fd}_i}}{r_{\text{fd}_i}} \tag{2.31}$$

Substituting L_{d_i}, L'_{d_i}, E'_{q_i}, E_{fd_i}, and T'_{d0_i} from (2.30) and (2.31) into (2.25) we get

$$\dot{E}'_{q_i} = \frac{1}{T'_{d0_i}} \left(-E'_{q_i} - \omega \left(L_{d_i} - L'_{d_i} \right) i_{ds_i} + E_{\text{fd}_i} \right) \tag{2.32}$$

For synchronous machine, the d-axis of the rotating frame is aligned with the rotor flux axis and δ is the angle between the rotating q-axis and the phase of the a-axis quantity [8, p. 96], i.e., $\phi_{r_i} = \delta_i - \frac{\pi}{2}$, and $\phi_{s_i} = 0$. Substituting this in (2.6), we get

$$\begin{bmatrix} v_{ds_i} \\ v_{qs_i} \end{bmatrix} = \begin{bmatrix} \sin \delta_i & -\cos \delta_i \\ \cos \delta_i & \sin \delta_i \end{bmatrix} \begin{bmatrix} v_{D_i} \\ v_{Q_i} \end{bmatrix} \tag{2.33}$$

The above matrix relationship can also be expressed as:

$$v_{ds_i} + J v_{qs_i} = \left(v_{D_i} + J v_{Q_i} \right) e^{J \left(\frac{\pi}{2} - \delta_i \right)} \tag{2.34}$$

With the above definitions in (2.30), Eqs. (2.28)–(2.29) can be written as:

$$\begin{bmatrix} v_{ds_i} \\ v_{qs_i} \end{bmatrix} = \begin{bmatrix} -r_{s_i} & \omega L'_{q_i} \\ -\omega L'_{d_i} & -r_{s_i} \end{bmatrix} \begin{bmatrix} i_{ds_i} \\ i_{qs_i} \end{bmatrix} + \begin{bmatrix} 0 \\ E'_{q_i} \end{bmatrix} \tag{2.35}$$

The above equation can be written in DQO frame as ($R(\phi_{r_i})$ is the matrix in Eq. (2.33)):

$$\begin{bmatrix} v_{D_i} \\ v_{Q_i} \end{bmatrix} = R^{-1}(\phi_{r_i}) \begin{bmatrix} -r_{s_i} & \omega L'_{q_i} \\ -\omega L'_{d_i} & -r_{s_i} \end{bmatrix} R(\phi_{r_i}) \begin{bmatrix} i_{D_i} \\ i_{Q_i} \end{bmatrix} + R^{-1}(\phi_{r_i}) \begin{bmatrix} 0 \\ \frac{\omega L_{md_i}}{L_{\mathrm{fd}_i}} \end{bmatrix} \lambda_{\mathrm{fd}_i} \quad (2.36)$$

2.2.1 The Model

The model consists of the three differential Eqs. (2.25)–(2.27), with

$$x_i = \begin{bmatrix} \lambda_{\mathrm{fd}_i} \\ \omega_{r_i} \\ \delta_{r_i} \end{bmatrix}, \quad u_i = v_{\mathrm{fd}_i}, \quad R(\phi_{r_i}) = \begin{bmatrix} \sin \delta_i & -\cos \delta_i \\ \cos \delta_i & \sin \delta_i \end{bmatrix} \quad (2.37)$$

and

$$Z_{DQ_i} = R^{-1}(\phi_{r_i}) \begin{bmatrix} -r_{s_i} & \omega L'_{q_i} \\ -\omega L'_{d_i} & -r_{s_i} \end{bmatrix} R(\phi_{r_i}), \quad D_{a_i} = R^{-1}(\phi_{r_i}) \begin{bmatrix} 0 & 0 & 0 \\ \frac{\omega L_{md_i}}{L_{\mathrm{fd}_i}} & 0 & 0 \end{bmatrix} \quad (2.38)$$

2.2.2 Equations in Per Unit System

The per unit system for synchronous machine is set up by first choosing the base power P_{b} and base voltage V_{b}, then the current base $I_{\mathrm{b}} = \frac{P_{\mathrm{b}}}{(3/2)V_{\mathrm{b}}}$, the flux base $\lambda_b = \frac{V_b}{\omega_b}$, and torque base $T_{\mathrm{b}} = \frac{P_{\mathrm{b}}}{(2/P)\omega_{\mathrm{b}}}$, where ω_{b} is normally the supply frequency.

For algebraic equations if all the quantities are changed to their per unit values, everything will balance out but extra care needs to be taken when time derivatives are involved. For example in (2.25), $\dot{\lambda}_{\mathrm{fd}_i}$ has the unit of voltage but $\frac{\dot{\lambda}_{\mathrm{fd}_i}}{V_{\mathrm{b}}}$ is not the per unit value, $\dot{\bar{\lambda}}_{\mathrm{fd}_i}$, instead

$$\frac{\dot{\lambda}_{\mathrm{fd}_i}}{V_{\mathrm{b}}} = \frac{1}{\omega_{\mathrm{b}}} \dot{\bar{\lambda}}_{\mathrm{fd}_i},$$

where bar denotes per unit quantities. The rotor flux Eq. (2.25) in per unit system is:

$$\frac{1}{\omega_{\mathrm{b}}} \dot{\bar{\lambda}}_{\mathrm{fd}_i} = -\frac{\bar{r}_{\mathrm{fd}_i}}{\bar{L}_{\mathrm{fd}_i}} \bar{\lambda}_{\mathrm{fd}_i} - \frac{\bar{r}_{\mathrm{fd}_i} \bar{L}_{md_i}}{\bar{L}_{\mathrm{fd}_i}} \bar{i}_{ds_i} + \bar{v}_{\mathrm{fd}_i} \quad (2.39)$$

Equation (2.26) is converted to the per unit system by dividing on both the sides by T_{b}

$$\frac{J_i \left(\frac{2}{P_i}\right) \omega_{\mathrm{b}} \frac{\dot{\omega}_{r_i}}{\omega_{\mathrm{b}}}}{\frac{P_{\mathrm{b}}}{(2/P_i)\omega_{\mathrm{b}}}} = \frac{T_{L_i} - \left(\frac{3}{2}\right) \left(\frac{P_i}{2}\right) \left(\left(L_{q_i} - L'_{d_i}\right) i_{qs_i} i_{ds_i} + \frac{L_{md_i}}{L_{\mathrm{fd}_i}} i_{qs_i} \lambda_{\mathrm{fd}_i}\right)}{\frac{P_{\mathrm{b}}}{(2/P)\omega_{\mathrm{b}}}}$$

$$\dot{\omega}_{r_i} = \frac{1}{2H_i} \left(\bar{T}_{L_i} - \left(\left(\bar{L}_{q_i} - \bar{L}'_{d_i}\right) \bar{i}_{qs_i} \bar{i}_{ds_i} + \frac{\bar{L}_{md_i}}{\bar{L}_{\mathrm{fd}_i}} \bar{i}_{qs_i} \bar{\lambda}_{\mathrm{fd}_i}\right)\right) \qquad (2.40)$$

where $H_i = \left(\frac{1}{2}\right) \left(\frac{2}{P_i}\right)^2 \frac{J_i \omega_{\mathrm{b}}^2}{P_{\mathrm{b}}}$. The angle δ is normally expressed in radians and not in a per unit system. For δ_{r_i} in radians and ω_{r_i} in per unit, Eq. (2.27) is written as:

$$\dot{\delta}_{r_i} = \omega_{\mathrm{b}}(\bar{\omega}_{r_i} - \bar{\omega}_{r_i}^0). \qquad (2.41)$$

2.2.3 Steady-State Conditions

For any simulation of the synchronous machine dynamics, first the equilibrium value of the variables, angle $\phi_{s_i}^0$, and voltages $v_{D_i}^0$, $v_{Q_i}^0$ are obtained from the load flow analysis and $v_{ds_i}^0$, $v_{qs_i}^0$ are written in terms of $v_{D_i}^0$, $v_{Q_i}^0$ using (2.33). Next, Eqs. (2.25), (2.26), (2.28), and (2.29) can be solved at steady-state (with $\dot{\lambda}_{\mathrm{fd}_i} = 0$, $\dot{\omega}_{r_i} = 0$), to obtain δ_i^0, $\lambda_{\mathrm{fd}_i}^0$, $i_{ds_i}^0$, $i_{qs_i}^0$, and $\omega_{r_i}^0 = 2\pi 50 \,\mathrm{rad}\,\mathrm{s}^{-1}$. These values provide all the initial conditions that are needed to obtain a numerical solution of the dynamic equations.

2.2.4 Single Machine Infinite Bus (SMIB)

A good understanding of the synchronous machine principles can be had by considering its operation when connected to an infinite bus. Since there is only one machine, the index subscript i is dropped in the SMIB analysis equations here.

Infinite bus is represented by a fixed voltage magnitue V_∞ and $\phi_s = 0$, then according to (2.4),

$$v_D = V_\infty, \text{ and } v_Q = 0.$$

The voltages v_{ds} and v_{qs} are then obtained from the transformation (2.33) and given as:

$$v_{ds} = V_\infty \sin\delta \text{ and } v_{qs} = V_\infty \cos\delta.$$

In the SMIB case the network equations do not need to be solved, since v_{ds} and v_{qs} are fixed, Eq. (2.35) can be solved only once for currents i_{ds} and i_{qs} and substituted in the differential Eqs. (2.25)–(2.27) and these equations can then be integrated.

2.2.4.1 Steady-State Equivalent When $L_d = L_q$

During the steady-state operation, the rate of change of rotor flux in (2.12) is zero and this gives the steady-state field current as,

$$i_{\text{fd}}^0 = \frac{v_{\text{fd}}}{r_{\text{fd}}}$$

Steady-state voltages and currents in (2.18)–(2.22) can be written as follows for $L_d = L_q$,

$$v_{ds}^0 + J v_{qs}^0 = -r_s \left(i_{ds}^0 + J i_{qs}^0\right) + \omega L_d \left(i_{qs}^0 - J i_{ds}^0\right) + J \frac{\omega L_{md} v_{\text{fd}}}{r_{\text{fd}}}$$

$$= -r_s \left(i_{ds}^0 + J i_{qs}^0\right) - J \omega L_d \left(i_{ds}^0 + J i_{qs}^0\right) + J \frac{\omega L_{md} v_{\text{fd}}}{r_{\text{fd}}}$$

$$i_{ds}^0 + J i_{qs}^0 = \frac{J \frac{\omega L_{md} v_{\text{fd}}}{r_{\text{fd}}} - \left(v_{ds}^0 + J v_{qs}^0\right)}{r_s + J \omega L_d}$$

When $r_s = 0$ and define $E_{\text{fd}}^0 = \frac{\omega L_{md} v_{\text{fd}}}{r_{\text{fd}}}$

$$v_{ds}^0 = V_\infty \sin \delta^0, \ v_{qs}^0 = V_\infty \cos \delta^0, \ i_{ds}^0 = \frac{E_{\text{fd}}^0}{\omega L_d} - \frac{v_{qs}^0}{\omega L_d}, \ i_{qs}^0 = \frac{v_{ds}^0}{\omega L_d}$$

The real power output of the synchronous machine is ($r_s = 0$):

$$P_o = \frac{3}{2} \Re\left(\left(v_{ds}^0 + J v_{qs}^0\right) \left(i_{ds}^0 - J i_{qs}^0\right)\right)$$

$$= \frac{3}{2} \frac{E_{\text{fd}}^0 V_\infty \sin \delta^0}{\omega L_d}$$

$$Q_o = \frac{3}{2} \Im\left(\left(v_{ds}^0 + J v_{qs}^0\right) \left(i_{ds}^0 - J i_{qs}^0\right)\right)$$

$$= \frac{3}{2} \frac{E_{\text{fd}}^0 V_\infty \cos \delta^0 - V_\infty^2}{\omega L_d}$$

2.2.4.2 Transient Analysis—Constant Flux Model

The development here has neglected stator transients and to be consistent with that it can be assumed that whenever there is a change in the steady-state operation, e.g., a fault or change in terminal voltage or a change in input power to the synchronous machine, stator currents will change their values. Transient analysis concerns itself about the changes in rotor flux due to the change in stator currents. A proper way to do the transient analysis is to solve the differential Eqs. (2.25)–(2.27) and that is what

Fig. 2.4 Voltage behind
transient inductance
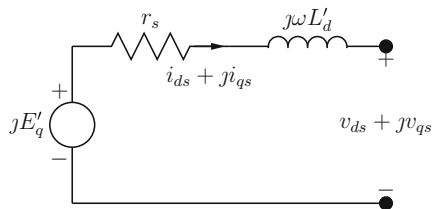
is normally done. For many synchronous machines, the time constant $\frac{L_{\text{lfd}_i}+L_{md_i}}{r_{\text{fd}_i}}$ in
differential Eq. (2.25) is of the order a few seconds thus it is possible to assume that
λ_{fd_i} is contstant for the first few milliseconds of the transient period. This suggests
that we can consider λ_{fd_i} constant at its pre-transient value. This means that we need
to solve only the differential equations that are for the mechanical part with constant
stator currents and voltages.

As seen above, currents i_{ds} and i_{qs} are easily calculated from an equivalent circuit
with a voltage source jE_{fd}, behind impdedance $r_s + j\omega L_d$, and connected to the
infinite bus. As soon as there is a change in stator currents E_{fd} changes thus the
simple model used above cannot be used for transient analysis. From observing the
rotor flux equation it can be seen that the quantity which does not change for intial
transient period is the quantity $\mathbf{E}'_q$ and thus Eq. (2.35) can be rearranged, in a similar
manner to what was done above for the steady-state analysis, to obtain an equivalent
"voltage behind a reactance" model.

A simplification is achieved when $L'_d = L'_q$. The currents i_{ds} and i_{qs} can be
obtained by solving (2.35),

$$
\begin{aligned}
v_{ds} + j v_{qs} &= -r_s\left(i_{ds} + j i_{qs}\right) + \omega L'_d\left(i_{qs} - j i_{ds}\right) + jE'_q \\
&= -r_s\left(i_{ds} + j i_{qs}\right) - j\omega L'_d\left(i_{ds} + j i_{qs}\right) + jE'_q \\
i_{ds} + j i_{qs} &= \frac{jE'_q - \left(v_{ds} + j v_{qs}\right)}{r_s + j\omega L'_d}
\end{aligned}
\tag{2.42}
$$

The equivalent circuit in Fig. 2.4 is a representation of the Eq. (2.42) above.

The real power output of the synchronous machine is ($r_s = 0$):

$$
\begin{aligned}
P_o &= \frac{3}{2}\Re\left(\left(v_{ds} + j v_{qs}\right)\left(i_{ds} - j i_{qs}\right)\right) \\
&= \frac{3}{2}\frac{E'_q V_\infty \sin\delta}{\omega L'_d}
\end{aligned}
$$

For the initial few milliseconds of the transient period the above value of output power
can be used along with the swing Eqs. (2.26) and (2.27) to solve for the mechanical
oscillations in the rotor angular position. This is a great simplification over having
to use the rotor flux differential equation in addition to the swing equations. If the

simulation duration extends beyond a few tens of milliseconds then the full model with three differential equations should be used.

Remark It must be noted that the reactance L_d' is not the reactance of the synchronous machine during the transient period in comparison with the reactance L_d which is known as the synchronous reactance and used for steady-state analysis. The transient reactance L_d' is a reactance behind a different "voltage" source and not E_{fd} thus they two should not be compared in that way. The best way to understand transient reactance L_d' is to realise that it is that reactance which enables us to write a simple model for the first few milliseconds of transient analysis.

Please note that the steady-state analysis can be performed with or without the constant flux assumptions. Since the use of the constant flux model is quite common for transient analysis and control design, it is common to obtain steady-state conditions using the constant flux model which requires the calculation of E_{q_i}', a step more than the calculation of E_{fd} which is done directly from the knowledge of the field voltage v_{fd}.

If there is no reason to do the transient analysis then transformation to dq-frame is not needed. A simple manipulation shows that for balanced steady-state transformation each phase is uncoupled and can be analysed as a voltage source behind "synchronous" reactance.

The following two exercises help to give a physical meaning to the concept of direct-axis and quadrature-axis transient inductance [9, vol. III].

2.2.5 Direct-Axis Transient Inductance

Let the relative position of the synchronous machines coils be as shown in Fig. 2.5 at $t = 0$ s, and let the currents in the stator coils in the synchronous machine in Fig. 2.5 be switched on at $t = 0$ s:

$$\begin{bmatrix} i_a \\ i_b \\ i_c \end{bmatrix} = \begin{bmatrix} I_m \cos \omega t \\ I_m \cos(\omega t + \frac{2\pi}{3}) \\ I_m \cos(\omega t - \frac{2\pi}{3}) \end{bmatrix} \text{A} \tag{2.43}$$

The field winding is short-circuited. Assume zero resistance for all the stator windings. As shown in Fig. 2.5 the rotating frame is aligned with the field-axis and transformation in (2.1) is used. This will result in $i_{qs} = 0$ and $i_{ds} = I_m$. Note that one can transform between the phasor quantities abc and the quantities $dq0$ using the transformation (2.1) with $\phi_s = 0$ and $\phi_r = 0$. In the following the ratio of phasor quantities which can be obtained by deriving the result in dq variables and then transforming them to phasor quantities are obtained.

1. At the instant the currents are switched on, the flux in the field coil is zero and it should remain zero for a very small time after that. Show that during that short time interval when λ_{fd} is zero:
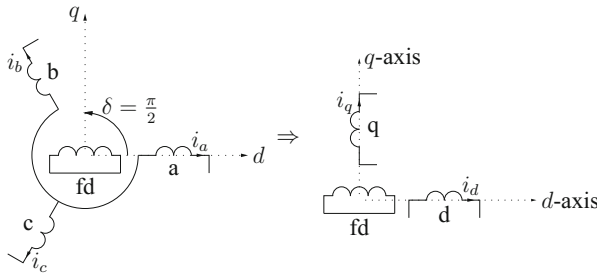
Fig. 2.5 Synchronous machine and direct-axis inductance

$$\frac{\vec{\lambda}_a}{-\vec{i}_a} = L'_d = \frac{L_{lfd}L_{md}}{L_{fd}} + L_{ls} \quad \text{(use (2.21) and (2.22))}.$$

2. A long time after the currents are switched-on, the field current will go to zero. Show that at steady-state:

$$\frac{\vec{\lambda}_a}{-\vec{i}_a} = L_d = L_{ls} + L_{md}.$$

Three-phase short-circuit There are many different ways to explain the physical meaning behind transient reactance and one of them is a description of what happens during a three-phase short-circuit. Let us consider a synchronous generator running at no-load and at synchronous speed. A three-phase short-circuit occurs at the synchronous machine terminals, i.e., $v_{as} = v_{bs} = v_{cs} = 0$ and thus $v_{ds} = v_{qs} = 0$. Show that when $r_s = 0$,

$$i_{ds} = \frac{E'_q}{\omega L'_d} \text{ and } i_{qs} = 0 \text{ (use (2.18)-(2.22))}.$$

2.2.6 Quadrature-Axis Transient Inductance

Repeat the analysis for the direct-axis transient inductance above, with the one where the relative position of the synchronous machine coils shown in Fig. 2.6 at $t = 0$ s ($\phi_s = 0$ and $\phi_r = -90°$), and prove that for both the initial condition and the steady-state the ratio is:

$$\frac{\vec{\lambda}_a}{-\vec{i}_a} = L'_q = L_q = L_{ls} + L_{mq}.$$

The above analysis shows that the "inductance" of stator coils is L'_d and L'_q during transient period for specific relative position of the rotor and stator coils. This

Fig. 2.6 Synchronous machine and quadrature-axis inductance
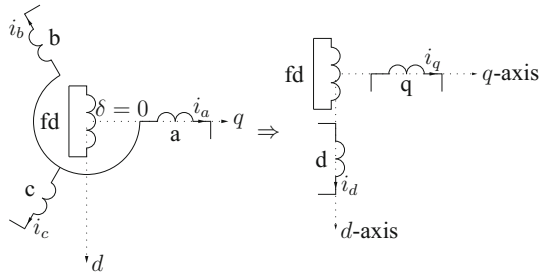
observation is also used to experimentally obtain the value of transient reactances. The rotor is physically locked to these positions and then measurements are made to obtain transient reactances.

2.2.7 Steady-State Output Power

The steady-state voltages and currents in (2.18)–(2.22) can be used to derive the following power-angle relationship for a salient pole machine (assume $r_s = 0$ and $E_{fd}^0 = \omega L_{md} i_{fd}^0$):

$$P_o = \frac{3}{2} \frac{E_{fd}^0 V_\infty}{\omega L_d} \sin \delta^0 + \frac{3}{2} V_\infty^2 \frac{L_d - L_q}{2\omega L_d L_q} \sin 2\delta^0 \qquad (2.44)$$

We can assume that $V_D = V_\infty$ and $V_Q = 0$, this gives $v_{ds}^0 = V_\infty \sin \delta^0$ and $v_{qs}^0 = V_\infty \cos \delta^0$. The following steps are useful in deriving the above relationship. Write

$$v_{ds}^0 + J v_{qs}^0 = -J\omega L_d \left(i_{ds}^0 + J i_{qs}^0 \right) + \omega \left(L_q - L_d \right) i_{qs}^0 + J\omega L_m i_{fd}^0$$

Equating the real and imaginary parts from above,

$$v_{ds}^0 = \omega L_q i_{qs}^0 \text{ and } v_{qs}^0 = -\omega L_d i_{ds}^0 + \omega L_m i_{fd}^0$$

$$\Re \left(\left(v_{ds}^0 + J v_{qs}^0 \right) \left(i_{ds}^0 - J i_{qs}^0 \right) \right) = -\omega i_{qs}^0 i_{ds}^0 \left(L_d - L_q \right) + \omega L_m i_{fd}^0 i_{qs}^0$$

$$P_o = \frac{3}{2} \Re \left(\left(v_{ds}^0 + J v_{qs}^0 \right) \left(i_{ds}^0 - J i_{qs}^0 \right) \right).$$

2.2.8 Voltage Behind Transient Inductance

An analysis similar to the one in Sect. 2.2.4 and Eq. (2.35) can be used to derive the following power-angle relationship for a salient pole machine (assume $r_s = 0$):

$$P_o = \frac{3}{2} \frac{E_q' V_\infty}{\omega L_d'} \sin \delta + \frac{3}{2} V_\infty^2 \frac{L_d' - L_q'}{2\omega L_d' L_q'} \sin 2\delta \qquad (2.45)$$

Note that the above formula for output power is valid both for transient and steady-state conditions, provided the appropriate value of E_q' is used.

2.2.9 Equivalence of the Two Models

It is easy to see that the two Eqs. (2.44) and (2.45) for steady-state output power give the same expression for the round rotor machines. For the definitions used in Sect. 2.2 verify the following:

$$L_d' = L_d - \frac{L_{md}^2}{L_{fd}}$$

$$E_q' = E_{fd}^0 - \omega \left(L_d - L_d' \right) i_{ds} \quad \text{(use (2.24) and the definition of } E_{fd}^0\text{)}$$

At steady-state verify that for round rotor machines:

$$\frac{E_{fd}^0}{L_d} = \frac{E_q'}{L_d'} - \frac{\omega \left(L_d - L_d' \right)}{\omega L_d L_d'} v_{qs}^0 \quad \text{(use } i_{ds}^0 \text{ in the exercise in Sect. 2.2.7)}$$

$$\frac{3}{2} \frac{E_{fd}^0 V_\infty \sin \delta^0}{\omega L_d} = \frac{3}{2} \frac{E_q' V_\infty}{\omega L_d'} \sin \delta^0 + \frac{3}{2} V_\infty^2 \frac{L_d' - L_q'}{2\omega L_d' L_q'} \sin 2\delta^0. \quad (L_q' = L_q = L_d)$$

2.2.10 Power Transfer Curves

A synchronous generator is directly connected to an infinite bus. The synchronous machine parameters and voltages are: $P_i = 2$; $V_\infty = V_m = (\sqrt{1/3})26$ kV; $J = 0.0658 \times 10^6$ kg m^2; $r_s = 0.00234\,\Omega$; $\omega_s = 2\pi 50$ rad s^{-1}; $L_{ls} = 4.6276 \times 10^{-4}$ H; $L_d = 0.0046$ H; $L_q = 0.0046$ H; $L_{md} = 0.0042$ H; $r_{fd} = 0.00075\,\Omega$; and $L_{lfd} = 3.6446 \times 10^{-4}$ H.

1. Show that when $P_m = 200 \times 10^6$ W and $v_{fd} = 11.3331$ V, the steady-state values are (assuming $r_s = 0\,\Omega$): $E_{fd}^0 = 19.820$ kV, $\delta^0 = 40.7659°$, $\lambda_{fd}^0 = 44.3806$ Wb, and $E_q' = 12.823$ kV.

2. Show that the electrical power transfer curves are given by the following equations (assuming $r_s = 0\,\Omega$):

   (a) $P_o = 306.29 \sin \delta$ MW: during steady-state conditions (use the analysis in Sect. 2.2.4).
   (b) $P_o = 1151.8 \sin \delta$ MW: during transient conditions (use the analysis in Sect. 2.2.4, assuming $L'_d = L'_q$).
   (c) $P_o = 1151.8 \sin \delta - 558.16 \sin 2\delta$ MW: during transient conditions (use the analysis in the exercise in Sect. 2.2.8, with $L'_q = L_q$).

   Plot the above three power curves. What conclusions can you draw from them?

2.2.11 Single-Machine-Infinite-Bus (SMIB) Simulation

The synchronous machine in the exercise in Sect. 2.2.10 is connected to an infinite bus.

1. Obtain steady-state values of the state variables for the differential Eqs. (2.25)–(2.27) when $P_m = 200 \times 10^6$ W and $v_{fd} = 11.3331$ V.
2. Simulate this SMIB system for 1 s, starting from the initial conditions obtained in the step above. Equation (2.27) is normally rewritten by defining a new state variable $\delta = \omega t - \delta_r$. At each integration step, currents i_D and i_Q are calculated using (2.36), where $v_D = V_m$, $v_Q = 0$,

$$
R(\phi_r) = \begin{bmatrix} \sin \delta & -\cos \delta \\ \cos \delta & \sin \delta \end{bmatrix}, \text{ and } \begin{bmatrix} i_{ds} \\ i_{qs} \end{bmatrix} = R(\phi_r) \begin{bmatrix} i_D \\ i_Q \end{bmatrix}
$$

3. Change the input power to $P_m = 250 \times 10^6$ W at 1 s and simulate for 10 s. Note that the initial conditions for this step are the final conditions in the above step.
4. Change the input power back to $P_m = 200 \times 10^6$ W at 10 s and simulate for another 10 s.
5. Show the simulation results using the plots for speed, angle, electrical torque, dq and phasor currents, flux linkages, real and reactive power.

The simulation plots are shown in Figs. 2.7, 2.8, 2.9, 2.10, 2.11 and 2.12. The plot is Fig. 2.12 is of special interest. Two output power versus delta plots for the constant voltage behind transient reactance model, with the $\sin 2\delta$ term, discussed in the exercise in Sect. 2.2.10 are plotted along with the simulated δ. One plot is for the equilibrium point with $P_m = 200$ MW and the other is for $P_m = 300$ MW. It can be seen that initially there is a good agreement between the simulated and constant flux model but as the transient dies out they separate. The plot joining both the equilibrim point is the steady-state power output versus delta curve.
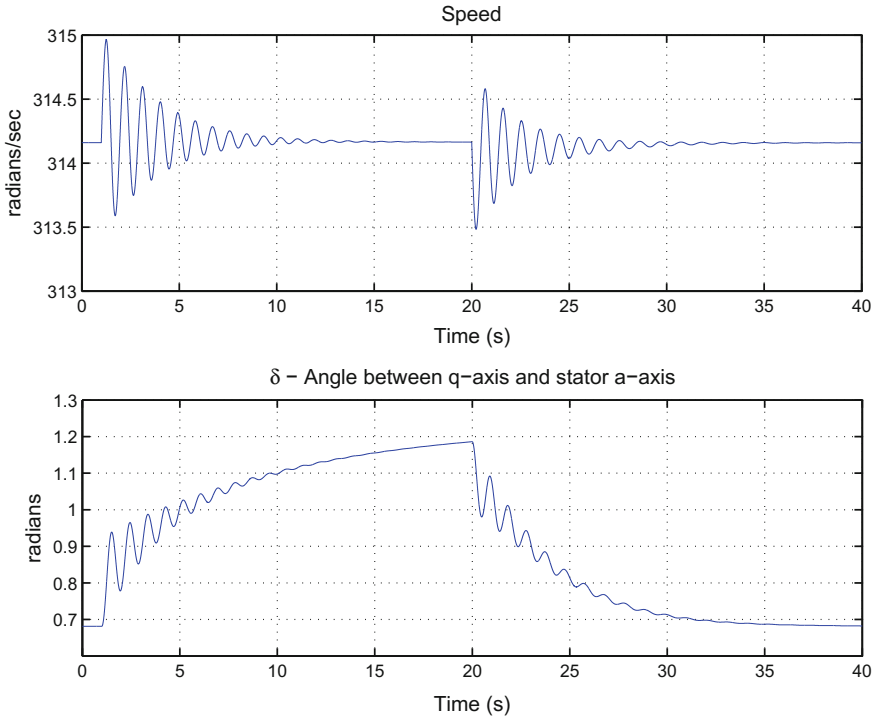
Fig. 2.7 Speed ω_r and angle δ

2.2.12 Steady-State δ^0 and i_{fd}^0

A synchronous generator is connected to an infinite bus and supplies power P_0 at a power factor PF. Let

$$\phi = \begin{cases} -\cos^{-1}(\text{PF}) & \text{lagging PF} \\ \cos^{-1}(\text{PF}) & \text{leading PF} \end{cases}$$

then $P_0 = (3/2)\,V_\infty I_m \cos \phi$.

1. For a round rotor, $(L_q = L_d)$, the steady-state δ^0 can be calculated using the following relationship:

$$\tan \delta^0 = \frac{r_s I_m \sin \phi + \omega L_d I_m \cos \phi}{V_\infty + r_s I_m \cos \phi - \omega L_d I_m \sin \phi}.$$

From Sect. 2.2.4 we can write the following

$$v_{ds}^0 = V_\infty \sin \delta \quad \text{and} \quad v_{qs}^0 = V_\infty \cos \delta$$
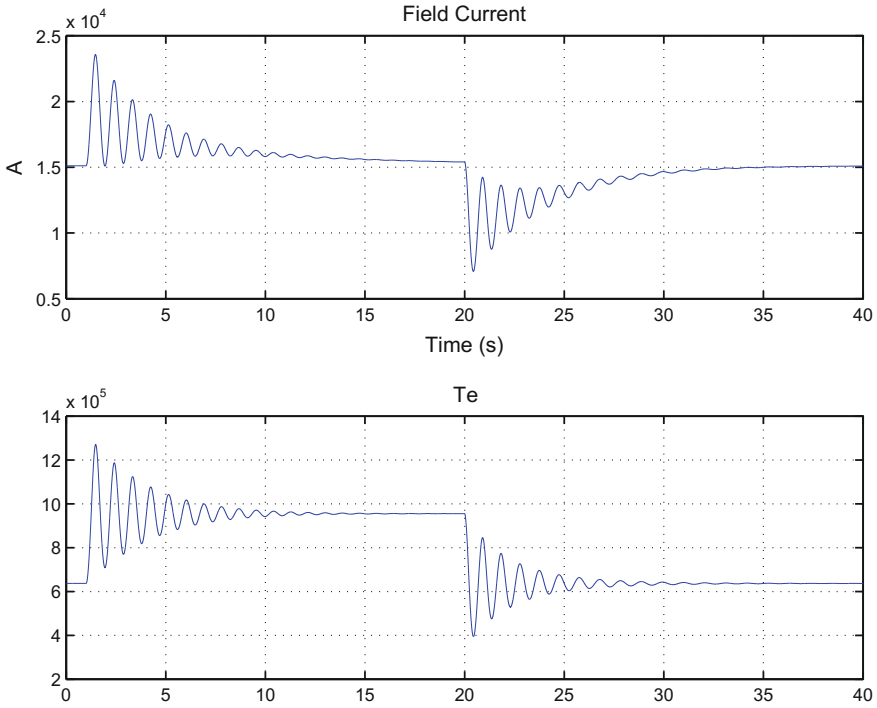
Fig. 2.8 i_{fd} and torque

and also

$$\begin{bmatrix} i_{ds}^0 \\ i_{qs}^0 \end{bmatrix} = \begin{bmatrix} \sin \delta & -\cos \delta \\ \cos \delta & \sin \delta \end{bmatrix} \begin{bmatrix} I_m \cos \phi \\ I_m \sin \phi \end{bmatrix}$$

Now use the analysis in Sect. 2.2.4 to write

$$v_{ds}^0 + J v_{qs}^0 = -r_s \left(i_{ds}^0 + J i_{qs}^0 \right) + \omega L_d \left(i_{qs}^0 - J i_{ds}^0 \right) + J \omega L_{md} i_{fd}^0$$

in terms of the above given expressions for $v_{ds}^0, v_{qs}^0, i_{ds}^0, i_{qs}^0$. Equate the real parts on both side of the above equation, collect the co-efficients of $\sin \delta^0$ on one side and $\cos \delta^0$ on the other side and then take their ratio.

2. For a salient pole machine, $(L_q \neq L_d)$, the steady-state δ^0 can be calculated using the following relationship:

$$\tan \delta^0 = \frac{r_s I_m \sin \phi + \omega L_q I_m \cos \phi}{V_\infty + r_s I_m \cos \phi - \omega L_q I_m \sin \phi}.$$

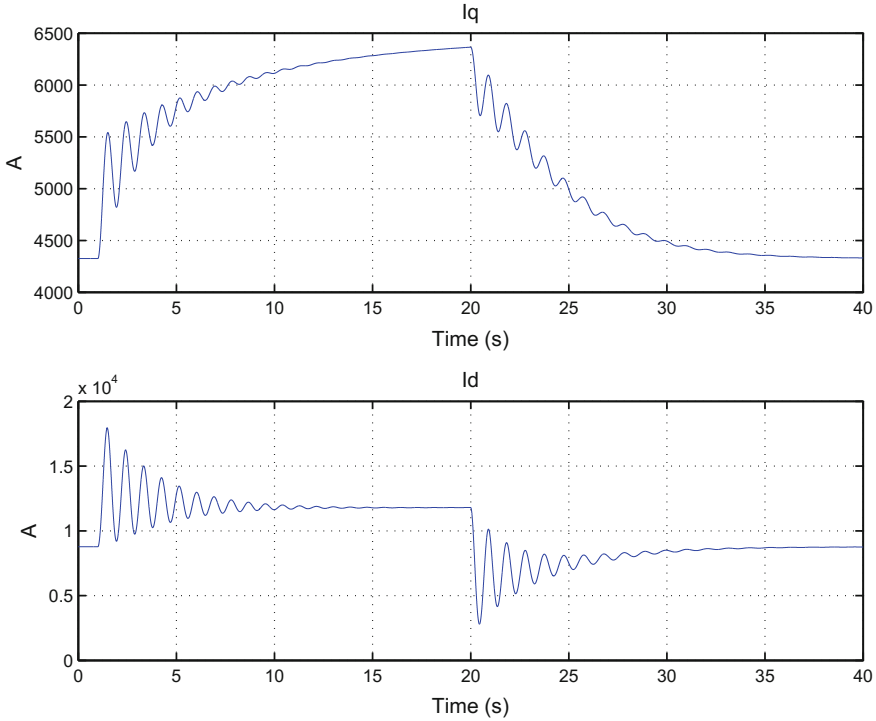Use the same process as in the first part of this exercise.

Fig. 2.9 i_{ds} and i_{qs}

3. Use (2.18) and (2.21) to show that:

$$i_{\text{fd}}^0 = \frac{v_{qs}^0 + r_s i_{qs}^0 + \omega L_d i_{ds}^0}{\omega L_{md}}.$$

Once δ^0 is known, v_{qs}^0, i_{ds}^0, and i_{qs}^0 can be written in terms of V_∞, δ^0, and ϕ.

2.2.13 Equal-Area Criterion

Equal-area criterion is a good way to understand the concept of first swing transient stability [9, vol. I & III]. It is best demonstrated with a SMIB system for a three-phase to ground fault on the synchronous machine terminals. Figure 2.13 is a graphical application of the criterion. The details are discussed next.

Let δ^0 be the steady-state angle of the synchronous machine, and a three-phase to ground fault occurs at the machine terminals. The electrical output power reduces to zero but the input mechanical power P_m^0 is unchanged. After a short time, when the machine angle is δ_{cl}, the fault is cleared. The acceleration energy applied to the rotor
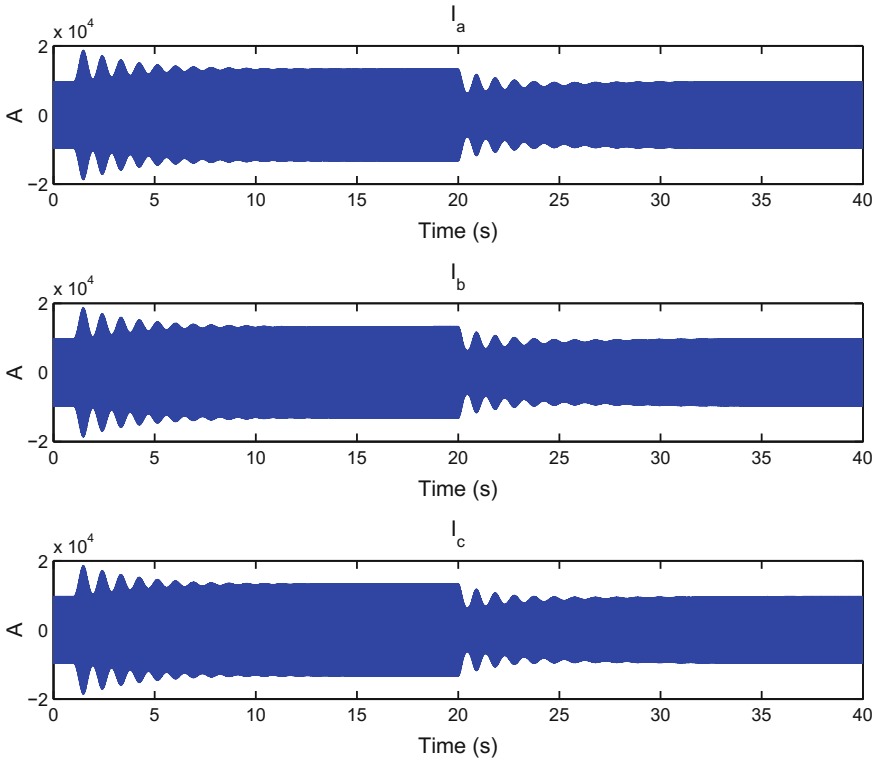
Fig. 2.10 i_a, i_b, and i_c

is the area in the rectangular box in Fig. 2.13. After the fault is cleared the output power is given by the power curve shown in Fig. 2.13 and the input mechanical power continues to be P_m^0. The deceleration energy is thus given by the shaded area between the output power curve and the constant P_m^0 line. If the acceleration energy is less than the deceleration energy then the generator has the first swing transient stability for the clearing angle δ_{cl}. The clearing angle for which the accelerating and decelerating energy are equal is called the critical clearing angle δ_{cr} and the corresponding time is called the critical clearing time t_{cr}.

1. Using the three different power output curves in the exercise in Sect. 2.2.10, calculate the critical clearing angle and time. Note that δ^0 using the steady-state and transient (with $\sin 2\delta$ term) power output expressions give the same δ^0 but for the transient power output expression, without the $\sin 2\delta$ term, a fictitious initial δ needs to be first calculated to match the steady-state input power.
2. Obtain the critical clearing angle and time using the numerical simulation in the exercise in Sect. 2.2.11. How does this compare with the critical values obtained with the three power output curves using the equal-area criterion? Which one is the closest to the t_{cr} obtained by numerical simulation?
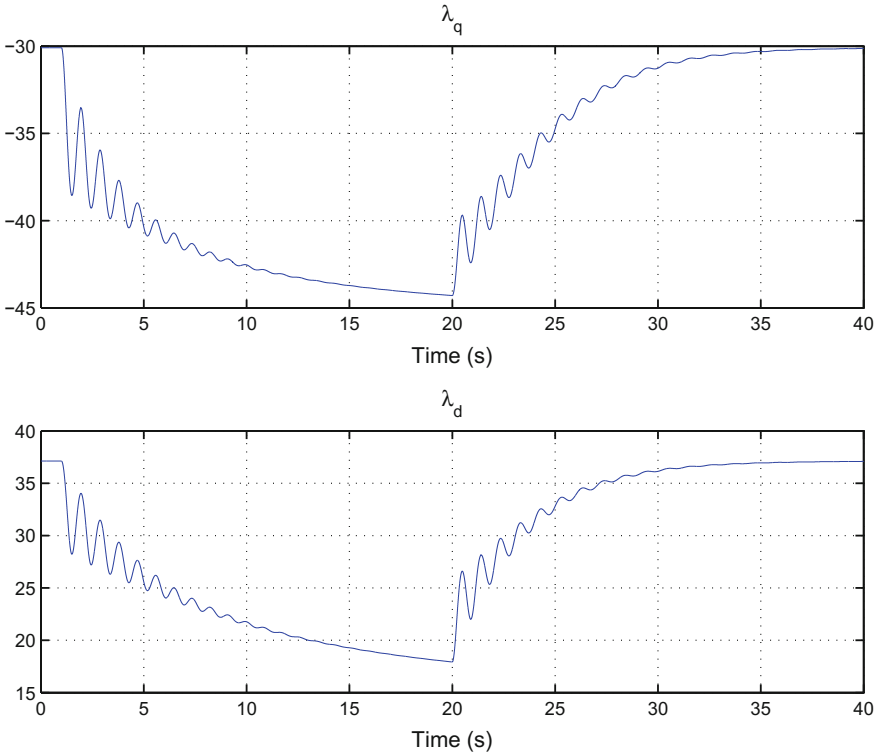
Fig. 2.11 λ_{ds} and λ_{qs}

2.2.14 Step Change in v_{fd} Simulation

Perform the steady-state analysis and the simulation for 1 s as in the exercise in Sect. 2.2.11. At 1 s change the field voltage v_{fd} to 11.4 V and simulate for 10 s. Plot i_{fd}, output power, and other variables.

2.2.15 Synchronous Machine V-Curves

Consider a SMIB system. For a fixed input power, the plot of the steady-state field-current versus the magnitude of the armature current is a V-curve such as shown in Fig. 2.14. Using Eqs. (2.18)–(2.21), show that the steady-state currents are:
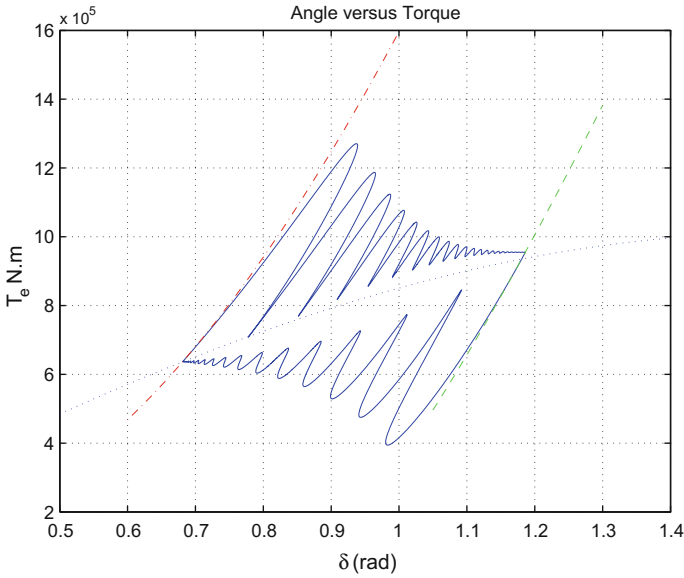
Fig. 2.12 Torque versus δ

Fig. 2.13 Equal-area criterion
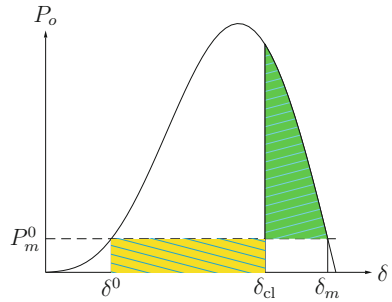
$$i_{ds}^0 = \frac{L_{md}}{L_d} i_{fd}^0 - \frac{v_{ds}^0}{\omega L_d}$$

$$i_{qs}^0 = \frac{v_{qs}^0}{\omega L_q}$$

For SMIB $v_{ds}^0 = V_\infty \sin \delta^0$, $v_{qs}^0 = V_\infty \cos \delta^0$, $i_a = i_{ds}^0 + J i_{qs}^0$, $v_a = v_{ds}^0 + J v_{qs}^0$, and PF $= \cos(\angle v_a - \angle i_a)$.

Plot the magnitude of the steady-state armature current and PF, as the field-current varies, for the synchronous machine data given in the exercise in Sect. 2.2.10. For each chosen value of i_{fd}^0 the expression in the exercise in Sect. 2.2.7 can be used to obtain δ^0 and then use the above expressions to obtain the plots.
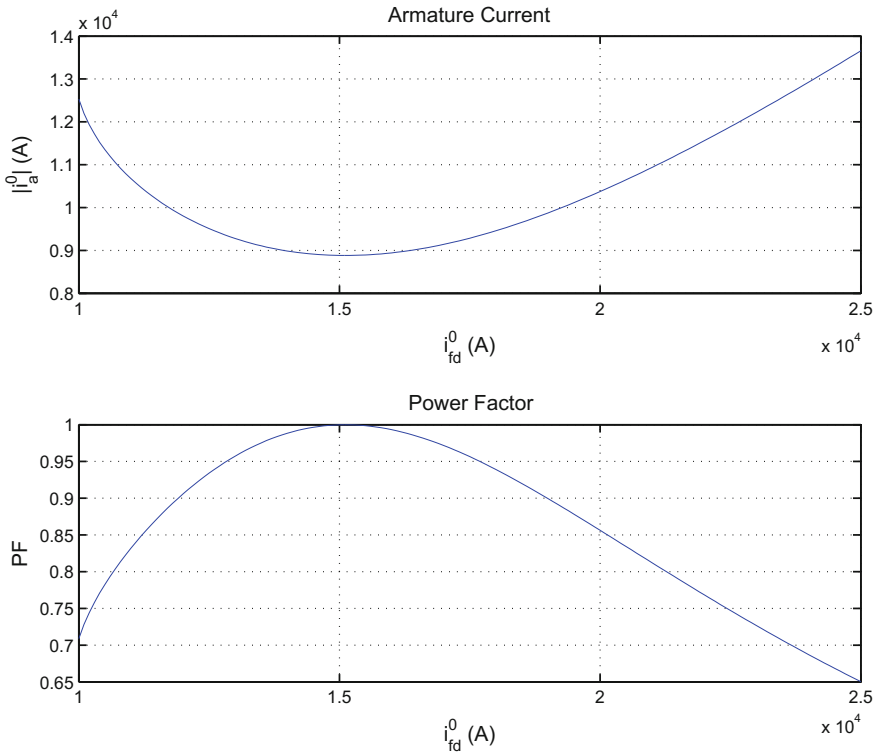
Fig. 2.14 Synchronous machine—V-curves

The ability of synchronous machine to deliver output electrical power at different power factors is the most important reason for it being the chosen machine as electrical generator. On the left side of the minimum point in the PF plot in Fig. 2.14, it supplies power to leading PF loads and on the right side to the lagging PF loads.

2.3 Phasor to dq-Frame Transformation

A detailed derivation of the synchronous machine model from the physical three-phase equations to the dq-frame is given below. The equations in the dq-frame are time-invariant and they are in a much simpler form than the equations in the three-phase variables. As shown in Part II of this derivation, the key simplification is achieved because of the sinusoidal form of the self and mutual inductance terms of the field and the armature coils.

Fig. 2.15 Synchronous
motor (currents in)
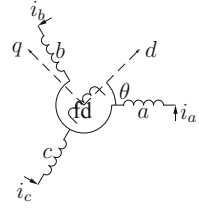
Fig. 2.16 Synchronous
generator (currents out)
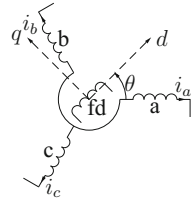
2.3.1 Phasor to dq-Frame—Part I

The phasor and dq-frame variables are related by

$$F_{dq0} = K_s F_{abc} \text{ and } F_{abc} = K_s^{-1} F_{dq0}$$

where abc, $dq0$ subscripts stand for phasor and dq-frame variables as in (2.2) and K_s, for transformation from abc to arbitrary dq-frame rotating at angular velocity ω, is given in (2.1) and reproduced here ($\dot{\theta} = \omega$),

$$K_s = \frac{2}{3} \begin{bmatrix} \cos(\theta) & \cos(\theta - \frac{2\pi}{3}) & \cos(\theta + \frac{2\pi}{3}) \\ -\sin(\theta) & -\sin(\theta - \frac{2\pi}{3}) & -\sin(\theta + \frac{2\pi}{3}) \\ \frac{1}{2} & \frac{1}{2} & \frac{1}{2} \end{bmatrix}$$

The schematic of synchronous machine is shown in Figs. 2.15 and 2.16. Here we consider *synchronous generator* equations, to get synchronous motor equations the directions of the currents need to be changed. For the synchronous machine with a field winding and three stator windings, the voltage equations can be written as:

$$v_{abcs} = -R_s i_{abcs} + \frac{d}{dt} \lambda_{abcs}$$

$$K_s^{-1} v_{dq0s} = -R_s K_s^{-1} i_{dq0s} + \frac{d}{dt} K_s^{-1} \lambda_{dq0}$$

$$v_{dq0s} = -K_s R_s K_s^{-1} i_{dq0s} + K_s \frac{d}{dt} K_s^{-1} \lambda_{dq0}, \text{ and}$$

$$v_{\text{fd}} = r_{\text{fd}} i_{\text{fd}} + \dot{\lambda}_{\text{fd}}$$

where $R_s = \text{diag}\,[r_s, r_s, r_s]$.

1. Show that

$$K_s^{-1} = \frac{3}{2}\bar{K}_s^T$$

   where $\bar{K}_s^T$ is the transpose of K_s but the third column is $\begin{bmatrix}1\ 1\ 1\end{bmatrix}^T$ instead of $\begin{bmatrix}\frac{1}{2}\ \frac{1}{2}\ \frac{1}{2}\end{bmatrix}^T$.

2. Show that

$$-K_s R_s K_s^{-1} = -R_s.$$

3. Show that

$$K_s \frac{d}{dt} K_s^{-1} = \omega \begin{bmatrix} 0 & -1 & 0 \\ 1 & 0 & 0 \\ 0 & 0 & 0 \end{bmatrix}$$

4. Show that the transformed equation, $K_s v_{abcs} = -K_s R_s K_s^{-1} i_{dq0} + K_s \frac{d}{dt} K_s^{-1}\lambda_{dq0}$, gives,

$$v_{ds} = -r_s i_{ds} - \omega\lambda_{qs} + \dot{\lambda}_{ds}$$
$$v_{qs} = -r_s i_{qs} + \omega\lambda_{ds} K_s^{-1} + \dot{\lambda}_{qs}$$
$$v_{0s} = -r_s i_{0s} + \dot{\lambda}_{0s}$$

2.3.2 Phasor to dq-Frame—Part II

The flux linkages for a synchronous machine with a field winding and three stator windings are written as:

$$\begin{bmatrix} \lambda_{abcs} \\ \lambda_{\mathrm{fd}} \end{bmatrix} = \begin{bmatrix} L_{ss} & L_{sr} \\ L_{sr}^T & L_{\mathrm{fd}} \end{bmatrix} \begin{bmatrix} -i_{abcs} \\ i_{\mathrm{fd}} \end{bmatrix}$$
$$K_s^{-1}\lambda_{dq0s} = -L_{ss} K_s^{-1} i_{dq0s} + L_{sr} i_{\mathrm{fd}}$$
$$\lambda_{dq0s} = -K_s L_{ss} K_s^{-1} i_{dq0s} + K_s L_{sr} i_{\mathrm{fd}}$$
$$\lambda_{\mathrm{fd}} = -L_{sr}^T K_s^{-1} i_{dq0s} + L_{\mathrm{fd}} i_{\mathrm{fd}}$$

where

$$L_{ss} = \begin{bmatrix} L_{ls} + L_A + L_B \cos 2\theta_r & -\frac{1}{2}L_A + L_B \cos 2\left(\theta_r - \frac{\pi}{3}\right) & -\frac{1}{2}L_A + L_B \cos 2\left(\theta_r + \frac{\pi}{3}\right) \\ -\frac{1}{2}L_A + L_B \cos 2\left(\theta_r - \frac{\pi}{3}\right) & L_{ls} + L_A + L_B \cos 2\left(\theta_r - \frac{2\pi}{3}\right) & -\frac{1}{2}L_A + L_B \cos 2\left(\theta_r + \pi\right) \\ -\frac{1}{2}L_A + L_B \cos 2\left(\theta_r + \frac{\pi}{3}\right) & -\frac{1}{2}L_A + L_B \cos 2\left(\theta_r + \pi\right) & L_{ls} + L_A + L_B \cos 2\left(\theta_r + \frac{2\pi}{3}\right) \end{bmatrix},$$

$L_{md} = \frac{3}{2}(L_A + L_B)$, $L_{mq} = \frac{3}{2}(L_A - L_B)$, $L_d = L_{ls} + L_{md}$, $L_q = L_{ls} + L_{mq}$,

$$L_{sr} = \begin{bmatrix} L_{md} \cos \theta_r \\ L_{md} \cos \left(\theta_r - \frac{2\pi}{3}\right) \\ L_{md} \cos \left(\theta_r + \frac{2\pi}{3}\right) \end{bmatrix}$$

When $\theta = \theta_r = \int_0^t \omega_r dt + \theta_r(0)$, where ω_r is the rotor angular velocity.

1. Show that

$$K_s L_{ss} K_s^{-1} = \begin{bmatrix} L_d & 0 & 0 \\ 0 & L_q & 0 \\ 0 & 0 & L_{ls} \end{bmatrix}$$

2. Show that

$$K_s L_{sr} = \begin{bmatrix} L_{md} \\ 0 \\ 0 \end{bmatrix}$$

3. Show that

$$L_{sr}^T K_s^{-1} = \begin{bmatrix} L_{md} & 0 & 0 \end{bmatrix}$$

4. Put all the above bits and pieces from Parts I and II together and form the Eqs. (2.18)–(2.22)and (2.25) when $\dot{\lambda}_{ds} = 0$ and $\dot{\lambda}_{qs} = 0$.
5. Let the steady-state voltages and currents for the synchronous machine shown in Fig. 2.16 be given by:

$$v_{abcs}^0 = \begin{bmatrix} V_m \cos(\omega t) \\ V_m \cos(\omega t - \frac{2\pi}{3}) \\ V_m \cos(\omega t + \frac{2\pi}{3}) \end{bmatrix} \text{ and } i_{abcs}^0 = \begin{bmatrix} I_m \cos(\omega t + \phi) \\ I_m \cos(\omega t + \phi - \frac{2\pi}{3}) \\ I_m \cos(\omega t + \phi + \frac{2\pi}{3}) \end{bmatrix}.$$

For a round rotor machine, the phasor relationship can be written as:

$$V_m \cos(\omega t) = -r_s I_m \cos(\omega t + \phi) - \omega L_d I_m \cos(\frac{\pi}{2} + \omega t + \phi) + \omega L_{md} i_{fd}^0 \cos(\omega t + \delta^0)$$

$$V_m \angle 0° = -r_s I_m \angle \phi - \jmath \omega L_d I_m \angle \phi + E_{fd}^0 \angle \delta^0,$$

where the rotor angular position $\theta_r = \omega t + \phi_r^0$, $\delta^0 = \frac{\pi}{2} + \phi_r^0$, $E_{fd}^0 = \omega L_{md} i_{fd}^0$, and ωL_d is known as the synchronous reactance (Fig. 2.17).

Fig. 2.17 Synchronous machine steady-state model
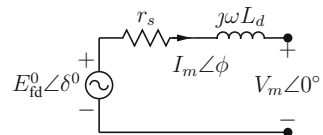
Fig. 2.18 Single machine
infinite bus—Load hlow
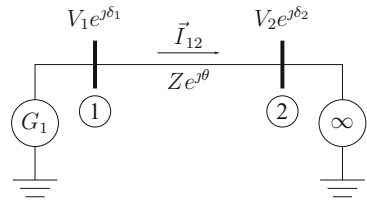
Fig. 2.19 SMIB via L_T
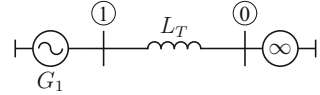
Exercise A synchronous machine, shown in the schematic in Fig. 2.18, is transferring
1 pu of real power to the mains. The mains voltage $V_m = 1$ pu, $E_{fd}^0 = 1$ pu, $r_s = 0.01$ pu, and $\omega L_d = 0.5$ pu. Calculate δ^0 and the reactive power transferred from the
synchronous machine to the mains.

2.3.3   Transmission Line L_T

The analysis above has been done for a synchronous machine directly connected to
the infinite-bus. Often the machine is connected via transmission line to the infinite-
bus. In this section we see the necessary changes to accommodate a transmission
line as seen in the single-line-diagram in Fig. 2.19.

1. A synchronous machine is directly connected to an infinite-bus with voltage V_∞.
   The voltage Eq. (2.35) can be written as:

$$\begin{bmatrix} V_\infty \sin \delta \\ V_\infty \cos \delta \end{bmatrix} = \begin{bmatrix} -r_s & \omega L'_q \\ -\omega L'_d & -r_s \end{bmatrix} \begin{bmatrix} i_{ds} \\ i_{qs} \end{bmatrix} + \begin{bmatrix} 0 \\ E'_q \end{bmatrix} \tag{2.46}$$

2. A synchronous machine, at bus 1, is connected to an infinite-bus, (∞ bus), with
   voltage V_∞, via a transmission line with inductance L_T and zero resistance, as
   shown in Fig. 2.19. The voltage Eq. (2.35) can be written as:

$$\begin{bmatrix} V_\infty \sin \delta_1 \\ V_\infty \cos \delta_1 \end{bmatrix} = \begin{bmatrix} -r_{s_1} & \omega(L'_{q_1} + L_T) \\ -\omega(L'_{d_1} + L_T) & -r_{s_1} \end{bmatrix} \begin{bmatrix} i_{ds_1} \\ i_{qs_1} \end{bmatrix} + \begin{bmatrix} 0 \\ E'_{q_1} \end{bmatrix}. \tag{2.47}$$

   Note that

$$(v_{D_1} + Jv_{Q_1}) - V_\infty = J\omega L_T(i_{D_1} + Ji_{Q_1}).$$

The above relationship can be obtained using:

$$v_{DQ0_1} = K_s \frac{d}{dt} K_s^{-1} K_s L_{TT} K_s^{-1} i_{DQ0_1} + v_{DQ0_0}$$

where L_{TT} is the transmission line inductance matrix):

$$L_{TT} = \begin{bmatrix} L_{TS} & L_{TM} & L_{TM} \\ L_{TM} & L_{TS} & L_{TM} \\ L_{TM} & L_{TM} & L_{TS} \end{bmatrix}$$

and $L_T = L_{TS} - L_{TM}$. Write the above equation as a matrix equation

$$\begin{bmatrix} v_{D_1} \\ v_{Q_1} \end{bmatrix} = \begin{bmatrix} 0 & -\omega L_T \\ \omega L_T & 0 \end{bmatrix} \begin{bmatrix} i_{D_1} \\ i_{Q_1} \end{bmatrix} + \begin{bmatrix} V_\infty \\ 0 \end{bmatrix}$$

and then transform DQ-variables to dq-variables using the $R(\phi_r)$ in the exercise in Sect. 2.2.11. Then eliminate v_{ds_1} and v_{qs_1} from the transformed version of the above equation and (2.35) to obtain the required relationship.

This exercise shows that for a synchronous machine connected to an infinite-bus via a transmission line, all the derived expressions for SMIB can be used for this case by replacing L'_{d_i} with $L'_{d_i} + L_T$ and L'_{q_i} with $L'_{q_i} + L_T$.

2.3.4 Terminal Voltage V_T

A synchronous machine, at bus 1, is connected to an infinite-bus, (∞ bus), with voltage V_∞, as shown in Fig. 2.19, via a transmission line with inductance L_T and zero resistance. For $r_{s_1} = 0$, show that

$$v_{ds_1} = \frac{L'_{q_1} v_{d0}}{L_T + L'_{q_1}} \text{ and } v_{qs_1} = \frac{L'_{d_1} v_{q0}}{L_T + L'_{d_1}} + \frac{L_T E'_{q_1}}{L_T + L'_{d_1}}.$$

Note that (L_{TT} is the transmission line inductance matrix):

$$v_{qd0_1} = K_s \frac{d}{dt} K_s^{-1} K_s L_{TT} K_s^{-1} i_{dq0_1} + v_{dq0_0}$$

$$\begin{bmatrix} v_{ds_1} \\ v_{qs_1} \end{bmatrix} = \begin{bmatrix} 0 & -\omega L_T \\ \omega L_T & 0 \end{bmatrix} \begin{bmatrix} i_{ds_1} \\ i_{qs_1} \end{bmatrix} + \begin{bmatrix} v_{d0} \\ v_{q0} \end{bmatrix}$$

Eliminate i_{ds_1} and i_{qs_1} from the above equation and (2.35) (with $r_{s_1} = 0$) to obtain the required result. The terminal voltage is:

$$V_{T_1} = \sqrt{v_{ds_1}^2 + v_{qs_1}^2}$$

2.4 Operational Impedance

A synchronous machine model that captures its entire dynamics is very complex and not much use in getting insights into the synchronous machine dynamics. This means that modelling techniques must be chosen where the complexity level of the model can be chosen depending on the application. A modelling technique that is very popular with engineering applications is to parameterise the models using time-constants. For a dynamic model each time-constant indicates the duration for which the transient associated with that time-constant will be a part of the solution. Once the time interval for the analysis is known, approximate models can be derived by neglecting the dynamics associated with smaller time-constants.

This process of parameterising the model using time-constants is greatly facilitated by using Laplace domain representation of dynamic equations. Strictly speaking Laplace representation can be used only for linear systems but nonlinear blocks can be inserted judiciously in Laplace representation based block diagram representation. This modelling technique is used by almost all commercial power system analysis software. Here we look at that technique in enough details such that the parameterisation used by most power system analysis packages is covered. The Laplace domain representation is known as the operational impedance method for synchronous machines.

For a synchronous machine with no damper windings, it can be seen that flux linkages and stator currents are related via the following Laplace transformed relationships:

$$\Lambda_{qs_i}(s) = -\hat{L}_{q_i} I_{qs_i}(s) \tag{2.48}$$

$$\Lambda_{ds_i}(s) = -\hat{L}_{d_i} \frac{1 + s\tau'_{d_i}}{1 + s\tau'_{do_i}} I_{ds_i}(s) + \frac{L_{md_i}}{1 + s\tau'_{do_i}} V_{\mathrm{fd}_i}(s) \tag{2.49}$$

where $\hat{L}_{q_i} = L_{q_i}, \hat{L}_{d_i} = L_{d_i}, \tau'_{d_i} = \frac{L'_{d_i} L_{\mathrm{fd}_i}}{r_{\mathrm{fd}_i}}$, and $\tau'_{do_i} = \frac{L_{\mathrm{fd}_i}}{r_{\mathrm{fd}_i}}$. Use (2.20) to derive (2.48) and use (2.12), (2.20), (2.21) to derive (2.49).

Now let us look at the approximations we can make to simplify the blocks in (2.49). If the time-constant τ'_{d_i} is much smaller than the time interval of interest, we can write (2.49) as:

$$\Lambda_{ds_i}(s) = -\hat{L}_{d_i} \frac{1}{1 + s\tau'_{do_i}} I_{ds_i}(s) + \frac{L_{md_i}}{1 + s\tau'_{do_i}} V_{\mathrm{fd}_i}(s)$$

Further if τ'_{do_i} is much smaller than the time interval of interest, we can write (2.49) as:

$$\Lambda_{ds_i}(s) = -\hat{L}_{d_i} I_{ds_i}(s) + L_{md_i} V_{\mathrm{fd}_i}(s)$$

The use of operational impedance model is most useful when damper windings on the rotor are included in the model. Next, we cover the subtransient model, i.e.,

the model that includes damper windings. Please note that the operational impedance model only includes the electrical part of the system and is mostly used to obtain parameters to model the electrical transients in the model.

2.4.1 Operational Impedance and Sub-transient Model

The synchronous machine dynamics is like a mass-spring system with very little mechanical damping. Electrical damping is introduced in the machine by putting extra sets of windings on the rotor and shorting them. When the rotational speed of the synchronous machine is different from its synchronous speed, currents are induced in these shorted rotor coils that dissipate energy and provide damping. Accurate synchronous machine models include the effect of the damper windings.

For the design of controllers for power oscillation damping, synchronous machine model with one rotor winding (stator transients neglected) gives acceptable transient period simulation. For the sake of completeness and comparison with other models existing in the literature, a detailed sub-transient model with three damper windings is derived in this section. The derivation follows the same ideas as for a single rotor winding—rotor coil fluxes are state variables and field voltage and stator dq-axis currents are the inputs to the dynamic equations.

The effect of the damper windings can be modelled by including three damper windings, two on the q-axis and one on the d-axis of the rotor, as shown in Fig. 2.20. The Laplace transformed flux linkage of each coil and voltages on the field coil and equivalent d and q-axis coils are given in the equations below:

Fig. 2.20 Synchronous machine with damper windings
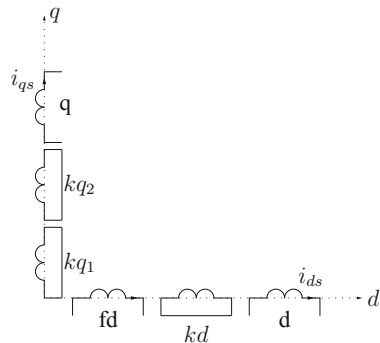
$$\Lambda_{ds} = -L_d I_{ds} + L_{md}(I_{\text{fd}} + I_{kd}) \tag{2.50}$$

$$\Lambda_{\text{fd}} = L_{\text{fd}} I_{\text{fd}} + L_{md}(-I_{ds} + I_{kd}) \tag{2.51}$$

$$\Lambda_{kd} = L_{kd} I_{kd} + L_{md}(-I_{ds} + I_{\text{fd}}) \tag{2.52}$$

$$V_{\text{fd}}(s) = r_{\text{fd}} I_{\text{fd}} + s\Lambda_{\text{fd}} \tag{2.53}$$

$$V_{kd}(s) = r_{kd} I_{kd} + s\Lambda_{kd} \tag{2.54}$$

The q-axis relationships can be obtained from the d-axis relationships (2.50)–(2.54) by changing fd $\rightarrow kq_1$ and kd $\rightarrow kq_2$.

$$\Lambda_{qs} = -L_q I_{qs} + L_{mq}(I_{kq_1} + I_{kq_2}) \tag{2.55}$$

$$\Lambda_{kq_1} = L_{kq_1} I_{kq_1} + L_{mq}(-I_{qs} + I_{kq_2}) \tag{2.56}$$

$$\Lambda_{kq_2} = L_{kq_2} I_{kq_2} + L_{mq}(-I_{qs} + I_{kq_1}) \tag{2.57}$$

$$V_{kq_1}(s) = r_{kq_1} I_{kq_1} + s\Lambda_{kq_1} \tag{2.58}$$

$$V_{kq_2}(s) = r_{kq_2} I_{kq_2} + s\Lambda_{kq_2} \tag{2.59}$$

The above Eqs. (2.50)–(2.59) are written as below after eliminating rotor variables:

$$\Lambda_{qs}(s) = -\hat{L}_q(s) I_{qs}(s) \tag{2.60}$$

$$\Lambda_{ds}(s) = -\hat{L}_d(s) I_{ds}(s) + G(s) V_{\text{fd}}(s) \tag{2.61}$$

Expressions for $\hat{L}_q(s)$, $\hat{L}_d(s)$, and $G(s)$, when all the three damper windings are short-circuited ($V_{kd} = V_{kq_1} = V_{kq_2} = 0$) are given below:

$$\Lambda_{qs}(s) = -\frac{s^2 \tau_{q_1} + s\tau_{q_2} + \tau_{q_3}}{\Delta_q(s)} I_{qs}(s) \tag{2.62}$$

where
$\Delta_q(s) = s^2(L_{kq_1} L_{kq_2} - L_{mq}^2) + s(L_{kq_1} r_{kq_2} + L_{kq_2} r_{kq_1}) + r_{kq_1} r_{kq_2}$
$\tau_{q_1} = L_{mq}^2(L_q + L_{kq_1} + L_{kq_2} - 2L_{mq}) - L_q L_{kq_1} L_{kq_2}$,
$\tau_{q_2} = -L_q(L_{kq_1} r_{kq_2} + L_{kq_2} r_{kq_1}) + L_{mq}^2(r_{kq_1} + r_{kq_2})$,
$\tau_{q_3} = -L_q r_{kq_1} r_{kq_2}$

$$\Lambda_{ds}(s) = -\frac{s^2 \tau_{d_1} + s\tau_{d_2} + \tau_{d_3}}{\Delta_d(s)} I_{ds}(s) + \frac{n(s)}{\Delta_d(s)} V_{\text{fd}}(s) \tag{2.63}$$

where
$n(s) = L_{md} r_{kd} + s(L_{md} L_{kd} - L_{md}^2)$, $\Delta_d(s) = s^2(L_{kd} L_{\text{fd}} - L_{md}^2) + s(L_{kd} r_{\text{fd}}$
$+ L_{\text{fd}} r_{kd}) + r_{kd} r_{\text{fd}}$
$\tau_{d_1} = L_{md}^2(L_d + L_{kd} + L_{\text{fd}} - 2L_{md}) - L_d L_{kd} L_{\text{fd}}$,
$\tau_{d_2} = -L_d(L_{kd} r_{\text{fd}} + L_{\text{fd}} r_{kd}) + L_{md}^2(r_{kd} + r_{\text{fd}})$,
$\tau_{d_3} = -L_d r_{kd} r_{\text{fd}}$

$$G(s) = \frac{n(s)}{\Delta_d(s)} = \frac{s(L_{md}L_{kd} - L_{md}^2) + L_{md}r_{kd}}{s^2(L_{kd}L_{fd} - L_{md}^2) + s(L_{kd}r_{fd} + L_{fd}r_{kd}) + r_{kd}r_{fd}} \tag{2.64}$$

Define:

$$
\begin{aligned}
&\hat{L}_d(s) = -\left.\frac{\Lambda_{ds}(s)}{I_d(s)}\right|_{\substack{v_{fd}=0 \\ v_{kd}=0}} \quad
\hat{L}_q(s) = -\left.\frac{\Lambda_{qs}(s)}{I_q(s)}\right|_{\substack{v_{kq_1}=0 \\ v_{kq_2}=0}} \\[4pt]
&L_d = \lim_{\substack{s\to 0 \\ r_{kd}\to\infty}} \hat{L}_d(s) \qquad\quad
L_q = \lim_{\substack{s\to 0 \\ r_{kq_2}\to\infty}} \hat{L}_q(s) \\[4pt]
&L'_d = \lim_{\substack{s\to\infty \\ r_{kd}\to\infty}} \hat{L}_d(s) \qquad\quad
L'_q = \lim_{\substack{s\to\infty \\ r_{kq_2}\to\infty}} \hat{L}_q(s) \\[4pt]
&L''_d = \lim_{s\to\infty} \hat{L}_d(s) \qquad\qquad
L''_q = \lim_{s\to\infty} \hat{L}_q(s)
\end{aligned}
\tag{2.65}
$$

The expressions for $\Lambda_{ds}(s)$ and $\Lambda_{qs}(s)$ in (2.62), (2.63) have ratio of second order polynomials. For practical values of synchronous machine inductances these polynomials have real roots and thus it is a common practice to write them as products of first-order polynomials as below.

$$\Lambda_{qs}(s) = -L_q \frac{(1+s\tau'_q)(1+s\tau''_q)}{(1+s\tau'_{qo})(1+s\tau''_{qo})} I_{qs}(s) = -L_q \frac{(1+\frac{L'_q}{L_q}s\tau'_{qo})(1+\frac{L''_q}{L'_q}s\tau''_{qo})}{(1+s\tau'_{qo})(1+s\tau''_{qo})} I_{qs}(s)$$

$$\Lambda_{ds}(s) = -L_d \frac{(1+s\tau'_d)(1+s\tau''_d)}{(1+s\tau'_{do})(1+s\tau''_{do})} I_{ds}(s) + \frac{n(s)}{(1+s\tau'_{do})(1+s\tau''_{do})} V_{fd}(s)$$

where $(1+s\tau'_d)(1+s\tau''_d) = (1+\frac{L'_d}{L_d}s\tau'_{do})(1+\frac{L''_d}{L'_d}s\tau''_{do})$. The parameters $\tau'_q, \tau''_q, \tau'_d$, and τ''_d are known as short-circuit parameters and $\tau'_{qo}, \tau''_{qo}, \tau'_{do}$, and τ''_{do} are open-circuit parameters. They are related by the definitions of the transient and sub-transient reactance in (2.65).

Exercise Show that

$$\left.\frac{I_{fd}(s)}{I_{ds}(s)}\right|_{V_{fd}=0} = sG(s)$$

where $G(s)$ is given in (2.64).

2.4.2 Synchronous Machine Sub-transient Model

The operational impedance sub-transient model developed in the previous section applies to the electrical transients, neglecting saturation and other nonlinear effects.

The operational impedance model is mostly used to obtain machine parameters using experimental frequency response measurements. Next a general sub-transient synchronous machine model is developed.

Equations (2.50)–(2.52) can be solved for rotor winding currents and stator d-axis flux and written in time-domain as:

$$i_{\text{fd}} = \frac{L_{\text{kd}}\lambda_{\text{fd}} - L_{md}\lambda_{\text{kd}} + (L_{md}L_{\text{kd}} - L_{md}^2)i_{ds}}{L_{\text{fd}}L_{\text{kd}} - L_{md}^2} \tag{2.66}$$

$$i_{\text{kd}} = \frac{-L_{md}\lambda_{\text{fd}} + L_{\text{fd}}\lambda_{\text{kd}} + (L_{md}L_{\text{fd}} - L_{md}^2)i_{ds}}{L_{\text{fd}}L_{\text{kd}} - L_{md}^2} \tag{2.67}$$

$$\lambda_{ds} = \frac{L_{md}L_{\text{kd}} - L_{md}^2}{L_{\text{fd}}L_{\text{kd}} - L_{md}^2}\lambda_{\text{fd}} + \frac{L_{fd}L_{md} - L_{md}^2}{L_{\text{fd}}L_{\text{kd}} - L_{md}^2}\lambda_{\text{kd}} + L_d''i_{ds}$$

$$\lambda_{ds} = \frac{L_d'' - L_{ls}}{L_d' - L_{ls}}\frac{E_q'}{\omega} + \frac{L_d' - L_d''}{L_d' - L_{ls}}\lambda_{\text{kd}} + L_d''i_{ds} \tag{2.68}$$

The above d-axis rotor winding currents can be used to write the dynamic equations as follows.

$$\dot{\lambda}_{\text{fd}} = -r_{\text{fd}}i_{\text{fd}} + v_{\text{fd}}$$

$$\frac{1}{\omega}\dot{E}_q' = -\frac{r_{\text{fd}}}{L_{\text{fd}}}\left(\frac{L_{\text{kd}}L_{\text{fd}}}{L_{\text{fd}}L_{\text{kd}} - L_{md}^2}\frac{E_q'}{\omega} - \frac{L_{md}^2}{L_{\text{fd}}L_{\text{kd}} - L_{md}^2}\lambda_{\text{kd}} + \frac{L_{md}(L_{md}L_{\text{kd}} - L_{md}^2)}{L_{\text{fd}}L_{\text{kd}} - L_{md}^2}i_{ds} - \frac{L_{md}}{r_{\text{fd}}}v_{\text{fd}}\right)$$

$$\frac{1}{\omega}\dot{E}_q' = -\frac{r_{\text{fd}}}{L_{\text{fd}}}\left(\frac{E_q'}{\omega} - \frac{L_{md}^2}{L_{\text{fd}}L_{\text{kd}} - L_{md}^2}(\lambda_{\text{kd}} - \frac{E_q'}{\omega}) - \frac{L_{md}(L_{md}L_{\text{kd}} - L_{md}^2)}{L_{\text{fd}}L_{\text{kd}} - L_{md}^2}i_{ds} - \frac{L_{md}}{r_{\text{fd}}}v_{\text{fd}}\right)$$

$$\frac{1}{\omega}\dot{E}_q' = -\frac{1}{T_{do}'}\left(\frac{E_q'}{\omega} - \frac{(L_d' - L_d'')(L_d - L_d')}{(L_d' - L_{ls})^2}(\lambda_{\text{kd}} - \frac{E_q'}{\omega}) + (L_d - L_d')\left(1 - \frac{L_d' - L_d''}{L_d' - L_{ls}}\right)i_{ds} - \frac{L_{md}}{r_{\text{fd}}}v_{\text{fd}}\right) \tag{2.69}$$

$$\dot{\lambda}_{\text{kd}} = -r_{\text{kd}}i_{\text{kd}}$$

$$\dot{\lambda}_{\text{kd}} = -\frac{r_{\text{kd}}L_{\text{fd}}}{L_{\text{fd}}L_{\text{kd}} - L_{md}^2}\left(\lambda_{\text{kd}} - \frac{E_q'}{\omega} + \frac{L_{md}L_{\text{fd}} - L_{md}^2}{L_{\text{fd}}}i_{ds}\right)$$

$$\dot{\lambda}_{\text{kd}} = -\frac{1}{T_{do}''}\left(\lambda_{\text{kd}} - \frac{E_q'}{\omega} + (L_d' - L_{ls})i_{ds}\right) \tag{2.70}$$

The derivations for simplification of the above equations are done next.

2.4.2.1 Basic d-Axis Relationships

First the a few definitions from Sect. 2.2 are reproduced here. The symbols have the same meaning as in Eqs. (2.23) and (2.30).

$$L_d = L_{ls} + L_{md}, \quad L_q = L_{ls} + L_{mq}, \quad L_{fd} = L_{lfd} + L_{md},$$

$$L_d' = \frac{L_{lfd}L_{md}}{L_{fd}} + L_{ls} = L_d - \frac{L_{md}^2}{L_{fd}}, \quad L_q' = L_{ls} + L_{mq}.$$

In the following all the inductance terms appearing in Eqs. (2.69) and (2.70) are rewritten in terms of L_d', L_d'', L_{ls}, L_q', L_q'', and time-constants. The inductance terms are also manipulated so that a physical meaning can be given to the machine parameters.

1. The transient inductance L_d' can be seen as a series and parallel combination of leakage and mutual inductances:

$$L_d' = L_{ls} + \frac{L_{md}L_{lfd}}{L_{fd}} = L_d - \frac{L_{md}^2}{L_{fd}} = L_{ls} + \frac{1}{\frac{1}{L_{md}} + \frac{1}{L_{lfd}}}$$

2. Field leakage written in terms of mutual, transient, and leakage inductances:

$$\frac{1}{L_{lfd}} = \frac{1}{L_d' - L_{ls}} - \frac{1}{L_{md}} = \frac{L_{md} - (L_d' - L_{ls})}{L_{md}(L_d' - L_{ls})} = \frac{L_d - L_{ls} - (L_d' - L_{ls})}{L_{md}(L_d' - L_{ls})}$$

$$\Rightarrow L_{lfd} = \frac{L_{md}(L_d' - L_{ls})}{L_d - L_d'}$$

3. Applying the definition in Eq. (2.65), we can write sub-transient inductance as a series and parallel combination of mutual and leakage inductances:

$$L_d'' = L_{ls} + \frac{1}{\frac{1}{L_{md}} + \frac{1}{L_{lfd}} + \frac{1}{L_{lkd}}}$$

4. The following progression of expressions derive relationships to arrive at Eqs. (2.69) and (2.70).

$$L_{lkd} = \frac{(L_d' - L_{ls})(L_d'' - L_{ls})}{L_d' - L_d''}$$

$$\frac{1}{L_{lkd}} = \frac{1}{L_d'' - L_{ls}} - \frac{1}{L_{md}} - \frac{1}{L_{lfd}}$$

$$= \frac{1}{L_d'' - L_{ls}} - \frac{1}{L_d' - L_{ls}}$$

$$\frac{L_{\mathrm{fd}}}{L_{\mathrm{fd}}L_{\mathrm{kd}} - L_{md}^2} = \frac{L_{\mathrm{fd}}}{(L_{l\mathrm{fd}} + L_{md})L_{l\mathrm{kd}} + L_{l\mathrm{fd}}L_{md}} = \frac{1}{L_{l\mathrm{kd}} + \frac{L_{l\mathrm{fd}}L_{md}}{L_{\mathrm{fd}}}}$$

$$\Rightarrow \frac{L_{\mathrm{fd}}}{L_{\mathrm{fd}}L_{\mathrm{kd}} - L_{md}^2} = \frac{1}{L_{l\mathrm{kd}} + (L_d' - L_{ls})} = \frac{L_d' - L_d''}{(L_d' - L_{ls})^2}$$

$$\frac{L_{md}^2}{L_{\mathrm{fd}}L_{\mathrm{kd}} - L_{md}^2} = \frac{L_{\mathrm{fd}}(L_d - L_d')}{L_{\mathrm{fd}}L_{\mathrm{kd}} - L_{md}^2} = \frac{(L_d' - L_d'')(L_d - L_d')}{(L_d' - L_{ls})^2}$$

$$\frac{L_{\mathrm{fd}}L_{\mathrm{kd}}}{L_{\mathrm{fd}}L_{\mathrm{kd}} - L_{md}^2} = 1 + \frac{L_{md}^2}{L_{\mathrm{fd}}L_{\mathrm{kd}} - L_{md}^2}$$

$$\frac{L_{md}^2 L_{l\mathrm{kd}}}{L_{\mathrm{fd}}L_{\mathrm{kd}} - L_{md}^2} = \frac{(L_d'' - L_{ls})(L_d - L_d')}{L_d' - L_{ls}}$$

$$\frac{L_{md}L_{\mathrm{fd}} - L_{md}^2}{L_{\mathrm{fd}}L_{\mathrm{kd}} - L_{md}^2} = \frac{L_{md}L_{l\mathrm{fd}}}{L_{\mathrm{fd}}L_{\mathrm{kd}} - L_{md}^2} = \frac{L_{md}L_{l\mathrm{fd}}}{L_{\mathrm{fd}}} \frac{L_{\mathrm{fd}}}{L_{\mathrm{fd}}L_{\mathrm{kd}} - L_{md}^2} = \frac{L_d' - L_d''}{L_d' - L_{ls}}$$

$$\frac{L_{md}L_{\mathrm{kd}} - L_{md}^2}{L_{\mathrm{fd}}L_{\mathrm{kd}} - L_{md}^2}\lambda_{\mathrm{fd}} = \frac{L_{md}L_{l\mathrm{kd}}}{L_{\mathrm{fd}}L_{\mathrm{kd}} - L_{md}^2}\lambda_{\mathrm{fd}} = \frac{L_{\mathrm{fd}}L_{l\mathrm{kd}}}{L_{\mathrm{fd}}L_{\mathrm{kd}} - L_{md}^2}\frac{E_q'}{\omega} = \frac{L_d'' - L_{ls}}{L_d' - L_{ls}}\frac{E_q'}{\omega}$$

$$L_{md}\frac{L_{md}L_{\mathrm{kd}} - L_{md}^2}{L_{\mathrm{fd}}L_{\mathrm{kd}} - L_{md}^2} = L_{md}\frac{L_{md}(L_{md} + L_{l\mathrm{kd}}) - L_{md}^2}{L_{\mathrm{fd}}L_{\mathrm{kd}} - L_{md}^2} = \frac{L_{md}^2 L_{l\mathrm{kd}}}{L_{\mathrm{fd}}L_{\mathrm{kd}} - L_{md}^2}$$

$$\Rightarrow L_{md}\frac{L_{md}L_{\mathrm{kd}} - L_{md}^2}{L_{\mathrm{fd}}L_{\mathrm{kd}} - L_{md}^2} = (L_d - L_d')\frac{L_d'' - L_{ls}}{L_d' - L_{ls}} = (L_d - L_d')\left(1 - \frac{L_d' - L_d''}{L_d' - L_{ls}}\right)$$

The q-axis relationships can be obtained from the d-axis relationships by changing $\mathrm{fd} \to kq_1$ and $\mathrm{kd} \to kq_2$.

Let,

$$E_{\mathrm{fd}} = \frac{v_{\mathrm{fd}}L_{md}}{r_{\mathrm{fd}}}, \quad E_q' = \omega\frac{L_{md}}{L_{\mathrm{fd}}}\lambda_{\mathrm{fd}}, \quad E_d' = \omega\frac{L_{md}}{L_{kq_1}}\lambda_{kq_1}$$

$$T_{do}' = \frac{L_{\mathrm{fd}}}{r_{\mathrm{fd}}}, \quad T_{do}'' = \frac{L_{\mathrm{fd}}L_{\mathrm{kd}} - L_{md}^2}{r_{\mathrm{kd}}L_{\mathrm{fd}}}$$

A block diagram representation of Eqs. (2.69) and (2.70) is shown in Fig. 2.21. A block diagram representation of the Eq. (2.68) is shown in Fig. 2.22.
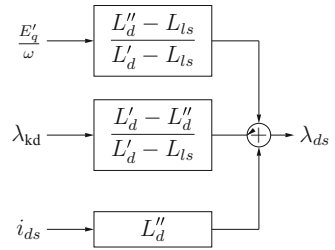
The q-axis relationships can be obtained from the d-axis relationships by changing $\mathrm{fd} \to kq_1$ and $\mathrm{kd} \to kq_2$. A block diagram representation of q-axis dynamic equations is shown in Fig. 2.23. A block diagram representation of the λ_{qs} is shown in Fig. 2.24.
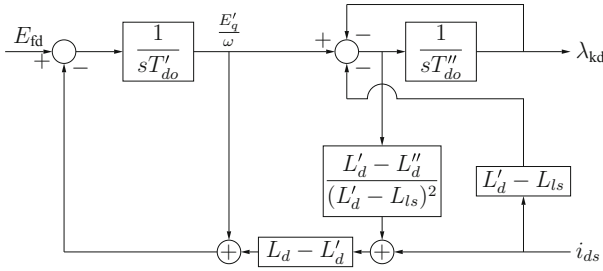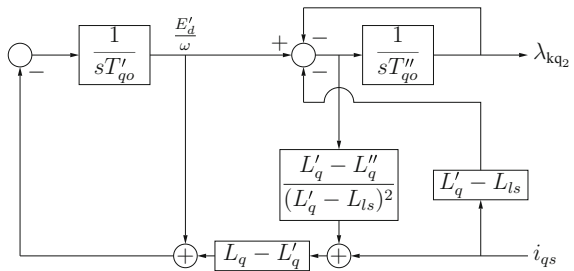
Fig. 2.21 Machine with damper windings—d-axis dynamics block
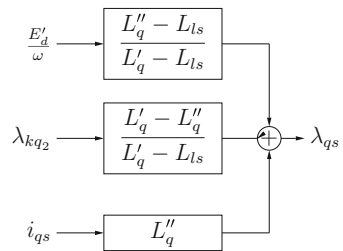

Fig. 2.22 Machine with damper windings—d-axis stator flux

Fig. 2.23 Machine with damper windings—q-axis dynamics block

Fig. 2.24 Machine with damper windings—q-axis stator flux

2.4.2.2 Typical Synchronous Machine Parameters [8, p. 153]

Parameter		Hydro	Thermal
Synchronous reactance	X_d	0.6–1.5	1.0–2.3
	X_q	0.4–1.0	1.0–2.3
Transient reactance	X'_d	0.2–0.5	0.15–0.4
	X'_q	–	0.3–1.0
Subransient reactance	X''_d	0.15–0.35	0.12–0.25
	X''_q	0.2–0.45	0.12–0.25
Transient open-circuit time constant	T'_{d0}	1.5–9.0 s	3.0–10.0 s
	T'_{q0}	–	0.5–2.0 s
Subtransient open-circuit time constant	T''_{d0}	0.01–0.05 s	0.02–0.05 s
	T''_{q0}	0.01–0.09 s	0.02–0.05 s
Stator leakage reactance	X_l	0.1–0.2	0.1–0.2
Stator resistance	r_s	0.002–0.02	0.0015–0.005

The reactances and resistances are in per units and the time-constants are in seconds.

2.4.2.3 Transient and Steady-State Models

Transient model can be dervided from the subtransient model by considering $r_{kd} \rightarrow \infty$, $r_{kq_1} \rightarrow \infty$, and $r_{kq_2} \rightarrow \infty$ in (2.65) for the expressions of sub-transient reactances. The steady-state model is obtained by setting $i_{\mathrm{fd}}^0 = \frac{v_{\mathrm{fd}}}{r_{\mathrm{fd}}}$ and then calculating the stator currents.

2.5 Induction Machine

Let us consider a P_i pole induction machine with the schematic shown in Fig. 2.25. Both the stator and rotor have three windings. The choice of symbols is the same as for the synchronous machine described in Sect. 2.2.

The dynamic equations for the rotor flux in the induction motor (for generator operation change the sign of the current terms) connected to bus i ([6, p. 150]),
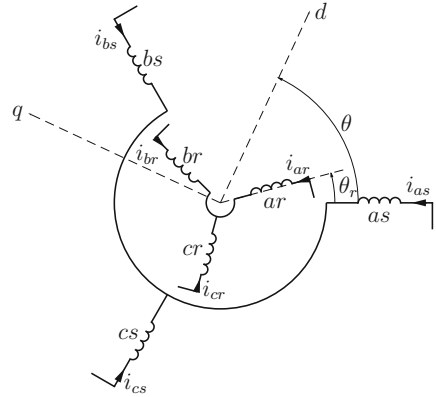
$$\dot{\lambda}_{qr_i} = -r_{r_i} i_{qr_i} - (\omega - \omega_{r_i})\lambda_{dr_i} + v_{qr_i} \tag{2.71}$$

$$\dot{\lambda}_{dr_i} = -r_{r_i} i_{dr_i} + (\omega - \omega_{r_i})\lambda_{qr_i} + v_{dr_i} \tag{2.72}$$

$$J_i \left(\frac{2}{P_i} \right) \dot{\omega}_{r_i} = T_{e_i} - T_{L_i} \tag{2.73}$$

where ω is the angular velocity of the rotating dq-frame,

Fig. 2.25 Induction machine

$$T_{e_i} = \left(\frac{3}{2}\right)\left(\frac{P_i}{2}\right)\left(\lambda_{qr_i} i_{dr_i} - \lambda_{dr_i} i_{qr_i}\right) \tag{2.74}$$

The angular velocity of the rotating dq-frame, ω, can be different from the supply frequency of $2\pi 50$ rad s^{-1} or $2\pi 60$ rad s^{-1}. In most cases ω is chosen equal to the supply frequency, but it can be different and this fact must be noted. Equations (2.71)–(2.73) are derived in full further in this chapter.

Algebraic equations or constraints for the induction machine connected to bus i,

$$v_{qs_i} = r_{s_i} i_{qs_i} + \omega \lambda_{ds_i} \tag{2.75}$$

$$v_{ds_i} = r_{s_i} i_{ds_i} - \omega \lambda_{qs_i} \tag{2.76}$$

$$\lambda_{qs_i} = L_{ls_i} i_{qs_i} + L_M \left(i_{qs_i} + i_{qr_i}\right) \tag{2.77}$$

$$\lambda_{ds_i} = L_{ls_i} i_{ds_i} + L_M \left(i_{ds_i} + i_{dr_i}\right) \tag{2.78}$$

$$\lambda_{qr_i} = L_{lr_i} i_{qr_i} + L_M \left(i_{qs_i} + i_{qr_i}\right) \tag{2.79}$$

$$\lambda_{dr_i} = L_{lr_i} i_{dr_i} + L_M \left(i_{ds_i} + i_{dr_i}\right) \tag{2.80}$$

The model of the induction machine is given by the differential Eqs. (2.71)–(2.73) and algebraic Eqs. (2.75) and (2.76) with λ_{ds_i}, λ_{qs_i}, i_{dr_i}, and i_{qr_i}, written in terms of i_{ds_i} and i_{qs_i}. Equations (2.77)–(2.80) are solved for λ_{ds_i}, λ_{qs_i}, i_{dr_i}, and i_{qr_i} in terms of i_{ds_i} and i_{qs_i}. The following material till Sect. 2.5.1 gives the details of these manipulations. On first reading these details can be skipped but please be sure to derive all the equations to get familiar with the model.

Eliminating λ_{ds}, λ_{qs}, i_{dr}, and i_{qr} from Eq. (2.77)–(2.80),

$$\lambda_{ds_i} = \frac{L_{M_i}}{L_{dr_i}} \lambda_{dr_i} + \frac{L_{ds_i} L_{dr_i} - L_{M_i}^2}{L_{dr_i}} i_{ds_i} \tag{2.81}$$

$$\lambda_{qs_i} = \frac{L_{M_i}}{L_{qr_i}} \lambda_{qr_i} + \frac{L_{qs_i} L_{qr_i} - L_{M_i}^2}{L_{qr_i}} i_{qs_i} \tag{2.82}$$

$$i_{dr_i} = \frac{\lambda_{dr_i}}{L_{dr_i}} - \frac{L_{M_i}}{L_{dr_i}} i_{ds_i} \tag{2.83}$$

$$i_{qr_i} = \frac{\lambda_{qr_i}}{L_{qr_i}} - \frac{L_{M_i}}{L_{qr_i}} i_{qs_i} \tag{2.84}$$

where $L_{qr_i} = L_{lr_i} + L_{M_i}$, $L_{dr_i} = L_{lr_i} + L_{M_i}$, $L_{qs_i} = L_{ls_i} + L_{M_i}$, and $L_{ds_i} = L_{ls_i} + L_{M_i}$. Note that $L_{qr_i} = L_{dr_i}$ and $L_{qs_i} = L_{ds_i}$, we also define $L_{rr_i} = L_{qr_i} = L_{dr_i}$ and $L_{ss_i} = L_{qs_i} = L_{ds_i}$.

The three differential Eqs. (2.71)–(2.73) can now be written as:

$$\dot{\lambda}_{qr_i} = -\frac{r_{r_i}}{L_{qr_i}} \lambda_{qr_i} - (\omega - \omega_{r_i}) \lambda_{dr_i} + \frac{r_{r_i} L_{M_i}}{L_{qr_i}} i_{qs_i} + v_{qr_i} \tag{2.85}$$

$$\dot{\lambda}_{dr_i} = -\frac{r_{r_i}}{L_{dr_i}} \lambda_{dr_i} + (\omega - \omega_{r_i}) \lambda_{qr_i} + \frac{r_{r_i} L_{M_i}}{L_{dr_i}} i_{ds_i} + v_{dr_i} \tag{2.86}$$

$$J_i \left(\frac{2}{P_i} \right) \dot{\omega}_{r_i} = \left(\frac{3}{2} \right) \left(\frac{P_i}{2} \right) \frac{L_{M_i}}{L_{dr_i}} \left(\lambda_{dr_i} i_{qs_i} - \lambda_{qr_i} i_{ds_i} \right) - T_{L_i} \tag{2.87}$$

The two algebraic Eqs. (2.75) and (2.76) can now be written as:

$$v_{qs_i} = r_{s_i} i_{qs_i} + \omega \frac{L_{ds_i} L_{dr_i} - L_{M_i}^2}{L_{dr_i}} i_{ds_i} + \omega \frac{L_{M_i}}{L_{dr_i}} \lambda_{dr_i} \tag{2.88}$$

$$v_{ds_i} = r_{s_i} i_{ds_i} - \omega \frac{L_{qs_i} L_{qr_i} - L_{M_i}^2}{L_{qr_i}} i_{qs_i} - \omega \frac{L_{M_i}}{L_{qr_i}} \lambda_{qr_i} \tag{2.89}$$

2.5.1 The Model

The model consists of the three differential Eqs. (2.85)–(2.87), with

$$x_i = \begin{bmatrix} \lambda_{dr_i} \\ \lambda_{qr_i} \\ \omega_{r_i} \end{bmatrix}, \quad u_i = \begin{bmatrix} v_{dr_i} \\ v_{qr_i} \end{bmatrix} \tag{2.90}$$

The dq-frame of the ith induction machine is aligned with the a-axis of the i bus voltage, thus $v_{D_i} = v_{ds_i}$, $v_{Q_i} = v_{qs_i}$, $i_{D_i} = i_{ds_i}$, and $i_{Q_i} = i_{qs_i}$, from this the algebraic constraint equations can be written as:

$$\begin{bmatrix} v_{D_i} \\ v_{Q_i} \end{bmatrix} = Z_{DQ_i} \begin{bmatrix} i_{D_i} \\ i_{Q_i} \end{bmatrix} + D_{a_i} x_i \tag{2.91}$$

where

$$Z_{DQ_i} = \begin{bmatrix} r_{s_i} & -\omega \dfrac{L_{qs_i} L_{qr_i} - L_{M_i}^2}{L_{qr_i}} \\ \omega \dfrac{L_{ds_i} L_{dr_i} - L_{M_i}^2}{L_{dr_i}} & r_{s_i} \end{bmatrix}, \quad D_{a_i} = \begin{bmatrix} 0 & -\dfrac{\omega L_{M_i}}{L_{qr_i}} & 0 \\ \dfrac{\omega L_{M_i}}{L_{dr_i}} & 0 & 0 \end{bmatrix} \quad (2.92)$$

The above equations in the per unit system are written exactly the same way as for the synchronous machine as discussed in Sect. 2.2.2.

2.5.2 Steady-State Conditions

At steady-state Eqs. (2.85)–(2.87) (with $\dot{\lambda}_{dr_i} = 0$, $\dot{\lambda}_{qr_i} = 0$, $\dot{\omega}_{r_i} = 0$), (2.88), (2.89) can be solved to obtain $\omega_{r_i}^0$, $\lambda_{dr_i}^0$, $\lambda_{qr_i}^0$, $i_{ds_i}^0$, $i_{qs_i}^0$, and $\omega = 2\pi 50\,\mathrm{rad\,s^{-1}}$. Alternatively, s_i^0, $i_{ds_i}^0$, $i_{qs_i}^0$, $i_{dr_i}^0$, $i_{qr_i}^0$ can be obtained from putting together the equivalent circuit in the exercise in Sect. 2.5.3 and steady-state torque expression in the exercise in Sect. 2.5.4. Finally, (2.79) and (2.80) can be used to obtain $\lambda_{dr_i}^0$ and $\lambda_{qr_i}^0$.
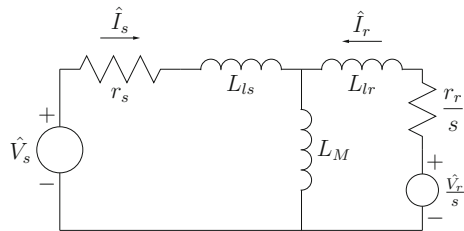
2.5.3 Steady-State Equivalent Circuit

Equations (2.71) and (2.72) (with $\dot{\lambda}_{qr_i} = 0$ and $\dot{\lambda}_{dr_i} = 0$), Eqs. (2.75)–(2.80), can be used to show that the circuit in Fig. 2.26 is an equivalent circuit for steady-state operation of an induction machine (eliminate flux variables and write the equations in terms of phasor current and voltage variables).

$$v_{ds} + jv_{qs} = r_s(i_{ds} + ji_{qs}) + j\omega L_{ss}(i_{ds} + ji_{qs}) + j\omega L_M(i_{dr} + ji_{qr})$$
$$v_{dr} + jv_{qr} = r_r(i_{dr} + ji_{qr}) + j(\omega - \omega_r)L_{rr}(i_{dr} + ji_{qr}) + j(\omega - \omega_r)L_M(i_{ds} + ji_{qs})$$

The phasor quantities in the equivalent circuit in Fig. 2.26 are $\hat{V}_s = v_{ds} + jv_{qs}$, $\hat{I}_s = i_{ds} + ji_{qs}$, $\hat{I}_r = i_{dr} + ji_{qr}$, and $\hat{V}_r = v_{dr} + jv_{qr}$.

Fig. 2.26 Induction machine steady-state equivalent circuit

2.5.4 Steady-State Output Power

Using the electrical torque expression in (2.87) it is easy to show that $T_e = \left(\frac{3}{2}\right)\left(\frac{P}{2}\right) L_M \Im(\hat{I}_r^* \hat{I}_s)$:

$$
\begin{aligned}
T_e &= \left(\frac{3}{2}\right)\left(\frac{P}{2}\right)\frac{L_M}{L_{dr}}\left(\lambda_{dr} i_{qs} - \lambda_{qr} i_{ds}\right) \\
&= \left(\frac{3}{2}\right)\left(\frac{P}{2}\right) L_M \left(i_{dr} i_{qs} - i_{qr} i_{ds}\right)
\end{aligned}
$$

Using the steady-state equivalent circuit in Fig. 2.26 we see that the steady-state output power is given by ($v_{dr} = v_{qr} = 0$, $s = \frac{\omega - \omega_r}{\omega}$):

$$
P_e = \omega_r T_e = \left(\frac{3}{2}\right)\left(\frac{P}{2}\right)\left|\hat{I}_r\right|^2 \frac{\omega_r r_r}{\omega - \omega_r} = \left(\frac{3}{2}\right)\left(\frac{P}{2}\right)\left|\hat{I}_r\right|^2 \frac{(1-s)r_r}{s}
$$

2.5.5 Steady-State Torque Versus Speed

Using the torque expression in the exercise in Sect. 2.5.4 and the equivalent circuit in Fig. 2.26 show that the steady-state is given by ($v_{dr} = v_{qr} = 0$, $s = \frac{\omega - \omega_r}{\omega}$):

$$
T_e = \frac{\frac{3}{2}\frac{P}{2}\omega L_M^2 r_r s |\hat{V}_s|^2}{\left(r_s r_r + s\omega^2 \left(L_M^2 - L_{ss} L_{rr}\right)\right)^2 + \omega^2 \left(r_r L_{ss} + s r_s L_{rr}\right)^2}
$$

Note that:

$$
\hat{I}_s = \frac{\hat{V}_s}{r_s + J\omega L_{ls} + \frac{J\omega L_M \left(J\omega L_{lr} + \frac{r_r}{s}\right)}{J\omega L_{rr} + \frac{r_r}{s}}},
$$

$$
\hat{I}_r = -\hat{I}_s \frac{J\omega L_M}{J\omega L_{rr} + \frac{r_r}{s}},
$$

and

$$
L_{ls} L_M + L_{lr} L_M + L_{ls} L_{lr} = L_{ss} L_{rr} - L_M^2.
$$

Exercise An induction motor is connected to an infinite bus and it has the following parameter values: $P = 2$; $T_L = \dfrac{2.4e3}{\omega}$ N m; $L_{ls} = 0.0139$ H; $L_{lr} = 0.01228$ H; $L_{ds} = 0.3826$ H; $L_{dr} = 0.38098$ H; $r_s = 1.77\,\Omega$; $r_r = 1.34\,\Omega$; $V_m = (\sqrt{2/3})460$ V; $v_{dr} = v_{qr} = 0$; $J = 0.025$ kg m^2. Assume the induction motor dq-frame aligned with the infinite bus DQ-frame, i.e., $v_{ds} = V_m$ and $v_{qs} = 0$.

For the steady-state operation of the above induction motor, plot

1. Electric torque versus speed (or slip)
2. Input current magnitude versus speed (or slip)
3. Reactive power input versus speed (or slip)

2.5.6 Doubly-Fed Induction Machine—Steady-State

A squirrel cage induction machine consumes reactive power both in the motor and generator modes. A doubly-fed induction machine can be both a consumer and a supplier of reactive power. In this exercise we see that by suitable adjustment of the rotor voltage the reactive power consumption of the machine can be controlled.

Parameters for a doubly-fed induction motor, in the given base values, are given below (quantities without units next to them are per unit values).

The base quantities are chosen as: $VA_b = 2.4 \times 10^3$ VA; $E_{s_b} = \sqrt{\frac{2}{3}}460$ V; $f_b = 50$ Hz; $I_{s_b} = \frac{VA_b}{(3/2E_{s_b})}$; $Z_{s_b} = \frac{E_{s_b}}{I_{s_b}}$; $\omega_b = 2\pi f_b$; $\omega_{m_b} = \omega_b$; $L_{s_b} = \frac{Z_{s_b}}{\omega_b}$; $\lambda_{sb} = L_{s_b} I_{s_b}$; $I_{r_b} = I_{s_b}$; $E_{r_b} = E_{s_b}$; $Z_{r_b} = \frac{E_{r_b}}{I_{r_b}}$; $L_{r_b} = \frac{Z_{r_b}}{omega_b}$; $J_b = \frac{VA_b}{\omega_{m_b}^2}$.

The parameters in per unit representation are: $\omega_0 = 2\pi 50$ rad s^{-1}, $\omega = \frac{\omega_0}{\omega_b}$; $P_e = \frac{2.4e3}{VA_b}$; $T_{load} = \frac{0.5Pe}{\omega}$; $L_{ss} = \frac{0.3826}{L_{s_b}}$; $L_{rr} = \frac{0.38098}{L_{r_b}}$; $L_{sm} = \frac{0.3687}{L_{s_b}}$; $r_s = \frac{1.77}{Z_{s_b}}$; $r_r = \frac{1.34}{Z_{r_b}}$; $L_{ls} = L_{ss} - L_{sm}$; $L_{lr} = L_{rr} - L_{sm}$; $V_m = \frac{\sqrt{2}460/\sqrt{3}}{E_{s_b}}$; $J = \frac{0.025}{J_b}$; $V_s = V_m(\cos(0) + \jmath \sin(0))$; $V_{rm} = 0.05$.

Show that when this induction motor is running at a slip of 0 05, the variation of the steady-state phase and amplitude of the stator current ($\hat{I}_s$ in Fig. 2.26) with the phase of the applied rotor voltage is as shown in Fig. 2.27. This curve is similar to the V-curve of the synchronous machine. Thus a doubly-fed induction machine can provide characteristics similar to synchronous machine during the steady-state operaion.

The parameters in this exercise are in terms of dq-axis, to work out the phasor rotor voltages the transformation matrix K_r in the exercise in Sect. 2.6.1 should be used.

2.5.7 Exercise—Voltage Behind Transient Inductance

Show that Eqs. (2.88) and (2.89) can be represented by the equivalent circuit shown in Fig. 2.28, where

$$L'_s = \frac{L_{ds}L_{dr} - L_M^2}{L_{dr}}, \; v'_d = -\omega\frac{L_M}{L_{qr}}\lambda_{qr}, \text{ and } v'_q = \omega\frac{L_M}{L_{dr}}\lambda_{dr}$$
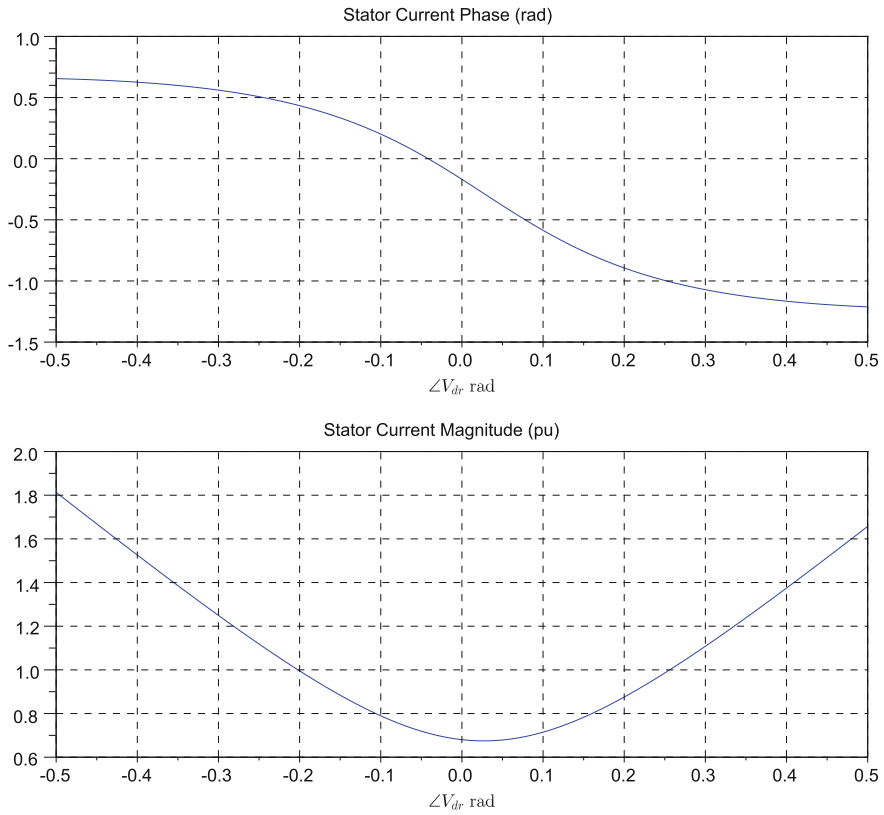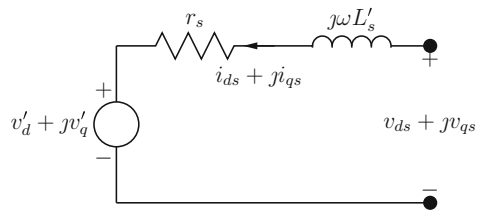
Stator Current Phase (rad)

$\angle V_{dr}$ rad

Stator Current Magnitude (pu)

$\angle V_{dr}$ rad

Fig. 2.27 DFIM—V-curves

Fig. 2.28 Voltage behind
transient inductance

2.5.8 Doubly-Fed Induction Machine

From the modelling point of view the chief difference between doubly-fed and short-circuited rotor machine is considering v_{dr_i} and v_{qr_i} in (2.85) and (2.86). In all the derivations done in the exercises here, if v_{dr_i} and v_{qr_i} are non-zero then it models a doubly-fed machine and for $v_{dr_i} = v_{qr_i} = 0$, it is a squirrel cage or short-circuited-

rotor induction machine. The actually applied rotor voltages and v_{dr_i}, v_{qr_i} are related by the transformation K_r in the exercise in Sect. 2.6.1.

2.5.9 Vector Control

In most power system simulations the dq-frame of the induction motor is aligned with the DQ-frame connected to the bus. There are many applications, vector control being one of the most useful one, where the dq-frame of the induction motor is positioned such that the d-axis is aligned with the rotor flux.

Repeat the simulations in the exercise in Sect. 2.5.5 with the d-axis of the dq-frame aligned with the rotor flux. Plot the angle between the d-axis and phase-a peak, given by δ below. The following changes need to be made in the simulation in Sect. 2.5.5 for this simulation.

1. Since the d-axis, rotating at an angular velocity ω_v, is chosen to be aligned with the rotor flux, we have $\lambda_{qr} = 0$ and $\dot{\lambda}_{qr} = 0$. This means that Eqs. (2.79) and (2.85) provide constraints and give ω_v, the angular velocity of the rotating dq-frame,

$$\omega_v = \omega_r + \frac{r_r L_M}{L_{qr}} \frac{i_{qs}}{\lambda_{dr}} + \frac{v_{qr}}{\lambda_{dr}} \ (\omega_r \text{ is the rotor angular velocity})$$

and we have to add the following equation to replace (2.85),

$$\dot{\delta} = \omega_v - \omega_s$$

where $\omega_s = 2\pi 50$.

2. dq and DQ currents are related as follows (for SMIB $v_D = V_m$, $v_Q = 0$),

$$R(\phi_r) = \begin{bmatrix} \sin\delta & -\cos\delta \\ \cos\delta & \sin\delta \end{bmatrix}, \quad \begin{bmatrix} i_{ds} \\ i_{qs} \end{bmatrix} = R(\phi_r) \begin{bmatrix} i_D \\ i_Q \end{bmatrix}, \quad \begin{bmatrix} v_{ds} \\ v_{qs} \end{bmatrix} = R(\phi_r) \begin{bmatrix} v_D \\ v_Q \end{bmatrix}$$

3. For steady-state values, solve Eqs. (2.86), (2.87) (with $\dot{\lambda}_{dr} = 0$, $\dot{\omega}_r = 0$), (2.88), (2.89) to obtain δ^0, λ_{dr}^0, i_{ds}^0, i_{qs}^0, and using Eq. (2.85) with $\dot{\lambda}_{qr} = 0$,

$$\omega_r^0 = 2\pi 50 - \frac{r_r L_M}{L_{qr}} \frac{i_{qs}^0}{\lambda_{dr}^0}$$

The above equations are a complete description of induction machine dynamics but to achieve vector control the following equation is needed to obtain v_{dqr} from v_{abcr}

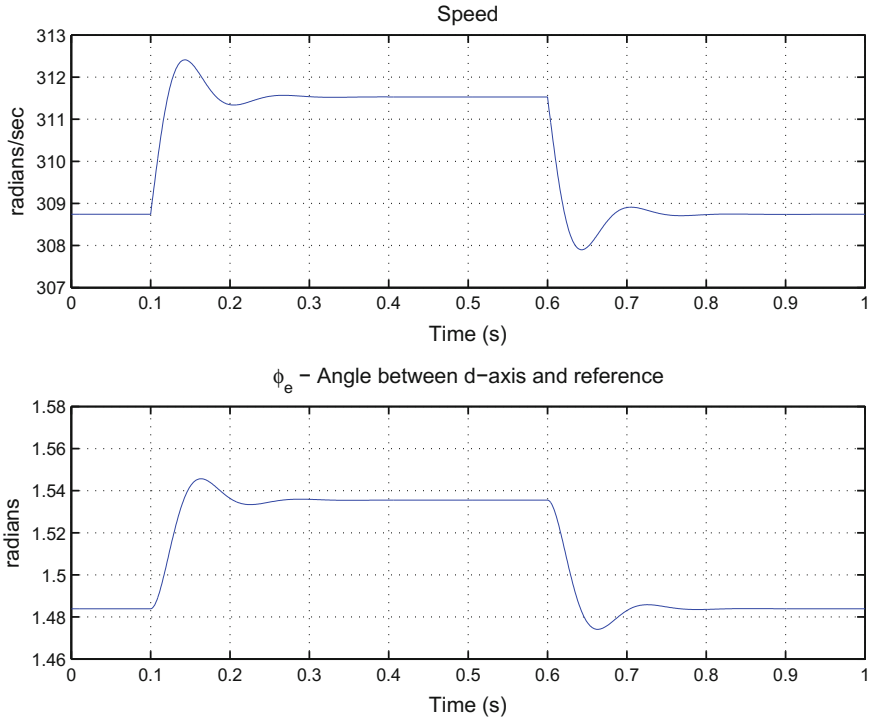$$\dot{\delta}_r = \omega_r - \omega_r^0 \text{ and } \theta_r = \omega_r^0 t + \delta_r.$$

Fig. 2.29 Speed ω_r and ϕ_e

The plots from the simulation using vector control are shown in Figs. 2.29, 2.30, 2.31 and 2.32.
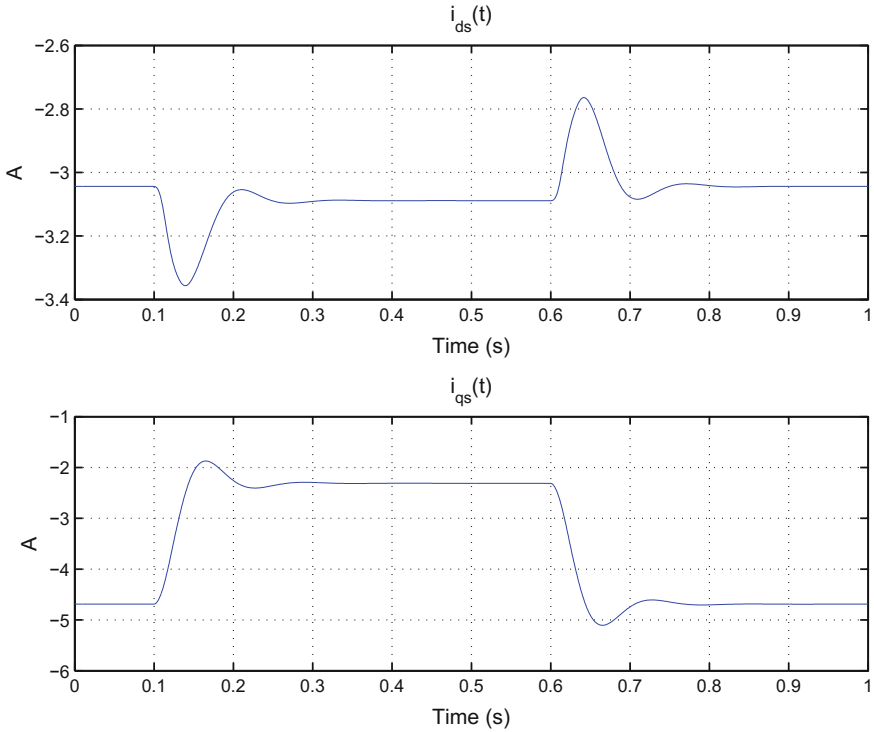
2.5.10 Dynamic Equations with δ

At times it is useful to write the dynamic equations for induction machines in a structure similar to the synchronous machine. The equations in the exercise in Sect. 2.5.9 can be used to write the SMIB equations as ($r_s = 0$):

$$\dot{\lambda}_{dr} = -\left(\frac{r_r}{L_{dr}} + \frac{r_r L_M^2}{L_{dr}^2 L_s'}\right)\lambda_{dr} + \frac{r_r L_M}{\omega_s L_{dr} L_s'}V_\infty \cos\delta + v_{dr} \qquad (2.93)$$

$$\dot{\delta} = -(\omega_s - \omega_r) - \frac{r_r L_M}{\omega_s L_{qr} L_s'}\frac{V_\infty \sin\delta}{\lambda_{dr}} + \frac{v_{qr}}{\lambda_{dr}} \qquad (2.94)$$

$$J\left(\frac{2}{P}\right)\dot{\omega}_r = \left(\frac{3}{2}\right)\left(\frac{P}{2}\right)\frac{L_M}{L_{dr}}\left(-\lambda_{dr}\frac{V_\infty \sin\delta}{\omega_s L_s'}\right) - T_L \qquad (2.95)$$

Fig. 2.30 i_{ds} and i_{qs}

Note that for the induction machine connected to the infinite-bus $v_{ds} = V_{\infty} \sin \delta$
and $v_{qs} = V_{\infty} \cos \delta$. Use the equivalent circuit in Fig. 2.28 to obtain the currents
$i_{ds} = \frac{-v'_q + V_{\infty} \cos \delta}{\omega_s L'_s}$ and $i_{qs} = \frac{-V_{\infty} \sin \delta}{\omega_s L'_s}$. Here we assume that the d-axis of the rotating
frame is aligned with the rotor flux and thus all the relationship in the exercise in
Sect. 2.5.9 can be applied to obtain the above dynamic equations.

2.6   Phasor to dq-Frame Transformation

Similar to the development of the dq-frame equations for the synchronous machine,
a derivation for induction machines is given below.
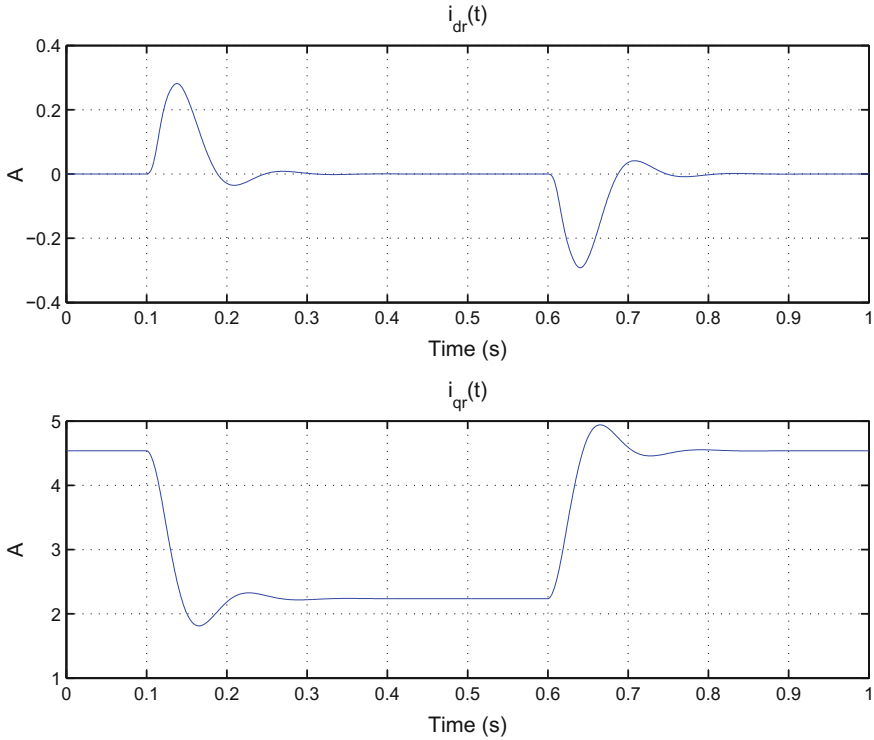
Fig. 2.31 i_{dr} and i_{qr}

2.6.1 Phasor to dq-Frame—Part I

For an induction machine with a schematic as shown in Fig. 2.25, the phasor and dq-frame variables are related by

$$F_{dq0} = K_s F_{abc} \text{ and } F_{abc} = K_s^{-1} F_{dq0}$$

where abc, $dq0$ subscripts stand for phasor and dq-frame variables as in (2.2) and K_s is given in (2.1) and reproduced here ($\dot{\theta} = \omega$),

$$K_s = \frac{2}{3} \begin{bmatrix} \cos(\theta) & \cos(\theta - \frac{2\pi}{3}) & \cos(\theta + \frac{2\pi}{3}) \\ -\sin(\theta) & -\sin(\theta - \frac{2\pi}{3}) & -\sin(\theta + \frac{2\pi}{3}) \\ \frac{1}{2} & \frac{1}{2} & \frac{1}{2} \end{bmatrix}$$

where $\theta = \int_0^t \omega dt + \theta_0$, ω can be any arbitray speed but here it is the synchronous speed, i.e., the frequency of the applied stator voltage and θ_0 is the position of the stator phase-a coil at time zero.
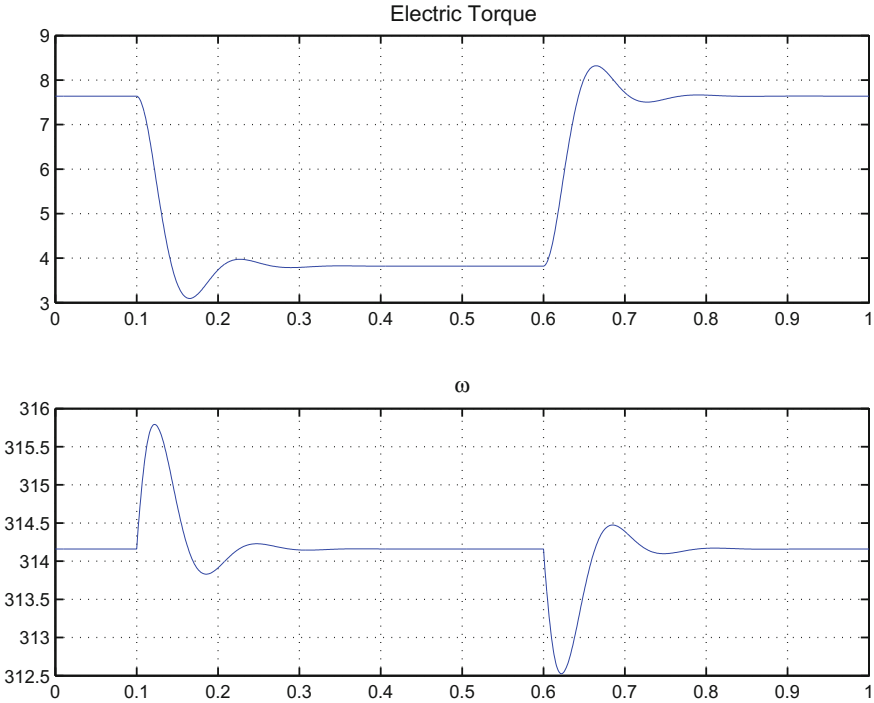
Fig. 2.32 Electric torque and ω

$$K_r = \frac{2}{3} \begin{bmatrix} \cos(\theta - \theta_r) & \cos(\theta - \theta_r - \frac{2\pi}{3}) & \cos(\theta - \theta_r + \frac{2\pi}{3}) \\ -\sin(\theta - \theta_r) & -\sin(\theta - \theta_r - \frac{2\pi}{3}) & -\sin(\theta - \theta_r + \frac{2\pi}{3}) \\ \frac{1}{2} & \frac{1}{2} & \frac{1}{2} \end{bmatrix}$$

where $\theta_r = \int_0^t \omega_r dt + \theta_r(0)$, ω_r is the angular velocity of the rotor and $\theta_r(0)$ is its initial position. Please note (see Fig. 2.25):

1. θ is the angle between the d-axis of the dq-frame rotating at angular velocity ω and stator phase-a coil.
2. $\theta - \theta_r$ is the angle between the rotor phase-a coil and the d-axis of the rotating frame. The angle between the rotor a-coil and stator a-coil is θ_r.

For a round rotor induciton motor with three stator windings and three rotor windings the voltage equations can be written as:

$$v_{abcj} = R_j i_{abcj} + \frac{d}{dt} \lambda_{abcj}$$

$$K_j^{-1} v_{dq0j} = R_j K_j^{-1} i_{dq0j} + \frac{d}{dt} K_j^{-1} \lambda_{abcj}$$

$$v_{dq0j} = K_j R_j K_j^{-1} i_{dq0j} + K_j \frac{d}{dt} K_j^{-1} \lambda_{dq0j}, \text{ and}$$

where j may be replaced by s for stator and r for rotor, $R_s = \text{diag}\,[r_s, r_s, r_s]$, and
$R_r = \text{diag}\,[r_r, r_r, r_r]$.

1. Show that

$$K_j^{-1} = \frac{3}{2} \bar{K}_j^T.$$

where $\bar{K}_j^T$ is the transpose of K_j but the third column is $\begin{bmatrix} 1 & 1 & 1 \end{bmatrix}^T$ instead of
$\begin{bmatrix} \frac{1}{2} & \frac{1}{2} & \frac{1}{2} \end{bmatrix}^T$.

2. Show that

$$K_j R_j K_j^{-1} = R_j.$$

3. Show that

$$K_s \frac{d}{dt} K_s^{-1} = \omega \begin{bmatrix} 0 & -1 & 0 \\ 1 & 0 & 0 \\ 0 & 0 & 0 \end{bmatrix}$$

4. Show that

$$K_r \frac{d}{dt} K_r^{-1} = (\omega - \omega_r) \begin{bmatrix} 0 & -1 & 0 \\ 1 & 0 & 0 \\ 0 & 0 & 0 \end{bmatrix}$$

5. Show that

$$v_{ds} = r_r i_{ds} - \omega \lambda_{qs} + \dot{\lambda}_{ds}$$
$$v_{qs} = r_r i_{qs} + \omega \lambda_{ds} + \dot{\lambda}_{qs}$$
$$v_{0s} = r_r i_{0s} + \dot{\lambda}_{0s}$$

6. Show that

$$v_{dr} = r_r i_{dr} - (\omega - \omega_r) \lambda_{qr} + \dot{\lambda}_{dr}$$
$$v_{qr} = r_r i_{qr} + (\omega - \omega_r) \lambda_{dr} + \dot{\lambda}_{qr}$$
$$v_{0r} = r_r i_{0r} + \dot{\lambda}_{0r}$$

2.6.2 Phasor to dq-Frame—Part II

The flux linkages for an induction machine with a field winding and three stator windings are written as:

$$\begin{bmatrix} \lambda_{abcs} \\ \lambda_{abcr} \end{bmatrix} = \begin{bmatrix} L_{ss} & L_{sr} \\ L_{sr}^T & L_{rr} \end{bmatrix} \begin{bmatrix} i_{abcs} \\ i_{abcr} \end{bmatrix}$$

$$\begin{bmatrix} \lambda_{dq0s} \\ \lambda_{dq0r} \end{bmatrix} = \begin{bmatrix} K_s L_{ss} K_s^{-1} & K_s L_{sr} K_r^{-1} \\ K_r L_{sr}^T K_s^{-1} & K_r L_{rr} K_r^{-1} \end{bmatrix} \begin{bmatrix} i_{dq0s} \\ i_{dq0r} \end{bmatrix}$$

where K_s and K_r are given in the exercise in Sect. 2.6.1,

$$L_{ss} = \begin{bmatrix} L_{ls} + L_{ms} & -\frac{1}{2}L_{ms} & -\frac{1}{2}L_{ms} \\ -\frac{1}{2}L_{ms} & L_{ls} + L_{ms} & -\frac{1}{2}L_{ms} \\ -\frac{1}{2}L_{ms} & -\frac{1}{2}L_{ms} & L_{ls} + L_{ms} \end{bmatrix},$$

$$L_{rr} = \begin{bmatrix} L_{lr} + L_{ms} & -\frac{1}{2}L_{ms} & -\frac{1}{2}L_{ms} \\ -\frac{1}{2}L_{ms} & L_{lr} + L_{ms} & -\frac{1}{2}L_{ms} \\ -\frac{1}{2}L_{ms} & -\frac{1}{2}L_{ms} & L_{lr} + L_{ms} \end{bmatrix},$$

$$L_{sr} = L_{ms} \begin{bmatrix} \cos\theta_r & \cos\left(\theta_r + \frac{2\pi}{3}\right) & \cos\left(\theta_r - \frac{2\pi}{3}\right) \\ \cos\left(\theta_r - \frac{2\pi}{3}\right) & \cos\theta_r & \cos\left(\theta_r + \frac{2\pi}{3}\right) \\ \cos\left(\theta_r + \frac{2\pi}{3}\right) & \cos\left(\theta_r - \frac{2\pi}{3}\right) & \cos\theta_r \end{bmatrix},$$

and $L_M = \frac{3}{2}L_{ms}$.

1. Show that

$$K_s L_{ss} K_s^{-1} = \begin{bmatrix} L_{ls} + L_M & 0 & 0 \\ 0 & L_{ls} + L_M & 0 \\ 0 & 0 & L_{ls} \end{bmatrix}$$

2. Show that

$$K_r L_{rr} K_r^{-1} = \begin{bmatrix} L_{lr} + L_M & 0 & 0 \\ 0 & L_{lr} + L_M & 0 \\ 0 & 0 & L_{lr} \end{bmatrix}$$

3. Show that

$$K_s L_{sr} K_r^{-1} = K_r L_{sr}^T K_s^{-1} = \begin{bmatrix} L_M & 0 & 0 \\ 0 & L_M & 0 \\ 0 & 0 & 0 \end{bmatrix}$$

4. Put all the above bits and pieces from Parts I and II together and form the Eqs. (2.71), (2.72), and (2.75)–(2.80) when $\dot{\lambda}_{ds} = 0$ and $\dot{\lambda}_{qs} = 0$.

2.7 Network Equations

Let n be the number of buses at which active generators or loads are connected and let m be the number of buses at which constant impedance loads are connected. A set of bus voltages and currents, with all elements real obtained from the elements of $\vec{V}_a$ and $\vec{I}_a$, and a $nn_i \times 1$ dimensional state-vector x, are defined as follows:

$$
V_a = \begin{bmatrix} v_{D_1} \\ \vdots \\ v_{D_n} \\ v_{Q_1} \\ \vdots \\ v_{Q_n} \end{bmatrix} ; \quad
I_a = \begin{bmatrix} i_{D_1} \\ \vdots \\ i_{D_n} \\ i_{Q_1} \\ \vdots \\ i_{Q_n} \end{bmatrix} ; \quad
V_{\bar{a}} = \begin{bmatrix} v_{D_{n+1}} \\ \vdots \\ v_{D_{n+m}} \\ v_{Q_{n+1}} \\ \vdots \\ v_{Q_{n+m}} \end{bmatrix} ; \quad
I_{\bar{a}} = \begin{bmatrix} i_{D_{n+1}} \\ \vdots \\ i_{D_{n+m}} \\ i_{Q_{n+1}} \\ \vdots \\ i_{Q_{n+m}} \end{bmatrix} ; \quad
x = \begin{bmatrix} x_1 \\ x_2 \\ \vdots \\ x_{nn_i} \end{bmatrix}
$$

$$(2.96)$$

Using the bus admittance matrix Y ($Y\vec{V} = \vec{I}$), we can rewrite the network relationships, in terms of the above defined vectors in (2.96) as

$$
\begin{bmatrix} Y_{aa} & Y_{a\bar{a}} & Y_{ao} \\ Y_{\bar{a}a} & Y_{\bar{a}\bar{a}} & Y_{\bar{a}o} \\ Y_{oa} & Y_{o\bar{a}} & Y_{oo} \end{bmatrix}
\begin{bmatrix} V_a \\ V_{\bar{a}} \\ V_o \end{bmatrix} =
\begin{bmatrix} I_a \\ 0 \\ I_o \end{bmatrix}
\tag{2.97}
$$

where the subscript o is used to denote slack bus quantities. At each active bus, let the current and voltage be related by

$$
S_i\left(\vec{V}_i, \vec{I}_i, x_i\right) = 0.
\tag{2.98}
$$

The above relationship (2.98) for some of the commonly used active load models can be written as:

1. Constant Impedance: $\frac{\vec{V}_i}{\vec{I}_i} = \text{constant}$
2. Constant Current: $\vec{I}_i = \text{constant}$
3. Constant Load: $\vec{V}_i \vec{I}_i^* = \text{constant}$
4. Constant MVA: $\vec{V}_i \vec{I}_i = \text{constant}$

The above Eqs. (2.97) and (2.98) are $2n + 2m + 2o + 2n$ and we have the following unknowns: $2n$ voltages V_a, $2n$ currents I_a, $2m$ voltages $V_{\bar{a}}$, and $2o$ currents I_o (known V_o). Thus the nonlinear Eqs. (2.97) and (2.98) can be solved after each integration step to obtain I_a, which is needed for the next integration step.

2.7.1 Machines as Active Loads

When the active loads can be expressed in certain forms, Eqs. (2.97) and (2.98) can be formulated as a system of linear equations. Electrical machines as active loads have a form which makes the solution of Eqs. (2.97) and (2.98) easier. From the machine stator equations we can write,

$$V_a = Z_a I_a + D_a x \tag{2.99}$$

Substituting (2.99) in (2.97), we get

$$V_{\bar{a}} = -Y_{\bar{a}\bar{a}}^{-1} \left(Y_{\bar{a}a} V_a + Y_{\bar{a}o} V_o \right) \tag{2.100}$$

$$= -Y_{\bar{a}\bar{a}}^{-1} \left(Y_{\bar{a}a} \left(Z_a I_a + D_a x \right) + Y_{\bar{a}o} V_o \right) \tag{2.101}$$

Substituting for $V_{\bar{a}}$ from (2.101) in the equation for I_a in the matrix Eq. (2.97),

$$\left(Y_{aa} Z_a - Y_{a\bar{a}} Y_{\bar{a}\bar{a}}^{-1} Y_{\bar{a}a} Z_a \right) I_a + \left(Y_{aa} - Y_{a\bar{a}} Y_{\bar{a}\bar{a}}^{-1} Y_{\bar{a}a} \right) D_a x - Y_{a\bar{a}} Y_{\bar{a}\bar{a}}^{-1} Y_{\bar{a}o} V_o + Y_{ao} V_o = I_a \tag{2.102}$$

Define (E is a $2n \times 2n$ identify matrix)

$$\bar{Y}_{aa} = Y_{aa} Z_a - E - Y_{a\bar{a}} Y_{\bar{a}\bar{a}}^{-1} Y_{\bar{a}a} Z_a \tag{2.103}$$

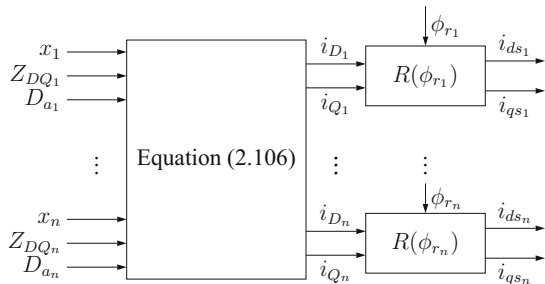$$\bar{D}_a = - \left(Y_{aa} - Y_{a\bar{a}} Y_{\bar{a}\bar{a}}^{-1} Y_{\bar{a}a} \right) D_a \tag{2.104}$$

$$\bar{Y}_{oo} = Y_{a\bar{a}} Y_{\bar{a}\bar{a}}^{-1} Y_{\bar{a}o} - Y_{ao} \tag{2.105}$$

Then from (2.102),

$$I_a = \bar{Y}_{aa}^{-1} \left(\bar{D}_a x + \bar{Y}_{oo} V_o \right) \tag{2.106}$$

Eq. (2.106) in a block diagram form is shown in Fig. 2.33.

Fig. 2.33 Network block diagram

2.7.2   Submatrices in Eq. (2.97)

To illustrate how the matrix in (2.97) is constructed, let us look at the submatrix Y_{aa}. We can write the relationship between bus voltages and currents, using the elements in the original Y matrix, as:

$$\begin{bmatrix} G_{aa} + {}_JB_{aa} & G_{a\bar{a}} + {}_JB_{a\bar{a}} & G_{ao} + {}_JB_{ao} \end{bmatrix} \begin{bmatrix} V_{Da} + {}_JV_{Qa} \\ V_{D\bar{a}} + {}_JV_{Q\bar{a}} \\ V_{Do} + {}_JV_{Qo} \end{bmatrix} = \begin{bmatrix} I_{Da} + {}_JI_{Qa} \end{bmatrix} \quad (2.107)$$

$$\begin{bmatrix} G_{aa} & -B_{aa} \\ B_{aa} & G_{aa} \end{bmatrix} \begin{bmatrix} V_{Da} \\ V_{Qa} \end{bmatrix} + \begin{bmatrix} G_{a\bar{a}} & -B_{a\bar{a}} \\ B_{a\bar{a}} & G_{a\bar{a}} \end{bmatrix} \begin{bmatrix} V_{D\bar{a}} \\ V_{Q\bar{a}} \end{bmatrix} + \begin{bmatrix} G_{ao} & -B_{ao} \\ B_{ao} & G_{ao} \end{bmatrix} \begin{bmatrix} V_{Do} \\ V_{Qo} \end{bmatrix} = \begin{bmatrix} I_{Da} \\ I_{Qa} \end{bmatrix} \quad (2.108)$$

Thus we get,

$$Y_{aa} = \begin{bmatrix} G_{aa} & -B_{aa} \\ B_{aa} & G_{aa} \end{bmatrix}, \quad Y_{a\bar{a}} = \begin{bmatrix} G_{a\bar{a}} & -B_{a\bar{a}} \\ B_{a\bar{a}} & G_{a\bar{a}} \end{bmatrix}, \quad Y_{ao} = \begin{bmatrix} G_{ao} & -B_{ao} \\ B_{ao} & G_{ao} \end{bmatrix} \quad (2.109)$$

In a similar manner all the submatrices of the matrix in (2.97) can be obtained from the original Y matrix.

2.7.3   Forming Z_a from Z_{a_i}

The matrix Z_a can be formed as follows (for $i = 1, 2, \ldots, n$):

$$Z_a(i, i) = Z_{DQ_i}(1, 1), \ Z_a(i, i + n) = Z_{DQ_i}(1, 2), \quad (2.110)$$
$$Z_a(i + n, i) = Z_{DQ_i}(2, 1), \ Z_a(i + n, i + n) = Z_{DQ_i}(2, 2), \quad (2.111)$$

and all other elements of Z_a are zero.

2.7.4   Forming D_a from D_{a_i}

Let the number of states in device j be n_j. The matrix D_a can be formed as follows (for $i = 1, 2, \ldots, n$):

$$D_a\left(i, \sum_{j=1}^{i-1} n_j + k\right) = D_{a_i}(1, k), \ k = 1, 2, \ldots, n_i, \quad (2.112)$$

$$D_a\left(i + n, \sum_{j=1}^{i-1} n_j + k\right) = D_{a_i}(2, k), \ k = 1, 2, \ldots, n_i, \quad (2.113)$$

and all other elements of D_a are zero.

2.7.5 Network Equations Referred to Machine Internal Variables

In special cases the synchronous machine parameters are such that they permit a simple electrical equivalent representation of the machine terminal variables, i.e., V_{D_i}, V_{Q_i}, and state variables, i.e., E'_{d_i}, E'_{q_i}. The terminal and state variables are related by Eq. (2.11), which cannot in general be converted into an electrical equivalent circuit like the ones in Figs. 2.4 or 2.28. In cases where an equivalent circuit representation is possible, e.g., when $L'_d = L'_q$, it is convenient to eliminate all the other bus nodes and write the network equations only in terms of the internal machine variables. This can be done by setting $Z_a = 0$ in Eq. (2.99), i.e., $V_a = D_a x$, and

$$
V_a = \begin{bmatrix} E'_{D_1} \\ \vdots \\ E'_{D_n} \\ E'_{Q_1} \\ \vdots \\ E'_{Q_n} \end{bmatrix}; \quad I_a = \begin{bmatrix} i_{D_1} \\ \vdots \\ i_{D_n} \\ i_{Q_1} \\ \vdots \\ i_{Q_n} \end{bmatrix}.
\tag{2.114}
$$

Using the above substitutions, and assuming that there is no infinite bus in the system, we can write Eq. (2.106) as

$$
I_a = \left(Y_{aa} - Y_{a\bar{a}} Y_{\bar{a}\bar{a}}^{-1} Y_{\bar{a}a} \right) V_a = Y_{\mathrm{red}} V_a
\tag{2.115}
$$

Each of the matrix, $Y_{aa}, Y_{a\bar{a}}, Y_{\bar{a}\bar{a}}, Y_{\bar{a}a}$, in (2.115) has a special structure as given in (2.109). It can be proved that the matrix $Y_{\mathrm{red}} = Y_{aa} - Y_{a\bar{a}} Y_{\bar{a}\bar{a}}^{-1} Y_{\bar{a}a}$ will also have a similar structure and we write,

$$
Y_{\mathrm{red}} = \begin{bmatrix} G & -B \\ B & G \end{bmatrix}
\tag{2.116}
$$

(Hint: The product of matrices in the form in (2.109) preserves the structure. To see that inverse is also of the same structure, let there exist matrices X and Y such that

$$
\begin{bmatrix} G_{aa} & -B_{aa} \\ B_{aa} & G_{aa} \end{bmatrix} \begin{bmatrix} X & Y \\ -Y & X \end{bmatrix} = \begin{bmatrix} G_{aa}X + B_{aa}Y & G_{aa}Y - B_{aa}X \\ B_{aa}X - G_{aa}Y & G_{aa}X + B_{aa}Y \end{bmatrix}
\tag{2.117}
$$

Matrices X and Y can be found such that $G_{aa}X + B_{aa}Y = \mathrm{diag}\{1, 1, \ldots, 1\}$ and $G_{aa}Y - B_{aa}X = 0$. Hence the same structure.)

Let G_{ij} and B_{ij} be the ijth elements of matrices G and B in (2.116), respectively. Then using (2.115) we can write

$$i_{D_i} + J i_{Q_i} = \sum_{j=1}^{n} \left(G_{ij} + J B_{ij} \right) \left(E'_{D_j} + J E'_{Q_j} \right) \tag{2.118}$$

$$\left(i_{d_i} + J i_{q_i} \right) e^{-J\left(\frac{\pi}{2} - \delta_i\right)} = \sum_{j=1}^{n} \left(G_{ij} + J B_{ij} \right) \left(E'_{d_j} + J E'_{q_j} \right) e^{-J\left(\frac{\pi}{2} - \delta_j\right)} \tag{2.119}$$

$$i_{d_i} + J i_{q_i} = \sum_{j=1}^{n} \left(G_{ij} + J B_{ij} \right) \left(E'_{d_j} + J E'_{q_j} \right) e^{J\delta_{ji}} \tag{2.120}$$

$$i_{d_i} = \sum_{j=1}^{n} \left(G_{ij} \cos \delta_{ji} - B_{ij} \sin \delta_{ji} \right) E'_{d_j} - \left(G_{ij} \sin \delta_{ji} + B_{ij} \cos \delta_{ji} \right) E'_{q_j} \tag{2.121}$$

$$i_{q_i} = \sum_{j=1}^{n} \left(G_{ij} \sin \delta_{ji} + B_{ij} \cos \delta_{ji} \right) E'_{d_j} + \left(G_{ij} \cos \delta_{ji} - B_{ij} \sin \delta_{ji} \right) E'_{q_j} \tag{2.122}$$

where Eq. (2.7) is used to transform betwen dq and DQ quantities in Eq. (2.119), and note that for synchronous machines $\phi_{r_i} = \delta_i - \frac{\pi}{2}$.

2.8   Simulation

Block diagram in Fig. 2.33 shows the network block and its inputs and outputs. The inputs come from individual devices such as the ones shown in the block diagram in Fig. 2.2, and again the outputs from the network block in Fig. 2.33 feedback into individual device blocks. An integration step is performed using n blocks of the type shown in Fig. 2.2 and then one algebraic step is performed as shown in the block diagram in Fig. 2.33. The alternating integration and algebraic solutions are repeated for the duration of the simulation. This simulation process consists of the following steps.

The equations for induction machine in Sect. 2.5 are for the motor convention but the currents in I_a in (2.106) are flowing into the network. To use this I_a for induction motor simulation a negative sign has to be place in front of Z_{DQ_i} given in (2.91) for induction motors and also negative of I_{a_i} has to be used in the differential Eqs. (2.85)–(2.87).

1. Form Y_{bus} matrix. Synchronous machines can be represented as PV buses and induction machines can be PQ buses.
2. Perform a load flow analysis. Obtain $\vec{V}_i$ and $\vec{I}_i$ for all the buses and form vectors in (2.96). This step is only to get an estimate of the bus voltages.
3. Convert PQ buses to constant impedance buses and modify Y_{bus}.

Fig. 2.34 Four-bus system
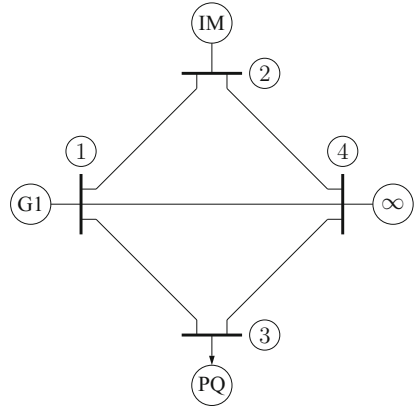
4. Form the matrices in the matrix Eq. (2.97), and matrices Z_a and D_a in (2.99). In general Z_a and D_a will depend on the current system state, develop functions to calculate these matrices for a given system state.
5. Find steady-state conditions by simultaneously solving the equilibrium conditions from differential equations and algebraic constrains. For this step the initial V_a^0 can be formed from the load flow solution, for this V_a^0 and steady-state state x^0 vector can be obtained for all the active devices. For this x^0, I_a^0 is obtained from (2.106). Iterations can stop when V_a^0 is equal to $Z_a^0 I_a^0 + D_a^0 x^0$ (Eq. (2.99)), if not then choose another value for V_a^0 and perform another iteration step. This entire step can be easily accomplished using the Matlab function fsolve.
6. Run a dynamic simulation starting from the steady-state solution obtained above for 1 s or so. After each integration step Eq. (2.106) should be used to obtain I_a and these current values are input for the next integration step.

    (a) Perform an integration step as shown in the block diagram in Fig. 2.2 for each device, and obtain x_i, Z_{DQ_i}, $R(\phi_{r_i})$, $i = 1, \ldots, n$.
    (b) Obtain I_a from (2.106). Go to Step 6a and continue till the end of the simulation period.

7. Apply a disturbance, e.g., increasing the input synchronous machine power by fifty per cent, and perform dynamic simulation.

2.8.1 Four-Bus System

A simple four-bus system with a synchronous generator, an induction motor, and an infinite bus, as shown in Fig. 2.34 is used to demonstrate the simulation process for a network.

The line impedances are: $z_{12} = 0.01 + j0.2$ pu, $z_{13} = 0.01 + j0.2$ pu, $z_{14} = 0.01 + j0.2$ pu, $z_{21} = 0.01 + j0.2$ pu, 0, 0, $z_{24} = 0.01 + j0.2$ pu, $z_{31} = 0.01 + j0.2$ pu, $z_{34} = 0.01 + j0.2$ pu, $z_{41} = 0.01 + j0.2$ pu, $z_{42} = 0.01 + j0.2$ pu, $z_{43} = 0.01 + j0.2$ pu. For the load flow: Bus 1 is a PV bus (0.2395, 1 pu); Bus 2 is a PQ bus (−1, −0.78 pu); Bus 3 is a PQ bus (−1, −0.1 pu); Bus 4 is an infinite or slack bus with voltage 1 pu. The synchronous machine parameters in per unit system are:

$$L_d : 1.7997, L_q : 1.7997, L_d' : 0.2254, L_q' : 1.7997, L_{md} : 1.6201, L_{mq} : 1.6201,$$
$$\omega_s : 1, L_{\mathrm{fd}} : 1.6673, r_s : 0, r_{\mathrm{fd}} : 3.0880 \times 10^{-4}, v_{\mathrm{fd}} : 2.5166 \times 10^{-4},$$
$$J : 7.7775, V_m : 1, P_m : 0.2395.$$

The induction motor parameters in per unit system are:

$$L_{ss} : 1.3633, L_{rr} : 1.3575, L_{sm} : 1.3138, \omega : 1, r_s : 0.0201, r_r : 0.0152,$$
$$J : 1.0281, V_m : 1, T_{\mathrm{load}} : 0.5000.$$

A simulation is performed for the two-machine four-bus system in Fig. 2.34. The input power to the synchronous machine is increased by fifty per cent and then again reduced to the normal value. The simulation results are shown in Figs. 2.35 and 2.36.

2.8.2 Matlab Scripts

The following matlab scripts can be obtained by sending an e-mail to h.pota@adfa.edu.au.
   The following scripts simulate a single machine connected to infinite bus.

1. indmcinitial.m
2. SynMachinedqSimulationNSTpu.m—SMIB synchronous machine simulation, neglecting stator transients.
3. iqd0dotNSTpu.m—$\dot{x}$ calculation function for SynMachinedqSimulation NSTpu.m.
4. getinitialconditions.m—initial conditions for synchronous machine
5. indmcdqsimulationpu.m—SMIB induction machine simulation, including stator transients.
6. indiqd0dotpu.m—$\dot{x}$ calculation function for indmcdqsimulationpu.m.
7. Torquesspu.m—calculate steady-state slip and then other states for a given load torque.
8. indmcdqsimulationNSTpu.m
9. indiqd0dotNSTpu.m—$\dot{x}$ calculation function for indmcdqsimulationNSTpu.m.
10. indssTvsw.m—Simple speed versus electric torque for induction motors.

The following scripts simulate the four-bus system.

1. loadflow.m—The initial load flow to get a rough estimate of the bus voltages.
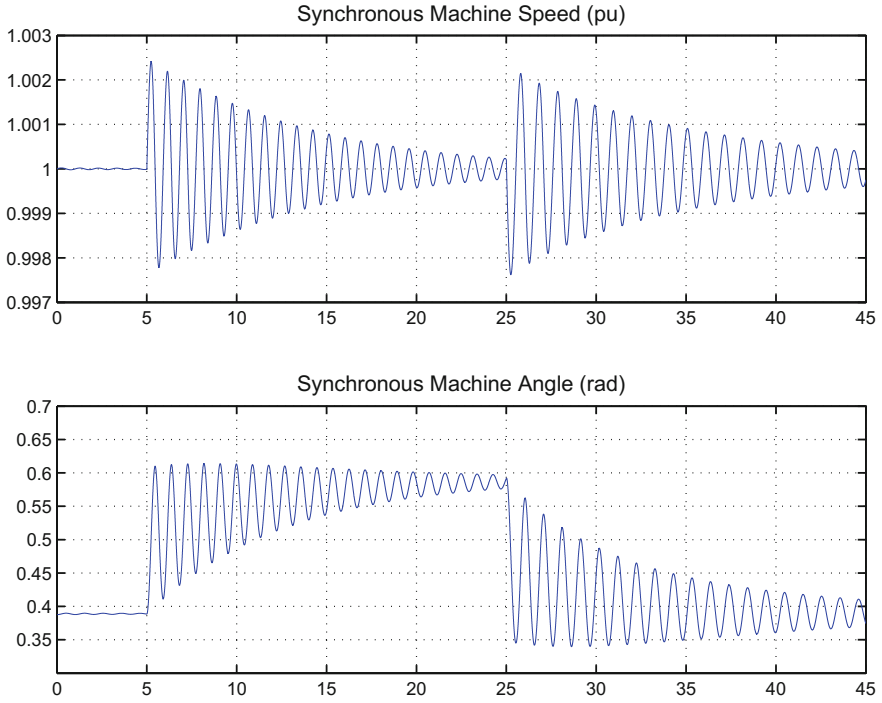
Synchronous Machine Speed (pu)

Synchronous Machine Angle (rad)

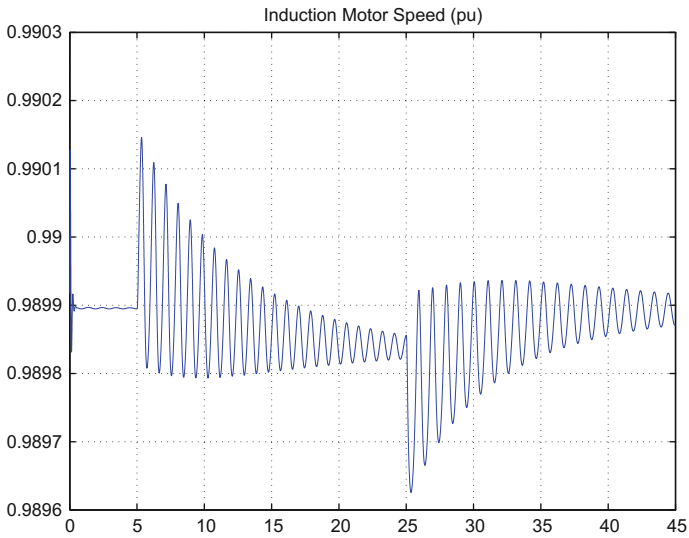**Fig. 2.35** SM angle and speed

Induction Motor Speed (pu)

Fig. 2.36 Induction motor speed

2. powerbal.m—load flow is done using Matlab's `fsolve` function and this function is called by `fsolve` to check if the power balance is achieved.
3. parameters.m—Puts the synchronous and induction machine parameters in Matlab `struct` form. This makes it easy to access these parameters without getting mixed up with symbols and using a long list of parameters in the `global` command.
4. networkequations.m—Forms all the matrices in Eq. (2.97); it iterates via `fsolve` as described in Step 5 in Sect. 2.8; sets up the simulation and then does the dynamic system simulation.
5. algbal.m—Function called by networkequations.m to get the initial conditions which satisfy both device and network constraints.
6. algconstraints.m—Function to calculate I_a given the current state x.
7. syncmcinitial.m—Get steady-state values for synchronous machines given the terminal voltage in DQ-frame.
8. indmcinitial.m—Get steady-state values for induction machines given the terminal voltage in DQ-frame.
9. syncmcza.m—Form the Z_{DQ_i} and D_{a_i} matrices for synchronous machines given the current state.
10. indmcza.m Form the Z_{DQ_i} and D_{a_i} matrices for induction machines. The sign of Z_{DQ_i} is reversed for induction motors.
11. networkdotpu.m—$\dot{x}$ calculation function for both synchronous and induction machines and called from networkequations.m. In the function, I_a is first obtained with algconstraints.m and then these currents are passed on to subfunctions which calculate $\dot{x}$ for synchronous and induction machines. In the induction motor $\dot{x}$ calculation $i_{ds_i} = -i_{D_i}$ and $i_{qs_i} = -i_{Q_i}$.

2.9 Saturation

In developing the models for synchronous machines and induction machines the saturation effects have not been considered. But the saturation effects have been anticipated in the models by using flux linkages of the coil as state variables instead of the currents through the coil as is the general practice in electrical circuits. Here we see how a minor modification in the integration routine can be made to do dynamic analysis with saturation effects.

For small values of excitation current there is a linear relationship between the flux and the current, as shown by the air-gap line in Fig. 2.37. For flux levels in synchronous machine and the magnetic materials used, the current-flux relationship is shown by the saturation curve in Fig. 2.37. The current needed to create flux λ is $K_{1s}\lambda$ for the air-gap but another term like $K_{2s}e^{K_{3s}\lambda}$ is added to it to model the saturation effect as shown in Fig. 2.38. The modelling of the saturation term can be done in many different ways but the important point to keep in mind is that including the effect of saturation is to include an extra term as shown in Fig. 2.38.
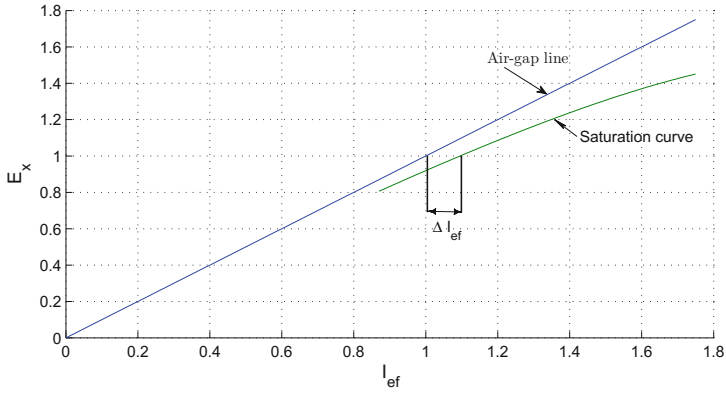
Fig. 2.37 Exciter load-saturation curve

Fig. 2.38 Induced emf and
total flux λ

$$v_i = Ri + \frac{d(\text{total flux})}{dt}$$
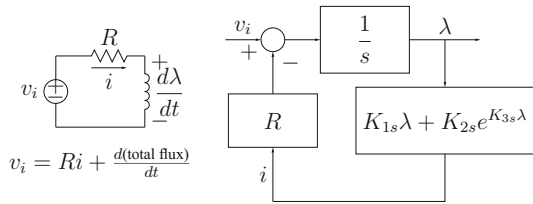
For linear circuits the flux linkages are related to current by the coil induc-
tance, $\lambda = Li$. There are many ways to model the saturation but most power
systems dynamic analysis packages model the flux linkages are related as: $i =
\left(K_{1s}\lambda + K_{2s}e^{K_{3s}\lambda}\right)\lambda$. The integration equation is shown in (2.124).

$$\dot{\lambda} = v_i - Ri \tag{2.123}$$
$$= v_i - R\left(K_{1s}\lambda + K_{2s}e^{K_{3s}\lambda}\right) \tag{2.124}$$

The above relationship (2.124) is for self flux linkages in a coil but the same idea
will work if there are multiple mutual linkages from other coils. As stated before the
use of flux linkages as state variables is a great advantage in keeping the equations
general enough to accommodate the saturation effects easily.

Chapter 3
Linear Control

3.1 Introduction

Automatic voltage regulator (AVR) and power system stabiliser (PSS) are two fundamental controllers which are important for the electrical engineering side of power systems. Although the impact of these two controllers is far reaching, they can be understood and designed using very elementary classical control ideas and tools. Power engineers will be able to design AVR and PSS for multi-machine system using the material in this chapter. Moreover, researchers will better understand nonlinear multi-device dynamics and control problem by the tools presented in this chapter.

Fundamental ideas to understand linear dynamic systems depend on the behaviour and solution of linear differential equations. An easy introduction and general solution method is introduced first and this is then used to introduce frequency response and other classical analysis and design tools.

A linear model for the synchronous machine is first derived and analysed for its dynamic properties. The analysis clearly identifies the role of AVRs and PSSs in maintaining the stability of interconnected power systems. Finally, a detailed introduction and design of AVRs and the PSS is done to bring all the classical analysis and design tools together. The aim of this chapter is also to get the reader to appreciate the characterisation of real interconnected power systems using Bode plots as shown in Fig. 3.1.

3.2 Time Domain Analysis

Time domain analysis is based on characterising a dynamic system based on differential equations. The techniques of the time domain analysis are meant to characterise the solution without actually solving the differential equations. To appreciate these methods let us first look at the basics of solving differential equations. The idea and solution methods for linear differential equations are rather straightforward. It
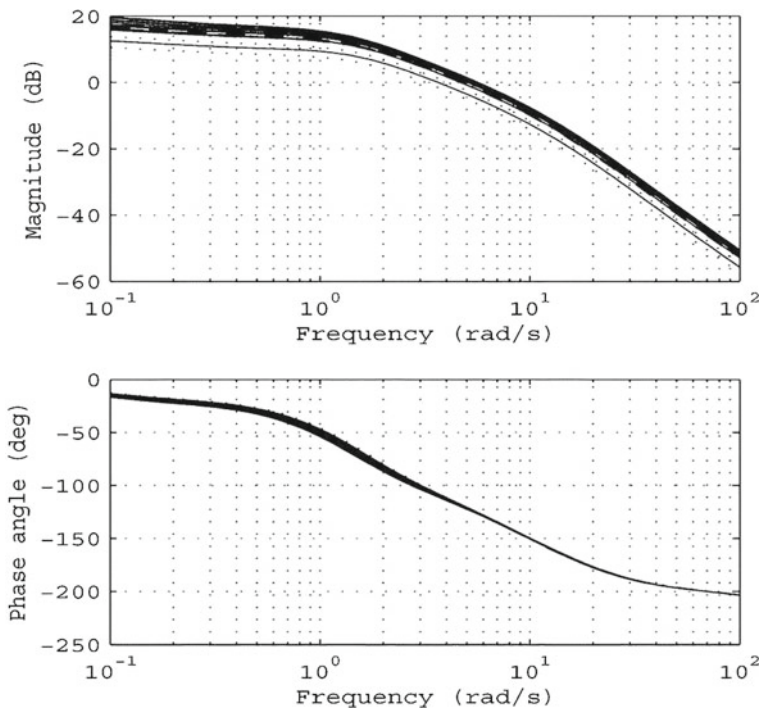
Fig. 3.1 Bode plots of $G_{PVr}(s)$ from [10]

is convenient to write a system of linear differential equations in a state-space form which in appearance and solution methods is like a first-order differential equation. For this reason we first look at the first-order equation in this section.

3.2.1   First Order Differential Equations

Let us look at the following simple first order linear differential equation:

$$\dot{x} = ax, \quad x(0) = x_0 \tag{3.1}$$

The solution of this Eq. (3.1) is a function which when differentiated is a constant times the function itself. Which function is that? The exponential function has this property,

$$\frac{de^{at}}{dt} = ae^{at}. \tag{3.2}$$

So $x(t) = e^{at}$ satisfies the differential Eq. (3.1) but not the initial condition. We need to modify our guess of $x(t)$ only slightly to satisfy the initial condition: $x(t) = x_0 e^{at}$. This solution is known as the initial condition solution.

Now we look at the forced first order equation:

$$\dot{x} = ax + bu(t), \quad x(0) = x_0 \tag{3.3}$$

where $u(t)$ is the forcing function.

As a first guess let's see how our initial condition solution can help us here. Let the guess be $x(t) = x_0 e^{at} + y(t)$, $y(t)$ is as yet unknown function. It would make sense to impose the condition $y(0) = 0$. Substituting this guess in Eq. (3.3) gives,

$$\begin{aligned} ax_0 e^{at} + \dot{y}(t) &= a\left(x_0 e^{at} + y(t)\right) + bu(t) \\ &\Rightarrow \dot{y}(t) = ay(t) + bu(t) \end{aligned} \tag{3.4}$$

Equation (3.4) is similar to the original equation but with zero intial condition.

As we did for the solution of the unforced Eq. (3.1), we guess a solution for the forced Eq. (3.4) as $y(t) = e^{at} z(t)$, where $z(t)$ is as yet unknown function. Substituting this guess in Eq. (3.4) we get,

$$\dot{y}(t) = ae^{at} z(t) + e^{at} \dot{z}(t) \tag{3.5}$$

From Eq. (3.5) we can see that if

$$\dot{z}(t) = e^{-at} bu(t) \tag{3.6}$$

then $y(t) = e^{at} z(t)$ is a solution of Eq. (3.4). This means that the solution of the original Eq. (3.3) is,

$$x(t) = x_0 e^{at} + e^{at} \int_0^t e^{-a\tau} bu(\tau) d\tau. \tag{3.7}$$

The solution of the first order differential (3.1), given in (3.7), has been derived by making repeated guesses. The solution can be found by other methods which can be found in many textbooks. Here the guess method is deliberately used to underline the fact that almost all problems are first solved by guessing a solution and then improving on it till a satisfactory solution is found. Unfortunately, later the "guess" tracks are hidden and a clean solution is presented. This removes students from the original insights and they miss on the most useful learning experience. Before accepting a solution, students should always think if they can guess a solution and how the first guess was made leading to the final solution.

Once the "guess" approach to solving a differential equations is understood, one never has to look for methods to solve differential equations, the methods can be invented as required.

3.2.2   Second Order Differential Equations

In many dynamical systems, an equivalent second order system dominates the system response and most systems can be approximated using a second order system. Next, we look at second order linear systems in detail.

Firstly we look at the solution of the following homogeneous second order linear differential equation:

$$\frac{d^2x}{dt^2} + a\frac{dx}{dt} + bx = 0, \quad x(0) = x_0, \ x'(0) = x'_0 \tag{3.8}$$

To find a solution of the above differential equation (3.8), we first guess a solution and then substitute it back in the equation and see if it satisfies the equation. To see what type of functions may provide a good guess we rewrite the above equation as: $\frac{d^2x}{dt^2} = -a\frac{dx}{dt} - bx$, and observe that higher order derivatives are expressed as a linear combination of the lower order derivatives. Which functions have this property? Polynomial functions in time don't have this property (why?). Sine and cosine functions differentiated twice result in a constant times the function itself, so sine and cosine functions show some promise and they are indeed good guesses for equations where the first derivative is missing, i.e., $\frac{d^2x}{dt^2} = -bx$, but for a general Eq. (3.8) it cannot be used.

Drill Substitute a general function $A\sin(\lambda x + \phi)$ in Eq. (3.8) and show that such a function cannot satisfy a general second order differential equation.

Since the sine function shows some promise let's go a step further and try a generalised trigonometric function, $ke^{\lambda t}$. On substituting $ke^{\lambda t}$ into Eq. (3.8) we get,

$$\lambda^2 ke^{\lambda t} + a\lambda ke^{\lambda t} + bke^{\lambda t} = 0. \tag{3.9}$$

For the above equation to hold we need,

$$\lambda^2 + a\lambda + b = 0 \tag{3.10}$$

Equation (3.10) is known as the characteristic equation for the system described by the Eq. (3.8). Let the solution of the characteristic be $\lambda = \lambda_1, \lambda_2$. Then the general solution of the differential equation (3.8) is given by:

$$x(t) = k_1 e^{\lambda_1 t} + k_2 e^{\lambda_2 t} \tag{3.11}$$

Real Roots (Overdamped Solution) The case where λ_1 and λ_2 are real and distinct needs no further comment except that the initial conditions are used to find the values of the constants k_1 and k_2. The case with equal real roots is interesting and is covered later.

Complex Roots (Underdamped Solution) When λ_1 and λ_2 are complex they have to be complex conjugate (why?). This means that, $\lambda_1, \lambda_2 = \alpha \pm j\omega$. The general solution can then be written as:

$$x(t) = k_1 e^{(\alpha+j\omega)t} + k_2 e^{(\alpha-j\omega)t}$$
$$= e^{\alpha t} \left((k_1 + k_2) \cos(\omega t) + j(k_1 - k_2) \sin(\omega t) \right) \tag{3.12}$$

To satisfy the given initial conditions it must be true that,

$$k_1 + k_2 = x(0) \tag{3.13}$$
$$j\omega(k_1 - k_2) + \alpha(k_1 + k_2) = x'(0) \tag{3.14}$$

From (3.13) and (3.14) above, for real values of $x(0)$ and $x'(0)$, k_1 and k_2 have to be complex conjugate.

Drill Prove that k_1 and k_2 are complex conjugate.

For complex conjugate k_1 and k_2 we see that $j(k_1 - k_2)$ is a real number. Denote:

$$k = \sqrt{(k_1 + k_2)^2 + (j(k_1 - k_2))^2} = 2k_1 k_2$$
$$\phi = \tan^{-1}\left(\frac{k_1 + k_2}{k_1 - k_2} \right)$$

with the above definitions of k and ϕ the general solution (3.12) can be written in the form:

$$x(t) = k e^{\alpha t} \sin(\omega t + \phi) \tag{3.15}$$

The two constants k and ϕ are solved for the given initial conditions.

Repeated Roots (Critically Damped Solution) When the roots of the characteristic equation (3.10) are equal then the solution is written differently from (3.11) above. The characteristic equation such as (3.10) has repeated roots when $b = a^2/4$ and then the differential equation (3.10) can be written as:

$$\frac{d}{dt}\left(\frac{dx}{dt} + \frac{a}{2}x \right) + \frac{a}{2}\left(\frac{dx}{dt} + \frac{a}{2}x \right) = 0 \tag{3.16}$$

Let

$$y \triangleq \frac{dx}{dt} + \frac{a}{2}x \tag{3.17}$$

with this definition of y, Eq. (3.16) and its solution can be written as:

$$\frac{dy}{dt} + \frac{a}{2}y = 0 \Rightarrow y = k e^{-\frac{a}{2}t}. \tag{3.18}$$

Substituting the above solution back into (3.17) we get:

$$\frac{dx}{dt} + \frac{a}{2}x = ke^{-\frac{a}{2}t} \Rightarrow x = k_1 te^{-\frac{a}{2}t} + k_2 e^{-\frac{a}{2}t} \tag{3.19}$$

Like the previous two cases the initial conditions are used to obtain values of the constants k_1 and k_2.

Forcing Functions For an equation with a forcing function $f(t)$, shown below,

$$\frac{d^2x}{dt^2} + a\frac{dx}{dt} + bx = f(t), \quad x(0) = x_0, \ x'(0) = x'_0, \tag{3.20}$$

what has been described before for the homogeneous equation is used to get the natural response.

To find particular solution for a general forcing function is a bit tedious. Particular solutions can be easily obtained for certain forcing functions. For example, particular solution due to a step forcing function is a constant, and due to a sinusoidal forcing function is a sinusoid itself with the frequency the same as that of the forcing function sinusoid but with a different magnitude and phase are different.

3.2.3   Simultaneous First Order Differential Equations or State-Space Representation

Earlier we saw that it was very simple to obtain a complete solution to the first order Eq. (3.3). In this section we use the same idea to obtain a solution of simultaneous first order differential equations.

The second order Eq. (3.20) can be written as two simultaneous first order equations. Define

$$x_1 := x \tag{3.21}$$
$$x_2 := \dot{x} \Rightarrow \dot{x}_2 = -ax_2 - bx_1 + f(t) \tag{3.22}$$

With the above definitions (3.21) and (3.22), the differential equation (3.20) can be written in a compact matrix form as:

$$\begin{bmatrix} \dot{x}_1 \\ \dot{x}_2 \end{bmatrix} = \begin{bmatrix} 0 & 1 \\ -b & -a \end{bmatrix} \begin{bmatrix} x_1 \\ x_2 \end{bmatrix} + \begin{bmatrix} 0 \\ 1 \end{bmatrix} f(t) \tag{3.23}$$

We now write the above equation in the form,

$$\dot{X} = AX + Bf(t) \tag{3.24}$$

where

$$X := \begin{bmatrix} x_1 \\ x_2 \end{bmatrix}; \quad A = \begin{bmatrix} 0 & 1 \\ -b & -a \end{bmatrix}; \quad B = \begin{bmatrix} 0 \\ 1 \end{bmatrix}. \tag{3.25}$$

We say that Eq. (3.24) is a vector version of Eq. (3.3). Looking at the solution of Eq. (3.3), given in Eq. (3.7), we write the solution of Eq. (3.24) as:

$$X(t) = \Pi(A, t) \left[X(0) + \int_0^t \Pi(A, -\tau) B f(\tau) d\tau \right]. \tag{3.26}$$

The solution (3.26) is valid provided the function $\Pi(A, t)$ satisfies two conditions:

$$\dot{\Pi}(A, t) = A \Pi(A, t) \text{ and } \Pi(A, t) \Pi(A, -t) = I$$

where I is an identity matrix. Note that

$$\frac{d}{dt} \int_0^t \Pi(A, -\tau) B f(\tau) d\tau = \Pi(A, -t) B f(t). \tag{3.27}$$

If $\dot{\Pi}(A, t) = A \Pi(A, t)$ then $\ddot{\Pi}(A, t) = A^2 \Pi(A, t)$, etc. We can use this fact to form a Taylor series for the function $\Pi(A, t)$ (note that $\Pi(A, 0) = I$, $\dot{\Pi}(A, 0) = A$, and $\ddot{\Pi}(A, 0) = A^2$, etc.)

$$\Pi(A, t) = I + At + \frac{A^2 t^2}{2!} + \frac{A^3 t^3}{3!} + \dots \tag{3.28}$$

When A is a diagonal matrix such that $a_{ii} = \lambda_i$ and $a_{ij} = 0, i \neq j$, then we write $A = \text{diag}\{\lambda_1, \dots, \lambda_n\}$, and from (3.28), we have

$$\Pi(A, t) = \text{diag}\{e^{\lambda_1 t}, \dots, e^{\lambda_n t}\}. \tag{3.29}$$

It can be verified by direct evaluation that for the definition of $\Pi(A, t)$ in (3.28),

$$\Pi(A, t) \Pi(A, -t) = I \text{ and } \Pi(A, t_1 + t_2) = \Pi(A, t_1) \Pi(A, t_2) = \Pi(A, t_2) \Pi(A, t_1).$$

There exist many different ways to calculate the state-transition matrix $\Pi(A, t)$. One of the easier ways is to use a computer. The factorial terms in Eq. (3.28) dominate after a few terms for small t. This with the property $\Pi(A, t_1 + t_2) = \Pi(A, t_1) \Pi(A, t_2)$ makes it very easy to calculate state-transition matrix using a computer.

An nth order differential equation can be written as a set of simultaneous first order differential equations. Let an nth order system be given as:

$$\frac{d^n x}{dt^n} + a_1 \frac{d^{n-1} x}{dt^{n-1}} + \dots + a_n x = f(t), \quad \frac{dx^i(0)}{dt^i} = x_0^i, \quad i = 0, 2, \dots, n-1. \tag{3.30}$$

Then define:

$$x_1 := x$$
$$x_i := \dot{x}_{i-1}, \quad i = 2, \ldots, n \tag{3.31}$$

This gives,

$$\dot{x}_n = -\sum_{i=1}^{n} a_i x_{n-i+1} + f(t). \tag{3.32}$$

The n first order simultaneous Eqs. (3.31) and (3.32) can be written as:

$$\dot{X} = AX + Bf(t), \quad X(0) = X_0 \tag{3.33}$$

where

$$X := \begin{bmatrix} x_1 \\ x_2 \\ \vdots \\ x_{n-1} \\ x_n \end{bmatrix}; \quad A = \begin{bmatrix} 0 & 1 & 0 & \cdots & 0 \\ 0 & 0 & 1 & \cdots & 0 \\ \vdots & \vdots & \vdots & & \vdots \\ 0 & 0 & 0 & \cdots & 1 \\ -a_n & -a_{n-1} & -a_{n-2} & \cdots & -a_1 \end{bmatrix}, \quad B = \begin{bmatrix} 0 \\ 0 \\ \vdots \\ 0 \\ 1 \end{bmatrix}, \quad X(0) := \begin{bmatrix} x_0^0 \\ x_0^1 \\ \vdots \\ x_0^{n-2} \\ x_0^{n-1} \end{bmatrix}. \tag{3.34}$$

The variables $x_1, x \ldots, x_n$ are called the state-variables and X is called the state-vector.

The solution of Eq. (3.33) is:

$$X(t) = \Pi(A, t) \left[X(0) + \int_0^t \Pi(A, -\tau) Bf(\tau) d\tau \right]. \tag{3.35}$$

3.2.4   Modal Analysis

A linear dynamic system can be represented as:

$$\dot{x} = Ax + Bu \tag{3.36}$$

x is an n-dimensional column vector and A is an $n \times n$ matrix. Modal analysis is a technique of analysing system behaviour looking at the properties of the matrix A in (3.36).

For an $n \times n$ matrix A, its characteristic equation is given by $\det(A - \lambda I) = 0$ where I is an identity matrix; n solutions $\lambda_i, i = 1, 2, \ldots, n$ are called eigenvalues of matrix A.

Let Φ_i be a column vector (right eigenvector) such that

$$A\Phi_i = \lambda_i \Phi_i, i = 1, \ldots, n$$

For dynamic systems (3.36), eigenvectors have an interesting interpretation. If the initial condition $x(0) = \Phi_i$ and $u = 0$, then according to Eq. (3.35),

$$x(t) = I + \lambda_i \Phi_i t + \frac{\lambda_i^2 \Phi_i t^2}{2!} + \frac{\lambda_i^3 \Phi_i t^3}{3!} + \cdots \qquad (3.37)$$

For λ_i real the solution continues along the vector Φ_i and for λ_i negative, it approaches zero along the eigenvector. It can be easily seen from the properties of the eigenvectors that any solution starting close to an eigenvector will approach the eigenvector and either go to zero or infinity along that eigenvector.

For complex $\lambda_i = a_i + jb_i$ and the associated eigenvector $\Phi_i = U_i + jV_i$, we have:

$$AU_i = a_i U_i - b_i V_i \qquad (3.38)$$

$$AV_i = a_i V_i + b_i U_i \qquad (3.39)$$

From (3.38)–(3.39), it can be seen that the real part of the eigenvalue a_i scales along the same direction but the imaginary part b_i flips the imaginary and the real parts of the eigenvector. So one can say that the real part moves the trajectory linearly and the imaginary part rotates it between vectors U_i and V_i

In the limit if $a_i = 0$, the trajectory if starting along the vector U_i or V_i is given by substituting (3.38)–(3.39) in (3.35),

$$x(t) = U_i \cos b_i t + V_i \sin b_i t \qquad (3.40)$$

From (3.40) one can say that the trajectory will keep rotating from U_i to V_i at frequency b_i. For eigenvalues with zero real part, i.e., $a = 0$, the trajectory will be a circle and the radius will depend on the initial conditions.

The relationship between eigenvectors and the system response can be seen for a simple system:

$$\ddot{x} + 2\zeta\omega_n\dot{x} + \omega_n^2 x = 0; \quad x(0) = x_0, \quad \dot{x}(0) = x_0'$$

For this system let $x_1 = x$, and $x_2 = \dot{x}$, then:

$$x = \begin{bmatrix} x_1 \\ x_2 \end{bmatrix} \text{ and } A = \begin{bmatrix} 0 & 1 \\ -\omega_n^2 & -2\zeta\omega_n \end{bmatrix}$$

Figure 3.2 shows trajectories when $\zeta = 1.25$, $\omega_n = 1$ rad s^{-1}, $\lambda_1 = -0.5$, $\lambda_2 = -2.0$, and $\Phi_1 = [0.89, \quad -0.44]^T$, $\Phi_2 = [-0.44, \quad 0.89]^T$. It can be seen that the trajectories move towards an eigenvector and then approach the origin along the eigenvector.

Figure 3.3 shows trajectories when $\zeta = 0.1$, $\omega_n = 14$ rad s^{-1}, $\lambda_1, \lambda_2 = -0.1 \pm j0.995$, and $\Phi_1 = [0.7071, \quad -0.0707 + 0.7036j]^T$, $\Phi_2 = [0.7071,$
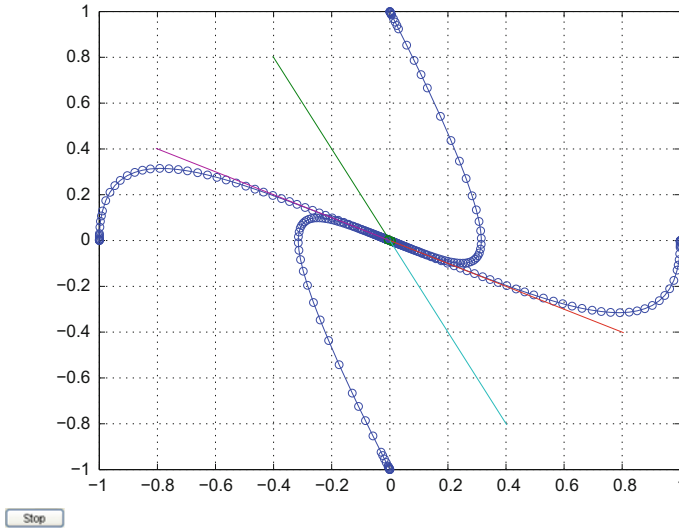
Fig. 3.2 Trajectories for a system with real eigenvalues
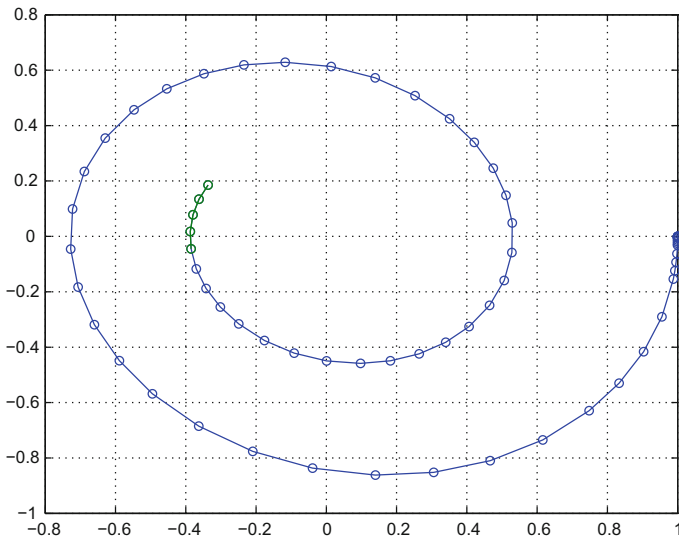
Fig. 3.3 Trajectories for a system with imaginary eigenvalues

$-0.0707 - 0.7036_J]^T$. It can be seen that the trajectory is spiralling towards the origin as expected for a system with imaginary eigenvalues (Fig. 3.3).

The correspondence between eigenvectors and the system response can be further systematised by considering all the eigenvectors together. Denoting Φ as the matrix, known as modal matrix, made up of all the column vector Φ_i, such that

$$\Phi = [\Phi_1, \ldots, \Phi_n].$$

We can see that

$$\Phi^{-1} A \Phi = \text{diag}\{\lambda_1, \ldots, \lambda_n\}$$

Often we write $\Lambda = \text{diag}\{\lambda_1, \ldots, \lambda_n\}$.

The left eigenvector, Ψ_i, is a row vector such that

$$\Psi_i A = \lambda_i \Psi_i.$$

Note that $A^T \Psi_i^T = \lambda_i \Psi_i^T$, we can make another modal matrix Ψ as,

$$\Psi = \left[\Psi_1^T, \ldots, \Psi_n^T\right]^T.$$

The left and right eigenvectors are such that, $\Psi_j \Phi_i = 0, i \neq j$, and, $\Psi_i \Phi_i = C_i$. This follows from $\Psi_j A \Phi_i = \lambda_j \Psi_j \Phi_i = \lambda_i \Psi_j \Phi_i$. Often the modal matrices are normalised such that $\Psi \Phi = I$.

Define a transformed vector z as $x = \Phi z$ (since $\Psi \Phi = I$, we have $z = \Psi x$), then (for u=0)

$$\dot{z} = \Phi^{-1} A \Phi z = \Lambda z.$$

The ith element of $z(t)$ is called the ith mode of the system corresponding to the eigenvalue λ_i. We have $z(t) = e^{\Lambda t} z(0)$ and $z_i(t) = e^{\lambda_i t} z_i(0) = e^{\lambda_i t} \Psi_i x(0)$ and finally

$$x(t) = \sum_{i=1}^{n} \Phi_i \Psi_i x(0) e^{\lambda_i t}.$$

The ith right eigenvector Φ_i is the mode shape corresponding to the eigenvalue λ_i. The jth element of the left eigenvector Ψ_i, Ψ_{ij}, gives the contribution of the jth state in the ith mode.

3.2.4.1 Evaluating Eigenvalues and Eigenvectors

Eigenvalues and eigenvectors are calculated in many different ways both numerically for a linear model and experimentally for power systems. It is helpful to remember a few properties of eigenvalues and eigenvectors to be able to make efficient use of the modal analysis.

For a matrix A with an eigenvalue λ and associated eigenvector X:

1. A^{-1} (if it exists) has an eigenvalue $\frac{1}{\lambda}$ with associated eigenvector X.
2. The matrix $(A - kI)$ has an eigenvalue $(\lambda - k)$ and associated eigenvector X.
3. The matrix $(A - kI)^{-1}$, i.e., the inverse (if it exists) of the matrix $(A - kI)$, has eigenvalue $\frac{1}{\lambda - k}$ and corresponding eigenvector X.

To obtain an eigenvalue of a matrix A closest to q [11]:

1. Let Z_0 be an arbitrary vector or a vector close to the expected eigenvector.
2. Solve for W_{k+1}:

$$(A - qI)W_{k+1} = Z_k$$

3. Compute the vector Z_{k+1} for the next iteration:

$$Z_{k+1} = \frac{W_{k+1}}{\max(W_{k+1})}$$

and return to the preceding step till there is a convergence.

Prony Analysis Modal information can be obtained from experimental measurements using Prony analysis [12–14]. The Prony method decomposes time-domain signals into damped sinusoids with four parameters per mode: frequency, damping, amplitude (relative weight), and phase:

$$y(t) = \sum A_i \exp(\sigma_i t) \cos(\omega_i t + \phi_i). \tag{3.41}$$

Prony analysis proceeds along the following steps.

1. Record output $y(t)$ for non-zero initial condition disturbance. Let the record $y(t)$ consist of N samples $y(t_k) = y(k), k = 0, 1, \ldots, N - 1$ evenly spaced by an amount Δt.
2. Fit the record $y(t)$ with a discrete linear prediction model of form (with SNR > 40 dB)

$$y_i(P + k) = a_1 y_i(P + k - 1) + \cdots + a_P y_i(k); \ \ SNR = 20 \log \mathrm{rms}\left(\frac{y(t)}{y(t) - y_i(t)}\right). \tag{3.42}$$

3. Find the roots of the characteristic polynomial, $\lambda_i = \sigma_i \pm J\omega_i$, associated with the model (3.42).
4. Using the roots of of the characteristic polynomial, $\lambda_i = \sigma_i \pm J\omega_i$, determine the amplitude (relative weight) and initial phase for each mode using (3.41) and the time-domain data.

Details of Prony analysis done by BPA using an output record that was obtained by applying a 1400 MW load for 0.5 s [12, 13].

3.2.5   Eigenvalue Sensitivity and Participation Matrix

A grid is an interconnection of several generators with the capability to provide control for voltage and frequency regulation. In the first instance it is desired that the

controls be decentralised or local. The first task is to decide which generators will
be used for control and their control authority. Every power system has continuous
oscillations and the primary purpose of the control is to damp those oscillations. Lin-
earised models of the complete power system give a very good idea of the oscillation
characteristics of power systems. The analysis consists in first evaluating the eigen-
values of the linearised model and analysing the damping properties of the dominant
eigenvalues. For the eigenvalues with less than acceptable damping control action is
provided.

Once the lowly damped dominant eigenvalues are identified, the sensitivity of
eigenvalues to changing the elements in the A matrix enables the identification of
the generators which can provide the control action for increasing the damping. Here
we look at the participation matrix method to evaluate the sensitivity.

We can use the basic eigenvalue algebra to write an expression for the sensitivity
of the eigenvalues of the system in terms of participation matrix elements as shown
below:

$$A\Phi_i = \lambda_i \Phi_i \tag{3.43}$$

$$\frac{\partial A}{\partial a_{kj}}\Phi_i + A\frac{\partial \Phi_i}{\partial a_{kj}} = \frac{\partial \lambda_i}{\partial a_{kj}}\Phi_i + \lambda_i \frac{\partial \Phi_i}{\partial a_{kj}} \tag{3.44}$$

$$\Psi_i \frac{\partial A}{\partial a_{kj}}\Phi_i = \frac{\partial \lambda_i}{\partial a_{kj}} \tag{3.45}$$

$$\frac{\partial \lambda_i}{\partial a_{kj}} = \Psi_{ik}\Phi_{ji}. \tag{3.46}$$

Equation (3.45) is possible since $\Psi_i \Phi_i = 1$ and $\Psi_i(A - \lambda_i I) = 0$ and finally only
the $(k, j)th$ element of A depends on a_{kj}. The eigenvalue sensitivity $\frac{\partial \lambda_i}{\partial a_{kj}}$ is given by
the expression in (3.46).

From the above sensitivity formula (3.46), let's see what happens if we change
the $(k, k)th$ element of the A matrix, i.e., provide a feedback in the state equation
for $\dot{x}_k$ from state variable x_k, i.e., provide a local control:

$$\frac{\partial \lambda_i}{\partial a_{kk}} = \Psi_{ik}\Phi_{ki} = p_{ki}. \tag{3.47}$$

This tells us that to change the ith mode the best thing to do is apply a control to
the state variable k such that p_{ki} is the largest participating factor. There is another
interpretation of the elements of the participation matrix. The dynamics of the $x_j = \sum_{i=1}^{n} \Phi_{ji}\Psi_i x(0)e^{\lambda_i t}$ state is made up of the dynamics of various modes and we see
that Φ_{ji} gives the participation of mode z_i in state x_j. We have $z_i = \sum_{j=1}^{n} \Psi_{ij}x_j$,
this means that $\Phi_{ji}\Psi_{ij}$ is the participation of mode i in state x_j and vice-versa. The
participation matrix P is made up of elements [8, 15]:

$$p_{ki} = \Phi_{ki}\Psi_{ik}.$$

Here are a few important points in the use of the participation factors.

1. The term, p_{ki}, gives the participation of the ith state in the kth mode and vice-versa.
2. States of a system are not unique, they can be scaled and eigenvectors may also be scaled by an arbitrary constant.
3. Participation factors are scale independent.
4. Participation factors are useful in the placement of PSS.

In many dynamic system applications eigenvectors are used for modal analysis and control design. In power systems participation factors are used. Although eigenvectors and participation factors are related, participation factors have an important property that their value is scale independent, i.e., is does not change with different scaling of the state variables, it is truly a property of the system dynamics.

Let the original system be:

$$\begin{bmatrix} \dot{x}_1 \\ \dot{x}_2 \end{bmatrix} = \begin{bmatrix} 0 & 1 \\ -1 & -1 \end{bmatrix} \begin{bmatrix} x_1 \\ x_2 \end{bmatrix} \tag{3.48}$$

The right eigenvectors are (columns of Φ):

$$\Phi = \begin{bmatrix} 0.7071 & 0.7071 \\ -0.3535 + 0.6123i & -0.3535 - 0.6123i \end{bmatrix} \tag{3.49}$$

The left eigenvectors are (rows of Ψ):

$$\Psi = \begin{bmatrix} 0.7071 - 0.4082i & -0.8165i \\ 0.7071 + 0.4082i & 0.8165i \end{bmatrix} \tag{3.50}$$

The two right eigenvectors above tell us that in both the modes both the states contribute equally magnitude wise but with a 180° phase difference. The participation matrix is:

$$P = \begin{bmatrix} 0.5000 - 0.2887i & 0.5000 + 0.2887i \\ 0.5000 + 0.2887i & 0.5000 - 0.2887i \end{bmatrix} \tag{3.51}$$

The above participation matrix clearly indicates that both the states contribute equally to both the modes. The same conclusion as from eigenvector analysis.

Now let us scale the first state variable and define a new variable as: $z_1 = 500x_1$. The above Eq. (3.48) becomes:

$$\begin{bmatrix} \dot{z}_1 \\ \dot{x}_2 \end{bmatrix} = \begin{bmatrix} 0 & 500 \\ \frac{-1}{500} & -1 \end{bmatrix} \begin{bmatrix} z_1 \\ x_2 \end{bmatrix} \tag{3.52}$$

The right eigenvectors are (columns of Φ):

$$\Phi = \begin{bmatrix} 1 & 1 \\ -0.001 + 0.0017i & -0.001 - 0.0017i \end{bmatrix} \tag{3.53}$$

The left eigenvectors are (rows of Ψ):

$$\Psi = \begin{bmatrix} 0.5 - 0.29i & -288.68i \\ 0.5 + 0.29i & 288.68i \end{bmatrix} \tag{3.54}$$

The right eigenvectors Φ_i indicate that state variable x_1 contributes much more to both the modes. Below the participation matrix of the scaled system is given and it is the same as in the first representation.

$$P = \begin{bmatrix} 0.5000 - 0.2887i & 0.5000 + 0.2887i \\ 0.5000 + 0.2887i & 0.5000 - 0.2887i \end{bmatrix} \tag{3.55}$$

From this we can see that the participation matrix is scale independent and it a property of the system itself.

3.3 Laplace Domain or Transfer Function Analysis

A power system, like most practical dynamic systems, is an interconnection of many subsystems. For analysis and control design a mathematical model of the complete system must be put together from subsystem models. In general this is a difficult task but of all the mathematical representations Laplace domain representation (also known as a transfer function representation) makes it the easiest to put together a complete system model from subsystem models. This is the reason for the popularity of transfer functions.

A transfer function is an input-output model of the system. It is a compact model. As we will see later in writing the model equations, $\frac{d}{dt}$ is replaced by s in transfer functions, resulting in economy of writing. At an advanced level, transfer functions capture unmodelled dynamics in a practical manner facilitating the design of robust control.

The Laplace transform, of a time function $f(t)$, is defined as:

$$F(s) = \mathcal{L}[f(t)] = \int_0^\infty e^{-st} f(t) dt \tag{3.56}$$

where s is a complex variable. It is a convention to denote time functions with lower case letters and Laplace transformed functions with upper case letters. Let us first derive a few frequently used time and Laplace transform pairs.

A unit-step $u(t)$ is defined as a function which is zero for time less than zero and unity at all other times. Then

$$U(s) = \int_0^\infty e^{-st} u(t) dt$$

$$= -\frac{1}{s} e^{-st} \Big|_0^\infty = \frac{1}{s}$$

Table 3.1 Laplace transform pairs

$f(t)$	$F(s)$
$e^{at} f(t)$	$F(s-a)$
$\frac{df}{dt}$	$sF(s) - f(0)$
$\frac{d^n f}{dt^n}$	$s^n F(s) - \sum_{k=1}^{n} s^{n-k} f^{k-1}(0)$
$f(t-a)u(t-a)$	$e^{-as} F(s)$
unit-step $u(t)$	$\frac{1}{s}$
$e^{-at} u(t)$	$\frac{1}{s+a}$
$\int g(\tau)d\tau$	$\frac{1}{s}G(s)$
$t^n u(t)$	$\frac{n!}{s^{n+1}}$
$\sin(\omega t)u(t)$	$\frac{\omega}{s^2+\omega^2}$
$\cos(\omega t)u(t)$	$\frac{s}{s^2+\omega^2}$

Let $f(t) = e^{-at}u(t)$, where $u(t)$ is a unit-step, then

$$F(s) = \int_0^\infty e^{-st} e^{-at} u(t)dt$$

$$= -\frac{1}{s+a} e^{-(s+a)t} \Big|_0^\infty = \frac{1}{s+a}$$

Let $g(t) = \frac{df}{dt}$, then

$$G(s) = \int_0^\infty \frac{df}{dt} e^{-st} dt$$

$$= f(t)e^{-st}\Big|_0^\infty + s \int_0^\infty e^{-st} f(t)dt = sF(s) - f(0)$$

Continuing the derivation process used above we can easily obtain Table 3.1 for the Laplace transform pairs.

Transfer Function For a single-input-single-output system, the Laplace transform of the output divided by the Laplace transform of the input, with zero initial conditions, is called the transfer function of the system. For a multi-input-multi-output system transfer functions are defined for every input-output pair and the collection of these transfer functions is normally represented in a matrix form.

For the types of systems considered in power system analysis, transfer functions are a ratio of two rational polynomials, i.e.,

$$G(s) = \frac{b(s)}{a(s)} = \frac{b_0 s^m + b_1 s^{m-1} + \ldots + b_m}{s^n + a_1 s^{n-1} + \ldots + a_n}$$

The roots of the numerator $b(s)$ are called the zeros of the system and the roots of the denominator $a(s)$ are called the poles of the system.

The transfer function for a system represented by an nth order equation can also be written quite easily. Let the nth order system be given as:

$$\frac{d^n x}{dt^n} + a_1 \frac{d^{n-1}x}{dt^{n-1}} + \cdots + a_n x = u(t), \quad \frac{dx^i(0)}{dt^i} = 0, \quad i = 0, 2, \ldots, n-1. \quad (3.57)$$

Let the output $y = x$, and let $u(t)$ be the input (not the unit-step as used before). Taking Laplace Transform of both the sides of Eq. (3.57), we get using Table 3.1,

$$s^n X(s) + a_1 s^{n-1} X(s) + \cdots + a_n X(s) = U(s). \quad (3.58)$$

From the above (3.58) gives, the transfer function as,

$$G(s) = \frac{Y(s)}{U(s)} = \frac{1}{s^n + a_1 s^{n-1} + \cdots + a_n}$$

In Sect. 3.2.3, we saw how an nth order differential equation can be represented in the state-space form:

$$\dot{x} = Ax + Bu \quad (3.59)$$

$$y = Cx + Du \quad (3.60)$$

x is an n-dimensional column vector; A is $n \times n$ matrix; B is $n \times m$ matrix; C is $p \times n$ matrix; D is $p \times p$ matrix; u is m-dimensional column vector; y is p-dimensional column vector; the system has m inputs and p outputs. The transfer function for the system in (3.59) and (3.60) can be obtained as follows:

$$sX(s) = AX(s) + BU(s)$$
$$X(s) = (sI - A)^{-1} BU(s)$$
$$Y(s) = CX(s) + DU(s)$$

where I is an $n \times n$ identity matrix with ones on its principal diagonal and zero elsewhere. Putting the above relations together we get the transfer function as:

$$G(s) = C (sI - A)^{-1} B + D$$

3.3.1 Block Diagrams

As mentioned above, one of the strengths of the Laplace domain analysis is the ability to represent a complex interconnected system as an interconnection of subsystem
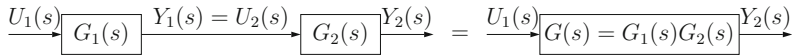
Fig. 3.4 Series connection
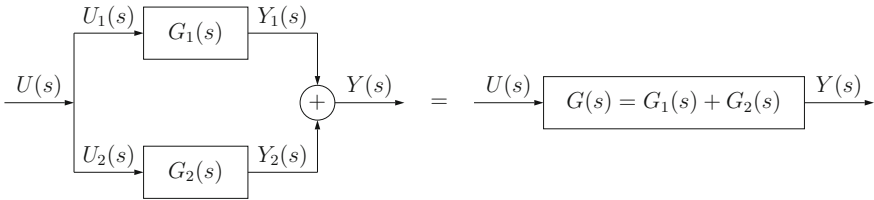
Fig. 3.5 Parallel connection

blocks. Here we look at elementary block diagram manipulations which are used to combine subsystem blocks into a complete system.

Figure 3.4 shows two transfer functions connected in series. The output of the first block is the input to the next block, the transfer function of the complete system is given as:

$$G(s) = \frac{Y_2(s)}{U_1(s)} = \frac{Y_1(s)}{U_1(s)} \frac{Y_2(s)}{Y_1(s)} = G_1(s)G_2(s)$$

Figure 3.5 shows two transfer functions connected in parallel. The input of both the blocks is the same and the output of the system is the sum of the two outputs, the transfer function of the complete system is given as:

$$G(s) = \frac{Y(s)}{U(s)} = \frac{Y_1(s) + Y_2(s)}{U(s)} = G_1(s) + G_2(s)$$

Figure 3.6 shows two transfer functions connected in a negative feedback configuration. The transfer function of the complete system is obtained as follows:

$$
\begin{aligned}
U_1(s) &= U(s) - Y_2(s) \\
&= U(s) - G_1(s)G_2(s)U_1(s) \\
&= \frac{U(s)}{1 + G_1(s)G_2(s)}
\end{aligned}
$$

From the above and $Y(s) = G_1(s)U_1(s)$, we get

$$G(s) = \frac{Y(s)}{U(s)} = \frac{G_1(s)G_2(s)}{1 + G_1(s)G_2(s)}$$

In general an interconnected system will be much more complicated than the three cases considered here but using these three block diagram manipulations one can obtain the complete transfer function of even the most complicated system.
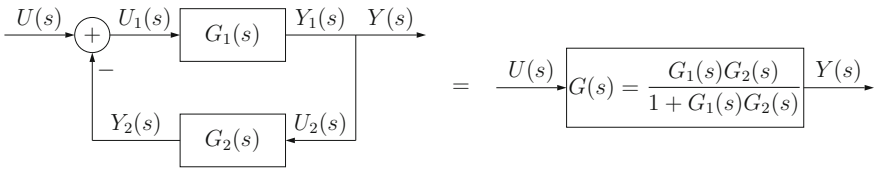
Fig. 3.6 Feedback connection

Subsequent to the combination of the subsystem blocks, one of the Laplace domain analysis method consists of evaluating the zeros and poles of the transfer function and then relating them to the time response of the dynamic system. Frequency response, obtained from the transfer function or experimentally, is another analysis method. We will look at the frequency response later in the chapter but next we see how dynamic system analysis is done using the poles and zeros of a transfer functions.

3.3.2 Second Order System Response

Transfer function for a second-order system (with $y(t) = x(t)$)

$$\ddot{x} + 2\zeta\omega_n\dot{x} + \omega_n^2 x = u(t); \ \ x(0) = 0, \ \dot{x}(0) = 0$$

can be written as,

$$G(s) = \frac{Y(s)}{U(s)} = \frac{\omega_n{}^2}{s^2 + 2\zeta\omega_n s + \omega_n{}^2} \tag{3.61}$$

where $\zeta, \omega_n > 0$. The transfer function is parameterised in terms of ζ and ω_n. The value of ω_n does not qualitatively change the system response but there are three important cases—with qualitatively different system behaviour—as ζ varies. The three cases are discussed below.

(a) $\zeta > 1$
This is known as an overdamped system. To see why, let's look at the step-response for this case.

$$Y(s) = \frac{1}{s}\frac{\omega_n{}^2}{(s + p_1)(s + p_2)}$$

$$= \frac{1}{s} - \frac{p_2}{p_2 - p_1}\frac{1}{s + p_1} + \frac{p_1}{p_2 - p_1}\frac{1}{s + p_2} \tag{3.62}$$

where $p_2 > p_1 > 0$, $p_1 = \omega_n(\zeta - \sqrt{\zeta^2 - 1})$, and $p_2 = \omega_n(\zeta + \sqrt{\zeta^2 - 1})$. This gives:

$$y(t) = 1 - \frac{1}{2}\left(\frac{\zeta}{\sqrt{\zeta^2 - 1}} + 1\right)e^{-\omega_n\left(\zeta - \sqrt{\zeta^2 - 1}\right)t} + \frac{1}{2}\left(\frac{\zeta}{\sqrt{\zeta^2 - 1}} - 1\right)e^{-\omega_n\left(\zeta + \sqrt{\zeta^2 - 1}\right)t}$$

$$= 1 - e^{-\omega_n t}\cosh\left(\omega_n\sqrt{\zeta^2 - 1}\right)t - \frac{\zeta}{\sqrt{\zeta^2 - 1}}e^{-\omega_n t}\sinh\left(\omega_n\sqrt{\zeta^2 - 1}\right)t \qquad (3.63)$$

In the above Eq. (3.63) it can be seen that

$$\cosh\left(\omega_n\sqrt{\zeta^2 - 1}\right)t > 0 \text{ and } \sinh\left(\omega_n\sqrt{\zeta^2 - 1}\right)t > 0, \quad \forall t > 0.$$

This means that two positive numbers are always subtracted in Eq. (3.63) from the steady-state value of 1. Hence the step-response $y(t)$ in Eq. (3.63) never goes above 1, hence the classification of overdamped.

(b) $\zeta < 1$
This is known as an underdamped system. To see why, let's look at the step-response for this case.

$$Y(s) = \frac{1}{s}\frac{\omega_n^2}{s^2 + 2\zeta\omega_n s + \omega_n^2}$$

$$= \frac{1}{s} - \frac{s + 2\zeta\omega_n}{s^2 + 2\zeta\omega_n s + \omega_n^2}$$

$$= \frac{1}{s} - \frac{\zeta\omega_n}{(s + \zeta\omega_n)^2 + \omega_n^2(1 - \zeta^2)} - \frac{s + \zeta\omega_n}{(s + \zeta\omega_n)^2 + \omega_n^2(1 - \zeta^2)} \quad (3.64)$$

This gives:

$$y(t) = 1 - \frac{\zeta e^{-\zeta\omega_n t}}{\sqrt{1 - \zeta^2}}\sin\omega_d t - e^{-\zeta\omega_n t}\cos\omega_d t$$

$$= 1 - \frac{e^{-\zeta\omega_n t}}{\sqrt{1 - \zeta^2}}\sin(\omega_d t + \psi) \qquad (3.65)$$

where $\omega_d = \omega_n\sqrt{1 - \zeta^2}$ and $\psi = \tan^{-1}\frac{\sqrt{1-\zeta^2}}{\zeta}$.

It can be clearly seen that the step-response in Eq. (3.65) will overshoot the steady-state value of 1 as the sinusoidal function takes negative values, hence the classification as underdamped system.

(c) $\zeta = 1$
This is the critically damped case. To see why let's look at the step-response.
Step-response:
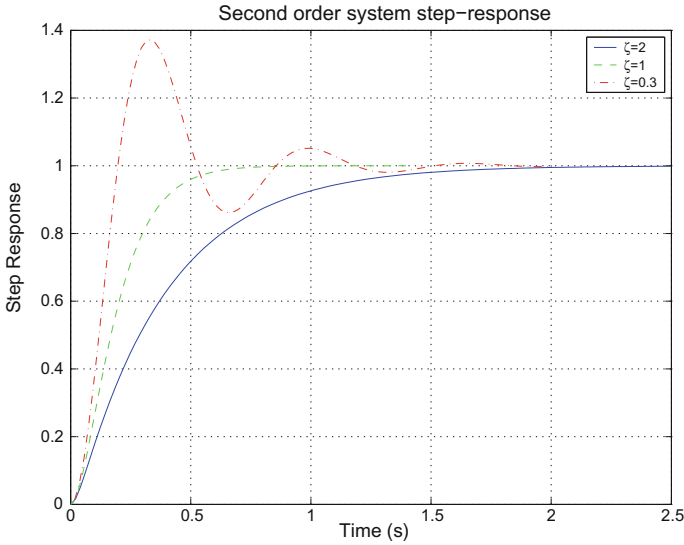
Fig. 3.7 Step-response of Second-order System ($\omega_n = 10$)

$$Y(s) = \frac{1}{s} \frac{\omega_n{}^2}{(s + \omega_n)^2}$$
$$= \frac{1}{s} - \frac{1}{s + \omega_n} - \frac{\omega_n}{(s + \omega_n)^2} \qquad (3.66)$$

This gives,

$$y(t) = 1 - e^{-\omega_n t} - \omega_n t e^{-\omega_n t}. \qquad (3.67)$$

Comparing the above expression (3.67) for the step-response with the expression for overdamped case in expression (3.63), we see that since (for $\zeta > 1$):

$$\cosh\left(\omega_n\sqrt{\zeta^2 - 1}\right) t > 1, \quad \forall t > 0 \text{ and } \frac{\zeta}{\sqrt{\zeta^2 - 1}} \sinh\left(\omega_n\sqrt{\zeta^2 - 1}\right) t > \omega_n t, \quad \forall t > 0,$$

the step-response of a critically damped system will always be higher than the over-damped system step-response ($\zeta > 1$). In other words, of all the second order damped systems with real poles (parameterised by ζ as in expression 3.61) this will reach the steady-state in the shortest time. That's why it's called critically damped. This can be clearly seen in Fig. 3.7.

An analysis for a second order system is done in the section. Almost every dynamic system has a much higher order than two, so why do we emphasise the second order analysis so much? The fact is that even for a hundredth order system the dominant dynamics is often given by just a couple of poles close to the imaginary axis, i.e., the

reduced order model of interest even for very high order systems is a second order system. Moreover, many design specifications are also given in terms of a second order system response. A good understanding and familiarity with the second order system dynamics is very important.

3.3.3 Frequency Domain Analysis

Frequency response for most systems can be experimentally obtained and this makes the study of the analysis and design methods based on frequency response very rewarding. Frequency response is a term used for the gain and phase shift between the input and output for sinusoidal forcing function in steady-state. In this section, first we prove that the steady-state output for a stable linear system, with sinusoidal inputs, is a sinusoid with the same frequency as the input sinusoid, with a different peak value and phase. This is the most vital element of linear analysis and design, thus it should be understood well.

    To make it accessible to students from different background, two proofs relating the transfer functions and state-space representations to the frequency response are presented next.

3.3.3.1 Transfer Function to Frequency Response

Let a stable system be described by a transfer function $H(s)$. Let us denote the input signal as $r(t)$ and the output signal as $y(t)$. For an input sinusoidal signal, i.e., $r(t) = A\sin(\omega_s t)$, the steady-state output $y(t) = A|H(j\omega)|\sin(\omega_s t + \angle H(j\omega))$.

Proof The Laplace transform of the input is:

$$\mathcal{L}[r(t)] = R(s) = \frac{A\omega_s}{s^2 + \omega_s^2}$$

and hence the output can be written as:

$$Y(s) = H(s)R(s) = H(s)\frac{A\omega_s}{s^2 + \omega_s^2}$$

Let

$$\frac{H(s)A\omega_s}{s^2 + \omega_s^2} = \frac{k}{s + j\omega_s} + \frac{k^*}{s - j\omega_s} + \sum_{i=1}^{n}\frac{\lambda_i}{s + \alpha_i} \qquad (3.68)$$

$$k = \frac{H(s)A\omega_s}{s^2 + \omega_s^2}(s + j\omega_s)\bigg|_{s=-j\omega_s} = \frac{H(-j\omega_s)A\omega_s}{-2j\omega_s} = \frac{jH(-j\omega_s)A}{2} \qquad (3.69)$$

Let

$$H(j\omega_s) \triangleq a(\omega_s) + jb(\omega_s)$$

This implies:

$$Y_{ss}(s) \triangleq \frac{k}{s + j\omega_s} + \frac{k^*}{s - j\omega_s} = \frac{j(a(\omega_s) - jb(\omega_s))A}{2(s + j\omega_s)} + \frac{-j(a(\omega_s) + jb(\omega_s))A}{2(s - j\omega_s)}$$

Then:

$$
\begin{aligned}
y_{ss}(t) = \mathcal{L}^{-1}[Y_{ss}(s)] &= \frac{(ja(\omega_s) + b(\omega_s))A}{2} e^{-j\omega_s t} + \frac{(-ja(\omega_s) + b(\omega_s))A}{2} e^{j\omega_s t} \\
&= A[\frac{ja(\omega_s)}{2}(e^{-j\omega_s t} - e^{j\omega_s t})] + A[\frac{b(\omega_s)}{2}(e^{-j\omega_s t} + e^{j\omega_s t})] \\
&= A[\frac{a(\omega_s)}{2j}(e^{j\omega_s t} - e^{-j\omega_s t})] + A[\frac{b(\omega_s)}{2}(e^{-j\omega_s t} + e^{j\omega_s t})] \\
&= A[a(\omega_s)\sin(\omega_s t) + b(\omega_s)\cos(\omega_s t)] \\
&= A\sqrt{(a^2(\omega_s) + b^2(\omega_s))}[\frac{a(\omega_s)}{\sqrt{(a^2(\omega_s) + b^2(\omega_s))}}\sin(\omega_s t) + \frac{b(\omega_s)}{\sqrt{(a^2(\omega_s) + b^2(\omega_s))}}\cos(\omega_s t)]
\end{aligned}
$$

Noting that

$$|H(j\omega_s)| = \sqrt{(a^2(\omega_s) + b^2(\omega_s))} \text{ and } \phi(\omega_s) \triangleq \angle H(j\omega_s) = \tan^{-1}\frac{b(\omega_s)}{a(\omega_s)}$$

we can write:

$$y_{ss}(t) = A|H(j\omega_s)|\sin(\omega_s t + \phi(\omega_s))$$

In the above we haven't paid any attention to the third part of the expression on the left hand side of the Eq. (3.68). Let us look at that expression now.

$$y_n(t) \triangleq \mathcal{L}^{-1}[\sum_{i=1}^{n}\frac{\lambda_i}{s + \alpha_i}] = \sum_{i=1}^{n}\lambda_i e^{-\alpha_i t}$$

Note that both λ_i and α_i can be either real or complex. When α_i is real then λ_i is also real. For complex α_i there will be another $\alpha_j = \alpha_i^*$ and in general we can write:

$$y_n(t) = \sum_{\forall \text{ real } \alpha_i}\lambda_i e^{-\alpha_i t} + \sum_{\forall \text{ complex } \alpha_i \& \alpha_i^*}k_i e^{-\Re(\alpha_i)t}\sin(\omega_s t + \psi)$$

It is easy to see that when (Real part of $(\alpha_i) > 0$) $\Re(\alpha_i) > 0$ then $\lim_{t\to\infty}y_n(t) = 0$.

For all passive RLC networks $\Re(\alpha_i)$ is always less than 0. The condition $\Re(\alpha_i) > 0$ also means that all the roots of the denominator of the transfer function $H(s)$ are in

the left half of the complex plane. Roots of the denominator of the transfer function are also known as the system poles; zeros are the roots of the transfer function numerator.

In other words for any system with the poles in the left half complex plane the steady-state response to a sinusoid of frequency w_s can be worked out by evaluating the magnitude and the phase of the complex number $H(jw_s)$ and then noting that the magnitude of the output is given by the magnitude of the input sinusoid times the magnitude of $H(jw_s)$ and the phase shift between the input sinusoid and the output is given by the phase of $H(jw_s)$.

3.3.3.2 State-Space Representation to Frequency Response

For a stable linear system,

$$\dot{x} = Ax + Bu \tag{3.70}$$
$$y = Cx + Du \tag{3.71}$$

let $u(t) = e^{st}$ where $s = iw$. Show that for this input $u(t)$ the steady-state output

$$y_{ss}(t) = Me^{i\theta}e^{st}$$

where

$$Me^{i\theta} = C(iwI - A)^{-1}B + D.$$

Use the above result to show that when

$$u(t) = \cos(\omega t) = \frac{1}{2}\left(e^{i\omega t} + e^{-i\omega t}\right)$$

then

$$y_{ss}(t) = M\cos(\omega t + \theta).$$

Proof We can write,

$$X(t) = e^{At}X(0) + \int_0^t e^{A(t-\tau)}Bu(\tau)d\tau = e^{At}X(0) + e^{At}\int_0^t e^{-A\tau}e^{i\omega\tau}d\tau B \tag{3.72}$$

Let

$$S = \int_0^t e^{-A\tau}e^{i\omega\tau}d\tau$$

then using the rule of integration by parts

$$S = \left. \frac{e^{-A\tau}e^{i\omega\tau}}{i\omega} \right|_0^t + \frac{A}{i\omega} \int_0^t e^{-A\tau}e^{i\omega\tau} d\tau \tag{3.73}$$

$$= \left. \frac{e^{-A\tau}e^{i\omega\tau}}{i\omega} \right|_0^t + \frac{A}{i\omega} S \tag{3.74}$$

$$\left(I - \frac{A}{i\omega} \right) S = \left. \frac{e^{-A\tau}e^{i\omega\tau}}{i\omega} \right|_0^t \tag{3.75}$$

$$= \frac{e^{-At}e^{i\omega t}}{i\omega} - \frac{I}{i\omega} \tag{3.76}$$

$$S = (i\omega I - A)^{-1} e^{-At} e^{i\omega t} - (i\omega I - A)^{-1} \tag{3.77}$$

$$= e^{-At} (i\omega I - A)^{-1} e^{i\omega t} - (i\omega I - A)^{-1} \tag{3.78}$$

The last step is possible only because the matrices $(i\omega I - A)^{-1}$ and e^{-At} commute. Putting S back in Eq. (3.72), we get

$$X(t) = e^{At} X(0) + e^{At} e^{-At} (i\omega I - A)^{-1} e^{i\omega t} - e^{At} (i\omega I - A)^{-1} \tag{3.79}$$

$$= e^{At} X(0) + (i\omega I - A)^{-1} e^{i\omega t} - e^{At} (i\omega I - A)^{-1} \tag{3.80}$$

If all the eigenvalues of A are in the left-half-plane then the first and third terms on the right-hand-side of the above equation go to zero as time goes to infinity. So we have

$$y_{ss}(t) = Me^{i\theta}e^{i\omega t} = \left(C (i\omega I - A)^{-1} B + D \right) e^{i\omega t}.$$

The steady-state output due to the input $e^{-i\omega t}$ is:

$$\left(C (-i\omega I - A)^{-1} B + D \right) e^{i\omega t} = Me^{-i\theta}e^{-i\omega t}.$$

Putting this together the steady-state output due to $cos(\omega t)$ is:

$$y_{ss}(t) = \frac{Me^{i\theta}e^{i\omega t} + Me^{-i\theta}e^{-i\omega t}}{2} \tag{3.81}$$

$$= \frac{Me^{i(\omega t + \theta)} + Me^{-i(\omega t + \theta)}}{2} \tag{3.82}$$

$$= Mcos(\omega t + \theta). \tag{3.83}$$

3.3.4 Bode Plots

Frequency response is normally represented as Bode plots. In this section we look at Bode plots with a view to using Bode plots in the design of controllers using frequency response data, either obtained analytically or experimentally.

A general transfer function, with real coefficients, can be represented in the following way:

$$H(s) = k \frac{\prod_{i=1}^{n_1}(1 + \alpha_i s) \prod_{i=1}^{n_2}\left(\frac{s}{\Omega_i}\right)^2 + \frac{2\xi_i s}{\Omega_i} + 1}{\prod_{i=1}^{n_3}(1 + \beta_i s) \prod_{i=1}^{n_4}\left(\frac{s}{\omega_i}\right)^2 + \frac{2\zeta_i s}{\omega_i} + 1} = \frac{\prod_{i=1}^{m} F_{z_i}}{\prod_{i=1}^{n} F_{p_i}}$$

Bode plot is a plot of $20 \log_{10} |H(\jmath\omega)|$ and the $\angle H(\jmath\omega)$ versus ω. It is a semilog plot where the x-axis is the log-axis and the y-axis is the linear axis. For complex numbers a and b, we have $\log(|a||b|) = \log |a| + \log |b|$ and $\angle ab = \angle a + \angle b$. For this reason we make a plot of each of the factors, $\left(F_{z_i}, F_{p_i}\right)$, separately and then add them up to give the Bode plot of $H(s)$. Next we look at Bode plots for first order and second order terms.

First Order Block—Bode Plot Let

$$H_1(s) = \frac{1}{1 + s\tau}, \quad H_1(\jmath\omega) = \frac{1}{1 + \jmath\omega\tau}$$

The sketch of the Bode plot of the first order term is obtain as follows:

$$20 \log_{10} |H_1(\jmath\omega)| = 20 \log_{10} \frac{1}{\sqrt{1 + \omega^2\tau^2}} = \begin{cases} 0 & \omega << \frac{1}{\tau}, \\ -3db & \omega = \frac{1}{\tau}, \\ -20 \log_{10}\omega - 20 \log_{10}\tau & \omega >> \frac{1}{\tau}. \end{cases}$$

$$\angle H_1(\jmath\omega) = -\tan^{-1}\frac{\omega\tau}{1} = \begin{cases} 0° & \omega << \frac{1}{\tau}\left(\frac{0.1}{\tau}\right) \\ -45° & \omega = \frac{1}{\tau}, \\ -90° & \omega >> \frac{1}{\tau}\left(\frac{10}{\tau}\right). \end{cases}$$

First order pole magnitude plots have a slope of -20 db/decade and the phase plot has a slope of –45 deg/decade (goes from 0 to $-90°$). First order zero magnitude plots have a slope of 20db/decade and the phase plot has a slope of 45 deg/decade (goes from 0 to 90°).

Bode plot for a first order term in the denominator is shown in Fig. 3.8 and for a first order term in the numerator is shown in Fig. 3.9.

Second Order Block—Bode Plot For transfer functions with complex poles or zeros, the transfer function cannot be reduced to a product of first order factors with real co-efficients. For such transfer functions Bode plots are sketched for the second order factors with complex poles or zeros. Next we discuss second order terms (Figs. 3.8 and 3.9).

Let a second order term be:

$$H_1(s) = \frac{1}{\left(\frac{s}{\omega_0}\right)^2 + \frac{2\zeta s}{\omega_0} + 1}$$

The frequency response for this term is:
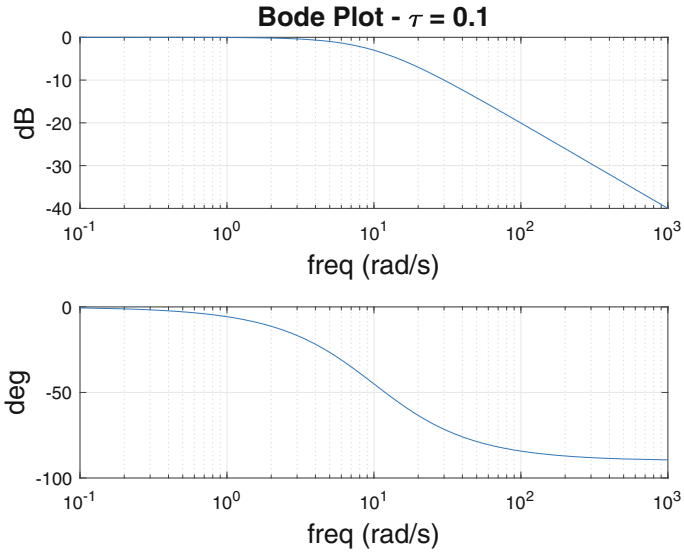
Fig. 3.8 Bode plot—$\frac{1}{1+s\tau}$
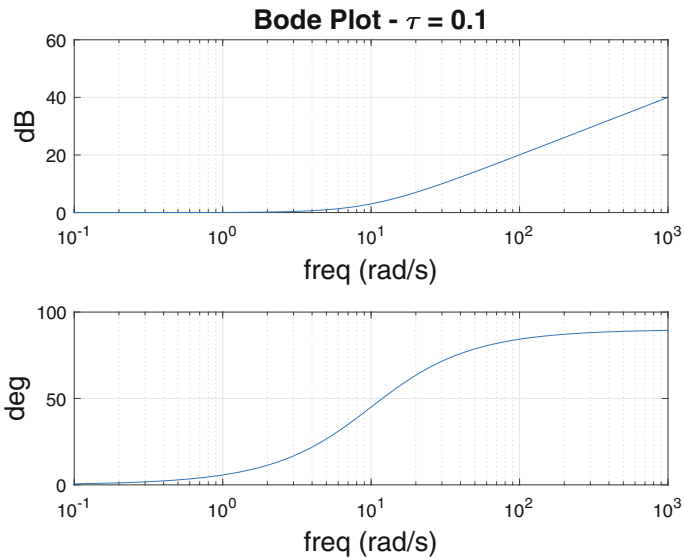
Fig. 3.9 Bode plot—$1 + s\tau$

$$H_1(J\omega) = \frac{1}{\left(\frac{J\omega}{\omega_0}\right)^2 + \frac{2\zeta J\omega}{\omega_0} + 1} = \frac{1}{1 - \left(\frac{\omega}{\omega_0}\right)^2 + \frac{2\zeta J\omega}{\omega_0}}$$

The magnitude of the frequency response is:

$$|H_1(J\omega)| = \frac{1}{\sqrt{\left(1 - \left(\frac{\omega}{\omega_0}\right)^2\right)^2 + 4\left(\frac{\zeta\omega}{\omega_0}\right)^2}}$$

Define $u \triangleq \frac{\omega}{\omega_0}$ and now the above expression can be written as:

$$|H_1(Ju)| = \frac{1}{\sqrt{\left(1 - (u)^2\right)^2 + 4\left(\zeta u\right)^2}} = \frac{1}{\sqrt{1 + 2u^2(2\zeta^2 - 1) + u^4}}$$

This magnitude function has a resonant peak in the Bode plot for certain values of *zeta*, the value of the peak, i.e., its maximum value is obtained next.

$$\frac{d\,|H_1(Ju)|}{du} = -\frac{1}{2}\frac{4u^3 + 4u(2\zeta^2 - 1)}{\left(1 + 2u^2(2\zeta^2 - 1) + u^4\right)^{\frac{3}{2}}}$$

$$\frac{d\,|H_1(Ju)|}{du} = 0 \text{ when } u = 0 \text{ or } u = \sqrt{1 - 2\zeta^2}, \text{ for u real } \zeta < \frac{1}{\sqrt{2}}$$

$$\left|H_1(J\sqrt{1 - 2\zeta^2})\right| = \frac{1}{\sqrt{1 - (1 - 2\zeta^2)^2}}$$

For $\zeta < \frac{1}{\sqrt{2}}$, we have $|H_1(Ju)| = \frac{1}{\sqrt{1+2u^2(2\zeta^2-1)+u^4}}$. The sketch for the second order term is obtained as follows:

$$20\log_{10}|H_1(Ju)| = \begin{cases} 0 & u \ll \sqrt{1 - 2\zeta^2}, \\ -10\log_{10}(\sqrt{1 - (1 - 2\zeta^2)^2}) & u = \sqrt{1 - 2\zeta^2}, \\ -40\log_{10} u & u \gg \sqrt{1 - 2\zeta^2}. \end{cases}$$

$$\angle H_1(Ju) = -\tan^{-1}\frac{2\zeta u}{1 - u^2} = \begin{cases} 0° & u \ll 1 \\ -90° & u = 1 \\ -180° & u \gg 1. \end{cases}$$

Second order pole magnitude plots have a slope of -40 db/decade and the phase plot goes from 0 to $-180°$ in the vicinity of the resonant frequency. Second order zero magnitude plots have a slope of 40db/decade and the phase plot goes from
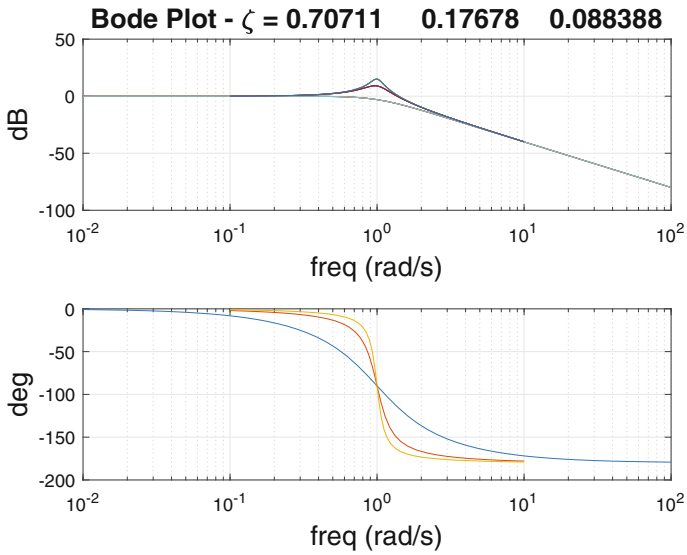
Fig. 3.10 Bode plot— $\frac{1}{s^2+2\zeta s+1}$
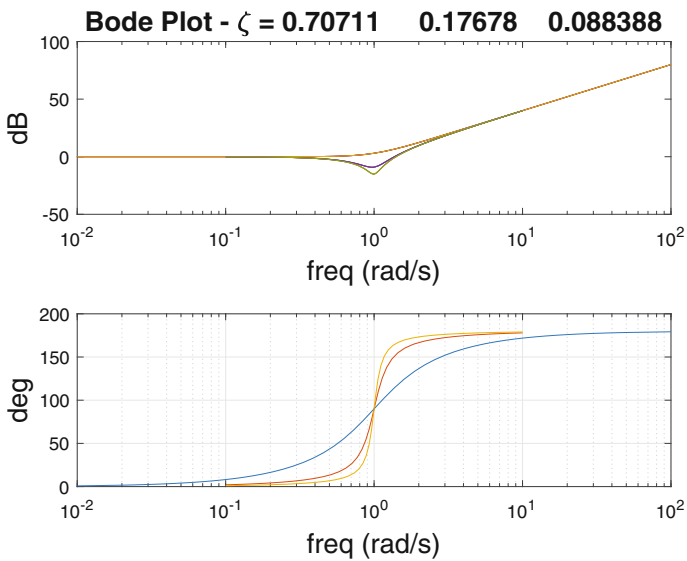
Fig. 3.11 Bode plot— $s^2 + 2\zeta s + 1$

0 to 180° in the vicinity of the resonant frequency. The sharpness of the phase plot as it switches from 0 to −180° depends on the damping ratio ζ as can be seen in Figs. 3.10 and 3.11.

Fig. 3.12 Feedback block
diagram
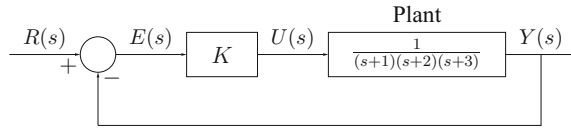
When sketching by hand, individual Bode plots for the first and second order terms are put together to obtain the complete Bode plot. With the ready availability of the computers, there is little need to sketch Bode plots by hand but hand sketching exercise helps to understand what information is contained in Bode plots and how one can use them to design controllers.

3.3.5   Root-Locus

In the preceding part of the chapter, time and frequency domain analysis was discussed. Root-locus is a technique which is a combination of both time and frequency domain analysis ideas. Root-locus is a handy tool to tune the gain of automatic voltage regulators and power system stabilisers in power systems.

Root-locus is the loci of all the poles of the closed-loop system as the gain K varies from 0 to ∞. As computers are used for plotting the root-locus, the rules required to plot a root-locus are not given here. It is more important to understand what information can be obtained from the root-locus than the rules to draw it.

For the system in Fig. 3.12, the root-locus is given in Fig. 3.13. The open-loop poles of this system are at: $\{-1, -2, -3\}$; from the root-locus in Fig. 3.13 it can be seen that as the gain K increases one closed-loop poles travels left along the negative real-axis but two poles go to the right-half-plane. There is a critical value of K for which two of the closed-loop poles are on the imaginary axis. If one were using the root-locus method to tune the parameter K, they would first decide if they wanted overdamped, critically damped, or underdamped (with the damping ratio) response, and then choose K to achieve that response. In short, root-locus gives all the possible locations of the closed-loop poles as the gain K changes and gives a good overview of how a constant gain controller can change the closed-loop dynamics. Root-locus is a very useful analysis and design tool for linear control.

3.3.6   Frequency Domain Control Design

In this section we discuss the design of the controller $H(s)$ shown in Fig. 3.14. In many practical situation we know only the frequency response of the plant $G(\jmath\omega)$, so the design method can use only this information and not the state-space representation or the transfer function of the system.

The closed-loop transfer function (also known as the closed-loop gain) is:
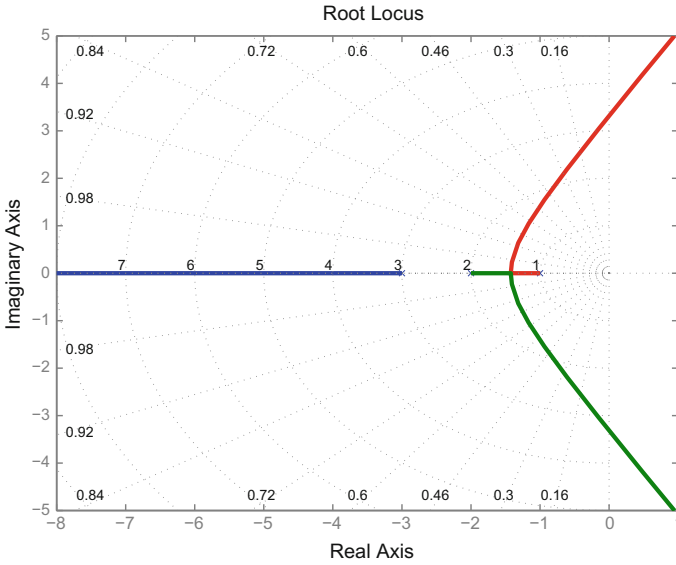
Fig. 3.13 Root locus (Matlab script `basicrlocus.m`)

$$\frac{Y(s)}{R(s)} = \frac{G(s)H(s)}{1 + G(s)H(s)}.$$

The above closed-loop system is stable only if all the roots of the equation $1 + G(s)H(s) = 0$ are in the left-half-plane.

For the closed-loop system in Fig. 3.14, the loop-gain is defined as $L(s) = G(s)H(s)$. This is the gain as we go around the loop from the input to the feedback summing junction. The loop-gain is also called the open-loop system. The stability of the closed-loop system can be evaluated from the frequency response of the loop-gain by evaluating the gain margin or the phase margin. For the closed-loop system to be stable both GM and PM (calculated with open-loop transfer function) should be positive if all the poles and zeros of the open-loop are in the left-half-plane.

Gain Margin (GM) GM of a system is the gain in dB of the loop-gain when the phase is $-180°$, i.e., $\text{GM} = -20 \log_{10} |L(J\omega^\dagger)|$, where $\angle L(J\omega^\dagger) = 180°$.

Phase Margin (PM) PM of a system is $180 + \angle L(J\hat{\omega})$ where $|L(J\hat{\omega})| = 1$.

A more general stability is given in terms of the Nyquist stability criterion using the frequency response of the open-loop system.

Fig. 3.14 Feedback block diagram
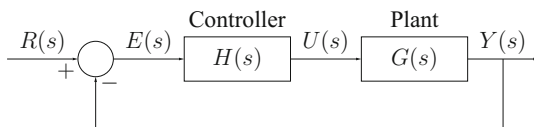
3.3.6.1   Design Specifications

The specifications for the design of the feedback controller $H(s)$ Fig. 3.14 in classical control design are normally specified in terms of four conditions:

1. Steady-state error, $\lim_{t \to \infty} e(t)$, for a chosen input $R(s)$.
2. The bandwidth or the zero gain crossover frequency of the loop-gain, i.e., ω_{BW}, such that, $|L(J\omega_{BW})| = 1$. The bandwidth is related to the speed of response.
3. Phase margin, normally chosen as sixty degrees.
4. Gain margin, normally chosen as higher than 6 dB.

Please note that the last three specifications above are in terms of the frequency response of the loop-gain. This means that we can use the frequency response of the plant to complete the design. Next we look at the relationship between the above design specifications and the closed-loop response.

3.3.6.2   Steady-State Error

The following analysis refers to the feedback system shown in Fig. 3.14. Assume that the feedback system is stable, then

$$E(s) = R(s) - G(s)H(s)E(s) \tag{3.84}$$

$$\Rightarrow (1 + G(s)H(s))E(s) = R(s) \tag{3.85}$$

$$\Rightarrow \frac{E(s)}{R(s)} = \frac{1}{1 + G(s)H(s)} \tag{3.86}$$

For unit step reference $R(s) = \frac{1}{s}$ and using the final value theorem ($\lim_{t \to \infty} f(t) = \lim_{s \to 0} sF(s)$, if the limit exists), we have

$$\lim_{t \to \infty} e(t) = \lim_{s \to 0} s \frac{1}{s} \frac{1}{1 + G(s)H(s)}$$

$$e_{ss} = e(\infty) = \frac{1}{1 + G(0)H(0)} \tag{3.87}$$

The values $G(0)$ and $H(0)$ are the DC gains of these transfer functions. From (3.87) it is obvious that if either the plant or the controller has an integrator, i.e., the $\frac{1}{s}$ term, then the steady-state error to a step-reference is zero. This is the reason why an integrator is a part of most of the controllers.

3.3.6.3   Open-Loop Bandwidth and Rise-Time

For the feedback system shown in Fig. 3.12, let $H(s) = K$ and $G(s) = \frac{1}{1+sT}$. It can be shown that:

1. The open-loop system bandwidth ω_{BW}, i.e., the 0 dB crossover of the Bode plot of $G(s)H(s)$, is approximately $\omega_{\mathrm{BW}} \approx \frac{K}{T}$.
2. The closed-loop system rise-time t_r (for a unit step input) is:

$$t_r \approx \frac{2.3}{\omega_{\mathrm{BW}}} \tag{3.88}$$

where t_r is the time at which the output reaches 90 per cent of its final or steady-state value.

Equation (3.88) connects bandwidth and rise time and it is very useful. Although this relationship is true only for a first order system, it is a good approximation for ever higher order system. Equation (3.88) tells that to achieve a fast response (small t_r), the open-loop or loop-gain bandwidth should be large. In this first order example the bandwidth can be increased by increasing K This rule of thumb is often used by control designers; to achieve a faster response, the gain of the loop is increased.

3.3.6.4 Phase-Margin and Damping

Let $G(s)$ be the plant transfer function and $H(s) = 1$, for the block diagram shown in Fig. 3.12. The closed-loop transfer function is,

$$T(s) = \frac{G(s)}{1 + G(s)}.$$

Let ω_p be such that $|G(\jmath\omega_p)| = 1$ and $\angle G(\jmath\omega_p) = \phi$, then

$$|T(\jmath\omega_p)| = \frac{1}{2 \sin \frac{\phi_m}{2}} \tag{3.89}$$

where phase margin $\phi_m = 180 + \phi, \quad -180° \leq \phi \leq 180°$.

Equation (3.89) is an important relationship that links phase-margin with peak value of the frequency response at the gain crossover point. As we saw previously the peak of the Bode plot for second order underdamped system is an indicator of the damping of the system. In general we want $|T(\jmath\omega_p)|$ to be less than one and it can be seen from (3.89) that for this to happen the phase-margin ϕ_m must be greater than 60°. This also means that the desired damping can be specified in terms of the phase-margin of the system. This is particularly useful since phase-margin can be directly adjusted using frequency domain techniques using experimentally measured data.

Next we look at a lead block which is the most important block in providing the right phase-margin. A good understanding of the frequency response of the lead block is very helpful in the design of AVRs and PSSs for power systems. Another

commonly used block is called a lag controller. The utility and characteristics of these two blocks will become clear when we look at their application to power systems.

3.3.7   Lead Block Relationships

The transfer function of a lead block can be written as:

$$C(s) = \frac{1 + s/\omega_z}{1 + s/\omega_p}$$

where $\omega_p > \omega_z$ Let ω_l be the frequency at which $\angle C(J\omega_l)$ is maximum over all $\omega > 0$. Then it can be shown that

$$\omega_l = \sqrt{\omega_z \omega_p}, \ \phi_l \triangleq \angle C(J\omega_l) = \sin^{-1}\left(\frac{\omega_p/\omega_z - 1}{\omega_p/\omega_z + 1}\right), \ \text{and}$$

$$20\log_{10}|C(J\omega_l)| = 10\log_{10}(\omega_p/\omega_z).$$

The ratio $\frac{\omega_p}{\omega_z}$ is often expressed as m.

It can also be seen that

$$m = \frac{1 + \sin\phi_l}{1 - \sin\phi_l}, \ \omega_l = \sqrt{\omega_z \omega_p} = \omega_z\sqrt{m}, \ \text{and} \ \log\omega_l = \frac{1}{2}\left(\log\omega_z + \log\omega_p\right)$$

The above relationships mean that for a lead compensator the maximum phase lead is provided at the frequency which is the geometric mean of the pole and zero frequencies of the lead block. The actual phase lead is a function of the separation of the pole and zero, the larger the separation the larger is the phase lead. Of course the maximum possible phase lead is 90° and to achieve that the pole and zero have to be two decades apart. For the control design, a specification is given in terms of the phase-margin and the lead controller is used if the desired phase-margin is higher than the existing phase-margin. The phase lead required to achieve the desired phase-margin is provided by the lead block. This is illustrated with a design example next.

Fig. 3.15 Feedback block diagram
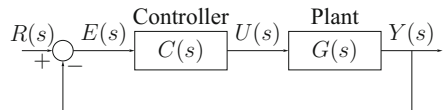
3.3.7.1 Example—Lead-Lag Controller Design

In Fig. 3.15, let

$$G(s) = \frac{10}{(s + 1)(s + 5)}.$$

Design a controller $C(s)$ such that,

1. The closed-loop system has zero steady-state error to unit step reference input;
2. The crossover frequency is above 100 rad s^{-1};
3. There is a minimum 60° phase margin.

A lead-lag controller, as explained below, can meet these specifications:

$$C(s) = K \frac{1 + \frac{s}{\alpha}}{s} \frac{1 + \frac{s}{\omega_z}}{1 + \frac{s}{\omega_p}}$$

From the system transfer function we can see that there is no integrator in the system. To achieve a zero steady-state error an integrator has to be a part of the system. Also from the frequency response of the open-loop system, shown in Fig. 3.16, it can be seen that the crossover frequency is 1.62 rad s^{-1}. To increase the crossover frequency we need to introduce gain at low frequencies. These two requirements can be met using a lag block: $\frac{1 + \frac{s}{\alpha}}{s}$. We need to choose an appropriate α to meet the crossover frequency requirement.

From Fig. 3.16 it can be seen that a gain of 1000 is needed at 100 rad s^{-1} for the crossover frequency to be at 100 rad s^{-1}. This gain can be achieved with $\alpha = 0.001$. The frequency response of the system with this lag block, i.e., $\frac{1 + 1000s}{s} G(s)$, is shown in Fig. 3.17. It can be seen that the phase-margin is no now only 3.44°. A lead compensator is needed to increase the phase margin to 60°.

Using the relationship derived above:

$$m = \frac{1 + \sin \phi_l}{1 - \sin \phi_l}, \omega_l = \sqrt{\omega_z \omega_p} = \omega_z \sqrt{m}, 100 \, \text{rad s}^{-1} \text{ and } \log \omega_l = \frac{1}{2} \left(\log \omega_z + \log \omega_p \right)$$

with $\omega_l = 100$ rad s^{-1} and $\phi_l = 56.56°$, we obtain $\omega_z = 30.0351$ rad s^{-1} and $\omega_p = 332.9438$ rad s^{-1}. The extra gain introduced by the lead block is 3.3294, to compensate for this $K = \frac{1}{3.3294}$ is chosen.

The frequency response of $C(s)G(s)$ is plotted in Fig. 3.18. From the figure we see that it meets both the bandwidth and phase-margin requirements. The closed-loop step-response is shown in Fig. 3.19.

A good understanding of the sequence of ideas used in this design problem can be very effectively used to design commercial grade AVRs and PSSs. As we will see later, the design of lag-lead controller in this design exercise can be used to design a PID controller by re-parametrising the controller. Next we see a popular method to directly design a PID controller.

Bode Diagram
Gm = Inf dB (at Inf rad/s) , Pm = 104 deg (at 1.62 rad/s)

Fig. 3.16 $G(s)$ Bode plot

Bode Diagram
Gm = Inf dB (at Inf rad/s) , Pm = 3.43 deg (at 100 rad/s)
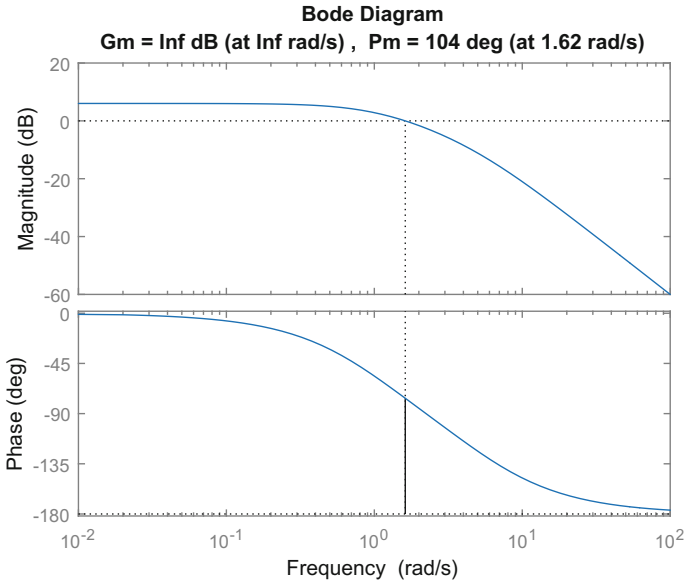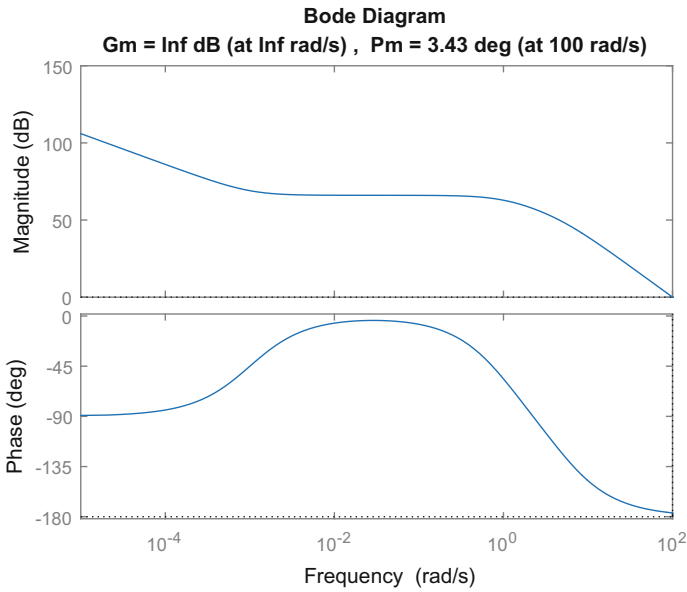
Fig. 3.17 Bode plot—Plant with lag compensator ($\alpha = 0.001$)
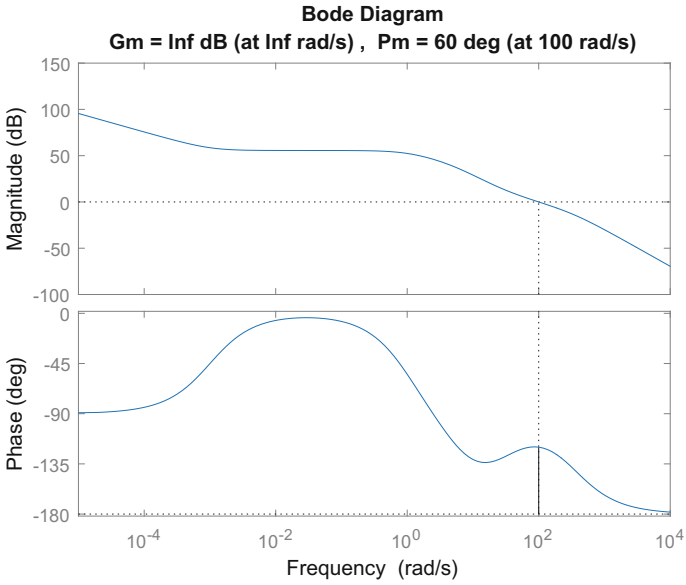
Fig. 3.18   Plant with Lead-lag compensator
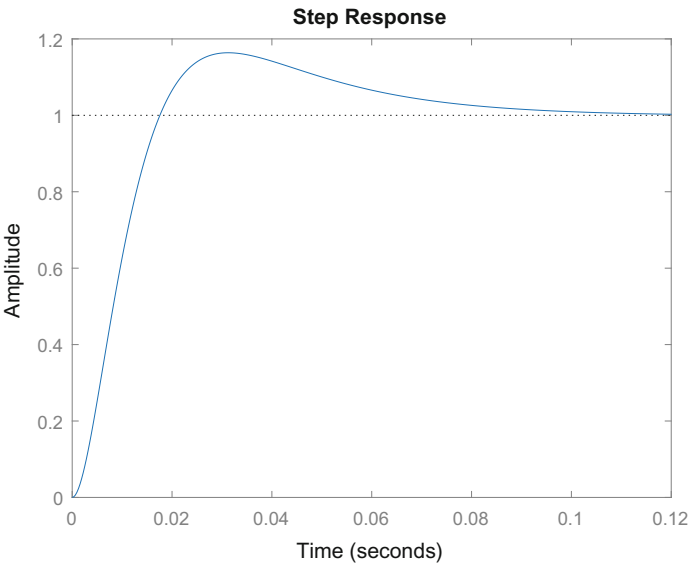
Fig. 3.19   Closed-loop step response

Fig. 3.20 Feedback block
diagram
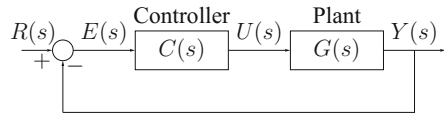
3.4   Ziegler-Nichols Tuning Method for PID Control

Ziegler-Nichols method to tune PID controller gains is mostly used for industrial
systems where a full mathematical model is not available but it is acceptable to
perform tests on the plant itself to tune a controller. For the unity feedback block
diagram in Fig. 3.20, let the PID controller be respresented as:

$$C(s) = K_P \left[1 + \frac{1}{T_i s} + T_d s \right].$$

The Ziegler-Nichols method provides guidelines to tune the parameters, K_P, T_i,
and T_d.

The first step is to perform experiments on the system in closed-loop, as shown
in Fig. 3.20, with $\frac{1}{T_i} = 0$ and $T_d = 0$. The gain K_P is varied till there is a sustained
oscillation in the system. The value of K_P for which the sustained oscillations are
observed is called the critical gain K_c. Let the period of the oscillations be T_c. The PID
controller parameters are obtained in terms of the critical gain K_c and the oscillation
period T_c as shown in Table 3.2. Depending on the desired closed-loop response
different parameter selections can be made.

3.4.1   PID Control of Governors

Synchronous machine governors respond to change in frequency by adjusting the
input mechanical power. In a given power system there are multiple generators hence
multiple governors. Two features distinguish control design for governors from that
of the AVRs. Firstly, governors are deliberately designed so that the frequency error

Table 3.2 Zeigler-Nichols parameters

Control	K_P	T_i	T_d
P only	$0.5K_c$		
PI	$0.45K_c$	$0.833T_c$	
PID tight control	$0.6K_c$	$0.5T_c$	$0.125T_c$
PID some overshoot	$0.33K_c$	$0.5T_c$	$0.33T_c$
PID no overshoot	$0.2K_c$	$0.3T_c$	$0.5T_c$
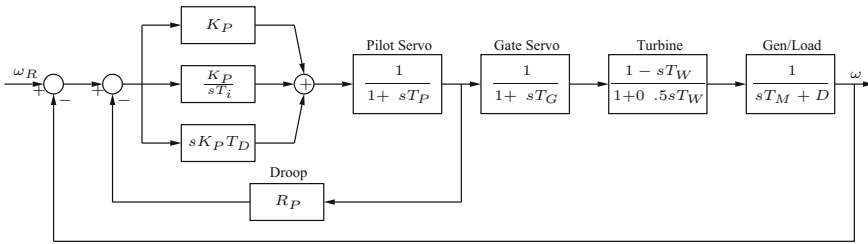
Fig. 3.21   Governor PID control

does not go to zero with changing output electrical power. This is done so that governors do not compete with each other in compensating for the mismatched power. The frequency of the generator is decreased with increasing output power, and this is known as droop, as shown in the droop block in Fig. 3.21. Secondly, governors have a slow response time, in the order of tens of seconds, and the turbines, valves, servomechanisms have significant built-in delays. For these systems Ziegler-Nichols method for tuning PID controllers has been very successful.

For governor control design a first-order synchronous machine model is used since governor dynamics is slow there is no loss of accuracy if only the mechanical movement is modelled and the electrical dynamics are neglected. In the model chosen for control, shown in Fig. 3.21, a pilot servo, gate servo, and turbine are all modelled as first-order systems. The turbine model has a right-half-plane zero which models the flexibility of the turbine shaft.

The design method is illustrated for a system with the following parameters: $T_P = 0.05$, $T_G = 0.2$, $T_W = 3$, $T_M = 10$, $R_P = 0.0.04$, $D = 1$.

The controller for the governor in Fig. 3.21 has three blocks. Firstly only the top, proportional gain, block is included in the system and the other two blocks are taken out. In the closed-loop the proportional gain is varied and for $K_c = 4.195$ sustained oscillations are observed with a period $T_c = 12.44s$, as shown in Fig. 3.22. PID controller parameters are tuned with these two values as shown in Table 3.2. Closed-loop step-responses for various choices of response are obtained; Fig. 3.23 shows the plot for proportional control only; Fig. 3.24 is for PI control; Fig. 3.25 shows tight PID control; Fig. 3.26 shows response for PID with some over-shoot, and finally Fig. 3.27 is for a PID control which is designed to result in no overshoot. As can be seen from the plots the responses do not fully match the performance criterion but they are close enough for practical purposes. Ziegler-Nichols method is robust to modelling uncertainties and it is a good practical method to tune PID controller parameters.
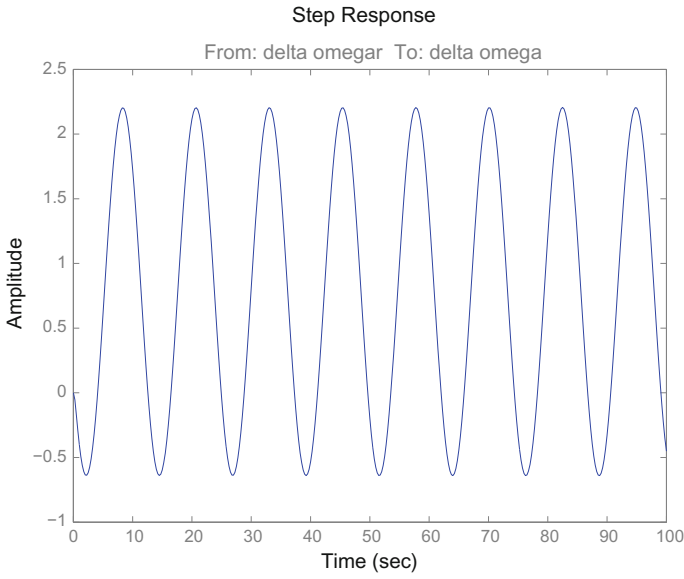
Fig. 3.22 PID Tuning—Governor—Sustained oscillations $K_c = 4.195$, $T_c = 12.44$ s
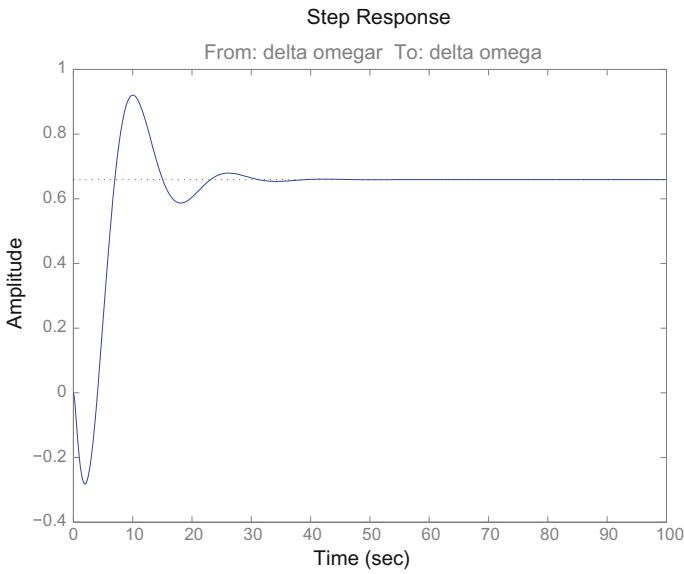
Fig. 3.23 PID Tuning—Governor—P only—$K_P = 0.5K_c$
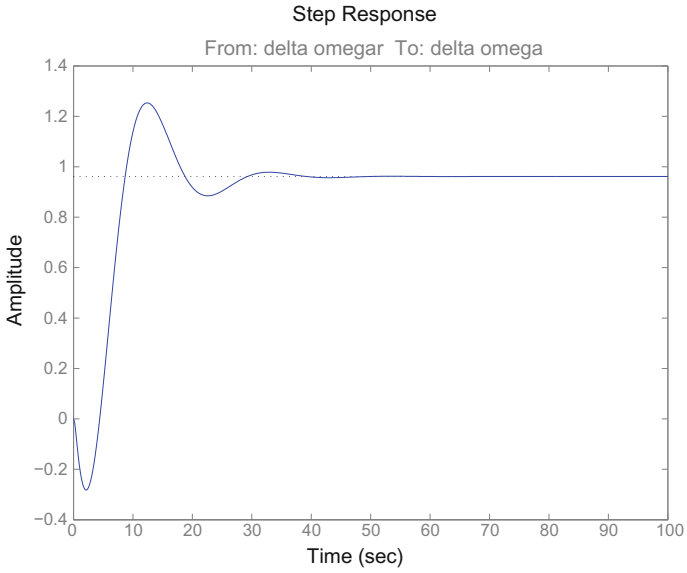
Fig. 3.24 PID Tuning—Governor—PI—$K_P = 0.45K_c$, $T_i = 0.833T_c$
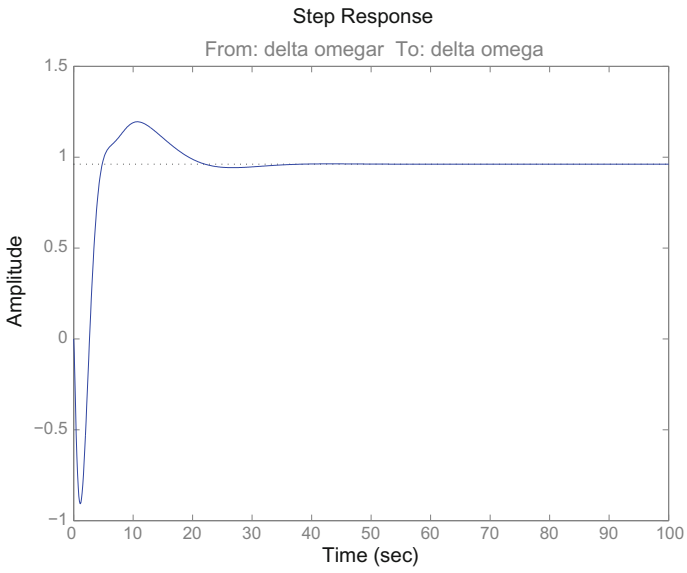
Fig. 3.25 PID Tuning—Governor—PID tight—$K_P = 0.6K_c$, $T_i = 0.5T_c$, $T_d = 0.125T_c$

Step Response

From: delta omegar To: delta omega
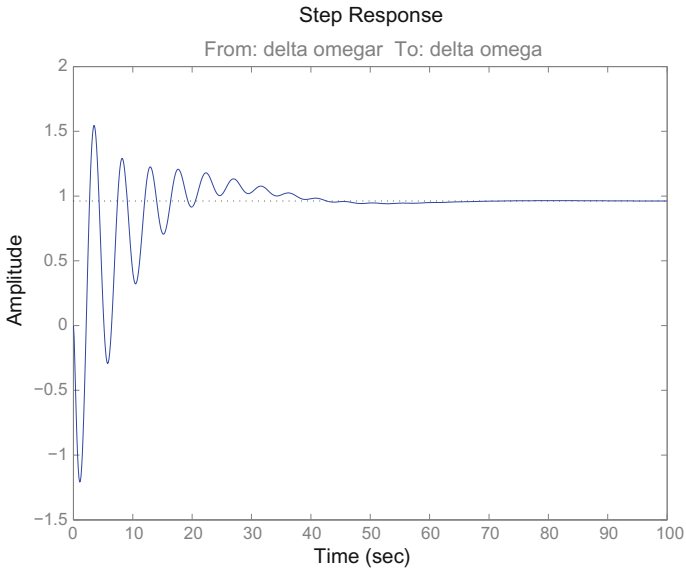
Fig. 3.26 PID Tuning—Governor—PID some overshoot—$K_P = 0.33K_c$, $T_i = 0.5T_c$, $T_d = 0.33T_c$

Step Response

From: delta omegar To: delta omega
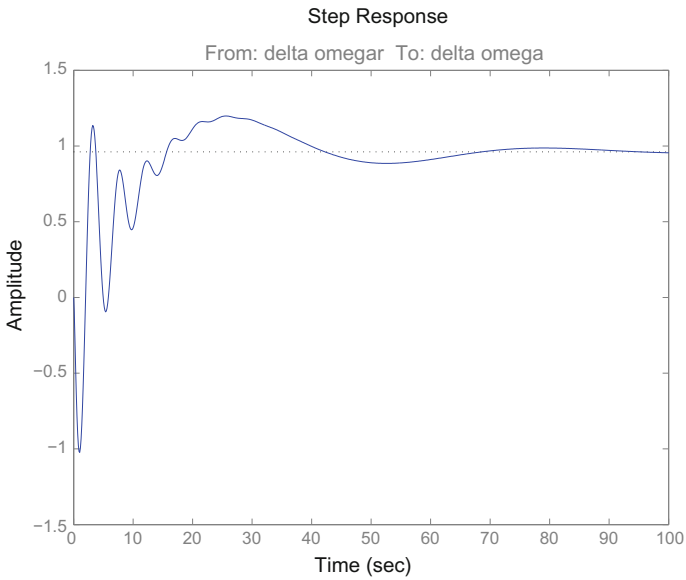
Fig. 3.27 PID Tuning—Governor—PID no overshoot—$K_P = 0.2K_c$, $T_i = 0.3T_c$, $T_d = 0.5T_c$

3.4.1.1 Exercise—Lead-lag Controller

In the above Fig. 3.15, let

$$G(s) = \frac{100}{(s/10 + 1)(s/20 + 1)}.$$

Design a controller $C(s)$ such that,

1. The closed-loop system has zero steady-state error to unit step reference input;
2. The crossover frequency is above 500 rad s^{-1};
3. There is a minimum 60° phase margin.

3.5 Linearisation

Most dynamic systems can only be described by a nonlinear model but for the purposes of designing a controller a linear model is often used. Linear control theory is a very convenient tool to design controllers even for nonlinear systems so to be able to use linear control ideas nonlinear models are first linearised. In this section we look at an analytical and also a numerical linearisation method.

Let a general nonlinear system have the following state-space representation:

$$\dot{x} = f(x, u) \tag{3.90}$$

In the above Eq. (3.90) x and $f(x, u)$ are n-dimensional vectors, u is an m-dimensional vector, and the ith element of each of these vectors is x_i, $f_i(x, u)$, u_i, respectively.

Linearisation is done about an equilibrium point, say (x_0, u_0), such that $f(x_0, u_0) = 0$. Taylor series expansion of $f(x, u)$ about the equilibrium point, (x_0, u_0), is put together from the Taylor series expansion for each element, $f_i(x, u)$, of $f(x, u)$:

$$f_i(x_0 + \Delta x, u_0 + \Delta u) = f_i(x_0, u_0) + \left.\frac{\partial f_i(x, u)}{\partial x_1}\right|_{\substack{x=x_0 \\ u=u_0}} \Delta x_1 + \left.\frac{\partial f_i(x, u)}{\partial x_2}\right|_{\substack{x=x_0 \\ u=u_0}} \Delta x_2 + \cdots \tag{3.91}$$

$$\left.\frac{\partial f_i(x, u)}{\partial x_n}\right|_{\substack{x=x_0 \\ u=u_0}} \Delta x_n + \cdots + \left.\frac{\partial f_i(x, u)}{\partial u_1}\right|_{\substack{x=x_0 \\ u=u_0}} \Delta u_1 + \cdots + \left.\frac{\partial f_i(x, u)}{\partial u_m}\right|_{\substack{x=x_0 \\ u=u_0}} \Delta u_m. \tag{3.92}$$

where $\Delta x_i = x_i - x_{i_0}$ and $\Delta u_i = u_i - u_{i_0}$.

For small changes in Δx and Δu we can write a linearised version of the differential equation (3.90) by neglecting all the terms with higher powers of Δx_i and Δu_j, to obtain the following linearised system:

$$\Delta \dot{x} = A \Delta x + B \Delta u \tag{3.93}$$

where

$$\Delta x = \begin{bmatrix} \Delta x_1 \\ \Delta x_2 \\ \vdots \\ \Delta x_n \end{bmatrix} \text{ and } \Delta u = \begin{bmatrix} \Delta u_1 \\ \Delta u_2 \\ \vdots \\ \Delta u_n \end{bmatrix}$$

$$A = \begin{bmatrix} \frac{\partial f_1(x,u)}{\partial x_1}\Big|_{\substack{x=x_0 \\ u=u_0}} & \frac{\partial f_1(x,u)}{\partial x_2}\Big|_{\substack{x=x_0 \\ u=u_0}} & \cdots & \frac{\partial f_1(x,u)}{\partial x_n}\Big|_{\substack{x=x_0 \\ u=u_0}} \\ \frac{\partial f_2(x,u)}{\partial x_1}\Big|_{\substack{x=x_0 \\ u=u_0}} & \frac{\partial f_2(x,u)}{\partial x_2}\Big|_{\substack{x=x_0 \\ u=u_0}} & \cdots & \frac{\partial f_2(x,u)}{\partial x_n}\Big|_{\substack{x=x_0 \\ u=u_0}} \\ \vdots & \vdots & \vdots & \vdots \\ \frac{\partial f_n(x,u)}{\partial x_1}\Big|_{\substack{x=x_0 \\ u=u_0}} & \frac{\partial f_n(x,u)}{\partial x_2}\Big|_{\substack{x=x_0 \\ u=u_0}} & \cdots & \frac{\partial f_n(x,u)}{\partial x_n}\Big|_{\substack{x=x_0 \\ u=u_0}} \end{bmatrix} \quad (3.94)$$

$$B = \begin{bmatrix} \frac{\partial f_1(x,u)}{\partial u_1}\Big|_{\substack{x=x_0 \\ u=u_0}} & \frac{\partial f_1(x,u)}{\partial u_2}\Big|_{\substack{x=x_0 \\ u=u_0}} & \cdots & \frac{\partial f_1(x,u)}{\partial u_m}\Big|_{\substack{x=x_0 \\ u=u_0}} \\ \frac{\partial f_2(x,u)}{\partial u_1}\Big|_{\substack{x=x_0 \\ u=u_0}} & \frac{\partial f_2(x,u)}{\partial u_2}\Big|_{\substack{x=x_0 \\ u=u_0}} & \cdots & \frac{\partial f_2(x,u)}{\partial u_m}\Big|_{\substack{x=x_0 \\ u=u_0}} \\ \vdots & \vdots & \vdots & \vdots \\ \frac{\partial f_n(x,u)}{\partial u_1}\Big|_{\substack{x=x_0 \\ u=u_0}} & \frac{\partial f_n(x,u)}{\partial u_2}\Big|_{\substack{x=x_0 \\ u=u_0}} & \cdots & \frac{\partial f_n(x,u)}{\partial u_m}\Big|_{\substack{x=x_0 \\ u=u_0}} \end{bmatrix} \quad (3.95)$$

Matrices A and B are also called the Jacobian matrices.

3.5.1 Perturbation Method

In many situations the partial derivatives are hard or inconvenient to obtain and in those situations perturbation analysis can be used to obtain a linearised model. The $(i, j)th$ element of the matrix A in the linearised model (3.93) are obtained numerically as:

$$a_{ij} = \frac{f_i(x_0 + \varepsilon_j, u_0) - f_i(x_0, u_0)}{\varepsilon_j}$$

where ε_j is a vector the same size as x with all its elements zero other than its jth element which is a small number ε.

The $(i, j)th$ element of matrix B can be obtained numerically as:

$$b_{ij} = \frac{f_i(x_0, u_0 + \varepsilon_j) - f_i(x_0, u_0)}{\varepsilon_j}$$

where ε_j is a vector the same size as u with all its elements zero other than its jth element. This is a simple method and works well in practice.

3.6 Linear Models for Synchronous Machine

Synchronous machine models are inherently nonlinear due to the fact that the electrical power is proportional to the sine of the power angle δ. Other types of nonlinearities are also present, such as magnetic saturation effects, but these effects are not important for the control design. To get familiar with the linearisation process the linearising of a SMIB system, shown in Fig. 3.28, is considered next.

3.6.1 Single Machine Infinite Bus Equations (Without AVR)

The differential equations for SMIB system are obtained from the Eqs. (2.25)–(2.27) in Chap. 2.

$$\dot{\delta} = \omega_0 \omega_r - \omega_0 \tag{3.96}$$

$$\dot{\omega}_r = \frac{1}{2H} (T_m - T_e - K_D \omega_r) \tag{3.97}$$

$$\dot{E}'_q = \frac{1}{\tau'_{do}} \left(E_{\mathrm{fd}} - E'_q - \left(x_d - x'_d \right) I_d \right) \tag{3.98}$$

where $E'_q = \frac{L_{md}}{L_{\mathrm{fd}}} \lambda_{\mathrm{fd}}, \tau'_{do} = \frac{L_{\mathrm{fd}}}{\omega_0 r_{\mathrm{fd}}}, E_{\mathrm{fd}} = \frac{L_{md}}{r_{\mathrm{fd}}} v_{\mathrm{fd}}, K_D$ is the mechanical damping. Algebraic equations ($r_e = 0$):

$$I_d = \frac{E'_q - V_\infty \cos \delta}{x'_d + x_e} \tag{3.99}$$

$$I_q = \frac{V_\infty \sin \delta}{x'_q + x_e} \tag{3.100}$$

$$V_q = E'_q - x'_d I_d \tag{3.101}$$

$$V_d = x'_q I_q \tag{3.102}$$

$$T_e = E'_q I_q + \left(x'_q - x'_d \right) I_q I_d \tag{3.103}$$

Note that the per unit numerical values of the torque and power are the same. The first step in linearising is defining the deviation of the state variables from their equilibrium value as new state variables. Let x^0 denote the equilibrium values of a state variable

Fig. 3.28 Single Machine Infinite Bus (SMIB)
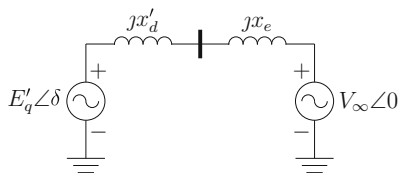
x, then the new states are defined as $\Delta x = x - x^0$, e.g., $\Delta\delta = \delta - \delta^0$. Please note that as the equilibrium value is a constant, giving $\Delta\dot{x} = \dot{x}$. The equilibrium per unit value of the speed is 1 so $\Delta\omega_r = \omega_r - 1$. The linear version of Eqs. (3.96)–(3.98) is obtained by writing these equations in terms of the new state variables. This means writing the linear approximation for all the nonlinear algebraic functions on the right-hand side of Eqs. (3.96)–(3.98). Following this procedure and taking Laplace transform of each of the elements of the equations, the linearised equations of the synchronous machine connected to an infinite-bus through a transmission line can be written as:

$$\Delta\delta(s) = \frac{\omega_0}{s}\Delta\omega_r(s) \tag{3.104}$$

$$\Delta\omega_r(s) = \frac{\Delta T_m(s) - \Delta T_e(s)}{2Hs + K_D} \tag{3.105}$$

$$s\Delta E'_q(s) = \frac{1}{\tau'_{do}}\left(\Delta E_{\mathrm{fd}}(s) - \Delta E'_q(s) - (x_d - x'_d)\left(\Delta\delta(s)\left.\frac{\partial I_d}{\partial\delta}\right|_{(.)=(.)^0} + \Delta E'_q(s)\left.\frac{\partial I_d}{\partial E'_q}\right|_{(.)=(.)^0}\right)\right) \tag{3.106}$$

where $(.) = (.)^0$ means that the function has to be evaluated at the equilibrium value of all the states on which it depends. The linearised electric torque from (3.103) can be written as:

$$\Delta T_e(s) = \Delta\delta(s)\left.\frac{\partial T_e}{\partial\delta}\right|_{(.)=(.)^0} + \Delta E'_q(s)\left.\frac{\partial T_e}{\partial E'_q}\right|_{(.)=(.)^0}$$

$$= K_1\Delta\delta(s) + K_2\Delta E'_q(s) \tag{3.107}$$

With the definitions of the K-parameters given below, we can write (3.106) as,

$$\Delta E'_q(s) = \frac{K_3}{1 + sT_3}\left(\Delta E_{\mathrm{fd}}(s) - K_4\Delta\delta(s)\right) \tag{3.108}$$

Figure 3.29 is a block diagram representation of Eqs. (3.105)–(3.108).

For the above linearised equations it is easy to derive the following expressions of the K-parameters:

$$K_1 = \frac{E'^0_q V_\infty \cos\delta^0}{x'_q + x_e} + \frac{(x'_q - x'_d)\left(E'^0_q V_\infty \cos\delta^0 - V^2_\infty \cos 2\delta^0\right)}{(x'_d + x_e)(x'_q + cx_e)}$$

$$K_2 = \frac{V_\infty \sin\delta^0}{x'_d + x_e}$$

$$K_3 = \frac{x'_d + x_e}{x_e + x_d}, \quad T_3 = \tau'_{do}K_3, \quad K_4 = \frac{x_d - x'_d}{x'_d + x_e}V_\infty \sin\delta^0$$

It can be shown that the transfer function (with $\Delta T_m = 0$) is:

$$\frac{\Delta \delta(s)}{\Delta E_{fd}(s)} = \frac{-K_2 K_3 \omega_0}{(1 + sT_3)\left(2Hs^2 + K_D s + K_1 \omega_0\right) - K_2 K_3 K_4 \omega_0} \tag{3.109}$$

Let the K-parameters for a synchronous machine be given as:

$$K_1 = 1.591, \, K_2 = 1.5, \, K_3 = 0.333, \, K_4 = 1.8, \, T_3 = 1.91, \, K_5 = -0.12, \, K_6 = 0.3$$

$$T_R = 0.03, \, H = 3.0, \, K_D = 0.0, \, \omega_0 = 2\pi 60.$$

For these parameter values, the roots of characteristic equation of just the mechanical part, $2Hs^2 + K_D s + K_1 \omega_0$ are, has roots at $\pm j9.9983$.

The poles of the transfer function in (3.109) are: $0.1470 \pm j10.00, -0.8175$.

The resonant mode is still at $9.99\,\mathrm{rad\,s^{-1}}$ but the inclusion of the field circuit has added a little damping to the mode.

3.6.1.1 Linear Model—State-Space Representation

From the block diagram in Fig. 3.29, it can be shown that the state-space representation of the linearised synchronous machine without an AVR can be written as:

$$\begin{bmatrix} \Delta \dot{\omega} \\ \Delta \dot{\delta} \\ \Delta \dot{E}'_q \end{bmatrix} = \begin{bmatrix} -\frac{K_D}{2H} & -\frac{K_1}{2H} & -\frac{K_2}{2H} \\ \omega_0 & 0 & 0 \\ 0 & -\frac{K_4 K_3}{T_3} & -\frac{1}{T_3} \end{bmatrix} \begin{bmatrix} \Delta \omega \\ \Delta \delta \\ \Delta E'_q \end{bmatrix} + \begin{bmatrix} \frac{1}{2H} & 0 \\ 0 & 0 \\ 0 & \frac{K_3}{T_3} \end{bmatrix} \begin{bmatrix} \Delta T_m \\ \Delta E_{\mathrm{fd}} \end{bmatrix} \tag{3.110}$$

For a system with the following parameter values, $P_m = 0.5$; $x_q = 1.0$; $x_d = 1.81$; $H = 3.5$; $K_D = 1$; $\tau'_{d0} = 8.0$; $T_R = 0.02$; $K_A = 200$; $x'_d = 0.8$; $x'_q = 0.8$; $x_e = 0.6$; $\omega_0 = 2\pi 50$; $V_\infty = 0.995$; $E'_{q0} = 1.2$, the A-matrix using the above linearised model representation in (3.110) and using linearisation by perturbation are given below. It can be seen that there is a good agreement between the two matrices (Analytical (left) and Perturbation Method (right)).

$$\begin{bmatrix} -0.1429 & -0.0987 & -0.05952 \\ 314.2 & 0 & 0 \\ 0 & 0.0526 & -0.03482 \end{bmatrix}, \quad \begin{bmatrix} -0.1429 & -0.09834 & -0.05952 \\ 314.2 & 0 & 0 \\ 0 & 0.05297 & -0.03482 \end{bmatrix} \tag{3.111}$$
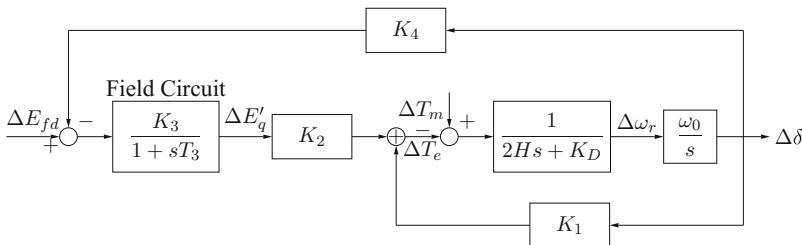
Fig. 3.29 Synchronous machine (without AVR)

3.6.2 Single Machine Infinite Bus Equations (with AVR)

Automatic Voltage Regulator (AVR) is needed to regulate the terminal voltage of synchronous generators. The input to the AVR is the difference between the set reference voltage and the measured terminal voltage. Modern AVRs or exciters are solid-state devices and owing to their fast response they can be modelled as a static gain to get an insight into the role of AVRs in maintaining system stability.

The modified equations of a synchronous machine with an AVR are written as:

$$\dot{\delta} = \omega_0 \omega - \omega_0 \tag{3.112}$$

$$\dot{\omega} = \frac{1}{2H} \left(P_m - E'_q I_q + \left(x'_d - x'_q \right) I_q I_d \right) \tag{3.113}$$

$$\dot{E}'_q = \frac{1}{\tau'_{do}} \left(K_A \left(V_{\text{ref}} - V_o + V_s \right) - E'_q - \left(x_d - x'_d \right) I_d \right) \tag{3.114}$$

$$\dot{V}_o = \frac{1}{T_R} \left(V_t - V_o \right) \tag{3.115}$$

Equation (3.115) represents the sensor dynamics that is used to measure the root-mean-square value of the terminal voltage.

The algebraic equations for this system are ($r_e = 0$):

$$I_d = \frac{E'_q - V_\infty \cos \delta}{x'_d + x_e} \tag{3.116}$$

$$I_q = \frac{V_\infty \sin \delta}{x'_q + x_e} \tag{3.117}$$

$$V_q = E'_q - x'_d I_d \tag{3.118}$$

$$V_d = x'_q I_q \tag{3.119}$$

$$V_t = \sqrt{V_q^2 + V_d^2}$$
$$= \sqrt{(x'_q I_q)^2 + (E'_q - x'_d I_d)^2} \tag{3.120}$$

3.6.3 K-Paramters: K_5 and K_6

To obtain the linear model with terminal voltage as one the state-variables two more K-parameters are required. Small changes in the terminal voltage V_t in (3.120) can be expressed as a linear function of $\Delta \delta(s)$ and $\Delta E'_q$:

$$\Delta V_t(s) = K_5 \Delta \delta(s) + K_6 \Delta E'_q(s). \tag{3.121}$$

From (3.120) we can write,

$$2V_t^0 \Delta V_t(s) = 2(x_q')^2 I_q^0 \left(\Delta\delta(s) \left. \frac{\partial I_q}{\partial \delta} \right|_{(.)=(.)^0} + \Delta E_q'(s) \left. \frac{\partial I_q}{\partial E_q'} \right|_{(.)=(.)^0} \right)$$
$$+ 2(E_q'^0 - x_d' I_d^0) \left(\Delta E_q'(s) - x_d' \left(\Delta\delta(s) \left. \frac{\partial I_d}{\partial \delta} \right|_{(.)=(.)^0} + \Delta E_q'(s) \left. \frac{\partial I_d}{\partial E_q'} \right|_{(.)=(.)^0} \right) \right)$$
$$(3.122)$$

Obtaining expressions for the partial derivatives and evaluating them about the equilibrium point the following expressions for K_5 and K_6 are obtained.

$$K_5 = \frac{1}{V_t^0} \left((x_q')^2 I_q^0 \frac{V_\infty \cos \delta^0}{x_q' + x_e} - (E_q'^0 - x_d' I_d^0) x_d' \frac{V_\infty \sin \delta^0}{x_d' + x_e} \right)$$

$$K_6 = \frac{1}{V_t^0} \left((E_q'^0 - x_d' I_d^0) - (E_q'^0 - x_d' I_d^0) \frac{x_d'}{x_d' + x_e} \right)$$

Putting (3.109) and (3.121) together, we get (3.123).

$$\frac{\Delta V_t(s)}{\Delta E_{fd}(s)} = \frac{-(K_5 - (K_6 K_4) K_2 K_3 \omega_0}{(1 + s T_3) \left(2H s^2 + K_D s + K_1 \omega_0 \right) - K_2 K_3 K_4 \omega_0} + \frac{K_6 K_3}{1 + s T_3}$$
$$(3.123)$$

Block diagram of the linearised system with AVR is shown in Fig. 3.30.

3.6.3.1 State-Space Representation with AVR

From the block diagram in Fig. 3.30, the state-space representation of the synchronous machine with an AVR can be written as:
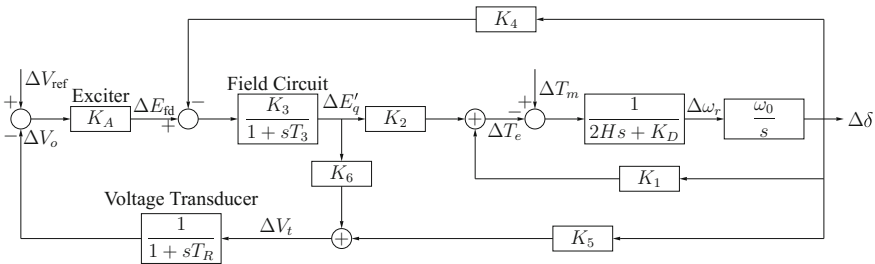
Fig. 3.30 Synchronous machine linear model (with AVR)

$$
\begin{bmatrix} \Delta\dot{\omega} \\ \Delta\dot{\delta} \\ \Delta\dot{E}'_q \\ \Delta\dot{V}_o \end{bmatrix} = \begin{bmatrix} -\frac{K_D}{2H} & -\frac{K_1}{2H} & -\frac{K_2}{2H} & 0 \\ \omega_0 & 0 & 0 & 0 \\ 0 & -\frac{K_4 K_3}{T_3} & -\frac{1}{T_3} & -\frac{K_A K_3}{T_3} \\ 0 & \frac{K_5}{T_R} & \frac{K_6}{T_R} & -\frac{1}{T_R} \end{bmatrix} \begin{bmatrix} \Delta\omega \\ \Delta\delta \\ \Delta E'_q \\ \Delta V_o \end{bmatrix} + \begin{bmatrix} \frac{1}{2H} & 0 \\ 0 & 0 \\ 0 & \frac{K_A K_3}{T_3} \\ 0 & 0 \end{bmatrix} \begin{bmatrix} \Delta T_m \\ \Delta V_{\text{ref}} \end{bmatrix}
$$

$$\text{(3.124)}$$

For the following numerical values, $P_m = 0.5$; $x_q = 1.0$; $x_d = 1.81$; $H = 3.5$; $K_D = 1$; $\tau'_{d0} = 8.0$; $T_R = 0.02$; $K_A = 200$; $x'_d = 0.8$; $x'_q = 0.8$; $x_e = 0.6$; $\omega_0 = 2\pi$ 50; $V_\infty = 0.995$; $E'_{q0} = 1.2$, the linearised representation using analytical (left) and perturbation Method (right) are given below. It can be seen that the matrices are accurate to three decimal places. Analytically obtained A:

$$
\begin{bmatrix} -0.1429 & -0.0987 & -0.05952 & 0 \\ 314.2 & 0 & 0 & 0 \\ 0 & 0.0526 & -0.03482 & -25 \\ 0 & -8.444 & 20.58 & -50 \end{bmatrix}, \begin{bmatrix} -0.1429 & -0.09834 & -0.05952 & 0 \\ 314.2 & 0 & 0 & 0 \\ 0 & 0.05297 & -0.03482 & -25 \\ 0 & -8.383 & 20.28 & -50 \end{bmatrix}
$$

$$\text{(3.125)}$$

3.6.3.2   K-Parameters: K_7 and K_8

In many situations the AVR is used to adjust the terminal voltage of the synchronous machine to deliver a set reactive power or power at a set power factor. The linearised expression for the reactive power is required in the design and analysis is these situations.

The reactive power delivered by a synchronous machine can be written as from (2.9):

$$Q = V_q I_d - V_d I_q \tag{3.126}$$

$$= \left(E'_q - x'_d I_d\right) I_d - x'_q I_q^2 \tag{3.127}$$

$$\Delta Q(s) = K_7 \Delta\delta(s) + K_8 \Delta E'_q(s) \tag{3.128}$$

Following the method to obtain the K-parameters K_1–K_6, we can obtain expressions for K_7 and K_8 from (3.128), as follows:

$$
\begin{aligned}
K_7 &= \frac{E'^0_q V_\infty \sin\delta^0}{x'_d + x_e} - 2x'_d \frac{E'^0_q - V_\infty \cos\delta^0}{x'_d + x_e} \frac{V_\infty \sin\delta^0}{x'_d + x_e} - 2x'_q \frac{\left(V_\infty \sin\delta^0\right)^2}{\left(x'_q + x_e\right)^2} \\
&= \frac{\left(x_e - x'_d\right) E'^0_q V_\infty \sin\delta^0 + x'_d V^2_\infty \sin 2\delta^0}{(x'_d + x_e)^2} - 2x'_q \frac{\left(V_\infty \sin\delta^0\right)^2}{\left(x'_q + x_e\right)^2}
\end{aligned}
\tag{3.129}
$$

$$K_8 = \frac{E_q'^0}{x_d' + x_e} + \left(x_e - x_d'\right) \frac{E_q'^0 - V_\infty \cos \delta^0}{(x_d' + x_e)^2}$$

$$= \frac{2x_e E_q'^0 - \left(x_e - x_d'\right) V_\infty \cos \delta^0}{(x_d' + x_e)^2} \tag{3.130}$$

Next we derive an expression for small changes in the power factor. This expression is very useful when analysing AVRs that are used to deliver power at a constant power factor.

$$Q = P \tan \phi$$
$$\Delta P = K_1 \Delta \delta(s) + K_2 \Delta E_q'(s) \text{ from (3.107)}$$
$$\Delta Q = \Delta P \tan \phi^0 + \frac{P^0 \Delta \phi}{\cos^2 \phi^0}$$
$$\Delta \phi = \frac{\cos^2 \phi^0 \left(\Delta Q - \Delta P \tan \phi^0\right)}{P^0}$$
$$\Delta \cos \phi = - \sin \phi^0 \Delta \phi$$
$$\Delta \cos \phi = - \frac{\cos^2 \phi^0 \sin \phi^0}{P^0} \left(K_7 \Delta \delta + K_8 \Delta E_q' - K_1 \Delta \delta \tan \phi^0 - K_2 \Delta E_q' \tan \phi^0\right)$$
$$= - \frac{\cos^2 \phi^0 \sin \phi^0}{P^0} \left(\Delta \delta \left(K_7 - K_1 \tan \phi^0\right) + \Delta E_q' \left(K_8 - K_2 \tan \phi^0\right)\right)$$

The above expression for the linearised power factor involves four K-parameters, instead of the usual two for other variables, as the power factor depends on both the real and reactive power terms and they each depend on two K-parameters.

Chapter 4
Design of the Automatic Voltage Regulator

AVRs are primarily used to regulate the output voltage of synchronous generators. In this chapter we will cover the tuning of exciters as recommended by the IEEE committee for excitation system models [16, 17]. The exciter tuning is in line with the recommended IEEE committee practice report in [18]. Although recent literature has confirmed that these models provide good agreement with detailed models [19], new models continue to be introduced for specialised situations [20]. Advanced control methods have appeared in the literature [21, 22] but it appears that the tuning based on classical control ideas has plenty of applications [23, 24]. The IEEE committee report [25] has some essential classical control ideas based on an interesting paper, which discusses the estimation of closed-loop poles from open-loop poles and frequency response [26]. AVRs are also known to enhance the transient stability of synchronous generators and some of the easy to follow classical papers on this subject are: [3, 27–29].

4.1 Synchronous Machine Model for AVR Tuning

For the initial AVR design synchronous generator is modelled as a first order system. Subsequent to this design the performance of this AVR is evaluated for the machine connected to the grid. The first order model is justified by looking at the SMIB system in Eqs. (3.96)–(3.98). For unloaded generator, i.e., the generator stator current is zero, E_q' is equal to the terminal voltage and thus Eq. (3.98) describes the dynamics between the field and terminal voltages. Most of the exicter design is done for unloaded generator. Setting $I_d = 0$ in (3.98), we get the following transfer function for the synchronous machine:

$$\frac{\Delta V_t(s)}{\Delta E_{\mathrm{fd}}(s)} = \frac{1}{1 + sT_{d0}'} \tag{4.1}$$
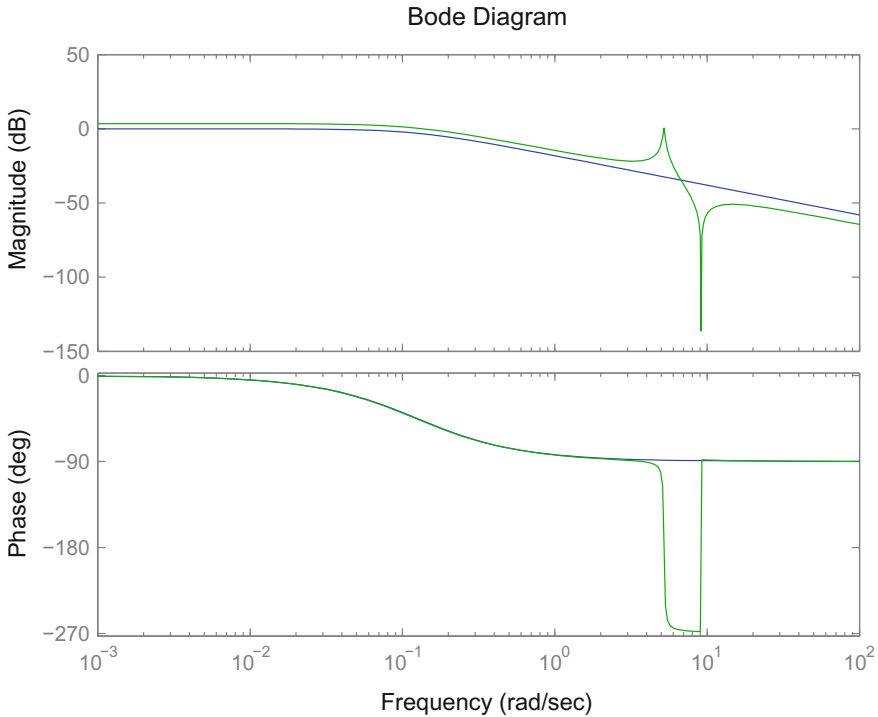
Fig. 4.1 Synchronous machine—frequency response $\frac{\Delta V_t(s)}{\Delta V_{\text{ref}}(s)}$

Although unloaded machine model is used for AVR tuning, it proves to be quite robust even when the machine is loaded. Figure 4.1 shows frequency responses of an unloaded generator and the same generator loaded at 0.9 pu. A few points need to be carefully observed about the two frequency responses in Fig. 4.1.

1. At low frequencies the exact plot has a higher gain than the approximate plot. This means that the steady-state error in practice will be lower than the designed value.
2. At higher frequencies the exact plot has a lower gain than the approximate plot. This means that the system will have higher gain margin than the designed value.
3. The biggest difference between the two plots is for a complex pole-zero pair. It can be seen that the phase and magnitude contribution due to the pair appears only near the electromechanical frequency of oscillation. A good AVR compensation method should not alter the frequency response in the range of this complex pole-zero pair. This also enables an independent design of the excitation system and the power system stabiliser.

AVR Models

IEEE recommended practice for excitation system models covers four DC commutator exciters, eight alternator-supplied rectifier exciters, and seven static excitation systems [16]. In what follows we will look at tuning the parameters of one exciter from each of the three groups. To understand the fundamentals of exciter tuning it is sufficient to look at a simple exciter model and tune its gain to meet performance specifications. Once it is understood how the gain for a simple AVR can be tuned the rest will follow rather easily.

A good understanding of the tuning process is achieved by considering a first order AVR model

$$\frac{K_A}{1 + sT_A}$$

where for practical systems K_A ranges between 200 and 500 and T_A is about 10 ms.

4.2   AVR Performance Requirements

The terminal voltage of a syncrhonous generator has to be maintained at a certain level. Due to the varying load conditions, and the resulting change in voltage drop across the stator reactance, the terminal voltage varies. Feedback control is one easy way to make sure that the terminal voltage is at a set value regardless of the changing load conditions. The correction needs to be made as quickly as possible, i.e., it must be a fast acting feedback controller. From Sect. 3.3.6 we know that to obtain a fast response, the open-loop bandwidth has to be large and to ensure a small steady-state error we know from Eq. (3.87) that the DC gain of the transfer function has to be large.

Formal performance specifications for AVR performance are given in IEEE guide [18] and a committee report [25]. The material covered here will enable the tuning of AVR parameters in most cases to satisfy the requirements in [18] and [25]. As the implemented AVRs are nonlinear, some fine tuning or empirical adjustments may be needed for practical systems.

4.2.1   AVR Tuning—K_A and Phase-Margin

The main issues involved with the design of an AVR can be illustrated using a simple example from [24]. The block diagram for this example is shown in Fig. 4.2 with $T_A = 0.04$ and $T'_{d0} = 1$.

The immediate problem is the selection of gain K_A such that it has a fast rise-time and small steady-state error. A block diagram of an AVR and a generator is shown in Fig. 4.3. In the block diagram the disturbance term $\Delta d(s)$ represents the weakening

Fig. 4.2 AVR tuning block diagram
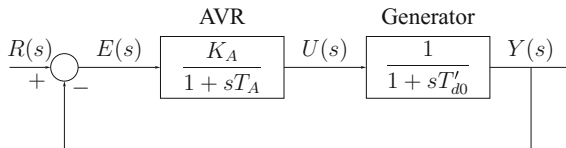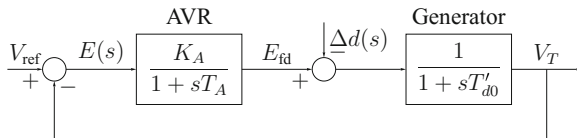
AVR   Generator

$$R(s) \quad E(s) \quad \boxed{\dfrac{K_A}{1+sT_A}} \quad U(s) \quad \boxed{\dfrac{1}{1+sT'_{d0}}} \quad Y(s)$$

Fig. 4.3 AVR tuning—steady-state error

AVR   Generator

$$V_{\mathrm{ref}} \quad E(s) \quad \boxed{\dfrac{K_A}{1+sT_A}} \quad E_{\mathrm{fd}} \quad \Delta d(s) \quad \boxed{\dfrac{1}{1+sT'_{d0}}} \quad V_T$$

of the flux due to armature reaction, etc. In other words, $\Delta d(s)$, models the effect of all the disturbances which change the terminal voltage. Typically: $T_A = 0.05$, $T'_{do} = 5$, $K_A = 50$; with these values and for a unit step change in reference voltage and disturbance $\Delta d(s)$,

$$e_{ss} = \lim_{s \to 0} s \left(\frac{1}{s} \frac{(1+sT_A)(1+sT'_{do})}{(1+sT_A)(1+sT'_{do}) + K_A} + \frac{1}{s} \frac{(1+sT_A)}{(1+sT_A)(1+sT'_{do}) + K_A} \right) = \frac{2}{1+K_A} = 3.92\%$$

Steady-state error of this magnitude is not acceptable and a way is needed to increase the low frequency gain. Next we see what happens when K_A is increased.

For the closed-loop system in Fig. 4.2, the frequency and step response are plotted in Figs. 4.4 and 4.5 for gains: $K_A = \{1, 10, 20, 50\}$. The phase-margins corresponding to these four gains are: 180°, 75.6°, 59.8°, and 40.5°, respectively. From the previous analysis we can expect that higher values of K_A result in faster response and lower values of phase-margin result in response with low damping. This can be seen in the time responses in Fig. 4.5.

It can be seen that higher gain results in lower steady-state error and faster response. But higher gains also mean oscillations. It is important to realise that there is a trade-off between the exciter gain and the closed-loop system damping. At times it is possible to find a value of K_A that meets both the steady-state error and speed of response requirements. In most cases a constant gain AVR is not suitable for obtaining a satisfactory transient and steady-state response. A lag block can be used to provide the desired steady-state response and acceptable transients. For achieving a damped and fast response with small steady-state error the controller can be augmented with a lag block. Next we look at how to tune the parameters of the lag block to meet AVR performance specifications.

Bode Plot - K$_A$ = 1 10 20 50

Fig. 4.4 Bode plot

Step Response - K$_A$ = 1 10 20 50
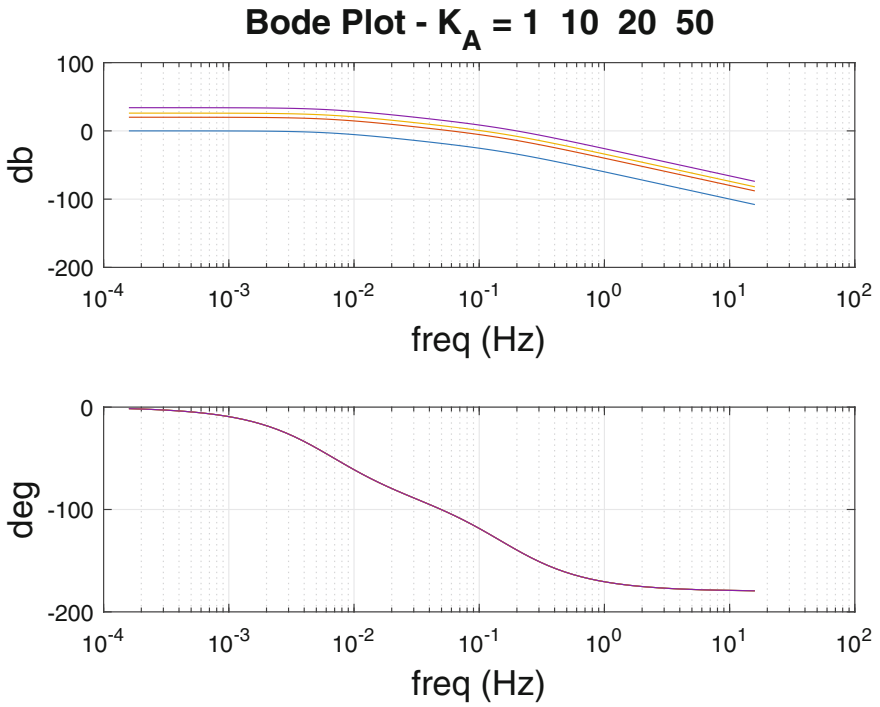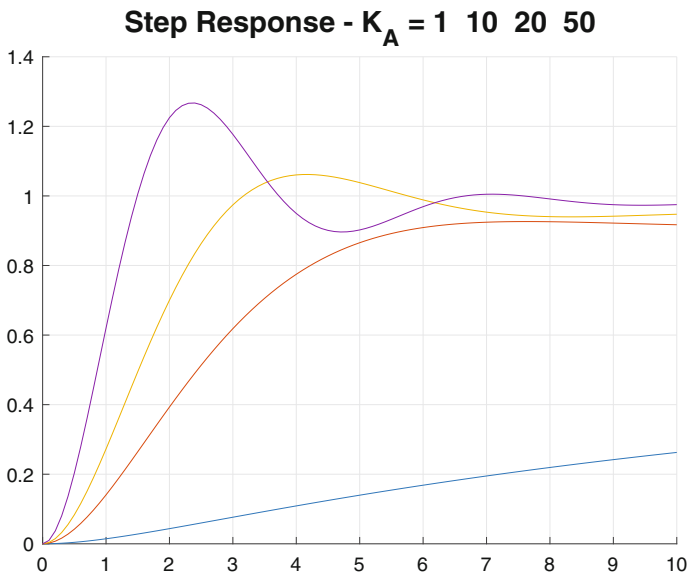
Fig. 4.5 Step response

4.2.2 AVR Tuning—Lag Block

A lag block is used to reduce gain at higher frequencies without reducing the DC gain and that's why it is also known as transient gain reduction block. In the example we have considered above, let us say that we need the steady-state error to be less than 0.5%. A gain $K_A = 500$ will give us a steady-state error of 0.4%. This choice of K_A gives a phase-margin of 25.4° and the cross-over frequency is 42.5 rad s^{-1}. We know that a phase-margin less than 60° is likely to lead to an oscillatory system. To increase the phase-margin at the expense of reducing the bandwidth or the response time one easy way is to use a lag block,

$$\frac{1 + sT_C}{1 + sT_B}, \quad T_B > T_C$$

Block diagram of the closed-loop system with a lag block is shown in Fig. 4.6.

The next design issue is the selection of time constants T_B and T_C. For a 0.25 s rise-time we need the open-loop bandwidth to be approximately 10 rad s^{-1}, i.e., the magnitude of the open-loop gain at 10 rad s^{-1} should be 1. The open-loop gain without the lag block is approximately 20 dB at 10 rad s^{-1} thus we need to choose T_B and T_C such that they result in the pole and zero one decade apart to reduce the gain by 20dB at higher frequencies. To provide a good phase-margin the net phase contribution due to the lag block near the cross-over frequency should be approximately zero. With this, we can choose $T_B = 10$ and a decade below $T_C = 1$. The frequency response of the open-loop system with these parameter values is shown in Fig. 4.7. The step-response of the closed-loop system with and without the lag block is shown in Fig. 4.8. From the figure it is clear that the lag compensator provides damping without affecting the steady-state error.

4.2.3 AVR Tuning—Rate-Feedback

There are many AVRs in practice which use a rate feedback block shown in Fig. 4.9. The system shown in Fig. 4.9 includes a rotating exciter modelled as a first-order block. There are two feedback loops in the system. The first feedback loop has the rate feedback block $\frac{sK_F}{1+sT_F}$ in the feedback path. In this design problem, appropriate values of T_F and K_F need to be chosen where all the other parameters are specified.
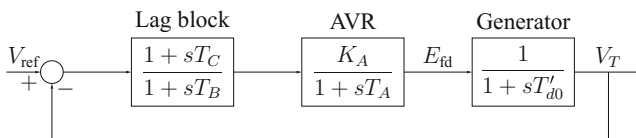
Fig. 4.6 AVR tuning lag compensator
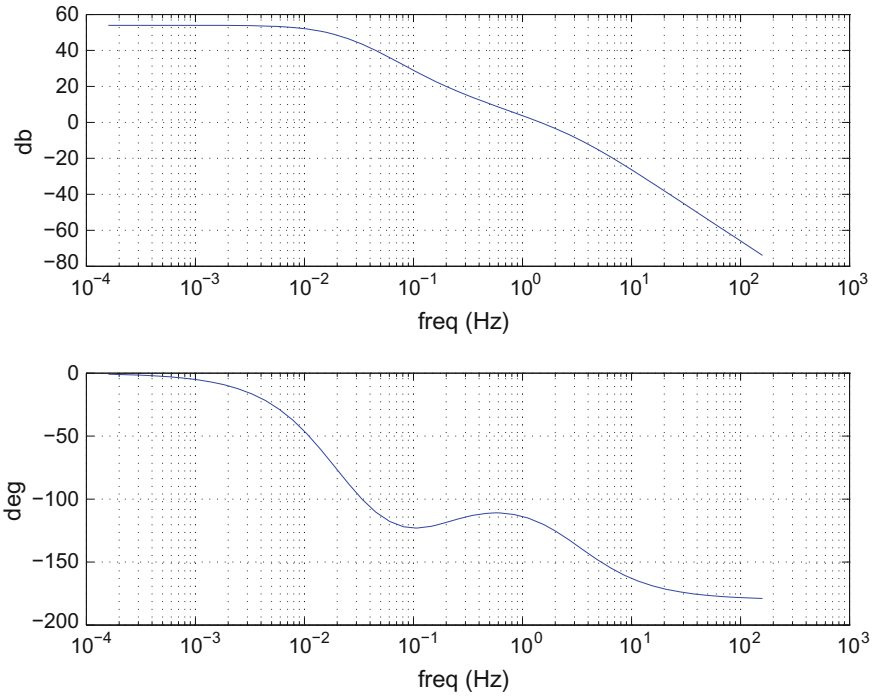
Fig. 4.7 Bode plot with compensator
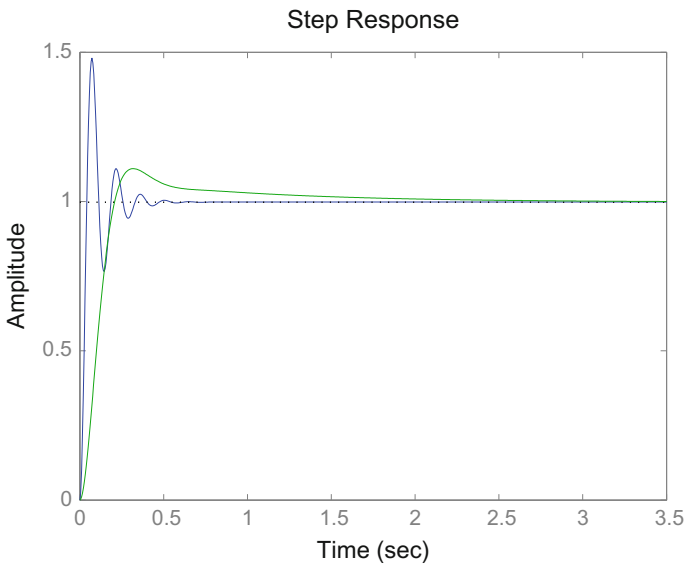
Fig. 4.8 Step-response with and without lag compensator
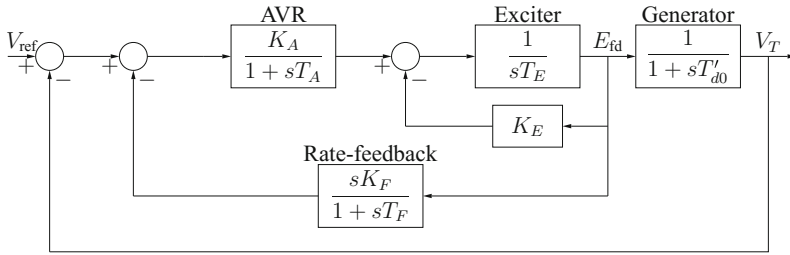
Fig. 4.9 AVR tuning rate-feedback compensator

The design objective is to have a fast response time and a small steady-state error to a step input. Typical parameters are: $K_A = 120$, $T_A = 0.15$, $T_E = 0.5$, $K_E = 1.0$, $T'_{d0} = 5$; in most designs $T_F \approx 10T_A$.

The purpose of the inner loop with rate feedback is to provide high DC gain and reduce high frequency gain to provide stability to the closed-loop system. To see how the inner loop with rate feedback provides this capability let us consider a feedback system with transfer function g in the forward path and h in the feedback path with the closed-loop transfer function $gh_{cl} = \frac{g}{1+gh}$. Approximate frequency response of the closed-loop will be the same as that of g when $|gh| << 1$ and $\frac{1}{h}$ when $|gh| >> 1$.

The cascade of the exciter and AVR blocks, with transfer function $g = \frac{K_A}{(1+sT_A)(K_E+sT_E)}$, provides a high DC gain of $\frac{K_A}{K_E}$; the first break point is at $\frac{K_E}{T_E}$ rad s^{-1} and the second break point is at $\frac{1}{T_A}$ rad s^{-1}. The rate feedback block, $h = \frac{sK_F}{1+sT_F}$, has a DC gain of $-\infty$, a low frequency reponse of 20 dB/decade, and a break point at $\frac{1}{T_F}$ rad s^{-1}. Since we have $\frac{K_A}{K_E} < \frac{1}{T_F} < \frac{1}{T_A}$, the closed-loop magnitude response for the inner loop is: DC gain of $\frac{K_A}{K_E}$, then -20 dB/decade from $\frac{K_E}{T_E}$ rad s^{-1}, flat from $\frac{1}{T_F}$ rad s^{-1}, and again -20 dB/decade from $\frac{1}{T_A}$ rad s^{-1}. The gain in the flat part is $\frac{T_F}{K_F}$. The frequency response for the inner loop is shown in Fig. 4.10 where the flat section can be clearly seen.

In this design, it is aimed that the open-loop crossover frequency for the entire loop in Fig. 4.9 is in the flat section of the inner loop gain. It is a common practice to have the crossover frequency as the geometric mean of the two end-points of the flat section.

The following steps give the design process.

1. If K_A is not already specified, choose it to satisfy the steady-state error specifications.
2. $T_F \approx 10T_A$
3. Choose $\omega_c = \sqrt{\dfrac{1}{T_F}\dfrac{1}{T_A}}$
4. Find the gain which needs to be applied to the generator transfer function such that the crossover is at ω_c. This extra gain $K_{\omega_c} = |1 + \jmath\omega_c T'_{d0}|$.
5. Set $K_F = K_{\omega_c} T_F$
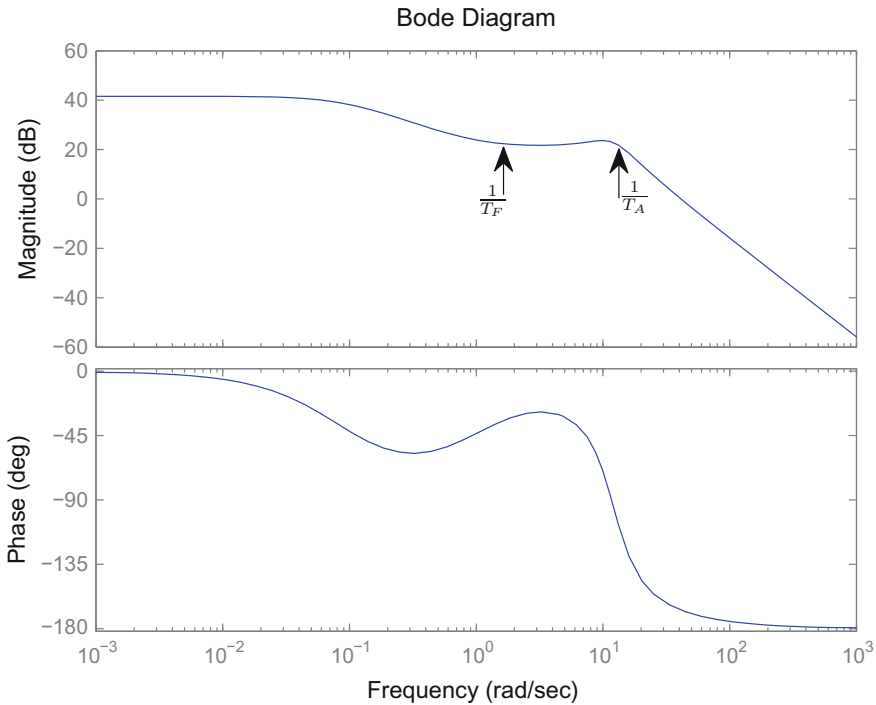
Fig. 4.10 Rate feedback—inner-loop frequency response

Following the above steps we get for the parameters given above $T_F = 1$, and $K_F = 0.0772$. The open-loop frequency response for the entire loop is shown in Fig. 4.11 and the closed-loop step response is shown in Fig. 4.12. From the figures it is clear that the design specifications are met.

4.2.4 AVR Tuning—PID Design

The steady-state error due to a step input with a PID controller is zero. For this reason majority of AVRs have a PID block as a part of the AVR structure. The main design objective with a PID control is to get a fast response with good damping. Fast and a well-damped response is achieved with large open-loop bandwidth and a large phase margin.

Here we illustrate the design of a PID controller using the example of a very popular AVR known as IEEE AC7B compensator shown in Figs. 4.13 and 4.14.

Let us say that the desired open-loop gain crossover frequency is ω_c, which is between 1 and 10 rad s^{-1}, and the desired phase margin is ϕ_d, which is between 60° and 90°.
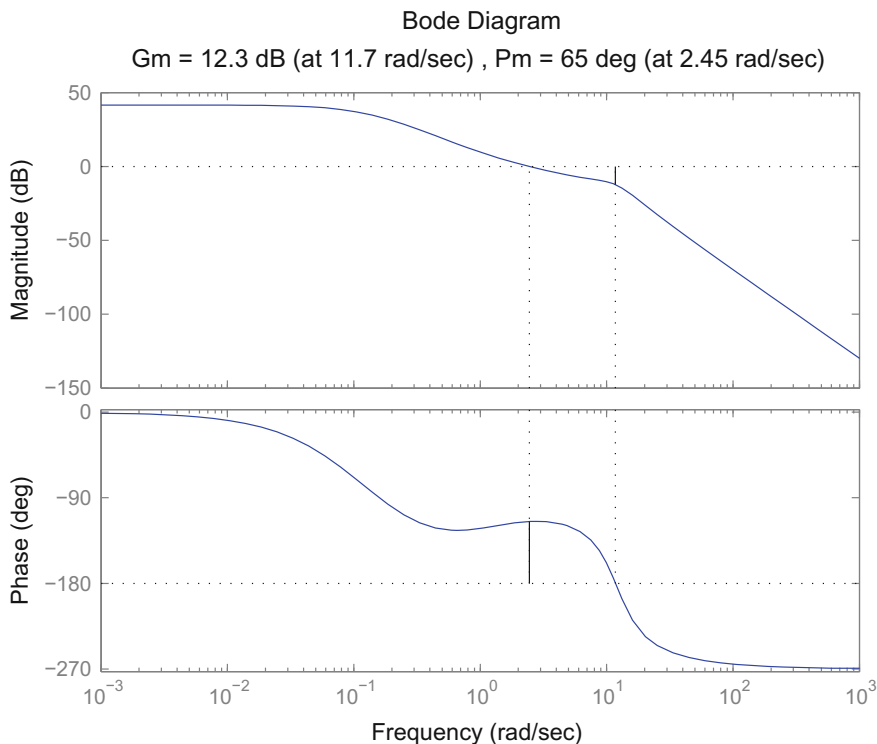
Fig. 4.11 Rate feedback—open-loop frequency response

In the design the following assumptions are made:

1. F_{ex} is unity.
2. In per unit system $I_{fd} = V_T$.
3. The correction for exciter saturation $V_x = 0$.
4. Either use the PID block $C_R(s)$ or the rate-feedback block ($K_{F3} \neq 0$).
5. $K_P V_T$ is unity.
6. Compensator voltage, $V_C = V_T$, in Fig. 4.13.

Exercise: Redraw the block diagrams in Figs. 4.13 and 4.14 with the above simplifying assumptions. (Hint: the outputs of the shaded boxes in Fig. 4.13 are either 0 or 1.)

The transfer function between X and E_{fd} in Fig. 4.14 is:

$$G_{xE_{fd}}(s) = \frac{\frac{C_A(s)}{sT_E + K_E}}{1 + \frac{K_{F1}C_A(s)}{sT_E + K_E}} \qquad (4.2)$$
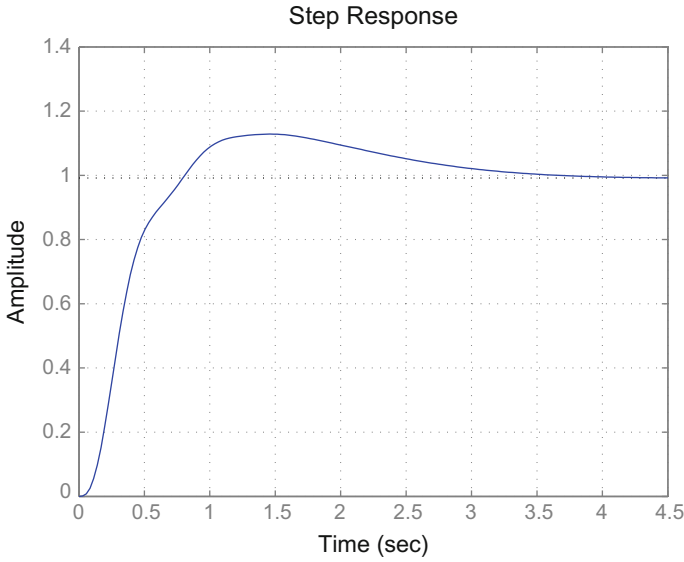
Fig. 4.12 Rate feedback—closed-loop step response
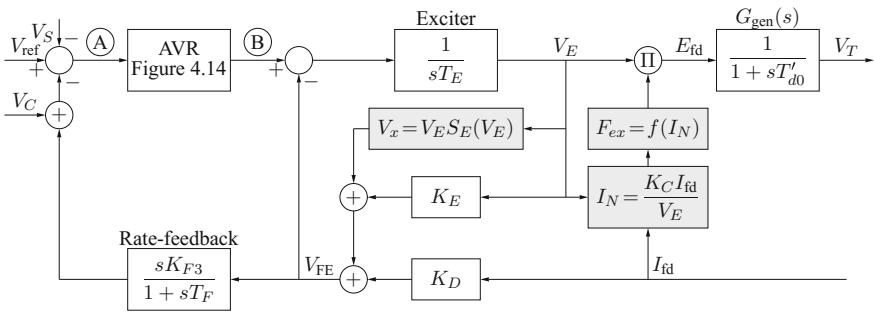
Fig. 4.13 AVR tuning IEEE AC7B compensator—block 1
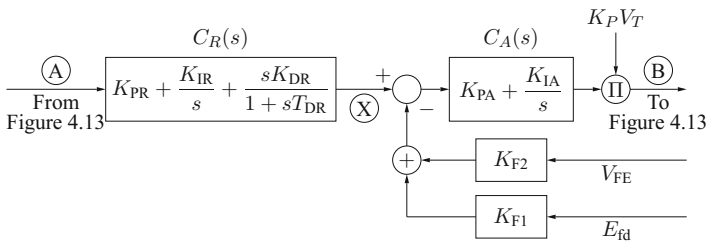
Fig. 4.14 AVR tuning IEEE AC7B compensator—block 2

where the feedback from the K_D block is ignored. Input $K_P V_T$ to the multiplier block in Fig. 4.14 is to account for the main supply to the exciter, which is from the generator terminals. In exciter tuning $K_P V_T$ can be considered as unity.

The first step in the design process is to design for the inner loop. The steps are:

1. Choose the inner loop crossover $\omega_{c_i} = 2\omega_c$.
2. Choose the location of the zero of the PI controller a decade below the crossover frequency, i.e., $\frac{K_{IA}}{K_{PA}} = \frac{\omega_{c_i}}{10}$.
3. Choose K_{PA} such that the inner loop crossover frequency is at ω_{c_i}.

The second stage in the design process is to choose controller $C_R(s)$ to achieve the overall bandwidth ω_c and the phase margin ϕ_d. First note that the inner loop transfer function is:

$$G_{in} = \frac{G_{xE_{fd}}(s)}{1 + G_{xE_{fd}}(s)K_D G_{gen}(s)} \tag{4.3}$$

The open-loop gain then is (with $K_{F3} = 0$):

$$G_{ol} = C_R(s)G_{in} \tag{4.4}$$

The controller $C_R(s)$ is written as $C_R(s) = K_x C_{lag}(s) C_{lead}(s)$ and

$$C_{lag}(s) = \frac{\frac{\beta}{\omega_c}s + 1}{s} \text{ and } C_{lead}(s) = \frac{\frac{s}{\omega_z} + 1}{\frac{s}{\omega_p} + 1} \tag{4.5}$$

The following steps can be used to choose the gains for the PID controller $C_R(s)$.

1. Select $\beta = 10$.
2. Find out the phase margin ϕ with $C_{lag}(s)G_{in}$.
3. The extra phase lead ϕ_l needed to achieve the desired phase margin is $\phi_d - \phi$.
4. Choose ω_z, ω_p, and K_x according to Sect. 3.3.7.
5. Equating the co-efficeints of $C_R(s)$ and $K_x C_{lag}(s)$, we can obtain

$$T_{DR} = \frac{1}{\omega_p}; K_{IR} = K_x; K_{DR} = \frac{\beta K_{IR}}{\omega_z \omega_p} - K_{PR} T_{DR}; K_{PR} = \left(\frac{\beta}{\omega_c} + \frac{1}{\omega_z}\right) K_{IR} - K_{IR} T_{DR}.$$

Let us look at a system with the following parameters: $K_{F1} = 0.212$, $K_{F2} = 0.0$, $K_{F3} = 0.0$, $T_E = 0.36$, $K_E = 1.0$, $K_C = 0.30$, $K_D = 1.04$, $T_R = 0.01$, $T'_{d0} = 8.9$, $K_E = 1$, $K_D = 0.6$. The controller parameters for $\omega_c = 5 \text{ rad s}^{-1}$ and $\phi_d = 65\%$ are: $K_{PA} = 17.5366$, $K_{IA} = 17.5366$, $T_{DR} = 0.1803$, $K_{PR} = 11.0192$, $K_{IR} = 5.3972$, $K_{DR} = 0.4091$. The open-loop frequency response and the closed-loop step response is shown in Figs. 4.15 and 4.16.

Bode Diagram
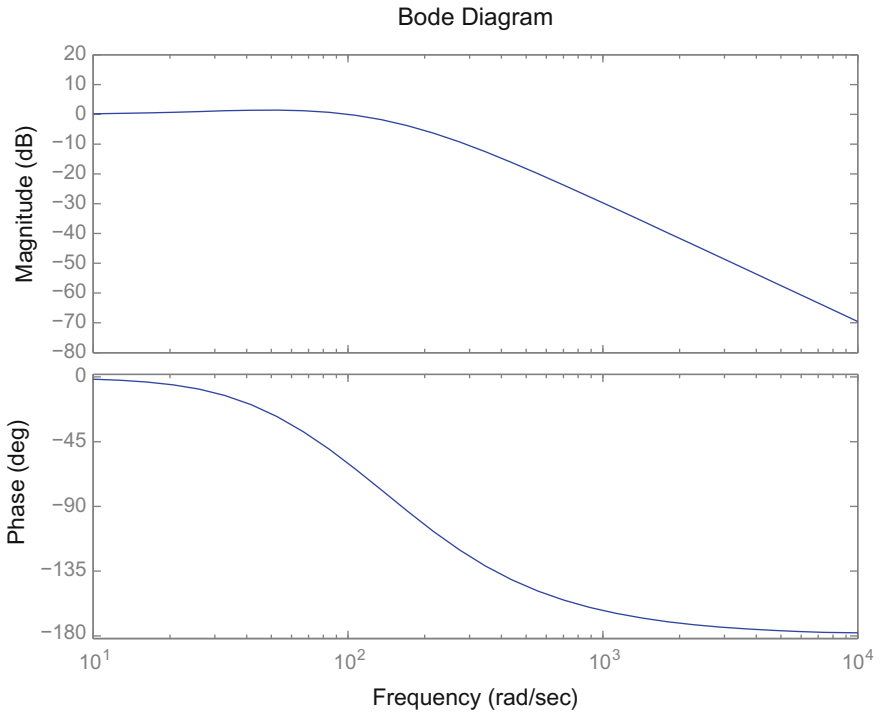
Fig. 4.15 Lead-lag compensator

Step Response
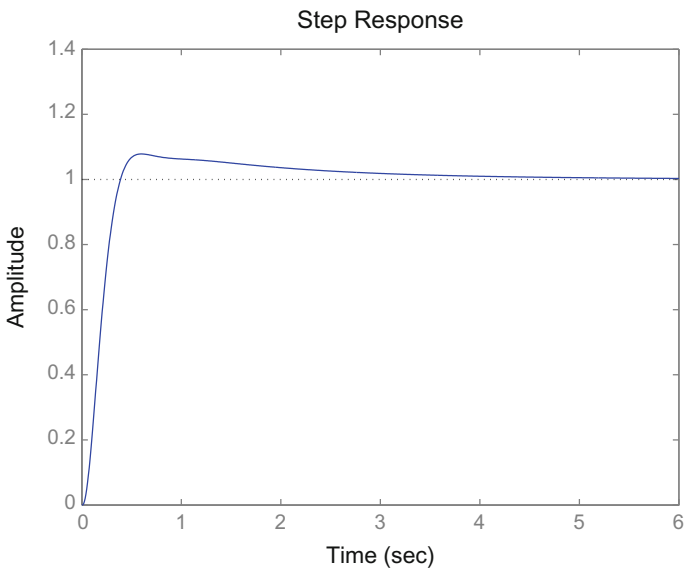
Fig. 4.16 Lead-lag compensator

4.3 AVR Models

All AVRs fall in one of the follwing three categories:

1. DC generator directly connected to the synchronous generator field.
2. AC generator connected to the synchronous generator field via a solid-state rectifier.
3. Solid-state rectifiers supplied from the synchronous terminal voltage and connected to the synchronous generator field.

In the following we look at some of the common features of the exciters so that we can model them appropriately for AVR tuning.

4.3.1 Rotating Exciters

Rotating exciters can be either AC or DC generators. In the literature AC generators are also known as brushless machines [30, 31]. DC generators and alternators still exist as exciters in old generators, but static exciters are becoming common for new generators.

In all rotating exciters there is a field coil and its electrical properties form the most important part of the exciter model. The field voltage supplied to the synchronous generator, E_{fd}, the output of the exciters, is proportional to the total flux linkages, λ in the exciter field coil. For rotating generators we can take it that the generated voltage $E_{\text{fd}} = k_f \omega_{\text{ex}} \lambda$, where ω_{ex} is the exciter angular velocity which can be considered constant, λ are the total flux linkages in the exciter field coil, and k_f is a proportionality constant. Further let $k_\lambda = k_f \omega_{\text{ex}}$, and so we can write $E_{\text{fd}} = k_\lambda \lambda$. Let us first look at the relationship between λ and the applied voltage to the exciter field coil.

4.3.2 Current-Flux Relationship in Coils with Saturation

The modelling of the saturation term can be done in many different ways but the important point to keep in mind is that including the effect of saturation is to include an extra term as shown in Fig. 4.17. Instead of using the exponential function to model saturation, e.g., in Fig. 2.38, some simulations use a quadratic relationship, e.g.,

$$S_e(E_{\text{fd}}) = \frac{B\,(E_{\text{fd}} - A)^2}{E_{\text{fd}}}. \tag{4.6}$$

In general, we are able to write a relationship between exciter field current and synchronous machine field voltage E_{fd} as, $i = E_{\text{fd}}\,(K_E + S_e(E_{\text{fd}}))$.

Fig. 4.17 Rotating exciter
block diagram
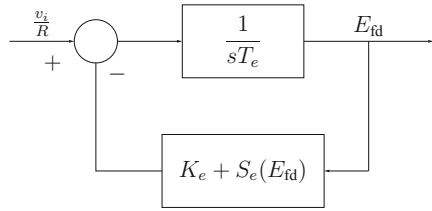
For the exciter field circuit shown in Fig. 2.38, we write

$$v_i = Ri + \frac{d\lambda}{dt}$$

$$v_i = RE_{\text{fd}}\left(K_E + S_e(E_{\text{fd}})\right) + \frac{1}{k_\lambda}\frac{dE_{\text{fd}}}{dt} \tag{4.7}$$

So with $T_e = \frac{1}{Rk_\lambda}$, $K_e = K_E$, we obtain the block diagram in Fig. 4.17 to represent the model in (4.7).

The block diagram in Fig. 4.17 is used to represent field coil in both DC and AC exciters, with suitable adjustments in the parameters T_e and K_e. In excitation systems with only solid-state components, there is a saturable core reactance which is used to control the input to the rectifier and this can be also modelled using the block diagram in Fig. 4.17. Thus this block is a common feature of almost all excitation systems.

4.4 Practical Exciters

In this section we look at two of the popular exciters and see how we can use the methods detailed in this chapter to tune the parameters of these two exciters. These two popular exciters are: an AC machine exciter IEEE AC1A and a solid-state exciter IEEE ST2A. The block diagrams of these two exciters are shown in Figs. 4.19 and 4.20. Let us look at the components in these block diagrams with a view to make assumptions about their dynamics in the AVR tuning process.

4.4.1 AC Exciter

The block diagram for a synchronous machine in Fig. 2.21, with damper windings neglected, can be used to represent a brushless AC exciter as shown in Fig. 4.18. The exciter supplies an inductive load so the terminal voltage, which is the main generator's field voltage E_{fd}, is proportional to E_q'. The block $K_E + S(E_{\text{fd}}')$ in Fig. 4.18 represents the gain adjustment and the extra exciter field current needed due to sat-
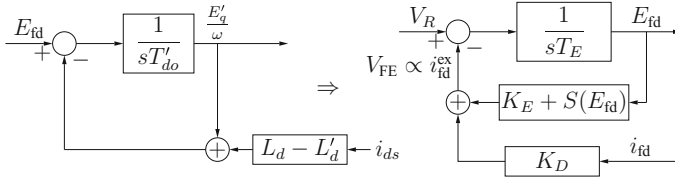
Fig. 4.18 Brushless exciter block diagram

uration. In most cases $K_D = L_d - L'_d$. The input to the integrator block $\dfrac{1}{sT_E}$ is $\dot{\lambda}^{\mathrm{ex}}_{\mathrm{fd}} = V_R - r^{\mathrm{ex}}_{\mathrm{fd}} i^{\mathrm{ex}}_{\mathrm{fd}}$, where the superscript 'ex' is used for exciter quantities. This means that the quantity being subtracted from V_R in Fig. 4.18 is proportional to the exciter field current. In many exciter control schemes the exciter field current is fedback through a rate block for a faster exciter response.

4.4.2 Rectifier Equivalent Representation

The voltage drop in the rectifier is modelled using the block $f(I_N)$ in Figs. 4.19 and 4.20, which is defined as follows:

$$f(I_N) = \begin{cases} 1 - 0.577 I_N, & I_N < 0.433 \\ \sqrt{0.75 - I_N^2}, & 0.433 < I_N < 0.75 \\ 1.732(1 - I_N), & 0.75 < I_N < 1.0 \\ 0, & I_N > 1. \end{cases} \tag{4.8}$$

The effect of the voltage drop due to the commutating inductance in the system is modelled as a voltage drop as a function of the load current. It can be written as:

$$E_{\mathrm{fd}} = E^0_{\mathrm{fd}} - X_{\mathrm{comm}} I_{\mathrm{fd}} \Rightarrow \frac{E_{\mathrm{fd}}}{E^0_{\mathrm{fd}}} = 1 - \frac{X_{\mathrm{comm}} I_{\mathrm{fd}}}{E^0_{\mathrm{fd}}}$$

where X_{comm} is the effective commutating reactance and the formula in (4.8) models this term. The multiplication block in Fig. 4.19 models this as a gain term due to the rectification process. The block $V_E = |K_P V_T + {}_J K_I I_T|$ in Fig. 4.20 is to compensate voltage drop between the terminal voltage and some other point at which the AVR is designed to regulate the voltage.
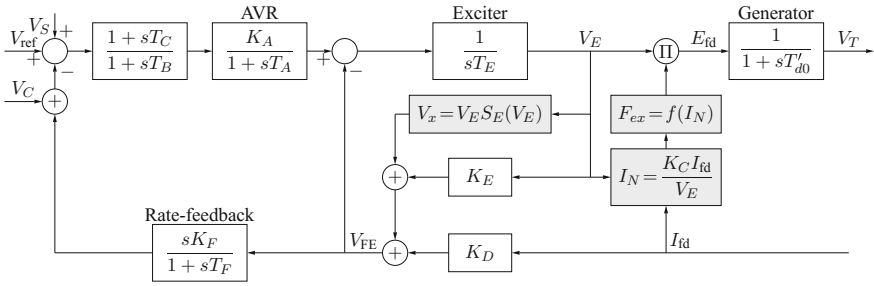
Fig. 4.19 AVR tuning IEEE AC1A compensator
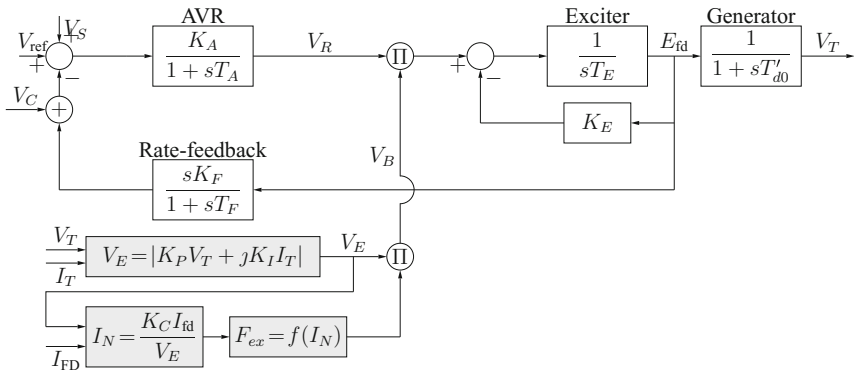
Fig. 4.20 AVR tuning IEEE ST2A compensator

4.4.3 Compensating Voltage V_C and VAR Droop

Details about the compensating voltage V_C in Figs. 4.13, 4.19, and 4.20 are given in [16]. This term is needed to provide a droop for reactive power sharing amongst generators. For a fast exciter without the V_C term,

$$E_{\text{fd}} = K_A (V_{\text{ref}} - V_T) \text{ and } Q \approx \frac{E_{\text{fd}} - V_T}{X_s}$$

$$V_T = \frac{K_A V_{\text{ref}}}{1 + K_A} - \frac{X_s Q}{1 + K_A} \qquad (4.9)$$

From (4.9) one can see that for large K_A, the terminal voltage and reactive power output Q are very weakly coupled and regulating V_T will not properly regulate Q. A compensating voltage

$$V_C = |\bar{V}_T + (R_C + {}_J X_C) \, \bar{I}_T|$$

can help with this. The terminal current $I_T = I_P - {}_JI_Q$, where I_P is the current in phase with the terminal voltage V_T. From this one can write for change only in reactive component as,

$$V_T = \frac{K_A V_{\text{ref}}}{1 + K_A} - \frac{(X_s + K_A X_c)I_Q}{1 + K_A} \tag{4.10}$$

where X_c can be selected to provide a reactive power droop or load compensation or several of the other things as suggested in [16]. Voltage V_S in Figs. 4.13, 4.19, and 4.20 is a stablising voltage term (normally the output of a PSS) which can be considered to be zero for AVR tuning.

4.4.4 Assumptions for AVR Tuning

It can be seen that the compensation for loading and rectifier voltage drop is applied as a product term. For the purposes of AVR tuning these values can be assumed to be 1pu and thus removed from the representation for the purposes of design. The block diagrams in Figs. 4.19 and 4.20 are generally simplified with the result that the resulting block diagram takes the form of the block diagram (without the shaded boxes) with either a constant-gain or a lag, or a rate-feedback, or a PID controller. It can be seen that once the product terminals are removed from the block diagrams in Figs. 4.19 and 4.20, it is straightforward to use them to tune AVR parameters.

Chapter 5
Design of the Power System Stabliser

The mechanical part of the synchronous generator is analogous to a spring-mass system with very little mechanical damping. For small disturbances it is effectively an oscillator. Some electrical damping is provided by the AVR control action but for higher values of AVR gain, the electrical damping can become negative, which turns the oscillator into an unstable system. Most synchronous generators are equipped with power system stabilisers (PSS) which provide a feedback to increase the damping and prevent the system from oscillating.

Power System Stabilisers (PSS) are very clever devices which achieve a lot with very little effort. A carefully designed and located PSS can damp oscillations in interconnected power systems with tens of synchronous machines. In essence a PSS is a lead compensator block which can be a first order block. To make the PSS design effective we have to first understand what is it that PSS does and what is the best location for the PSS in a multimachine system. In this chapter we analyse the role of synchronous and damping torques for a synchronous machine, methods to choose a location for the PSS, and tuning the PSS.

5.1 Synchronising and Damping Torques

As the electrical loading or the mechanical power of the synchronous machine changes, a restoration force is generated within the machine to change the power angle δ such that an equilibrium is reached between the input and output power. As mentioned above the essential dynamics of a synchronous machine is that of a mass-spring system but there is a little damping that makes the post-disturbance trajectory converge to its equilibrium value. In a second order linear position feedback system, with low damping, the damping is increased with velocity feedback and the position feedback pulls the system to the new set position. Similarly in a synchronous machine feedback from the angular velocity provides damping and the

feedback from the angle synchronises the machine. It so happens that in most cases the damping torque in a synchronous machine is too small and the PSS is designed to increase that damping torque. Next we analyse the damping and synchronising torque in a synchronous machine.

The linearised SMIB system with an AVR shown in Fig. 5.1 can be redrawn as shown in Fig. 5.2 which gives a better idea of the synchronising and damping torques. The blocks $K_\omega(s)$ and $K_\delta(s)$ in Fig. 5.2 are:

$$K_\omega(s) = -\frac{K_2 K_3 K_4 T_R}{T_3 T_R s^2 + s(T_3 + T_R) + 1 + K_A K_3 K_6} \tag{5.1}$$

$$K_\delta(s) = -\frac{K_2 K_3 (K_4 + K_A K_5)}{T_3 T_R s^2 + s(T_3 + T_R) + 1 + K_A K_3 K_6} \tag{5.2}$$

The damping introduced by $K_\omega(s)$ and $K_\delta(s)$ at any resonant mode can be estimated by the imaginary part of $K_\delta(J\omega_{\text{resonant}})$ and real part of $K_\omega(J\omega_{\text{resonant}})$. Here the assumption being that $K_\omega(s)$ and $K_\delta(s)$ do not greatly affect the resonant mode but only the damping at the resonant mode. For a given frequency real values of $K_\omega(s)$ and $K_\delta(s)$ give damping and synchronising torques, respectively, and their imaginary values give synchronising and damping torques, respectively.

Table 5.1 gives the K-parameters for different output power operation of a synchronous machine with the following numerical values of the parameters,
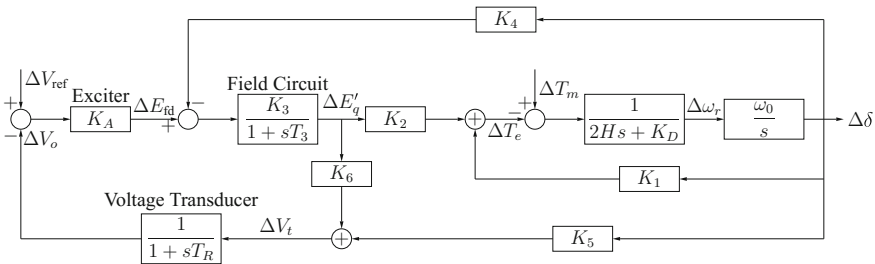
Fig. 5.1 Synchronous machine linear model (with AVR)
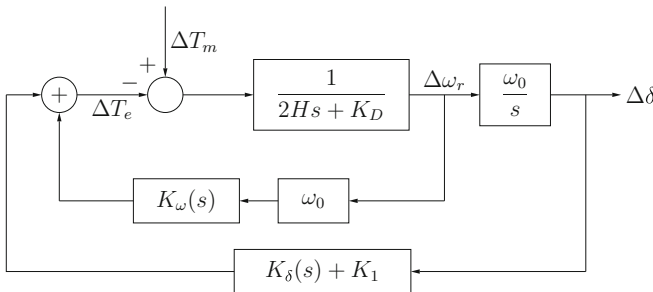
Fig. 5.2 Synchronising and damping torques

Table 5.1 K-parameters

$P + jQ$	$0.5 + j0.1$	$0.6 + j0.2$	$0.7 - j0.1$	$0.8 - j0.2$
K_1	0.6909	0.6061	0.4872	0.2956
K_2	0.4167	0.5	0.5833	0.6667
K_3	3.59	3.59	3.59	3.59
K_4	0.4208	0.505	0.5892	0.6733
K_5	−0.1689	−0.2055	−0.2449	−0.2909
K_6	0.4116	0.3932	0.367	0.3233

Table 5.2 $K_\delta(s)$ and $K_\omega(s)$ for mid-range K_A

	$K_\omega(s)$	$K_\delta(s)$
$s \approx j0$	$-\dfrac{K_2 K_3 K_4 T_R}{1 + K_A K_3 K_6}$	$-\dfrac{K_2 K_3 (K_4 + K_A K_5)}{1 + K_A K_3 K_6}$
$s \approx j\omega_{\text{resonant}}$	$j\dfrac{K_2 K_3 K_4 T_R}{\omega(T_3 + T_R)}$	$j\dfrac{K_2 K_3 (K_4 + K_A K_5)}{\omega(T_3 + T_R)}$

$x_q = 1.0$; $x_d = 1.81$; $H = 3.5$; $K_D = 1$; $\tau'_{d0} = 8.0$; $T_R = 0.02$; $K_A = 200$; $x'_d = 0.8$; $x'_q = 0.8$; $x_e = 0.6$; $\omega_0 = 2\pi 50$; $V_\infty = 0.995$; $E'_{q0} = 1.2$.

With the values of K-parameters in Table 5.1, we get an estimate of the steady-state damping and synchronising torques due to $K_\omega(s)$ and $K_\delta(s)$ terms from the expressions in Table 5.2 for different operating points.

The total synchronising torque is given by the term $K_\delta(s) + sK_\omega(s)$ since the derivative of the angular velocity is the angular position. The expressions for $K_\omega(s)$ and $K_\delta(s)$ in (5.1) and (5.2) can be used to obtain the following expressions for the synchronising torques when there is no AVR ($\lim_{K_A \to 0}$) and when there is a high-gain AVR ($\lim_{K_A \to \infty}$).

$$\lim_{K_A \to 0} K_\delta(s) + sK_\omega(s) = -\frac{K_2 K_3 K_4 (1 + sT_R)}{(1 + sT_R)(1 + sT_3)} = -\frac{K_2 K_3 K_4}{(1 + sT_3)} \tag{5.3}$$

$$\lim_{K_A \to \infty} K_\delta(s) + sK_\omega(s) = -\frac{K_2 K_5}{K_6} \tag{5.4}$$

Using the Equations in (5.3), (5.4), and Table 5.2, the results are summarised in Table 5.3. Terms marked in Table 5.3 with * may change sign with a sign change in K_5. The indications of positive or negative torque for the starred terms is for negative values of K_5.

In Table 5.3 synchronising torque only due to $K_\omega(s)$ and $K_\delta(s)$ is given. The total synchronisatin torque is obtained by adding K_1 to that value. Increasing load leads to smaller value of K_1, thus lower synchronising torque. Higher values of K_A make the damping torque $K_\omega(s)$ smaller at low frequencies but increase the synchronising torque needed for increased transient stability limit.

Table 5.3 Synchronising and damping terms

	$K_A \approx 0$	K_A mid-range	$K_A \to \infty$
$s \approx j0$	zero damp. −ve sync.	−ve damp. +ve sync.*	zero damp. +ve sync.*
$s \approx j\omega_{resonant}$	+ve damp. zero sync.	−ve damp.* +ve sync.	zero damp. +ve sync.*

5.1.1 Multimachine Systems

Expressions for damping and synchronising torques for multimachine system are developed [1, p. 98] in this section. Let

$$\Delta\delta = [\delta_1, \delta_2, \ldots, \delta_n]^T ,$$

$$\Delta\omega = [\omega_1, \omega_2, \ldots, \omega_n]^T ,$$

and let x_d be the state vector of all other states, like exciter, AVR, governor, turbines and every other dynamic elements in the system. The state-space representation for a multimachine power system can be written as:

$$\frac{d\Delta\delta}{dt} = \omega_0 \Delta\omega \tag{5.5}$$

$$2H\frac{d\Delta\omega}{dt} = \Delta T_m - \Delta T_e - D_\omega \Delta\omega \tag{5.6}$$

$$\frac{dx_d}{dt} = A_d x_d + B_{d\delta}\Delta\delta + B_{d\omega}\Delta\omega \tag{5.7}$$

The input to the mechanical system (5.5)–(5.7) are the mechanical and electrical torques which can be written in terms of all other state variables as follows for a closed-loop system:

$$\Delta T_e = c_{te}x_d + D_{d\delta}\Delta\delta + D_{d\omega}\Delta\omega \tag{5.8}$$

$$\Delta T_m = c_{tm}x_d + D_{m\delta}\Delta\delta + D_{m\omega}\Delta\omega \tag{5.9}$$

Replacing $\frac{d}{dt}$ by s,

$$X_d(s) = (sI - A_d)^{-1} (B_{d\delta} + sB_{d\omega}) \Delta\delta(s) \tag{5.10}$$

$$\Delta T_e(s) = \left(c_{te} (sI - A_d)^{-1} (B_{d\delta} + sB_{d\omega}) + (D_{d\delta} + sD_{d\omega})\right) \Delta\delta(s) \tag{5.11}$$

$$\Delta T_m(s) = \left(c_{tm} (sI - A_d)^{-1} (B_{d\delta} + sB_{d\omega}) + (D_{m\delta} + sD_{m\omega})\right) \Delta\delta(s) \tag{5.12}$$

Once an expression for $\Delta T_e(s)$ is obtained it can be written as $T_s(s) + sT_d(s)$ where $T_s(s)$ is the synchronising torque and $T_d(s)$ is the damping torque.

Let us apply the above formulation for a SMIB machine with an AVR (block diagram in Fig. 3.30) and compare it with the results we have already obtained in the Sect. 5.1. The state-space representation of a SMIB with an AVR can be written from Eq. (3.124):

$$\Delta\dot{\delta} = \omega_0\Delta\omega_r \tag{5.13}$$

$$2H\Delta\dot{\omega}_r = -K_D\Delta\omega_r - K_2\Delta E'_q - K_1\Delta\delta + \Delta T_m \tag{5.14}$$

$$T_3\Delta\dot{E}'_q = -E'_q + K_3K_A(V_{\text{ref}} - \Delta v_1) - K_3K_4\Delta\delta \tag{5.15}$$

$$T_R\Delta\dot{v}_1 = -\Delta v_1 + K_6\Delta E'_q + K_5\Delta\delta \tag{5.16}$$

$$x_1 \overset{\triangle}{=} \Delta\delta,\, x_2 \overset{\triangle}{=} \Delta\omega_r,\, x_3 \overset{\triangle}{=} \Delta E'_q,\, x_4 \overset{\triangle}{=} \Delta v_1,\, x_d = [x_3, x_4]^T \tag{5.17}$$

$$c_{te} = \begin{bmatrix} -K_2 & 0 \end{bmatrix}, \qquad D_{d\delta} = -K_1, \qquad D_{d\omega} = -K_D \tag{5.18}$$

$$c_{tm} = \begin{bmatrix} 0 & 0 \end{bmatrix}, \qquad D_{m\delta} = 0, \qquad D_{m\omega} = 0 \tag{5.19}$$

$$A_d = \begin{bmatrix} -\frac{1}{T_3} & -\frac{K_AK_3}{T_3} \\ \frac{K_6}{T_R} & -\frac{1}{T_R} \end{bmatrix}, \quad B_{d\delta} = \begin{bmatrix} -\frac{K_3K_4}{T_3} \\ \frac{K_5}{T_R} \end{bmatrix}, \quad B_{d\omega} = \begin{bmatrix} 0 \\ 0 \end{bmatrix} \tag{5.20}$$

Using the Maple script KdKw.ma we get:

$$\left(c_{te}(sI - A_d)^{-1}(B_{d\delta} + sB_{d\omega}) + (D_{d\delta} + sD_{d\omega})\right) = T_s + sT_d \tag{5.21}$$

where

$$T_d(s) = -\frac{K_2K_3K_4T_R}{T_3T_Rs^2 + s(T_3 + T_R) + 1 + K_AK_3K_6}$$

$$T_s(s) = K_1 - \frac{K_2K_3(K_4 + K_AK_5)}{T_3T_Rs^2 + s(T_3 + T_R) + 1 + K_AK_3K_6}$$

These are the same expressions as obtained for damping and synchronising torque in Sect. 5.1.

5.2 Design of Power System Stabilisers

Equations (3.96) and (3.97) model the mechanical behaviour of a synchronous machine. The damping constant K_D in (3.97) models mechanical damping which is very small. A way to damp the mechanical oscillations then seems to be to change the applied electrical torque $\Delta T_e(s)$, shown in Fig. 5.1, in proportion to the change in the speed of the machine. A practical way to achieve this is to apply a control
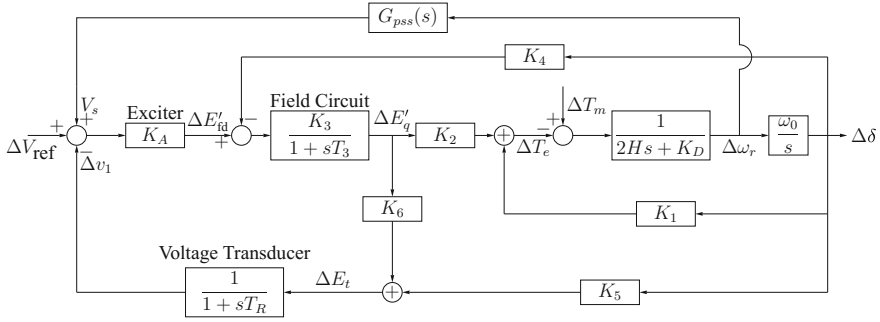
Fig. 5.3 Synchronous machine with PSS

signal to the AVR such that it changes the input electrical torque in proportion to the change in the angular velocity. Damping can also be increased by changing the input mechanical torque proportional to the change in the speed, as done by the governor, but this is a slow process due to the large response time of the valves and turbines, and it does not provide fast enough damping. Conventional PSS measures the change in the speed and applies a control signal to the AVR as shown in the block diagram in Fig. 5.3.

From the block diagram in Fig. 5.3, we can write

$$\Delta T_e(s) = \frac{K_A K_2 K_3 \left(1 + s T_R\right) G_{\mathrm{PSS}}(s)}{(1 + s T_R)(1 + s T_3) + K_A K_3 K_6} \Delta \omega_r(s) + \frac{K_A K_2 K_3 \left(1 + s T_R\right)}{(1 + s T_R)(1 + s T_3) + K_A K_3 K_6} \Delta V_{\mathrm{ref}}(s)$$

$$+ \frac{K_1 \left(1 + s T_R\right)\left(1 + s T_3\right) - K_2 \left(K_4 \left(1 + s T_R\right) + K_A K_5\right)}{(1 + s T_R)(1 + s T_3) + K_A K_3 K_6} \Delta \delta(s)$$

$$(5.22)$$

The PSS, $G_{\mathrm{PSS}}(s)$, is designed to make sure that the net phase shift, at the electromechanical oscillation frequency ω^*, from $\Delta \omega_r(s)$ to $\Delta T_e(s)$ is zero. From Eq. (5.22), it can be seen that this will happen if

$$\angle G_{\mathrm{PSS}}(\jmath \omega^*) + \angle G_{\mathrm{PVr}}(\jmath \omega^*) = 0.$$

where $G_{\mathrm{PVr}}(s)$ is the transfer function

$$G_{\mathrm{PVr}}(s) = \frac{K_A K_2 K_3 \left(1 + s T_R\right)}{(1 + s T_R)(1 + s T_3) + K_A K_3 K_6}.$$

From (5.22), it can be seen that $G_{\mathrm{PVr}}(s)$ is the transfer function between $\Delta T_e(s)$ and $\Delta V_{\mathrm{ref}}(s)$, without $G_{\mathrm{PSS}}(s)$, and with blocked rotor, i.e, $\Delta \delta(s) = 0$ or $H \to \infty$.

A classical PSS block is shown in Fig. 5.4. It has the following transfer function:

$$G_{\mathrm{PSS}}(s) = K_{\mathrm{stab}} \frac{s T_W}{1 + s T_w} \frac{1 + s T_1}{1 + s T_3} \frac{1 + s T_2}{1 + s T_4}$$

Washout   Phase Lead   Phase Lead V_{max}

$\Delta\omega_r$ K_{stab} $\dfrac{sT_w}{1+sT_w}$ $\dfrac{1+sT_1}{1+sT_3}$ $\dfrac{1+sT_2}{1+sT_4}$ V_s

V_{min}
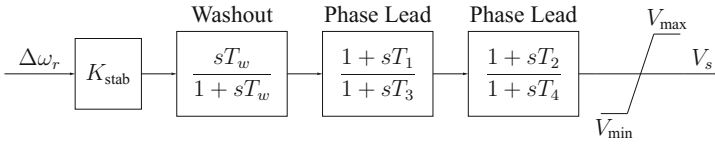
Fig. 5.4 A PSS block

The washout block filters out constant and low frequency changes in the speed. The generic PSS has two lead blocks in case a lead larger than say 90 degrees is required.

In subsequent PSS design methods, e.g., Gibbard method, phase lead has to be provided over a range of frequencies, instead of just at the resonant frequency. Practical application of a design method which requires phase lead over a range of frequencies is discussed in [32].

From Fig. 2 in [32] it can be seen that the desired phase lead changes from approximately 0 deg at 0.2 Hz to 75 deg at 2 Hz. Although the total phase lead required is less than 90 deg (which one lead block can provide), the rate at which phase lead is required is more than 45 degrees per decade hence the need for two phase lead blocks.

Similarly in many PSS designs the phase lead required may exceed 45 degree per decade and in those situations a double phase lead block is required.

Let us see the Bode plot in Fig. 5.5 for the double lead block transfer function with $T_1 = T_2 = 0.118s$, $T_3 = T_4 = 0.044s$. From the plot in Fig. 5.5 we can see that the double block provides approximately the phase lead needed for the PSS in [32].

PSS Design Steps

One can proceed with the following steps to design a classical PSS.

1. Find out the resonant mode frequency of the system ω^*.
2. Obtain the frequency response between the ΔV_{ref} and ΔT_e by holding the change in rotor speed to zero, i.e., obtain the transfer function $G_{\text{PVr}}(s)$. Calculate the phase lag at the resonant frequency, i.e., $G_{\text{PVr}}(J\omega^*)$.
3. Choose parameters for the lead compensator in Fig. 5.4 to provide the phase lead equal to the phase lag obtained in the previous step.
4. Use root-locus to select gain K_{stab} for maximum damping.
5. Alternatively increase the gain of the PSS till the closed-loop system oscillates and then set the gain K to be one third of this gain [10].
6. Choose T_W for the washout filter so that it does not interfere with the phase compensator dynamics.

The PSS design is explained here using a numerical example for the system in Sect. 3.6.3 with: $P_m = 0.5$; $x_q = 1.0$; $x_d = 1.81$; $H = 3.5$; $K_D = 1$; $\tau'_{d0} = 8.0$; $T_R = 0.02$; $K_A = 200$; $x'_d = 0.8$; $x'_q = 0.8$; $x_e = 0.6$; $\omega_0 = 2\pi 50$; $V_\infty = 0.995$; $E'_{q0} = 1.2$. All values are in per units.

1. First we find out the resonant mode frequency of the machine which has the following A matrix obtained using the linearisation techniques discusses in Chap. 3:
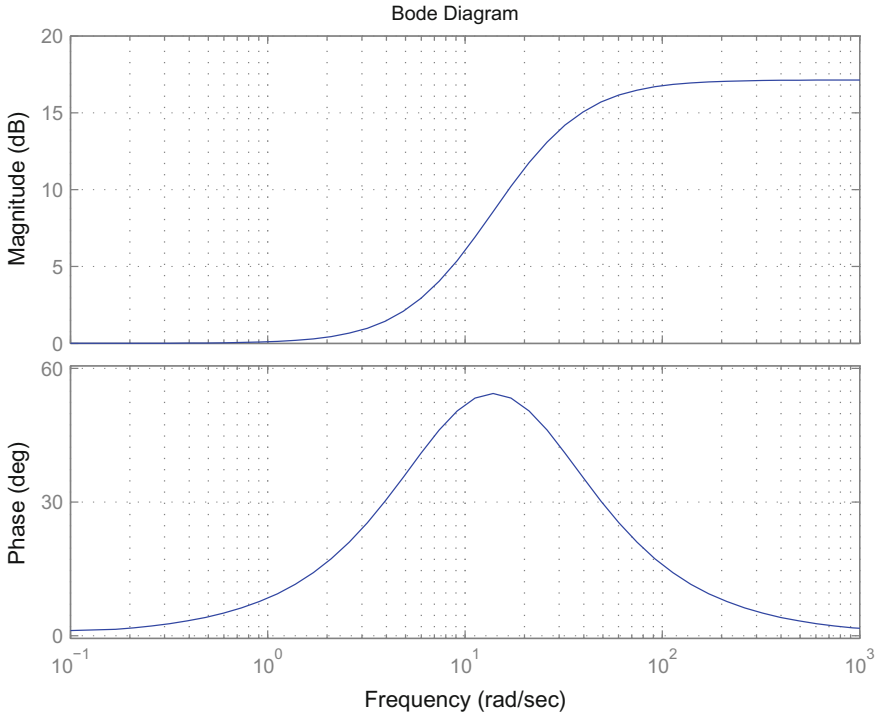
Fig. 5.5 Two lead blocks frequency response

$$A = \begin{bmatrix} 0 & -0.2652 & -0.25 & 0 \\ 377 & 0 & 0 & 0 \\ 0 & -0.3138 & -0.5236 & -0.1743 \\ 0 & -4 & 10 & -33.33 \end{bmatrix} \qquad (5.23)$$

The state vector is: $[\Delta \omega_r, \Delta \delta, \Delta E'_q, \Delta v_i]^T$.

The frequency response of the machine, without the PSS, is shown in Fig. 5.6. The resonant mode is clearly seen in the plot and from the eigenvalues given below it is clear that the electromechanical oscillation frequency is 9.99 rad s^{-1} and the damping constant is 0.013. The PSS is designed next to provide the right phase lead at this frequency.

The eigenvalues are:

$$\begin{bmatrix} -33.28 & -0.1389 + j9.99 & -0.1389 - j9.99 & -0.3006 \end{bmatrix} \qquad (5.24)$$

The right eigenvectors are:

$$\begin{bmatrix} 0 & -0.0003657 + j0.0263 & -0.0003657 - j0.0263 & -0.0005232 \\ 0.0004152 & 0.9925 & 0.9925 & 0.6561 \\ -0.005319 & -0.001845 + j0.02923 & -0.001845 - j0.02923 & -0.6966 \\ -1 & -0.1077 + j0.04123 & -0.1077 - j0.04123 & -0.2903 \end{bmatrix} \quad (5.25)$$

The participation matrix is:

$$\begin{bmatrix} -0 & 0.5004 - j0.00687 & 0.5004 + j0.00687 & -0.0008316 \\ 0 & 0.5004 - j0.00687 & 0.5004 + j0.00687 & -0.0008316 \\ -0.001676 & -0.001098 + j0.01391 & -0.001098 - j0.01391 & 1.004 \\ 1.002 & 0.0002213 - j0.0001655 & 0.0002213 + j0.0001655 & -0.002208 \end{bmatrix}$$
$$(5.26)$$

From the eigenvectors we can see that in the second and third oscillatory modes (second and third colums of the right eigenvector matrix), the second state $\Delta\delta$ has the highest contribution and $\Delta\omega_r$ has very little contribution thus the low damping. The participation matrix indicates that the two most effective states to feedback are $\Delta\delta$ and $\Delta\omega_r$. The low value of participation for the other two states means that there is little point in using the terminal voltage feedback to damp this electromechanical mode. We use the feedback from the state $\Delta\omega_r$ to damp this mode.

2. Next we obtain a frequency response between the ΔV_{ref} and ΔT_e by holding the change in rotor speed to zero. This frequency response is shown in Fig. 5.7.
3. We calculate the phase lag at the resonant frequency from the frequency response obtained in the last step. This is approximately 90°.
4. We then provide a lead compensator to provide a phase lead equal to the phase lag obtained in the previous step (at the resonant mode). The PSS is

$$G_{\text{PSS}}(s) = 10 \frac{1.4s}{1 + 1.4s} \frac{1 + \frac{s}{0.286}}{1 + \frac{1}{349.7}}.$$

The frequency response of the PSS with this phase lead is shown in Fig. 5.8. The gain is chosen using the root-locus method. The root-locus is shown in Fig. 5.9.

5.2.1   Other PSS Design Methods

As can be expected there are many PSS design methods and configurations. The essential idea remains the same as discussed in the previous section. Some of the methods that have been accepted in the power industry are mentioned below.

1. Compensation determination using residue angle [1, p. 145].
2. Larsen and Swann [33] suggest that the response of the phase angle of the generator terminal voltage magnitude is very close to that of the electrical torque. The response of the terminal voltage magnitude to changes in the voltage reference input is straightforward to measure. Therefore, it is a good signal with which to
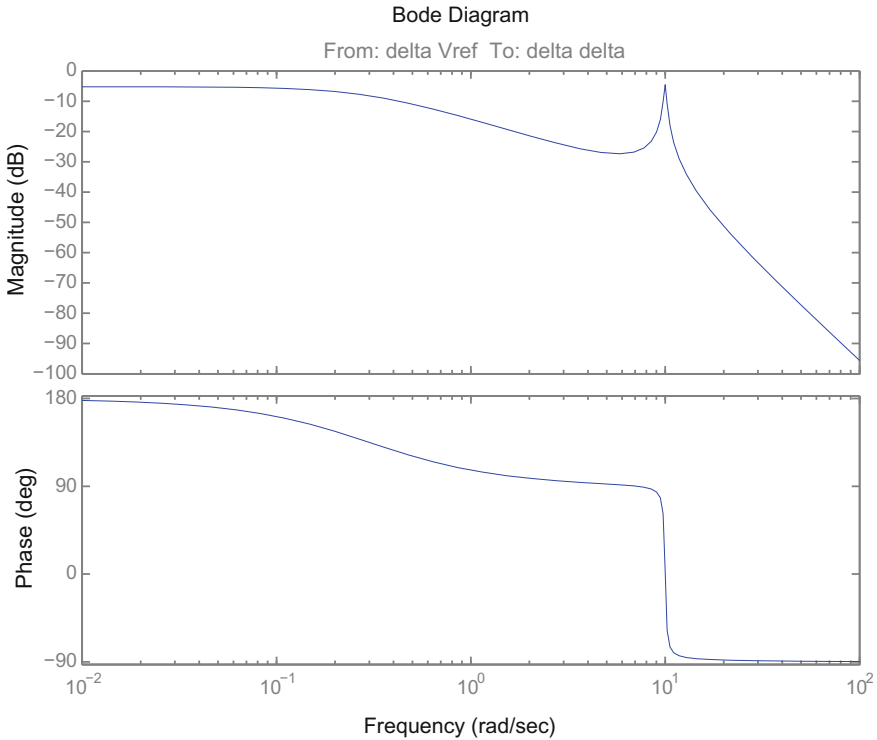
Fig. 5.6 PSS tuning—open-loop frequency response

validate the power system model used for the power system stabilizer design [1, pp. 156–157] (Fig. 5.10).

3. The transfer function of the PSS according to Gibbard method is [34]:

$$G_P(s) = \frac{DsT}{(1 + sT)(1 + sT_1)(1 + sT_2)} \frac{1}{kG_{PVr}(s)} \qquad (5.27)$$

Typical values: $T = 3$, $T_1 = 0.05$, $T_2 = 0.01$, $D = 20$. For the definition of $G_{PVr}(s)$ refer to Fig. 5.3; this is the transfer function between V_{ref} and ΔT_e. The frequency response of a typical PSS using this method is shown in Fig. 5.11 and the corresponding root-locus to tune for k is shown in Fig. 5.12.

5.3 Multimachine System PSS Design

Classical PSSs are successfully deployed for interconnected systems with many synchronous generators. The classical PSS is a single-input-single-output system
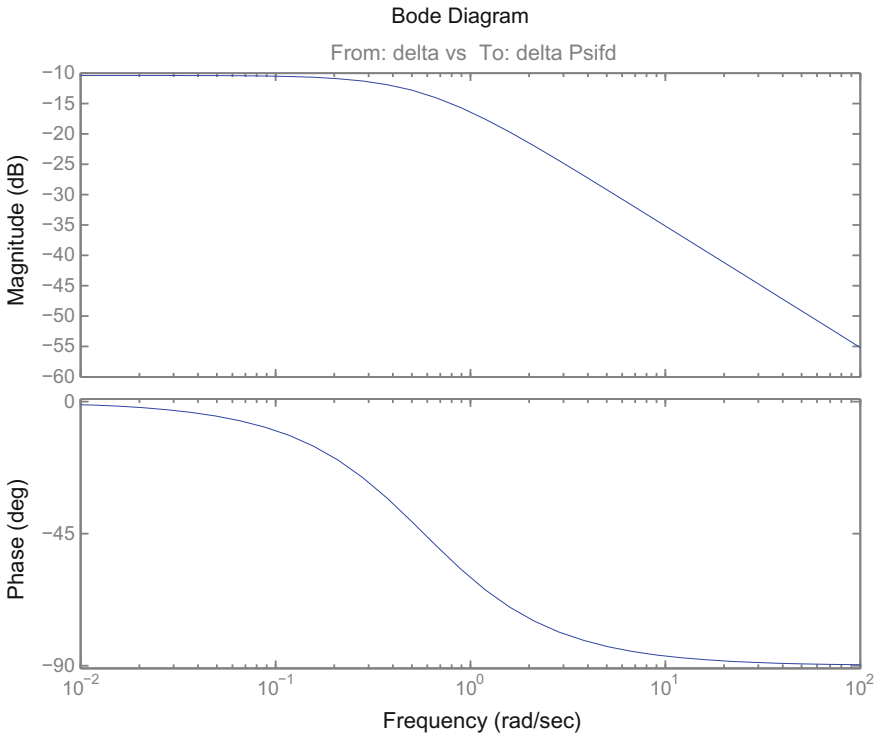
Fig. 5.7 Frequency response—ΔV_{ref} and ΔT_e

and for a multimachine system the most important question is the selection of a generator whose speed is fed back and also a generator whose electrical torque is changed via feedback. In most cases both the generators are the same and in that case the selection of that generator is important. Normally the feedback and the control happens at the same generator but with the availability of affordable phasor measurement units, it may be possible to take feedback from one generator and apply a proportional electrical damping torque to another generator. Next we look at the residue method for the selection of the generator pairs or a generator at which the PSS should be located to achieve maximum damping.

5.3.1 Dominant Residue Method

The transfer function of a system with poles at $p_1, \ldots, p_n$ can be written as:

$$G(s) = \frac{R_1}{s - p_1} + \frac{R_2}{s - p_2} + \cdots + \frac{R_n}{s - p_n}$$
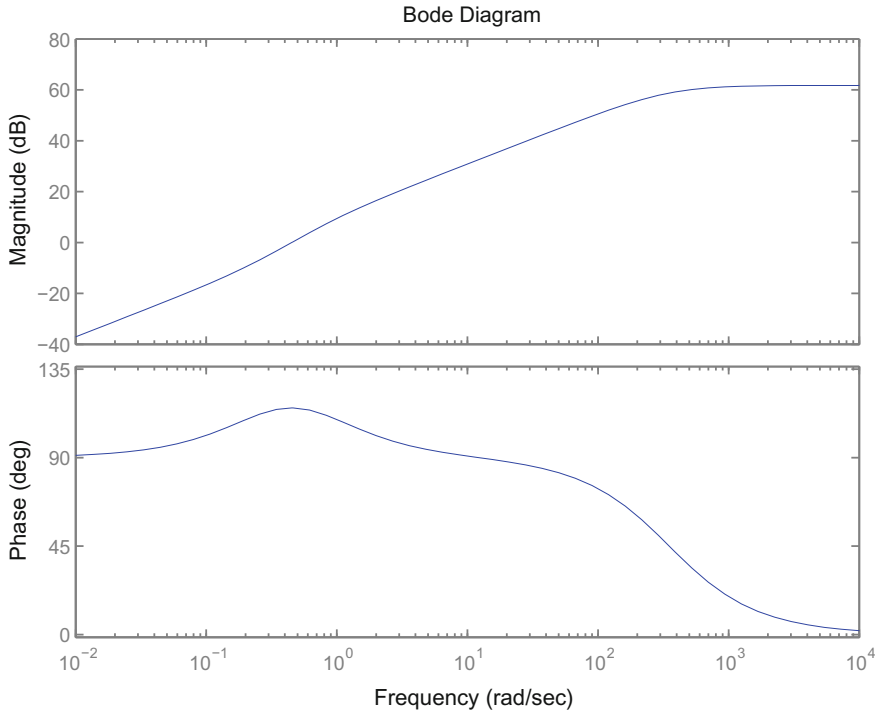
Fig. 5.8 PSS tuning—lead compensator frequency response
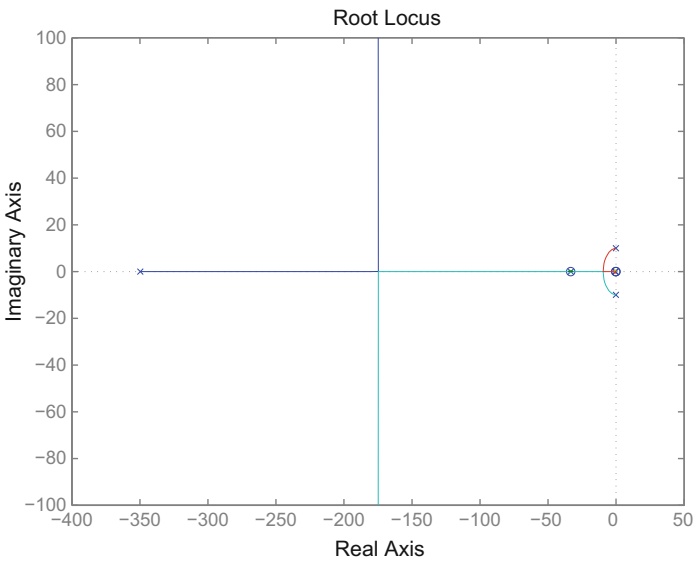
Fig. 5.9 PSS tuning—root-locus
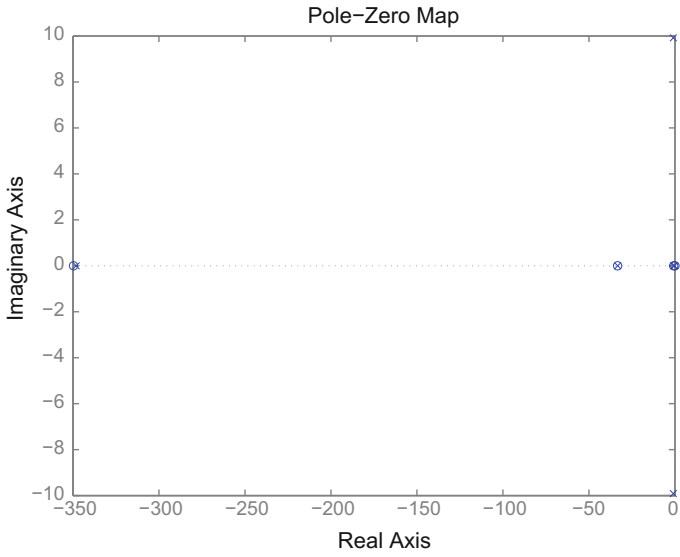
Fig. 5.10 PSS tuning—pole-zero Map
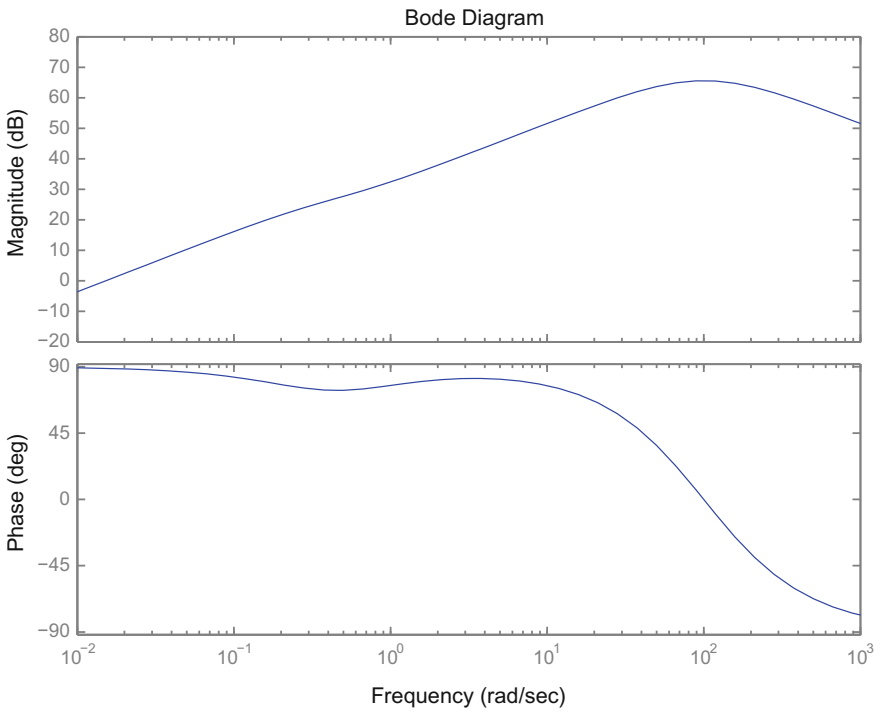
Fig. 5.11 PSS tuning—Gibbard PSS frequency response
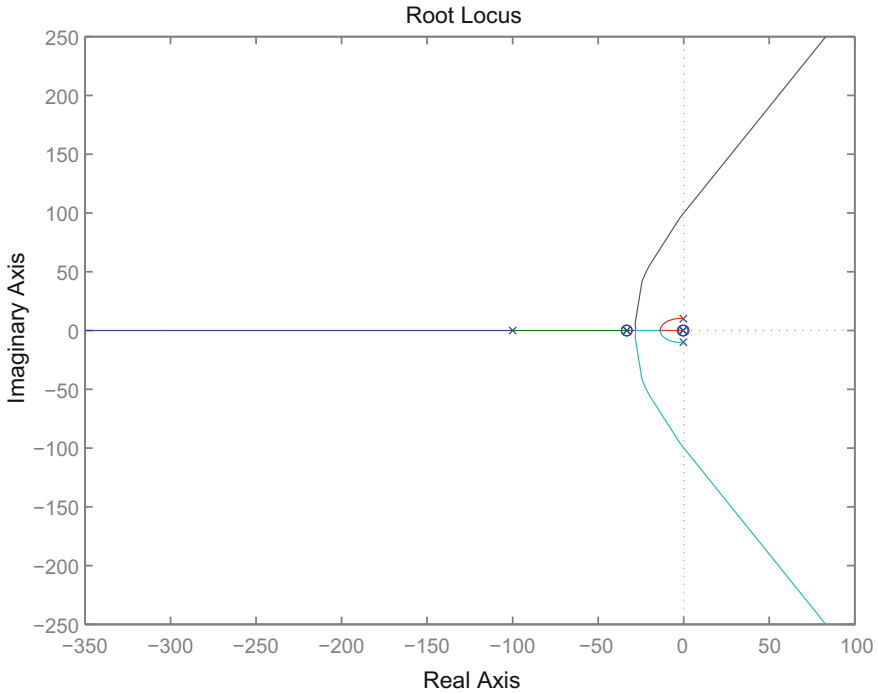
Fig. 5.12 PSS tuning—root-locus to choose k

where R_i, $i = 1, \ldots, n$, are the system residues. Let us first see what is the relationship between R_i and modal matrices.

Let the state-space respresentation of the same system be,

$$\dot{x} = Ax + Bu \tag{5.28}$$
$$y = Cx + Du \tag{5.29}$$

Define $x = \Phi z$, where Φ is the matrix with right eigenvectors as its columns, for this, $\dot{z} = \Phi^{-1}A\Phi z + \Phi^{-1}Bu$ and $y = C\Phi z$, for this we can write,

$$G(s) = C\Phi (sI - \Lambda)^{-1} \Phi^{-1}B = \sum_{i=1}^{n} \frac{C\Psi_i\Phi_i B}{s - p_i} \Rightarrow R_i = C\Psi_i\Phi_i B. \tag{5.30}$$

where Ψ_i, Φ_i are the left and right eigenvectors of the system. For an multi-input-multi-output (MIMO) system, R_i are matrices, and the element $R_i(j, k)$ gives the contribution in output j due to input k for mode i. This is exactly the same information conveyed by participation factors.

Fig. 5.13 Small gain in the feedback loop
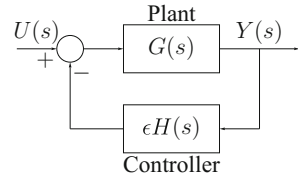
To see the influence of the residue in a feedback control design let us consider the feedback system in Fig. 5.13. Let $G(s) = \sum_{i=1}^{n} \frac{R_i}{s - \lambda_i}$, then the closed-loop transfer function is given as:

$$\frac{Y(s)}{U(s)} = \frac{G(s)}{1 + \epsilon H(s)G(s)} \tag{5.31}$$

$$= \frac{\sum_{i=1}^{n} \frac{R_i}{s - \lambda_i} \prod_{i=1}^{n}(s - \lambda_i)}{\prod_{i=1}^{n}(s - \lambda_i) + \epsilon H(s) \sum_{i=1}^{n} R_i \prod_{\substack{j=1 \\ j \neq i}}^{n}(s - \lambda_j)} \tag{5.32}$$

$$= \frac{\sum_{i=1}^{n} \frac{R_i}{s - \lambda_i} \prod_{i=1}^{n}(s - \lambda_i)}{(s - \lambda_k + \epsilon H(s)R_k) \prod_{\substack{j=1 \\ j \neq k}}^{n}(s - \lambda_j) + \epsilon H(s) \sum_{\substack{i=1 \\ i \neq k}}^{n} R_i \prod_{\substack{j=1 \\ j \neq i}}^{n}(s - \lambda_j)} \tag{5.33}$$

If we choose $H(s)$ such that:

$$H(s) = \begin{cases} 1 & s \text{ is close to } \lambda_k \\ 0 & s \text{ is not close to } \lambda_k \end{cases}$$

then the denominator of (5.32) near $s = \lambda_k$ is:

$$(s - \lambda_k + \epsilon R_k) \prod_{\substack{j=1 \\ j \neq k}}^{n}(s - \lambda_j) \tag{5.34}$$

The above Eq. (5.34) implies that as a result of the feedback shown in Fig. 5.13 the mode λ_k will shift by $-\epsilon R_k$ and all other modes will remain unchanged [35].

In a resonant system like a power system with angle oscillations, the above analysis shows that the strength of the feedback is governed by the residue of the resonant mode. This is because the system itself acts as a filter to feedback the oscillation mode signal with the strongest signal, i.e., $H(s)$ is a part of the dynamics of the system itself.

Let us now consider a MIMO system, let Fig. 5.14 be a block diagram representation of the system with the lth input and mth output.

$$Y_m(s) = (U_l(s) - \epsilon Y_m(s)) \sum_{i=1}^{n} \frac{R_i^{lm}}{s - p_i} \tag{5.35}$$

$$\frac{Y_m(s)}{U_l(s)} = \frac{\sum_{i=1}^{n} R_i^{lm} \prod_{\substack{j=1 \\ j \neq i}}^{n} (s - p_j)}{\prod_{j=1}^{n}(s - p_j) + \epsilon \sum_{i=1}^{n} R_i^{lm} \prod_{\substack{j=1 \\ j \neq i}}^{n} (s - p_j)} \tag{5.36}$$

When $R_k^{lm} >> R_i^{lm}$, $i = 1, \ldots, n$, $(i \neq k)$, we can write (5.36) as:

$$\frac{Y_m(s)}{U_l(s)} = \frac{\sum_{i=1}^{n} R_i^{lm} \prod_{\substack{j=1 \\ j \neq i}}^{n} (s - p_j)}{\left(s - p_k - \epsilon R_k^{lm}\right) \prod_{\substack{j \neq k \\ j=1}}^{n} (s - p_j)} \tag{5.37}$$

Equation (5.37) shows that the largest shift in the poles of the system will be realised by feeding back the input corresponding to the largest residue of the system. Thus to damp the kth mode choose l and m such that $R_k^{lm} >> R_i^{lm}$, $i = 1, \ldots, n$, $(i \neq k)$. Once an input-output pair is selected and the corresponding residue has been evaluated, the method discussed previously can be used to design a PSS. The following properties of the residues are helpful in the design process.

1.
$$R_i = \lim_{\lambda \to p_i} G(s)(s - p_i)$$

where p_i is not a multiple pole of $G(s)$.

2. The departure angle of root-locus of $G(s)$ from pole p_i is

$$\alpha_i = 180 - \angle \lim_{\lambda \to p_i} G(s)(s - p_i) = -180 + \angle R_i$$

3. When the feedback is positive (as in the case of PSS), the departure angle is, $\alpha_i = \angle R_i$. In classical PSS design it is aimed that the root-locus heads "left" from the underdamped pole. This can be achieved by providing a lead equal to $180 - \angle R_i$ such that the departure angle $\alpha_i = 180$.
4. Residues change the mode with "resonant" feedback.

5.3.2 $G_{PVr}(s)$ for Multi-machine Systems [1]

The first step in tuning PSS for multi-machine systems is to obtain the transfer function $G_{PVr}(s)$ between $\Delta V_{\text{ref}}(s)$ and $\Delta T_e(s)$. Let

$$\Delta \delta = [\delta_1, \delta_2, \ldots, \delta_n]^T,$$

$$\Delta \omega = [\omega_1, \omega_2, \ldots, \omega_n]^T,$$

and let x_d be the state vector of all other states, like exciter, AVR, governor, turbines and every other dynamic element in the system. The state-space representation can be written as:

Obtaining $G_{PVr}(s)$ for multi-machine systems [1]:

$$\frac{d\Delta\delta}{dt} = \omega_0 \Delta\omega \tag{5.38}$$

$$M\frac{d\Delta\omega}{dt} = \Delta T_m - \Delta T_e - D_\omega \Delta\omega \tag{5.39}$$

$$\frac{dx_d}{dt} = A_d x_d + B_{d\delta}\Delta\delta + B_{d\omega}\Delta\omega + B_v (V_{\text{ref}} + V_s) \tag{5.40}$$

$$\Delta T_e = c_{te} x_d + D_{d\delta}\Delta\delta + D_{d\omega}\Delta\omega \tag{5.41}$$

$$\Delta T_m = c_{tm} x_d + D_{m\delta}\Delta\delta + D_{m\omega}\Delta\omega \tag{5.42}$$

Replacing $\frac{d}{dt}$ by s

$$X_d(s) = (sI - A_d)^{-1} ((B_{d\delta} + s B_{d\omega}) \Delta\delta(s) + B_v (V_{\text{ref}} + V_s)) \tag{5.43}$$

$$\Delta T_e(s)|_{\Delta\delta=0} = c_{te} (sI - A_d)^{-1} B_v (V_{\text{ref}} + V_s) \tag{5.44}$$

We can write $G_{PVr}(s)$ as:

$$G_{PVr}(s) = c_{te} (sI - A_d)^{-1} B_v \tag{5.45}$$

Single Machine Infinite Bus

$$\Delta\dot{\delta} = \omega_0 \Delta\omega_r \tag{5.46}$$

$$2H\Delta\dot{\omega}_r = -K_D\Delta\omega_r - K_2\Delta E'_{q_{\text{fd}}} - K_1\Delta\delta + \Delta T_m \tag{5.47}$$

$$T_3\Delta\dot{E}'_{q_{\text{fd}}} = -E'_{q_{\text{fd}}} + K_3 K_A (V_{\text{ref}} + V_s - \Delta v_1) - K_3 K_4 \Delta\delta \tag{5.48}$$

$$T_R\Delta\dot{v}_1 = -\Delta v_1 + K_6 E'_{q_{\text{fd}}} + K_5\Delta\delta \tag{5.49}$$

$$x_1 \stackrel{\triangle}{=} \Delta\delta,\, x_2 \stackrel{\triangle}{=} \Delta\omega_r,\, x_3 \stackrel{\triangle}{=} \Delta E'_{q_{\text{fd}}},\, x_4 \stackrel{\triangle}{=} \Delta v_1,\, x_d = [x_3, x_4]' \tag{5.50}$$

$$c_{te} = \begin{bmatrix} -K_2 & 0 \end{bmatrix},\quad A_d = \begin{bmatrix} -\frac{1}{T_3} & -\frac{K_A K_3}{T_3} \\ \frac{K_6}{T_R} & -\frac{1}{T_R} \end{bmatrix},\quad B_v = \begin{bmatrix} \frac{K_A K_3}{T_3} \\ 0 \end{bmatrix} \tag{5.51}$$

Substituting the above matrices in the expression for $G_{PVr}(s)$ in (5.45) and using the Maple script KdKw.ma we get:

$$G_{PVr}(s) = \frac{K_2 K_3 K_A(sT_R + 1)}{T_3 T_R s^2 + s(T_3 + T_R) + 1 + K_A K_3 K_6} \tag{5.52}$$

A comparison is made between the frequency response obtained using the above anyalytical (5.52) expression of the transfer function and Gibbard's method of setting inertias to infinity in Figs. 5.15 and 5.16, respectively.

Next we look at the PSS design for the two-area system and a 30 bus system [1, p. 38].

Two-Area System

One line diagram of a two-area system from [1, p. 38] is shown in Fig. 5.17. It consists of four generators with two generators each in an area. Modal analysis is performed for this two-area system to obtain the dominant modes—oscillation frequency and mode shape. In this example of four generators, as they oscillate they can form the following possible oscillating groups: one group with all four generators oscillating independently, six groups with two generators paired together, two groups with three generators each, and one group with all the four generators. Modal analysis can work out which of the possible ten groupings for oscillations will be dominant. This example is called a two-area system because with the modal analysis we discover that this system has two dominant modes, one local mode and another inter-area mode where generators G_1 and G_2 oscillate coherently and so do G_3 and G_4, but they form two groups which oscillate with respect to each other.
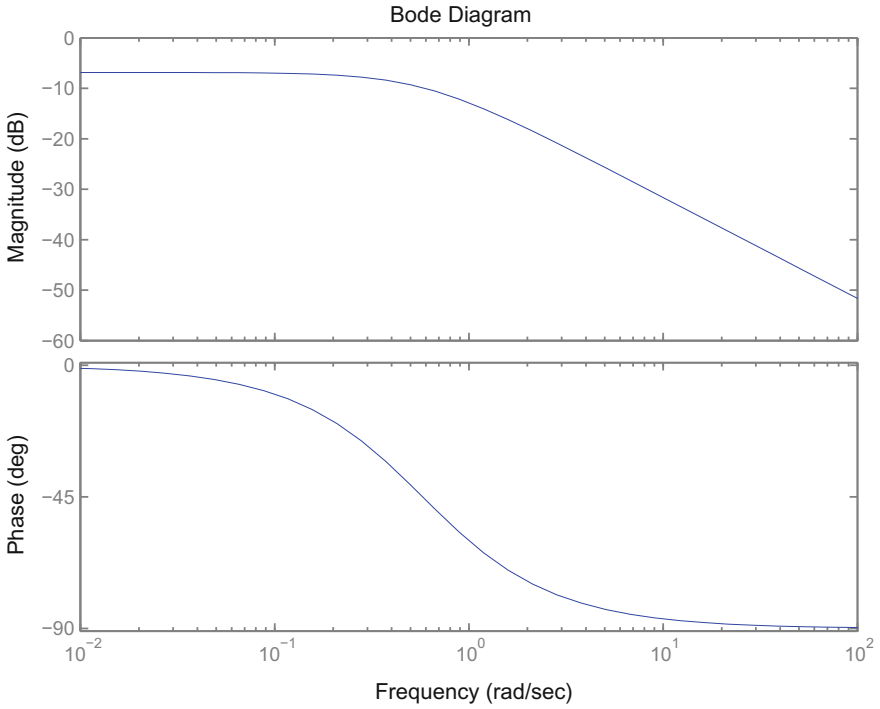
Fig. 5.15 Frequency response of analytical $G_{PVr}(s)$

The A matrix for four machine system, where the machines are represented using the classical swing equation, is:

$$\begin{bmatrix} 0 & 377 & 0 & 0 & 0 & 0 & 0 & 0 \\ -0.07442 & 0 & 0.0676 & 0 & 0.003688 & 0 & 0.003135 & 0 \\ 0 & 0 & 0 & 377 & 0 & 0 & 0 & 0 \\ 0.07182 & 0 & -0.08647 & 0 & 0.007151 & 0 & 0.007503 & 0 \\ 0 & 0 & 0 & 0 & 0 & 377 & 0 & 0 \\ 0.007307 & 0 & 0.01069 & 0 & -0.07802 & 0 & 0.06003 & 0 \\ 0 & 0 & 0 & 0 & 0 & 0 & 0 & 377 \\ 0.01135 & 0 & 0.01733 & 0 & 0.06725 & 0 & -0.09593 & 0 \end{bmatrix} \quad (5.53)$$

The state variables are:

$$\begin{bmatrix} \Delta\delta_1 & \Delta\omega_1 & \Delta\delta_2 & \Delta\omega_2 & \Delta\delta_3 & \Delta\omega_3 & \Delta\delta_4 & \Delta\omega_4 \end{bmatrix} \quad (5.54)$$

The eigenvalues of the above A matrix are:

$$\begin{bmatrix} 0.01148 & -0.01148 & -j3.532 & j3.532 & -j7.509 & j7.509 & -j7.575 & j7.575 \end{bmatrix} \quad (5.55)$$

Bode Diagram
From: delta Vref To: Out(1)
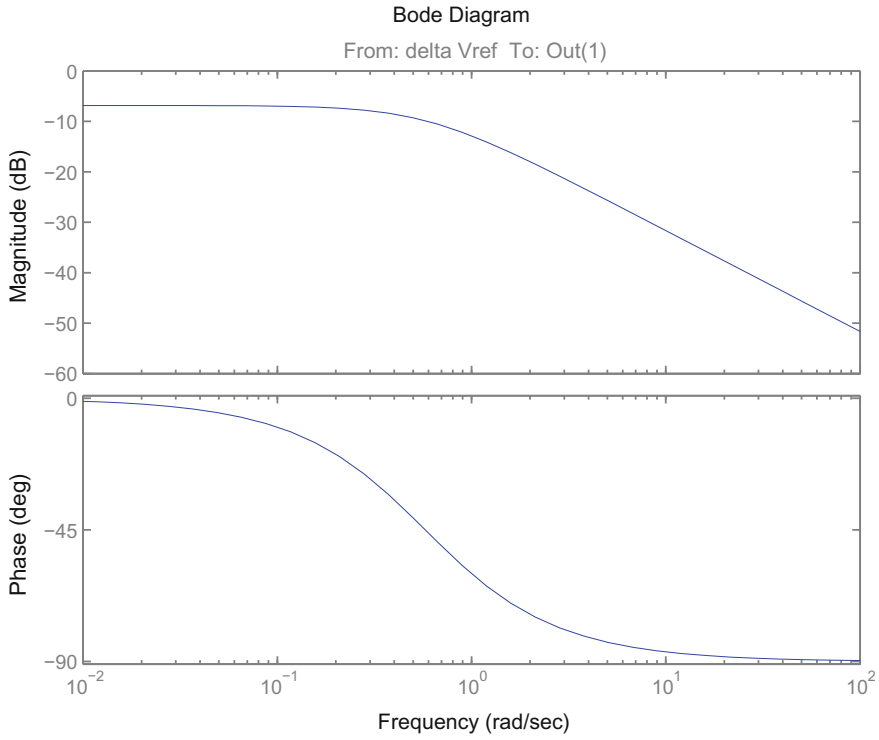
Fig. 5.16 Frequency response of numerical $G_{PVr}(s)$

Fig. 5.17 Two area system
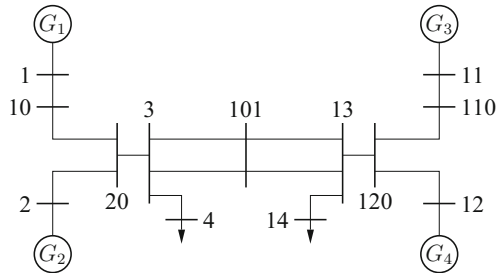
The right eigenvectors are:

$$
\begin{bmatrix}
0.5 & -0.5 & 0.3274 & 0.3274 & -0.4342 & -0.4342 & -0.3084 & -0.3084 \\
0 & 0 & -j0.003067 & j0.003067 & j0.008648 & -j0.008648 & j0.006196 & -j0.006196 \\
0.5 & -0.5 & 0.2651 & 0.2651 & 0.4838 & 0.4838 & 0.3575 & 0.3575 \\
0 & 0 & -j0.002484 & j0.002484 & -j0.009637 & j0.009637 & -j0.007183 & j0.007183 \\
0.5 & -0.5 & -0.6821 & -0.6821 & -0.5045 & -0.5045 & 0.5416 & 0.5416 \\
0 & 0 & j0.00639 & -j0.00639 & j0.01005 & -j0.01005 & -j0.01088 & j0.01088 \\
0.5 & -0.5 & -0.5977 & -0.5977 & 0.568 & 0.568 & -0.6953 & -0.6953 \\
0 & 0 & j0.005599 & -j0.005599 & -j0.01131 & j0.01131 & j0.01397 & -j0.01397
\end{bmatrix}
$$

$$(5.56)$$
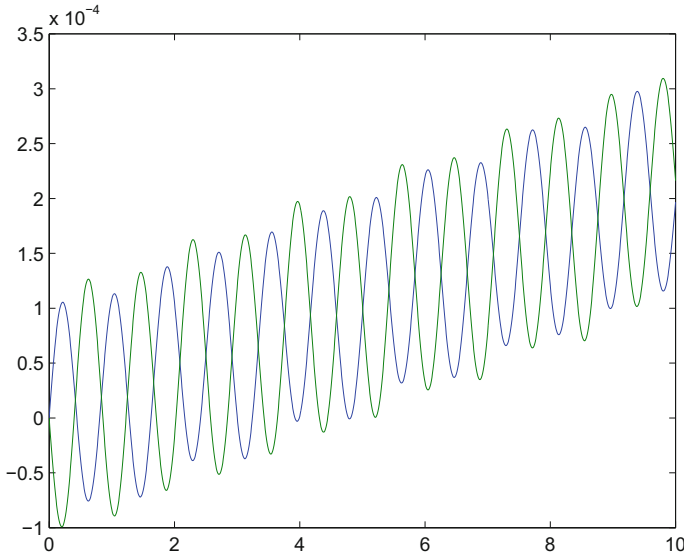
Fig. 5.18 Local mode—generators 1 and 2 speeds

The participation matrix is:

$$\begin{bmatrix}
0.1778 & 0.1778 & 0.09611 & 0.09611 & 0.1437 & 0.1437 & 0.08235 & 0.08235 \\
0.1778 & 0.1778 & 0.09611 & 0.09611 & 0.1437 & 0.1437 & 0.08235 & 0.08235 \\
0.1641 & 0.1641 & 0.06261 & 0.06261 & 0.1631 & 0.1631 & 0.1102 & 0.1102 \\
0.1641 & 0.1641 & 0.06261 & 0.06261 & 0.1631 & 0.1631 & 0.1102 & 0.1102 \\
0.08577 & 0.08577 & 0.1997 & 0.1997 & 0.09248 & 0.09248 & 0.122 & 0.122 \\
0.08577 & 0.08577 & 0.1997 & 0.1997 & 0.09248 & 0.09248 & 0.122 & 0.122 \\
0.07232 & 0.07232 & 0.1416 & 0.1416 & 0.1007 & 0.1007 & 0.1854 & 0.1854 \\
0.07232 & 0.07232 & 0.1416 & 0.1416 & 0.1007 & 0.1007 & 0.1854 & 0.1854
\end{bmatrix}$$

$$(5.57)$$

The local modes of this two area system can be seen by perturbing generators 1 and 2. The local mode can be seen in 5.18 and 5.19 where G_1 and G_2 oscillate with respect to each other and so do generators G_3 and G_4.

The inter-area mode can be excited by perturbing generators 1 and 3. The inter-area mode can be seen in Figs. 5.20 and 5.21 where G_1 and G_2 oscillate coherently and so do G_3 and G_4.

Figs. 5.22 and 5.23 show how G_1 and G_2 form one group and G_3 and G_4 another group and they oscillate with respect to each other.
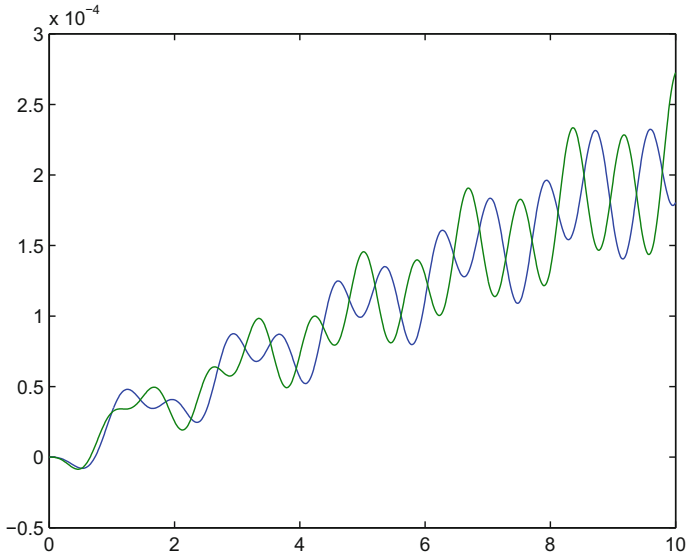
Fig. 5.19 Local mode—generators 3 and 4 speeds
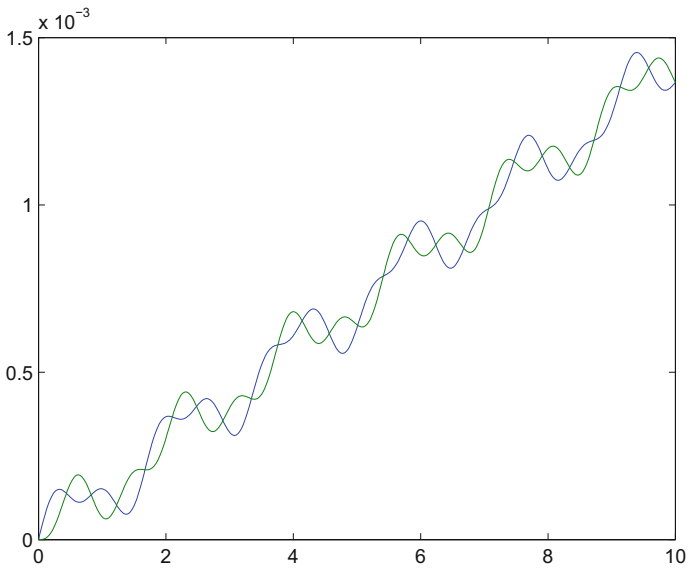
Fig. 5.20 Inter area mode—generators 1 and 2 speeds
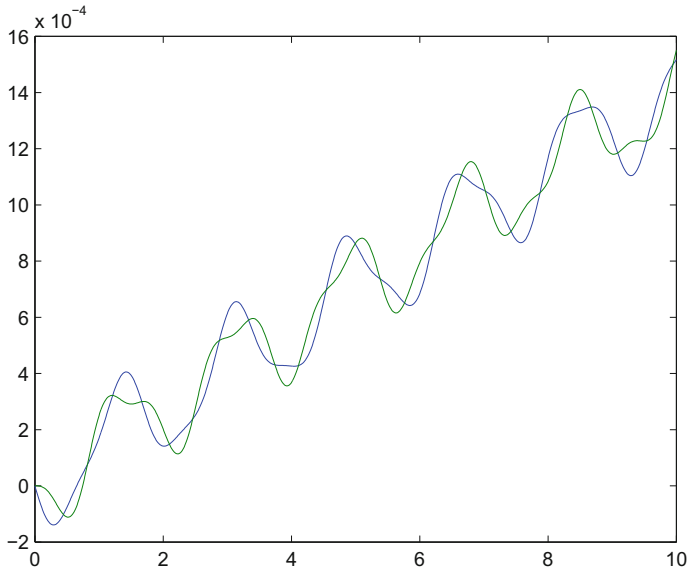
Fig. 5.21 Inter area mode—generators 3 and 4 speeds
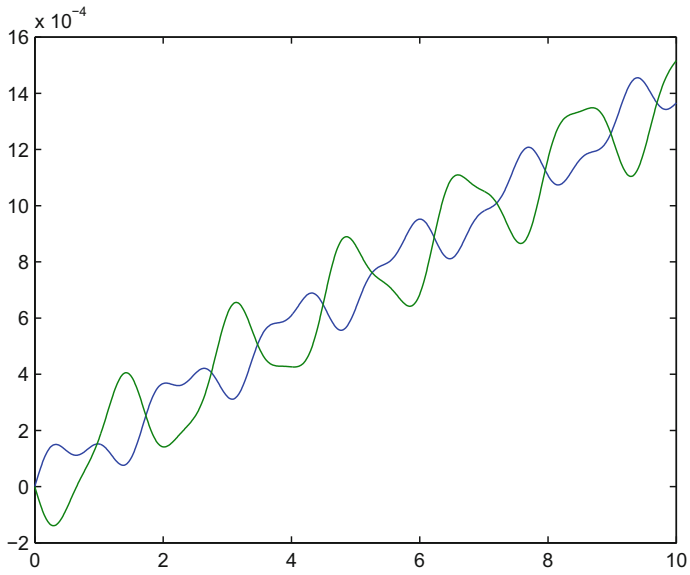
Fig. 5.22 Inter area mode—generators 1 and 3 speeds
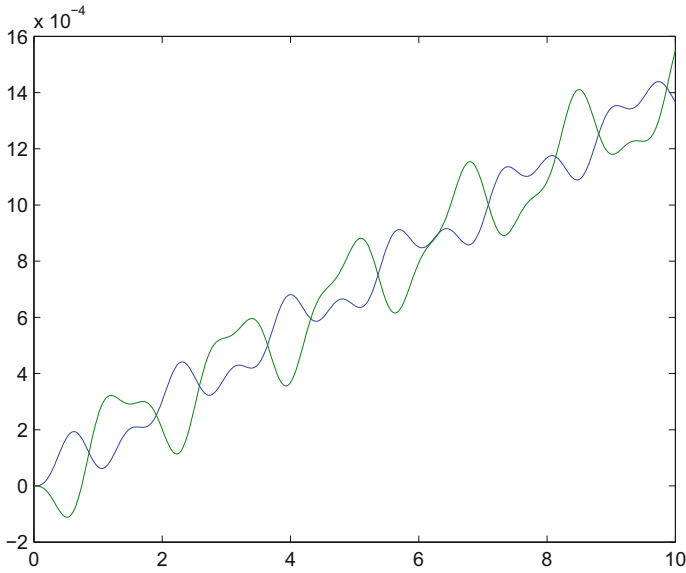
Fig. 5.23 Inter area mode—generators 2 and 4 speeds

A 30 Bus System
A one-line diagram of a 30 bus system with sixteen generators is shown in Fig. 5.24.

The system has two unstable roots: $0.3264 - 6.8364\jmath$ and $0.3264 + 6.8364\jmath$. The modes of this system are shown as a pole-zero plot in Fig. 5.25.

The non-negligible participation factor for the $0.3264 - 6.8364i$ mode are:

Participation factor	State	State name	Machine number
$0.1288 - 0.0624i$	8.0000	1.0000	2.0000
$0.0912 - 0.0783i$	9.0000	2.0000	2.0000
$0.0810 - 0.0646i$	15.0000	1.0000	3.0000
$0.9107 - 0.0783i$	57.0000	1.0000	9.0000
1.0000	58.0000	2.0000	9.0000
$0.1730 - 0.0790i$	59.0000	3.0000	9.0000
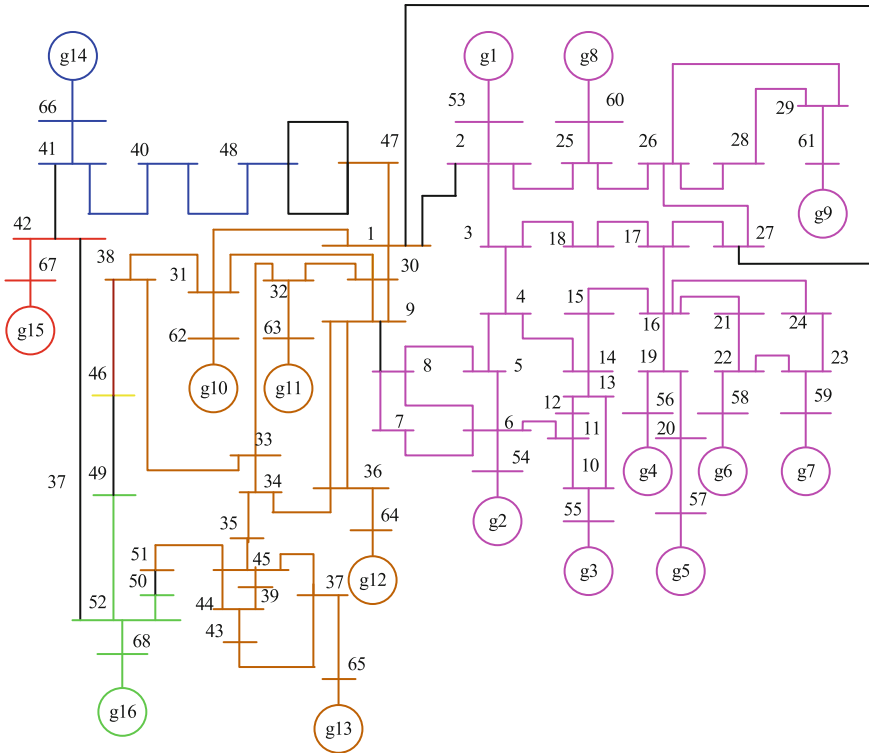
Fig. 5.24 Sixteen generator system [1, p. 351]

Based on the participation factors it is clear that the PSS must be located at generator 9. The phase lead that is required by the PSS at generator 9 is shown in Fig. 5.26. A PSS block with the following transfer function is designed,

$$G_P(s) = k \frac{sT_w}{1 + sT_w} \frac{1 + sT_1}{1 + sT_3} \frac{1 + sT_2}{1 + sT_4}$$

The values of the PSS parameters that provide the required lead as shown in Fig. 5.26 are: $T_w = 5$; $T_1 = 0.08$; $T_2 = 0.01$; $T_3 = \frac{1}{4\pi}$; $T_4 = \frac{1}{8\pi}$.

The root-locus plot in Fig. 5.27 is used to obtain the gain k of the PSS. The modes of the closed-loop system with the PSS are shown in Fig. 5.28.
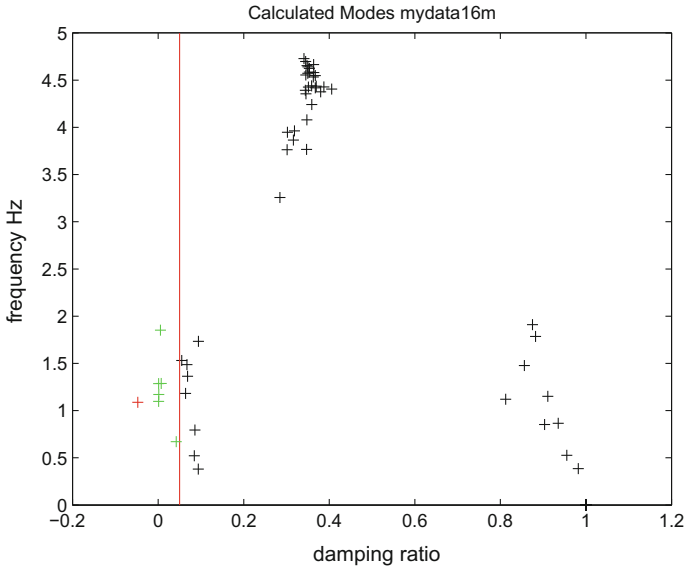
Fig. 5.25 Sixteen generator system—modes
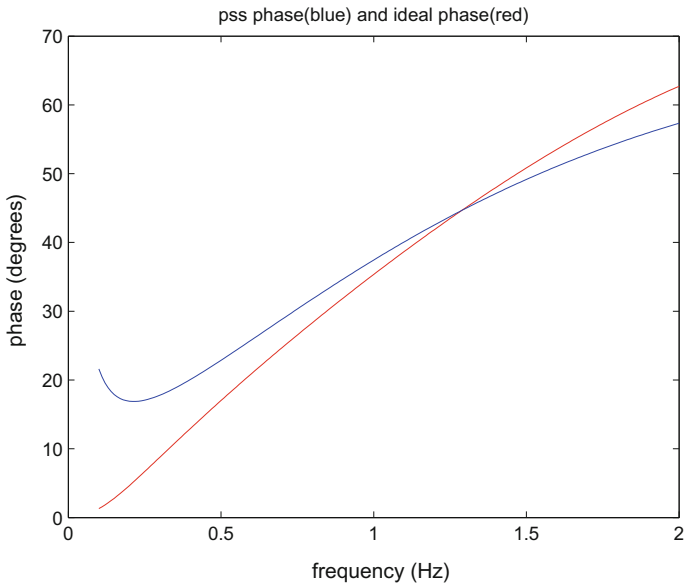
Fig. 5.26 Sixteen generator system—phase lead
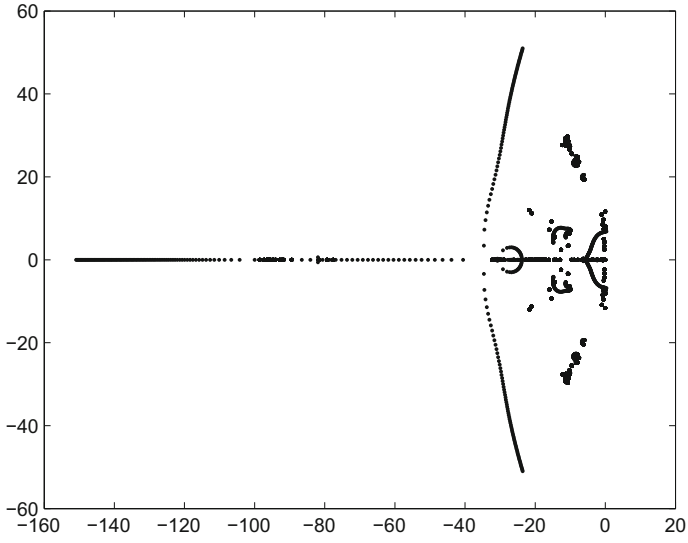
Fig. 5.27   Sixteen generator system—root-locus with PSS
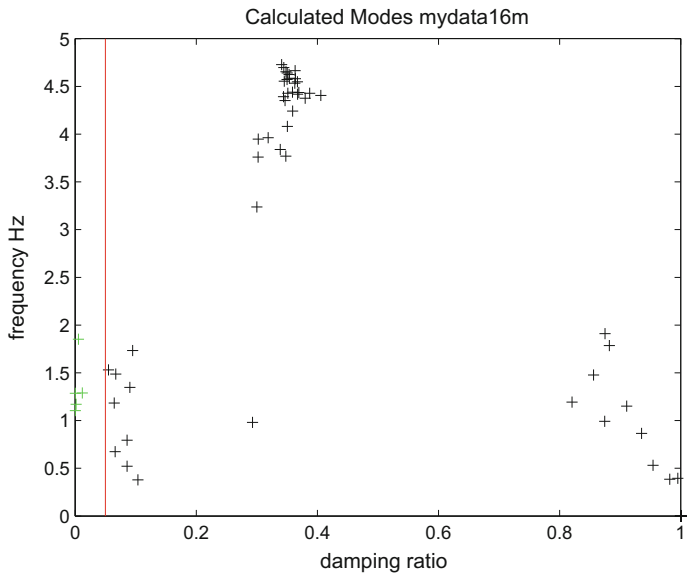
Fig. 5.28   Sixteen generator system—modes

Chapter 6
Exercises

6.1 Phasor Analysis

Exercise 6.1 In Fig. 6.1 the voltage $v(t) = 2\sin(2\pi 50t)$ V, $R = 1\,\Omega$, and $L = 0.0025$ H. Find the steady-state current $i(t)$. Draw the phasor equivalent circuit as shown on the right side of Fig. 6.1 with numerical values for all the phasor quantities.

Exercise 6.2 In Fig. 6.2 the voltage $v(t) = 100\sin(2\pi 50t)$ V, $R = 300\,\Omega$, and $C = 10\,\mu$F, and $v_c(0) = 50$ V. Find the steady-state capacitor voltage $v_c(t)$. Write the differential equation describing the circuit operation. Solve the differential equation numerically or otherwise to obtain $v_c(t)$ and plot the steady-state solution and the numerical solution on the same plot.

Exercise 6.3 Figure 6.3 is a one-line diagram of a three-bus system. The impedance of the lines connecting nodes i and j is given by $\bar{Z}_{ij} = 0.05 + j0.3$ pu, i.e., all the transmission lines have the same impedance. Obtain the Y_{Bus} matrix for this three-bus system.

Exercise 6.4 1. What is a V-curve? Describe the conditions under which a V-curve is plotted. How does the V-curve make synchronous generator the dominant device for electromechanical energy conversion?
  2. What is the essential condition in terms of flux linkages for electromechanical energy conversion?

Exercise 6.5 In Fig. 6.4 the voltage $v(t) = 2\sin(2\pi 50t)$ V, $R = 1\,\Omega$, $R = 300\,\Omega$, and $C = 10\,\mu$F, $v_c(0) = 50$ V, and $v_c'(0) = 0$. Solve the differential equation numerically or otherwise to obtain $v_c(t)$ and plot the steady-state solution and the numerical solution on the same plot.

Fig. 6.1 An RL circuit
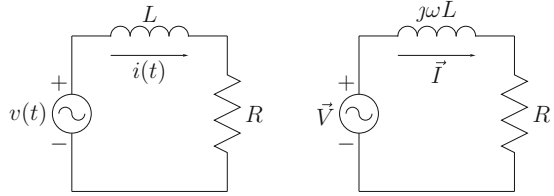
Fig. 6.2 An RC circuit
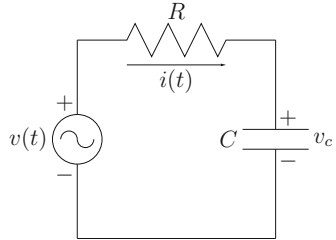
Exercise 6.6 In Fig. 6.5 the voltage $v_1(t) = 10\sin(2\pi 50t)$ V, $v_2(t) = 20\sin(2\pi 50t + 90°)$ V, $R = 300\,\Omega$, and $C = 100\,\mu$F, $L = 25$ mH. Calculate currents $i_1(t)$ and $i_2(t)$ using phasor analysis. Find the real and reactive power consumed by each element in the circuit and add them up to verify that the sum of complex power consumed by all the loads is equal to the generated complex power.
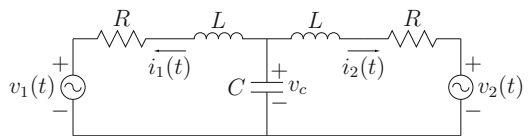
Fig. 6.3 Three bus system
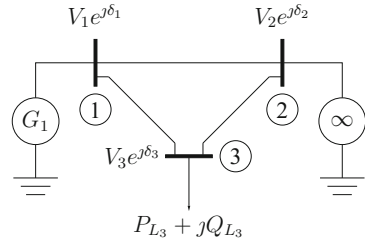
Fig. 6.4 An LCR circuit
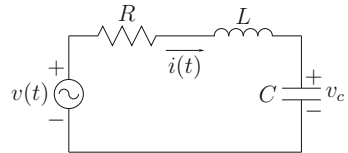
Fig. 6.5 A mesh circuit

Exercise 6.7   1. Figure 6.6 shows a three-phase star system.

In the three-phase star system shown in Fig. 6.6, the supply voltages are: $v_a(t) = 415\sin(2\pi 50t)$ V, $v_b(t) = 415\sin(2\pi 50t - 120°)$ V, $v_c(t) = 415\sin(2\pi 50t + 120°)$ V, and the load is: $R = 5\,\Omega$, and $L = 15$ mH. Calculate the total real and reactive power consumed by the load and generated by the three-phase voltage source.

2. Figure 6.7 shows a three-phase delta connected load.

In the three-phase Δ system shown in Fig. 6.7, the supply voltages are: $v_a(t) = 415\sin(2\pi 50t)$V, $v_b(t) = 415\sin(2\pi 50t - 120°)$ V, $v_c(t) = 415\sin(2\pi 50t + 120°)$ V, and the load is: $R = 5\,\Omega$, and $L = 15$ mH. Calculate the total real and reactive power consumed by the load and generated by the three-phase voltage source.

Exercise 6.8 Figure 6.8 shows a one-line diagram of a single machine infinite-bus system. Generator 1 is set to generate 0.5 pu real power, $Ze^{J\theta} = 0.25e^{J\frac{\pi}{2}}$, $V_1 = 1.0$ pu, $V_2 = 1.0$ pu, and $\delta_2 = 0°$. Calculate δ_1 and the reactive power generated by Generator 1. What is the real and reactive power generated or absorbed by the infinite-bus?
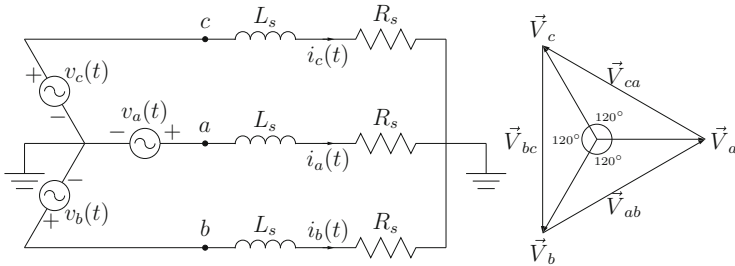
Fig. 6.6 A Three-Phase Star-Star connection
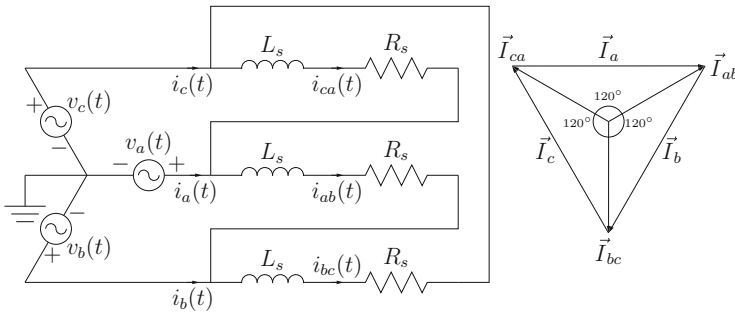
Fig. 6.7 A Three-Phase Star-Delta connection

Exercise 6.9 Figure 6.8 shows a one-line diagram of a single machine infinite-bus system. Generator 1 is set to generate 0.5 pu real power, $Ze^{j\theta} = 0.3e^{j\frac{\pi}{2}}$, $V_2 = 1.0$ pu, and $\delta_2 = 0°$. Plot the current magnitude $|\vec{I}_{12}|$ and the reactive power supplied by generator 1 as the magnitude of the voltage at bus 1, V_1, varies between 0.85 and 1.1 pu.

Exercise 6.10 Figure 6.9 is a one-line diagram of a three-bus system. The impedance of the lines connecting nodes i and j is given by $\vec{Z}_{ij} = 0.05 + j0.3$ pu, i.e., all the transmission lines have the same impedance.

1. Bus 1 is a PV bus, i.e., a generator bus: $P_{G_1} = 0.5$ pu and $V_1 = 1.1$ pu; Q_1 and δ_1 are unknown.
2. Bus 2 is a slack bus: $V_2 = 1$ pu and $\delta_2 = 0°$; P_2 and Q_2 are unknown.
3. Bus 3 is a PQ bus, i.e., a load bus: $P_{L_3} = 0.8$ pu and $Q_{L_3} = 0.2$ pu; V_3 and δ_3 are unknown.

All the values are expressed in per unit with $P_b = 100$ MW and $V_b = 138$ kV. Use the powerworld simulator or write a program using Matlab or any other package to obtain a power flow solution. Attach the one-line diagram and tabulate the results from the power flow solution.

Exercise 6.11 Figure 6.10 is a one-line diagram of a four-bus system. The impedance of the lines connecting nodes i and j is given by $\vec{Z}_{ij} = 0.01 + j0.2$ pu, i.e., all the transmission lines have the same impedance.

1. Bus 1 is a PV bus, i.e., a generator bus: $P_{G_1} = 1$ pu and $V_1 = 0.99$ pu; Q_1 and δ_1 are unknown.
2. Bus 2 is a PV bus, i.e., a generator bus: $P_{G_2} = 0.8$ pu and $V_2 = 1.01$ pu; Q_2 and δ_2 are unknown.
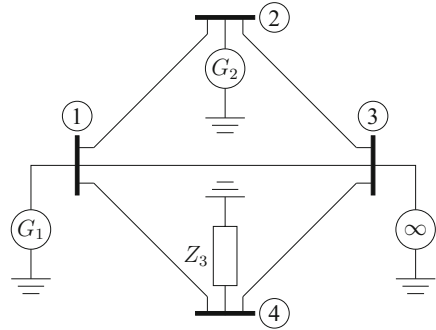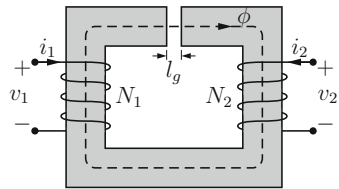
Fig. 6.8 SMIB—Load flow
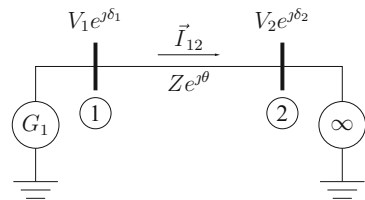
Fig. 6.9 Three bus system
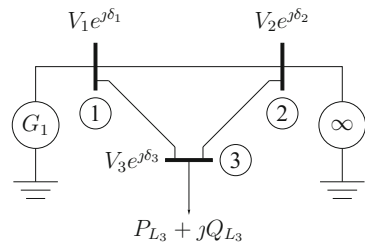
Fig. 6.10 Four bus circuit

Fig. 6.11 Core with an Airgap

3. Bus 3 is a slack bus: $V_3 = 1$ pu and $\delta_3 = 0°$; P_3 and Q_3 are unknown.
4. Bus 4 is a PQ bus, i.e., a load bus: $P_{L_4} = 1.5$ pu and $Q_{L_4} = 0.3$ pu; V_3 and δ_3 are unknown.

All the values are expressed in per unit with $P_b = 100$ MW and $V_b = 138$ kV. Please write a load-flow script (in a package of your choice) and obtain the complex power supplied by the swing bus to supply the load at bus 4.

Exercise 6.12 Two coils with turns $N_1 = 1000$ and $N_2 = 100$ are wound around an iron core with an airgap of $l_g = 2$ mm. The flux path in the iron core has a length of 5 cm and the cross-section area of the core is 2 cm^2. The relative permeability of the iron core is $\mu_r = 3000$ and $\mu_0 = 4\pi 10^{-7}$ V s A^{-1} m^{-1}. Find the inductance of both the coils (Fig. 6.11).

Exercise 6.13 The synchronous machine, in Fig. 6.12, has a sinusoidally distributed stator winding aa' and a round rotor with field coil ff'. A helical spring connects rotor to a fixed point. DC voltages are applied to the rotor and stator windings at time $t = 0$ s and $\theta(0) = 0.03$ rad. The parameters of the system are: $J = 1$ J s^2, $B = 0.2$ J s, $k_s = 0.2$ N m, $L_{aa} = 4$ mH, $L_{ff} = 4$ mH, $\hat{L}_{fa} = 3$ mH, $r_f = 1\,\Omega$, $r_a = 2\,\Omega$, $v_f = 10$ V, and $v_a = -10$ V. The mutual inductance is $L_{fa} = \hat{L}_{fa} \cos\theta$ where θ is the angle between the horizontal line and the magnetic "pole" of the rotor.

1. What is the equilibrium value of θ?
2. Plot the value of θ with time.

Fig. 6.12 Machine and spring
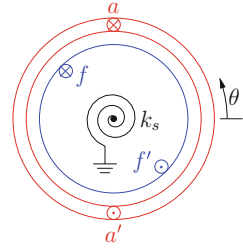
Fig. 6.13 Synchronous machine stator
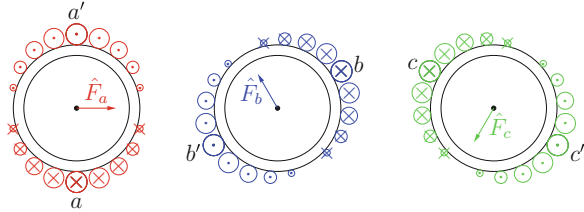
Exercise 6.14 Two magnetically coupled coils, a and f, have the following inductances: $L_{aa} = 3 + \cos 2\theta$ mH, $L_{af} = 0.1 \cos \theta\, H$, and $L_{ff} = 30 + 10 \cos 2\theta\, H$. The coil a is free to rotate about its centre and coil f is stationary. Find the torque $T_a(\theta)$ on the rotor coil a for $i_a = 1$ A and $i_f = 0.01$ A.

Exercise 6.15 The currents in N-turn stator windings aa', bb', and cc' of a synchronous machine as shown in Fig. 6.13 result in the following peak mmf values:

$$\hat{F}_a = N I_m \cos(\omega t); \ \ \hat{F}_b = N I_m \cos(\omega t - \frac{2\pi}{3}); \ \ \hat{F}_c = N I_m \cos(\omega t + \frac{2\pi}{3})$$

Prove that the resultant rotating mmf is:

$$
\begin{aligned}
F =& N I_m \cos(\omega t) \cos(\theta) + N I_m \cos(\omega t - \frac{2\pi}{3}) \cos(\theta - \frac{2\pi}{3}) \\
&+ N I_m \cos(\omega t + \frac{2\pi}{3}) \cos(\theta + \frac{2\pi}{3}) \\
=& \frac{3}{2} N I_m \cos(\omega t - \theta)
\end{aligned}
$$

where θ is measured counter-clockwise from the horizontal line.

Exercise 6.16 Please comment on the statement that the dynamics of a synchronous machine is similar to a mass-spring system dynamics. Justify your comments with appropriate equations.

Exercise 6.17

$$K_s = \frac{2}{3} \begin{bmatrix} \cos(\omega t + \phi_r + \phi_s) & \cos(\omega t + \phi_r + \phi_s - \frac{2\pi}{3}) & \cos(\omega t + \phi_r + \phi_s + \frac{2\pi}{3}) \\ -\sin(\omega t + \phi_r + \phi_s) & -\sin(\omega t + \phi_r + \phi_s - \frac{2\pi}{3}) & -\sin(\omega t + \phi_r + \phi_s + \frac{2\pi}{3}) \\ \frac{1}{2} & \frac{1}{2} & \frac{1}{2} \end{bmatrix}$$

The above matrix K_s is used to transform between abc and dq-frames: $F_{dq0} = K_s F_{abc}$. Obtain I_{dq0} when $\phi_r + \phi_s = 0$, and

$$I_{abc} = \begin{bmatrix} I_m \sin \omega t \\ I_m \sin(\omega t - 2\frac{\pi}{3}) \\ I_m \sin(\omega t + 2\frac{\pi}{3}) \end{bmatrix}$$

Exercise 6.18 The stator coil of a three-phase round rotor synchronous machine has: $r_s = 0.003$ pu, $\omega L_d = 1.5$ pu, $\omega L_q = 1.5$ pu, $\omega L_{md} = 1.4$ pu. The field coil has: $r_{fd} = 0.0006$ pu. The line voltage is $1e^{J0}$. Use the voltage-behind-synchronous-reactance model to find E_{fd}^0, δ_0, and i_{fd}^0 when the stator current is: (a) $1e^{J\frac{\pi}{4}}$ pu and (b) $1e^{-J\frac{\pi}{4}}$ pu.

Exercise 6.19 The stator coil of a three-phase round rotor synchronous machine has: $r_s = 0.003$ pu, $\omega L_d' = 1.5$ pu, $\omega L_q' = 1.5$ pu. The field coil has: $r_{fd} = 0.0006$ pu. The voltage $v_D + J v_Q = 1e^{J0}$ and $i_D + J i_Q = 1e^{-J\frac{\pi}{4}}$ pu. Obtain E_q' and δ_0. Use the voltage-behind-transient reactance model and note that (where F is either v or i):

$$\begin{bmatrix} F_{ds} \\ F_{qs} \end{bmatrix} = \begin{bmatrix} \sin \delta_0 & -\cos \delta_0 \\ \cos \delta_0 & \sin \delta_0 \end{bmatrix} \begin{bmatrix} F_D \\ F_Q \end{bmatrix} \tag{6.1}$$

Exercise 6.20 A synchronous generator is connected to an infinite bus, with voltage $V_\infty e^{J0}$, and supplies power P_0 at a power factor PF. Let

$$\phi = \begin{cases} -\cos^{-1}(PF) & \text{lagging PF} \\ \cos^{-1}(PF) & \text{leading PF} \end{cases}$$

then $P_0 = (3/2) V_\infty I_m \cos \phi$. Show that for a round rotor, $(L_q = L_d)$, the steady-state δ^0 can be calculated using the following relationship:

$$\tan \delta^0 = \frac{r_s I_m \sin \phi + \omega L_d I_m \cos \phi}{V_\infty + r_s I_m \cos \phi - \omega L_d I_m \sin \phi}.$$

Exercise 6.21 The synchronous machine in the exercise in Sect. 2.2.10 is connected to an infinite bus and it is supplying 200×10^6W power at 0.8 lagging power factor.

1. Obtain steady-state values of the state variables for the differential Eqs. (2.25)–
   (2.27). Since the machine is connected to the infinite bus $v_D = V_m$ and $v_Q = 0$.

$$\phi = -\cos^{-1} 0.8$$
$$200 \times 10^6 \, \text{W} = (3/2) V_m I_m \cos \phi \quad \text{(obtain } I_m)$$
$$i_D = I_m \cos \phi$$
$$i_Q = I_m \sin \phi$$
$$\begin{bmatrix} i_{ds} \\ i_{qs} \end{bmatrix} = R(\phi_r) \begin{bmatrix} i_D \\ i_Q \end{bmatrix} \quad (i_{ds}, i_{qs} \text{ in terms of } \delta)$$

   where $R(\phi_r)$ is the same as in the above exercise in Sect. 2.2.11. Obtain δ^0, λ_{fd}^0,
   i_{ds}^0, and i_{qs}^0 from (2.25), (2.35) and $P_o^0 = (3/2)(v_{ds}^0 i_{ds}^0 + v_{qs}^0 i_{qs}^0)$. Obtain i_{fd}^0 from
   (2.24) and then $v_{\text{fd}} = r_{\text{fd}} i_{\text{fd}}^0$.
2. Calculate the initial values of δ^0 and i_{fd}^0 based on the exercise in Sect. 2.2.12 and
   compare it with the values obtained above.
3. Simulate this SMIB system for 1 s. Please see the instructions in the exercise in
   Sect. 2.2.11.
4. Change the input power to $P_m = 250 \times 10^6 \, \text{W}$ at 1 s and simulate for 10 s. Note
   that the initial conditions for this step are the final conditions in the above step.
   Note that by changing the input power the output power will also change
5. Change the input power back to $P_m = 200 \times 10^6 \, \text{W}$ at 10 s and simulate for
   another 10 s.
6. Show the simulation results using the plots for speed, angle, electrical torque, dq
   and phasor currents, flux linkages, real and reactive power.

Exercise 6.22 Repeat Exercise 6.21 when the synchronous machine is supplying
$200 \times 10^6 \, \text{W}$ power at 0.8 leading power factor.

Exercise 6.23 The synchronous machine with parameters in Exercise 6.21 is oper-
ating at steady-state with zero input mechanical power. At $t = 1 \, \text{s}$, a three-phase
short-circuit is applied at the generator terminals. The short-circuit is removed at
$t = 5 \, \text{s}$. Simulate the response till $t = 10 \, \text{s}$ and plot all the outputs including phasor
currents. What can you say about the relative magnitude of the transient and syn-
chronous reactance of this synchronous machine from the plot of phasor currents?

Exercise 6.24 A single machine is connected to an infinite bus. The pre-fault power
transfer is: $2.25 \sin \delta$ pu and at steady-state the power transfer is 0.9 pu. There is a
fault that reduced the power transfer capability to $0.75 \sin \delta$ pu and when the fault is
cleared the power transfer capacity is $1.75 \sin \delta$ pu. Find the critical clearing angle.

Fig. 6.14 Induction machine steady-state equivalent circuit
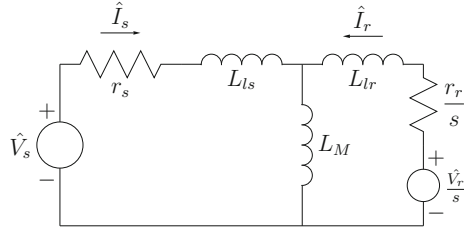
Exercise 6.25

$$
K_s = \frac{2}{3}
\begin{bmatrix}
\cos(\theta) & \cos(\theta - \frac{2\pi}{3}) & \cos(\theta + \frac{2\pi}{3}) \\
-\sin(\theta) & -\sin(\theta - \frac{2\pi}{3}) & -\sin(\theta + \frac{2\pi}{3}) \\
\frac{1}{2} & \frac{1}{2} & \frac{1}{2}
\end{bmatrix}
$$

$$
L_{sr} =
\begin{bmatrix}
L_{md} \cos \theta_r \\
L_{md} \cos \left(\theta_r - \frac{2\pi}{3}\right) \\
L_{md} \cos \left(\theta_r + \frac{2\pi}{3}\right)
\end{bmatrix}
$$

When $\theta = \theta_r = \int_0^t \omega_r dt + \theta_r(0)$, where ω_r is the rotor angular velocity. Show that

$$
K_s L_{sr} =
\begin{bmatrix}
L_{md} \\
0 \\
0
\end{bmatrix}
$$

Exercise 6.26 Show that the circuit in Fig. 6.14 is an equivalent circuit for steady-state operation (with $\dot{\lambda}_{qr} = 0$ and $\dot{\lambda}_{dr} = 0$) of an induction machine (eliminate flux variables and write the equations in terms of phasor current and voltage variables). To show that the circuit in Fig. 6.14 is an equivalent circuit, you need to show that in steady-state the following is true.

$$
v_{ds} + j v_{qs} = r_s(i_{ds} + j i_{qs}) + j\omega L_{ss}(i_{ds} + j i_{qs}) + j\omega L_M(i_{dr} + j i_{qr})
$$
$$
v_{dr} + j v_{qr} = r_r(i_{dr} + j i_{qr}) + j(\omega - \omega_r)L_{rr}(i_{dr} + j i_{qr}) + j(\omega - \omega_r)L_M(i_{ds} + j i_{qs})
$$

Please note that: $\hat{V}_s = v_{ds} + j v_{qs}$, $\hat{I}_s = i_{ds} + j i_{qs}$, $\hat{I}_r = i_{dr} + j i_{qr}$, $\hat{V}_r = v_{dr} + j v_{qr}$, $L_{qr} = L_{lr} + L_M$, $L_{dr} = L_{lr} + L_M$, $L_{qs} = L_{ls} + L_M$, and $L_{ds} = L_{ls} + L_M$. Note that $L_{qr} = L_{dr}$ and $L_{qs} = L_{ds}$, we also define $L_{rr} = L_{qr} = L_{dr}$ and $L_{ss} = L_{qs} = L_{ds}$.

Exercise 6.27 An induction motor is connected to an infinite bus and it has the following parameter values: $P = 1.5$; $L_{ls} = 0.014$ H; $L_{lr} = 0.012$ H; $L_{ds} = 0.39$ H; $L_{dr} = 0.39$ H; $r_s = 1.75\,\Omega$; $r_r = 1.30\,\Omega$; $V_m = (\sqrt{2/3})240$ V; $v_{dr} = v_{qr} = 0$. Assume the induction motor dq-frame aligned with the infinite bus DQ-frame, i.e., $v_{ds} = V_m$ and $v_{qs} = 0$.

For the steady-state operation of the above induction motor, plot for ω_r varying from 0 to 2ω. You can assume the synchronous speed $\omega = 2\pi\,50\,\text{rad s}^{-1}$ and the slip $s = \frac{\omega - \omega_r}{\omega}$.

1. Electric torque versus speed (or slip)
2. Input current magnitude versus speed (or slip)
3. Reactive power input versus speed (or slip)

Exercise 6.28 For the induction motor connected to an infinite bus system with parameters given Exercise 6.27:

1. The dq-frame is rotating with the angular velocity $\omega = 2\pi\,50\,\text{rad s}^{-1}$.
2. For steady-state values solve Eqs. (2.85), (2.86), (2.87) (with $\dot{\lambda}_{dr} = 0$, $\dot{\lambda}_{qr} = 0$, $\dot{\omega}_{r_i} = 0$), (2.88), (2.89) to obtain $\omega_{r_i}^0$, λ_{dr}^0, λ_{qr}^0, i_{ds}^0, i_{qs}^0.
3. Simulate this system for 0.1 s, starting from the initial conditions obtained in the step above. At each integration step for Eqs. (2.85), (2.86), currents i_{ds} and i_{qs} are calculated using (2.88)–(2.89), where $v_{ds} = V_m$, $v_{qs} = 0$.
4. At 0.1 s, change the load torque to 50% of the value used above and simulate for 1 s. Note that the initial conditions for this step are the final conditions in the above step.
5. Change the load torque back to the original value after 1 s and simulate for another 1 s.
6. Show the simulation results using the plots for speed, electrical torque, dq and phasor currents, flux linkages, real and reactive power.

Plot all the currents, voltages, real and reactive power output and other state variables.

Exercise 6.29 From the modelling point of view the chief difference between doubly-fed and short-circuited rotor machine is considering v_{dr_i} and v_{qr_i} in (2.85) and (2.86). In all the derivations done in the exercises here, if v_{dr_i} and v_{qr_i} are non-zero then it models a doubly-fed machine and for $v_{dr_i} = v_{qr_i} = 0$, it is a squirrel cage or short-circuited-rotor induction machine. The actually applied rotor voltages and v_{dr_i}, v_{qr_i} are related by the transformation K_r in the exercise in Sect. 2.6.1.

Repeat the Exercise 6.28 when $v_{dr} = 2\,\text{V}$ and $v_{qr} = 2\,\text{V}$.

Exercise 6.30 For the following parameter values, in per unit, obtain the A-matrix using the linearised model shown in Fig. 6.15: $P_m = 0.6$; $x_q = 1.3$; $x_d = 1.5$; $K_D = 1.0$; $H = 3.0$; $\tau'_{d0} = 7.0s$; $x'_d = 0.3$; $x'_q = 1.3$; $x_e = 0.6$; $\omega_0 = 2\pi\,60\,\text{rad s}^{-1}$; $V_\infty = 1$; $E'_{q0} = 1.2$. Assume values not given above. Please note that to get the A-matrix you will need to obtain the K-parameters first. For the A-matrix obtained here, obtain its eigenvalues and eigenvectors.
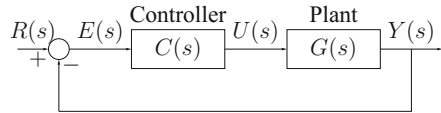
Exercise 6.31 In Fig. 6.16, let

$$G(s) = \frac{10}{(s+1)(s+10)}.$$
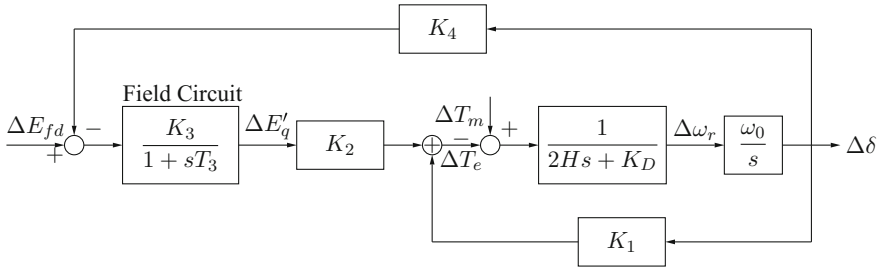
Fig. 6.15 Synchronous machine (without AVR)

Fig. 6.16 Feedback block diagram

Design controller $C(s)$ such that,

1. The closed-loop system has zero steady-state error to unit step reference input;
2. The crossover frequency is above $80\,\text{rad s}^{-1}$;
3. There is a minimum $50°$ phase margin.

A lead-lag controller can meet these specifications:

$$C(s) = K \frac{1 + \frac{s}{\alpha}}{s} \frac{1 + \frac{s}{\omega_z}}{1 + \frac{s}{\omega_p}}$$

Please provide sufficient justifications and explanations with the design.

Exercise 6.32 The differential equations describing DC motor dynamics are:

$$L\frac{di_a}{dt} + Ri_a + k_\omega \omega_r = v_m \tag{6.2}$$

$$J\frac{d\omega_r}{dt} + B\omega_r = k_a i_a \tag{6.3}$$

$$\frac{d\theta}{dt} = \omega_r \tag{6.4}$$

where v_m is the input motor voltage, ω_r, θ, i_a are the motor angular velocity, angular position, and armature current, respectively. Let the angle θ be the output and the voltage v_m be the system input.

Obtain a state-space realisation, i.e., $\{A, B, C, D\}$ matrices and the transfer function of the system, $\frac{\Theta(s)}{V_m(s)}$, for the system represented by Eqs. (6.2)–(6.4).

Exercise 6.33 A dynamical system is represented in the block diagram form as shown in Fig. 6.17.

Find the overall transfer function $\frac{Y(s)}{U(s)}$ in terms of the component blocks.

Exercise 6.34 A dynamical system is represented in the block diagram form as shown in Fig. 6.18.

Find the overall transfer function $\frac{Y(s)}{R(s)}$ in terms of the component blocks.

Exercise 6.35 Plot the bode plot for some of the following systems with $\tau = 1/10; \tau_1 = 1/20; \tau_2 = 1/30; \tau_3 = 1/100$:

1. $\frac{1}{1+\tau s}$

2. $\frac{1+\tau s}{s}$

3. $\frac{1}{(1+\tau_1 s)(1+\tau_2 s)}$
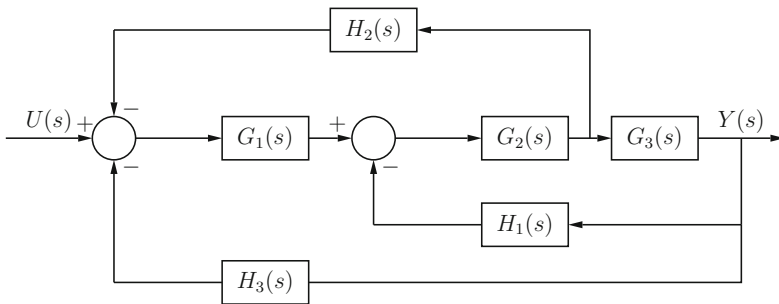
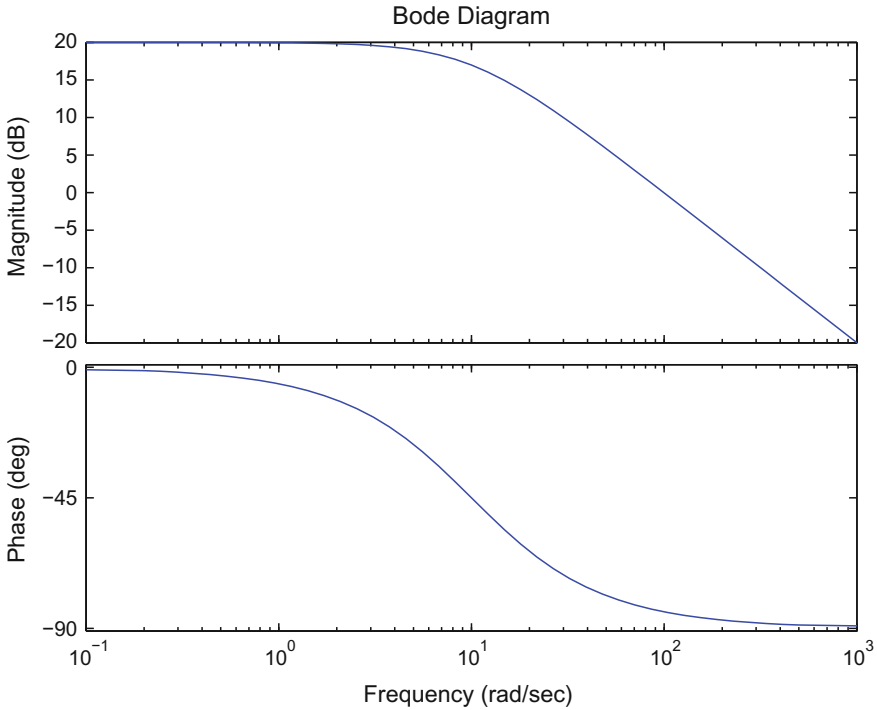**Fig. 6.17** Block diagram
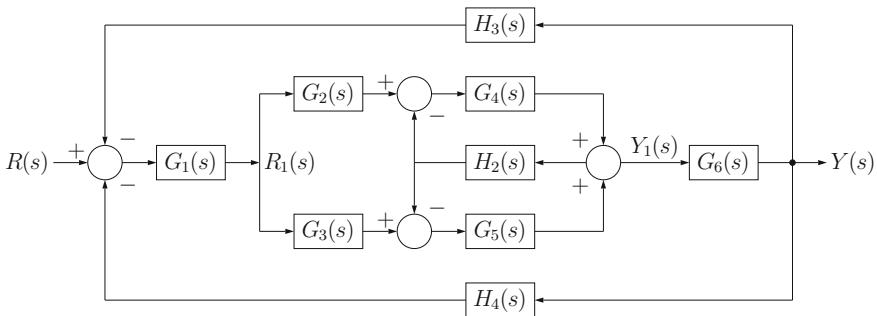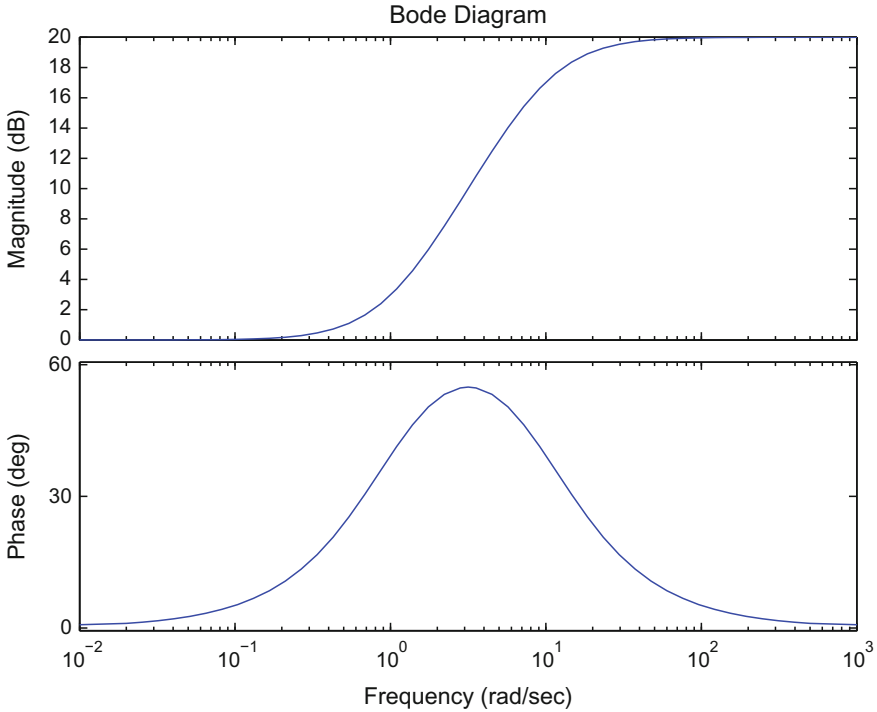

Fig. 6.18 Block diagram

Fig. 6.19 Frequency response

4. $\frac{1+\tau_1 s}{1+\tau_2 s}$

5. $\frac{1+\tau_3 s}{(1+\tau_1 s)(1+\tau_2 s)}$

6. $\frac{1+T_1 s}{1+T_3 s} \frac{1+T_2 s}{1+T_4 s}$, $T_1 = T_2 = 0.118\,s$, $T_3 = T_4 = 0.044\,s$.

7. $\frac{sT_W}{1+sT_W}$, $\frac{(sT_W)^2}{(1+sT_W)^2}$, $T_W = 10$.

8. $\frac{1-\tau_1 s}{1+\tau_2 s}$

Exercise 6.36 Obtain the transfer functions for the systems with the frequency response shown in Figs. 6.19, 6.20, 6.21 and 6.22.

Exercise 6.37 A block diagram of an AVR and a generator is shown in Fig. 6.23. In the block diagram the disturbance term $\Delta d(s)$ in the figure represents the weakening of the flux due to armature reaction, etc. In other words, $\Delta d(s)$, models the effect of all the disturbances which change the terminal voltage. Let: $T_A = 0.02$, $T'_{do} = 8$, $\Delta d(s) = 0$.

Fig. 6.20 Frequency response

Choose a value for K_A such that the steady-state error to a unit-step reference voltage V_{ref} is less than 3%. What is the settling time with this value of K_A?

Exercise 6.38 The block diagram of a closed-loop system with a lag block is shown in Fig. 6.24. Let: $T_A = 0.05$, $T'_{do} = 5$, $K_A = 500$.
Design the lag block in Fig. 6.24, i.e., choose T_C and T_B such that the open-loop (or the loop-gain) bandwidth is $12\,\text{rad}\,\text{s}^{-1}$.

Exercise 6.39 An AVRs with a rate feedback block is shown in Fig. 6.25. Let: $K_A = 120$, $T_A = 0.15$, $T_E = 0.5$, $K_E = 1.0$, $T'_{d0} = 5$.
Design the rate-feedback block in Fig. 6.25, i.e., choose T_F and K_F such that the open-loop (or the loop-gain) bandwidth is $12\,\text{rad}\,\text{s}^{-1}$.

Exercise 6.40 Let us look at an AVR, shown in Figs. 4.13 and 4.14, with the following parameters: $K_{F1} = 0.212$, $K_{F2} = 0.0$, $K_{F3} = 0.0$, $T_E = 0.36$, $K_E = 1.0$, $K_C =$
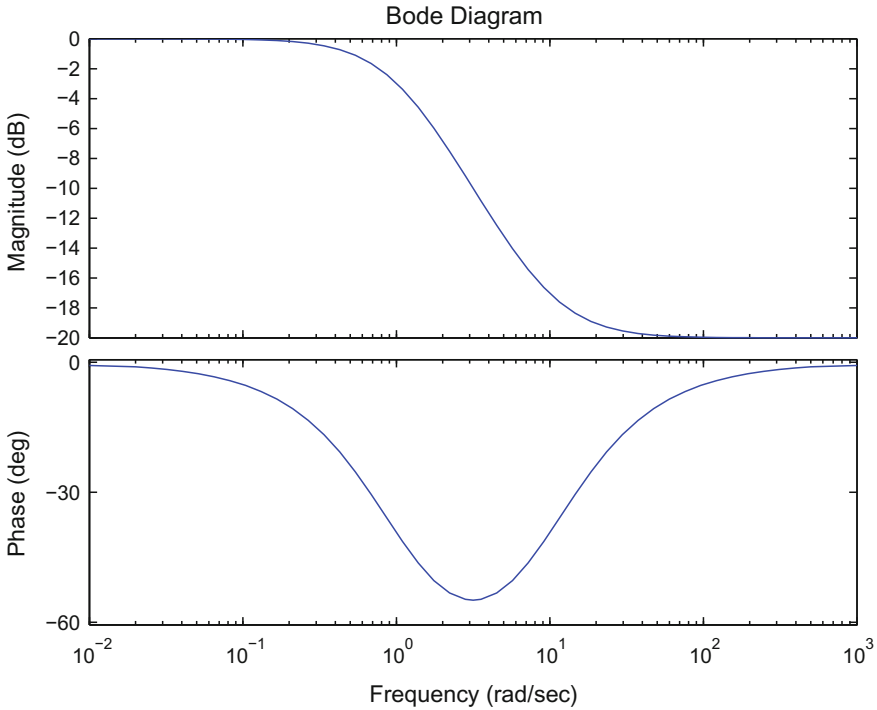
Fig. 6.21 Frequency response

0.30, $K_D = 1.04$, $T_R = 0.01$, $T'_{d0} = 8.9$, $K_E = 1$, $K_D = 0.6$. Assume a practical value of any parameter that is not given here. Design the PID controller $C_R(s)$, i.e., choose the parameters, K_{PA}, K_{IA}, T_{DR}, K_{PR}, K_{IR}, K_{DR}, such that the open-loop crossover frequency is $\omega_c = 4\,\text{rad s}^{-1}$ with a phase-margin $\phi_d = 60°$.

Exercise 6.41 A synchronous machine with a static AVR (gain K_A) is connected to the infinite-bus as shown in Fig. 6.26 and the SMIB has the following parameters, $x_q = 1.0$; $x_d = 1.81$; $H = 3.5$; $K_D = 1$; $\tau'_{d0} = 8.0$; $T_R = 0.02$; $K_A = 200$; $x'_d = 0.8$; $x'_q = 0.8$; $x_e = 0.6$; $\omega_0 = 2\pi 50$; $V_\infty = 1.0$; $P_e = 1.0$; $Q = 0.1$.

Design a PSS to fit into the overall scheme shown in Fig. 5.3. What is the maximum damping that can be provided by the PSS? A PSS block such as in Fig. 5.4 or any other PSS block can be used to damp the resonant mode.
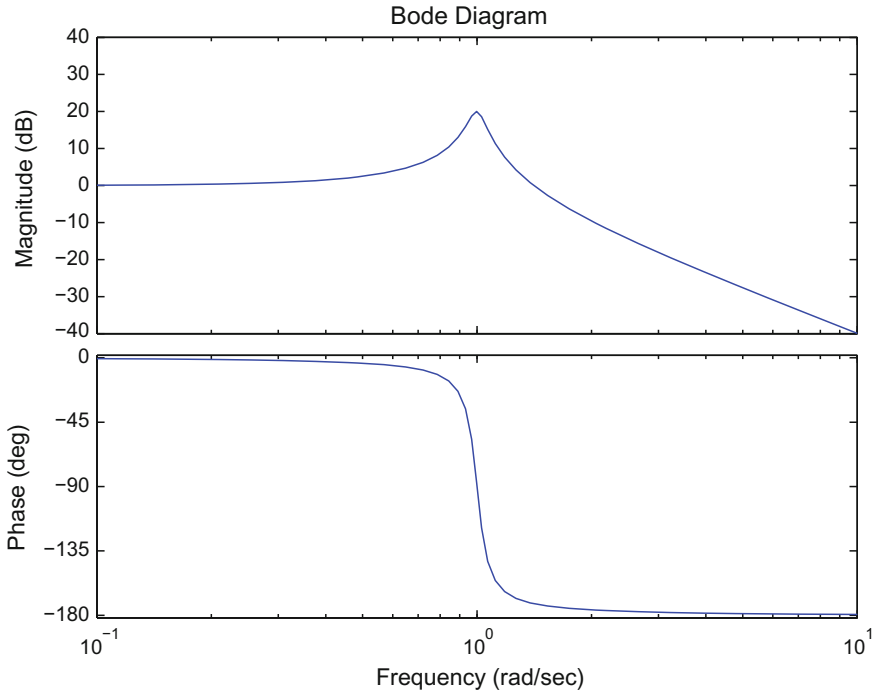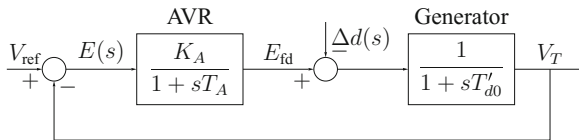
Fig. 6.22 Frequency response
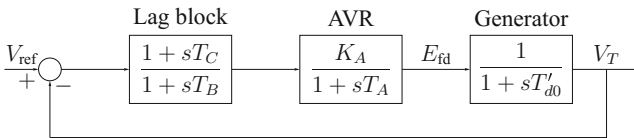

Fig. 6.23 AVR tuning—steady-state error

Fig. 6.24 AVR tuning lag compensator
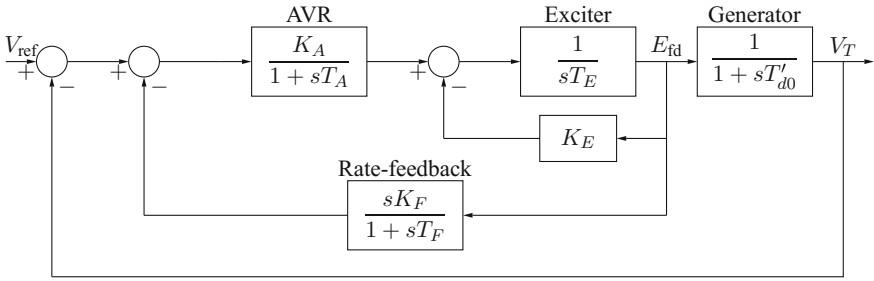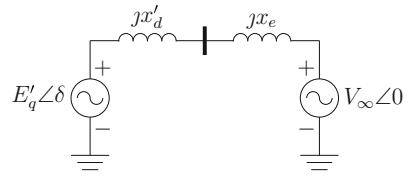
AVR   Exciter   Generator

Fig. 6.25 AVR tuning rate-feedback compensator

Fig. 6.26 Single machine
infinite bus (SMIB)
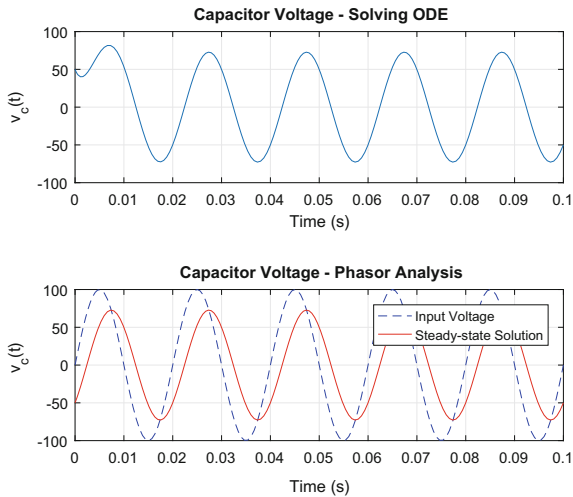

6.2 Answers

Exercise 6.1, *page* 201
$\vec{I} = 1.11e^{-J38.14°} A$ and $i_{ss}(t) = \sqrt{2} \times 1.11 \sin(2\pi 50t - 38.14°)$
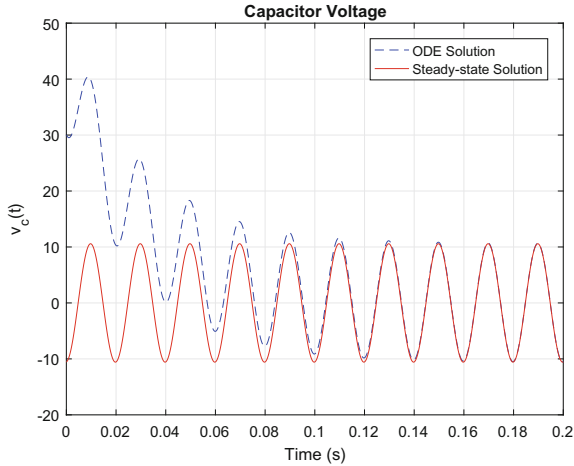
Exercise 6.2, *page* 201

Exercise 6.3, *page* 201

$$Y_{\text{BUS}} = \begin{bmatrix} 1.08 - j6.48 & -0.54 + j3.24 & -0.54 + j3.24 \\ -0.54 + j3.24 & 1.08 - j6.48 & -0.54 + j3.24 \\ -0.54 + j3.24 & -0.54 + j3.24 & 1.08 - j6.48 \end{bmatrix}$$

Exercise 6.4, *page* 201—To be included

Exercise 6.5, *page* 201

Exercise 6.6, *page* 202

$\vec{V}_c = 2.24 - j0.64$, $\quad \vec{I}_1 = -0.025 - j0.00146$, $\quad \vec{I}_2 = 0.0056 - j0.068$, $\quad S_{v_c} = -j0.170$, $S_{v_1} = 0.258 - j0.0014$.

Exercise 6.7, *page* 202

Star - $\vec{I}_a = 43.95 - j41.42$, $S_{\text{load}} = 18242 + j17192$, $S_{\text{gen}} = 3 \times (18242 + j17192)$. Delta - $\vec{I}_{ab} = 101.81 - j24.07$, $S_{\text{load}} = 54725 + j51577$, $S_{\text{gen}} = 3 \times (54725 + j51577)$.

Exercise 6.8, *page* 203

$\delta_1 = 7.49°$ and the complex power absorbed by the infinite-bus is $0.5 - j0.031$pu.

Exercise 6.9, *page* 203
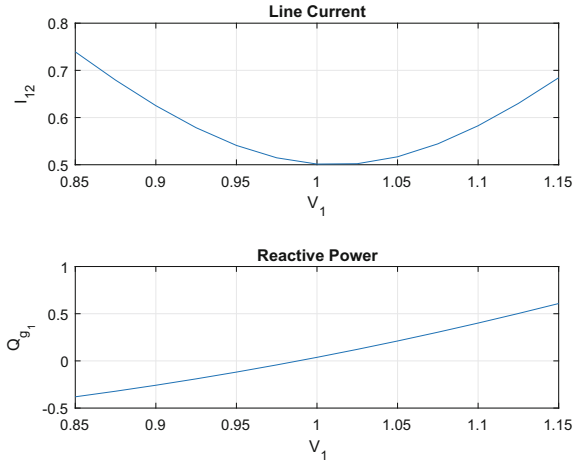
Exercise 6.10, *page* 204

V_1	Iteration	V_3	P_{L_2}	Q_{L_2}
1	1.004	1.019	0.000	0.000
2	0.999	1.013	0.027	−0.081
3	1.000	1.013	0.232	−0.064
4	1.000	1.013	0.284	−0.064
5	1.000	1.013	0.298	−0.064
6	1.000	1.013	0.302	−0.064
7	1.000	1.013	0.303	−0.064
8	1.000	1.013	0.303	−0.064
9	1.000	1.013	0.303	−0.064
10	1.000	1.013	0.303	−0.064

Exercise 6.11, *page* 204

Iteration	V_1	V_2	V_4	P_{L_3}	Q_{L_3}
1	0.996	1.016	0.979	−0.000	−0.000
2	0.990	1.009	0.969	−0.445	0.161
3	0.990	1.010	0.969	−0.399	0.206
4	0.990	1.010	0.969	−0.340	0.203
5	0.990	1.010	0.969	−0.312	0.201
6	0.990	1.010	0.969	−0.299	0.200
7	0.990	1.010	0.969	−0.294	0.200
8	0.990	1.010	0.969	−0.291	0.200
9	0.990	1.010	0.969	−0.290	0.200
10	0.990	1.010	0.969	−0.289	0.199
11	0.990	1.010	0.969	−0.289	0.199
12	0.990	1.010	0.969	−0.289	0.199

Exercise 6.12, *page* 205

$L_1 = 1.246\,\text{mH}$ and $L_2 = 0.1246\,\text{H}$.

Exercise 6.13, *page* 205
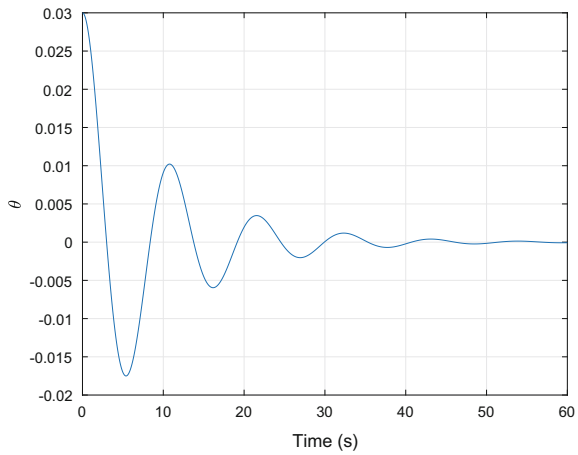
References

1. Rogers G (2000) Power system oscillations. Kluwer Academic Publishers, Boston
2. Dandeno PL, Kundur P, Schulz RP (1974) Recent trends and progress in synchronous machine modeling in the electric utility industry. Proc IEEE 62(7):941–950
3. Concordia C (1948) Steady-state stability of synchronous machines as affected by angle-regulator characteristics. Trans Am Institute Electrical Eng 67(1):687–690
4. IEEE guide for synchronous generator modeling practices in stability analyses. IEEE Std 1110-1991, p 1, (1991)
5. Concordia C, Poritsky H (1937) Synchronous machine with solid cylindrical rotor. Trans Am Institute Electrical Eng 56(1):49–179
6. Krause PC, Wasynczuk O, Sudhoff SD (2006) Analysis of electric machinery and drive systems, 2nd edn. Wiley-Interscience ISBN 9812-53-150-5
7. Sauer PW, Pai MA (2002) Power system dynamics and stability. Pearson Education, Asia
8. Kundur P (1994) Power system stability and control. McGraw-Hill Inc, New York
9. Edward Wilson Kimbark (1995) Power system stability: volumes I-elements of stability calculations, II-power circuit breakers III-synchronous machines. Wiley-Interscience. ISBN 9812-53-075-4
10. Gibbard MJ, David J (2004) Vowles. Reconciliation of methods of compensation for PSSs in multimachine systems. IEEE Trans Power Syst, 19(1):463–472
11. Martins N (1998) Efficient eigenvalue and frequency response methods applied to power system small-signal stability studies. IEEE Trans Power Syst, PWRS-1(1):217–224
12. Hauer JF (1991) Application of prony analysis to the determination of modal content and equivalent models for measured power system response. IEEE Trans Power Syst 6(3):1062–1068
13. Smith JR, Fatehi F, Woods CS, Hauer JF, Trudnowski DJ (1993) Transfer function identification in power system applications. IEEE Trans Power Syst 8(3):1282–1290
14. Grund CE, Paserba JJ, Hauer JF, Nilsson S (1993) Comparison of prony and eigenanalysis for power system control design. IEEE Trans Power Syst 8(3):964–971
15. Hashlamoun WA, Hassouneh MA, Abed EH (2009) New results on modal participation factors: revealing a previously unknown dichotomy. IEEE Trans Autom Control 54(7):1439–1449
16. IEEE recommended practice for excitation system models for power system stability studies (IEEE Std 421.5-2005, Revision of IEEE Std 421.5-1992) (2006)
17. IEEE Std 421.1-2007 (Revision of IEEE Std 421.1-1986). IEEE standard definitions for excitation systems for synchronous machines, 15 (2007)
18. IEEE Std 421.2-1990. IEEE guide for identification, testing, and evaluation of the dynamic performance of excitation control systems (1990)

19. Taborda J (2010) Comparison between detailed and simplified AC exciter models. In: Power and energy society general meeting, pp 1–8. IEEE
20. Glaninger-Katschnig A, Nowak F, Bachle M, Taborda J (2010) New digital excitation system models in addition to IEEE.421.5 2005. In: Power and energy society general meeting, pp 1–6. IEEE
21. Barakat A, Tnani S, Champenois G, Mouni E (2011) Monovariable and multivariable voltage regulator design for a synchronous generator modeled with fixed and variable loads. IEEE Trans Energy Convers 26(3):811–821
22. Kim K, Rao P, Burnworth JA (2010) Self-tuning of the PID controller for a digital excitation control system. IEEE Trans Industry Appl, 46(4):1518 –1524
23. Hsu Y-Y, Liu C-S, Luor T-S, Chang C-L, Liu A-S, Chen Y-T, Huang C-T (1996) Experience with the identification and tuning of excitation system parameters at the second nuclear power plant of Taiwan power company. IEEE Trans Power Syst 11(2):747–753
24. Koessler RJ (1988) Techniques for tuning excitation system parameters. IEEE Trans Energy Convers 3(4):785–791
25. IEEE Commitee Report. Excitation system dynamic characteristics. IEEE Trans Power Apparatus Syst, PAS-92(1):64 –75
26. Chen K (1957) A quick method for estimating closed-loop poles of control system. AIEE Trans Appl Industry 76:80–87
27. Dandeno PL, Karas AN, McClymont KR, Watson W (1968) Effect of high-speed rectifier excitation systems on generator stability limits. IEEE Tran Power Apparatus Syst, PAS-87(1):190–201
28. Schleif FR, Hunkins HD, Martin GE, Hattan EE (1968) Excitation control to improve powerline stability. IEEE Trans Power Apparatus Syst, PAS-87(6):1426–1434
29. Demello FP, Concordia C (1969) Concepts of synchronous machine stability as affected by excitation system. IEEE Trans Power Apparatus Syst, PAS-88(4):316–329
30. Ferguson RW, Herbst R, Miller RW (1959) Analytical studies of the brushless excitation system. Trans Am Institute Electrical Eng Power Apparatus Part III 78(4):1815–1821
31. Gayek HW (1964) Transfer characteristics of brushless aircraft generator systems. IEEE Trans Aerospace 2(2):913–928
32. Kundur P, Klein M, Rogers GJ, Zywno MS (1989) Application of power system stabilizers for enhancement of overall system stability. IEEE Trans Power Syst 4(2):614–626
33. Larsen EV, Swann DA (1981) Applying power system stabilizers part I: general concepts. IEEE Trans Power Apparatus Syst, PAS-100(6):3017–3024
34. Gibbard MJ (1991) Robust design of fixed parameter stabilizers over a wide range of operating conditions. IEEE Trans Power Syst 6(2):794–800
35. Martins N, Lima LTG (1990) Determination of suitable locations for power system stabilizers and static VAR compensators for damping electromechanical oscillations in large scale power systems. IEEE Trans Power Syst 5(4):1455–1469